Report No. CG-D-01-94

(2)

THERMAL RADIATION FROM MARINE FIRE BOUNDARIES:

EVALUATION AND ANALYSIS OF A-60, A-30, A-15, and A-0 BULKHEAD ASSEMBLIES

LeMoyne Boyer

Southwest Research Institute
San Antonio, Texas

FINAL REPORT
JULY 1993

Prepared for:

U.S. Coast Guard
Research and Development Center
1082 Shennecossett Road
Groton, Connecticut 06340-6096

and

U.S. Department of Transportation
United States Coast Guard
Office of Engineering, Logistics, and Development
Washington, DC 20593-0001

NOTICE

This document is disseminated under the sponsorship of the Department of Transportation in the interest of information exchange. The United States Government assumes no liability for its contents or use thereof.

The United States Government does not endorse products or manufacturers. Trade or manufacturers' names appear herein solely because they are considered essential to the object of this report.

The contents of this report reflect the views of the Coast Guard Research & Development Center. This report does not constitute a standard, specification, or regulation.

D. L. Motherway
Technical Director, Acting
United States Coast Guard
Research & Development Center
1082 Shennecossett Road
Groton, CT 06340-6096

Technical Report Documentation Page

1. Report No.	2. Government Accession No.	3. Recipient's Catalog No.
CG-D-01-94		

4. Title and Subtitle

Thermal Radiation From Marine Fire Boundaries:
Evaluation and Analysis of A-60, A-30, A-15,
and A-0 Bulkhead Assemblies

5. Report Date
April 1993

6. Performing Organization Code
SwRI 01-4580

7. Author(s)
LeMoyne Boyer

8. Performing Organization Report No.
CG R&DC 12/93

9. Performing Organization Name and Address

Southwest Research Institute
6220 Culebra Road
San Antonio, TX 78228

10. Work Unit No. (TRAIS)

11. Contract No. F4265087D0026
Delivery Order No. 5162

12. Sponsoring Agency Name and Address

Department of Transportation
U.S. Coast Guard
Office of Engineering, Logistics,
and Development
Washington, D.C. 20593-0001

U.S. Coast Guard
Research and Development Center
1082 Shennecossett Road
Groton, CT 06340-6096

13. Type of Report and Period Covered
Final Report
September 1991 - July 1993

14. Sponsoring Agency Code

15. Supplementary Notes

The Coast Guard technical contact and COTR is Mr. Louis Nash of the U.S. Coast Guard R&D Center. The Headquarter Project Officer is Mr. Klaus Wahle of the Office of Marine Safety, Security and Environmental Protection.

16. Abstract

This report presents the results of fire evaluation and analysis of several types of Class A insulated bulkheads, otherwise referred to as marine fire boundaries. The primary objective of this work was to determine the levels of thermal radiation and surface temperatures from the unexposed face of several assemblies, which barely meet the requirements for that classification. The tests were performed in accordance with IMO Resolution A.517(13), Recommendation on Fire Test Procedures for "A," "B," and "F" Class Divisions. Of secondary importance was the determination of the amount of insulation necessary to meet the thermal requirements of the standard whether the insulation was exposed to the fire or not. This work provides a baseline database to aid in the development of fire modeling, and of regulatory criteria for assemblies of alternate materials, e.g. windows, for the determination of acceptable levels of exposure in the event of a fire in an adjacent compartment.

Furnace calibration tests were performed to determine the total and radiative heat flux and temperature distribution within the furnace over the face of the bulkhead. A total of 21 full-scale fire tests were conducted on steel bulkheads insulated with mineral wool of varying thicknesses and densities, some in combination with calcium silicate marine panels, and uninsulated bulkheads to achieve Class A-60, A-30, A-15, and A-0 ratings. Finite-element heat transfer modeling was utilized to aid in the density / thickness selection for the tests. Radiative heat fluxes and surface temperatures were recorded for each test, with a test length of 60 minutes.

Analysis of the results included determining the peak heat flux and cumulative radiated energy flux associated with a given class of bulkhead. Heat fluxes (at 60 minutes) for the Class A-60 tests reached 2 kW/m^2, while the fluxes for the A-0 tests approached 50 kW/m^2. Cumulative radiated energy (at 60 minutes) for the A-60 and A-0 tests ranged from 0.5 to 100 MJ/m^2, respectively.

The data fit expected scaling behavior based on heat transfer concepts. A linear relationship was shown to exist between the insulation density times the thickness squared and the time to thermal failure. In addition, it was found that approximately twice the thickness of insulation of a given density was required when placed on the unexposed face compared to placing it on the exposed face. This information should prove to be useful in the prediction of exposure levels in the event of a fire and forms a basis for comparison with alternate materials.

17. Key Words	18. Distribution Statement		
Thermal Radiation, Fire Tests Marine Bulkhead IMO Res. A517(13) Heat Flux Measurement	Document is available to the U. S. Public through the National Technical Information Service, Springfield, VA 22161		
19. Security Classif. (of this report) UNCLASSIFIED	**20. Security Classif. (of this page)** UNCLASSIFIED	**21. No. of Pages**	**22. Price**

Form DOT F 1700.7 (8/72) **Reproduction of form and completed page is authorized**

METRIC CONVERSION FACTORS

Approximate Conversions to Metric Measures

Symbol	When You Know	Multiply By	To Find	Symbol
		LENGTH		
in	inches	* 2.5	centimeters	cm
ft	feet	30	centimeters	cm
yd	yards	0.9	meters	m
mi	miles	1.6	kilometers	km
		AREA		
in^2	square inches	6.5	square centimeters	cm^2
ft^2	square feet	0.09	square meters	m^2
yd^2	square yards	0.8	square meters	m^2
mi^2	square miles	2.6	square kilometers	km^2
	acres	0.4	hectares	ha
		MASS (WEIGHT)		
oz	ounces	28	grams	g
lb	pounds	0.45	kilograms	kg
	short tons (2000 lb)	0.9	tonnes	t
		VOLUME		
tsp	teaspoons	5	milliliters	ml
tbsp	tablespoons	15	milliliters	ml
fl oz	fluid ounces	30	milliliters	ml
c	cups	0.24	liters	l
pt	pints	0.47	liters	l
qt	quarts	0.95	liters	l
gal	gallons	3.8	liters	l
ft^3	cubic feet	0.03	cubic meters	m^3
yd^3	cubic yards	0.76	cubic meters	m^3
		TEMPERATURE (EXACT)		
°F	Fahrenheit temperature	5/9 (after subtracting 32)	Celsius temperature	°C

*1 in = 2.54 (exactly).

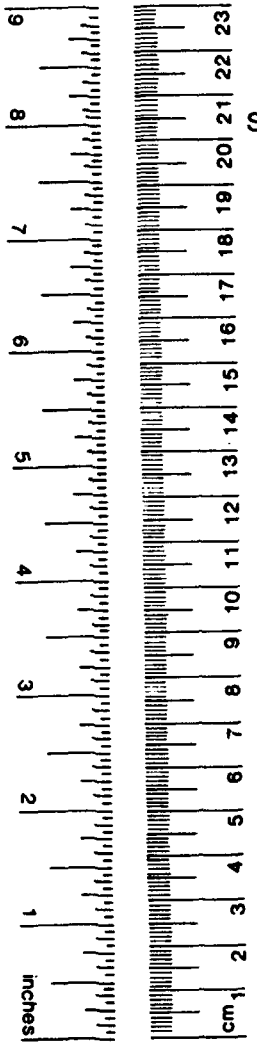

Approximate Conversions from Metric Measures

Symbol	When You Know	Multiply By	To Find	Symbol
		LENGTH		
mm	millimeters	0.04	inches	in
cm	centimeters	0.4	inches	in
m	meters	3.3	feet	ft
m	meters	1.1	yards	yd
km	kilometers	0.6	miles	mi
		AREA		
cm^2	square centimeters	0.16	square inches	in^2
m^2	square meters	1.2	square yards	yd^2
km^2	square kilometers	0.4	square miles	mi^2
ha	hectares (10,000 m^2)	2.5	acres	
		MASS (WEIGHT)		
g	grams	0.035	ounces	oz
kg	kilograms	2.2	pounds	lb
t	tonnes (1000 kg)	1.1	short tons	
		VOLUME		
ml	milliliters	0.03	fluid ounces	fl oz
l	liters	0.125	cups	c
l	liters	2.1	pints	pt
l	liters	1.06	quarts	qt
l	liters	0.26	gallons	gal
m^3	cubic meters	35	cubic feet	ft^3
m^3	cubic meters	1.3	cubic yards	yd^3
		TEMPERATURE (EXACT)		
°C	Celsius temperature	9/5 (then add 32)	Fahrenheit temperature	°F

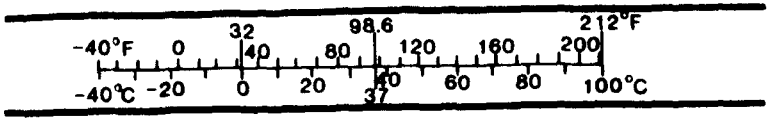

TABLE OF CONTENTS

TABLE OF CONTENTS

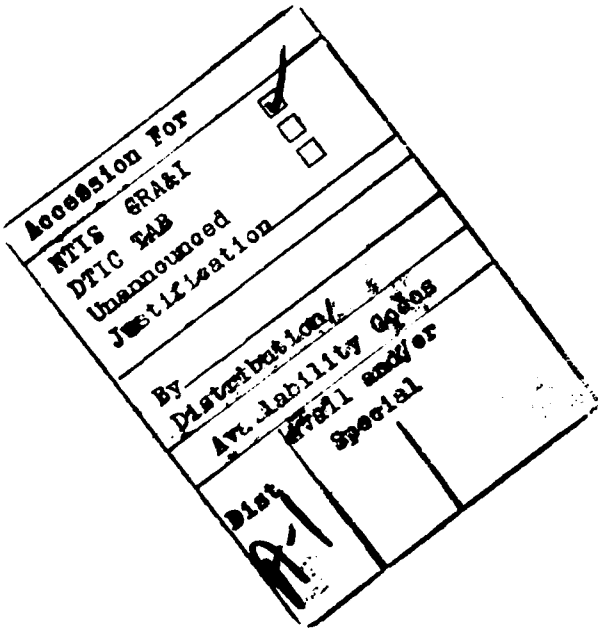

LIST OF FIGURES

LIST OF FIGURES (Continued)

LIST OF TABLES

NOMENCLATURE

A-60	Class A bulkhead thermally rated for 60 minutes; likewise for an A-30, A-15, and A-0 classification ; tests identified by class followed by number, e.g. A60-2 refers to the second class A-60 test in the series
c	Specific heat (J/kgK)
CAL	Designation for calibration test
Fo	Fourier number, $kt/\rho cL^2$ (-)
HF	Heat flux (kW/m^2)
HFT	Heat flux transducer
k	Thermal conductivity (W/mk)
L	Insulation thickness (mm)
Rad	Heat flux transducer designation, either total or radiative, numbered 1-6 (kW/m^2)
RHF	Radiative heat flux (kW/m^2)
S	Insulation thickness (mm)
t	Time (min)
Tamb	Ambient temperature (°C)
Tf	Furnace temperatures, numbered 1-5 (°C)
THF	Total heat flux [radiative plus convective components] (kW/m^2)
To	Initial surface temperature, average of Ts1-9 (°C)
Tr	Heat flux transducer body temperatures, numbered 1-6 (°C)
Ts	Surface temperatures, numbered 1-11 (10 and 11 over stiffeners) (°C)
Tsavg	Average bulkhead surface temperature (average of Ts1-9) (°C)
α	Surface absorptivity (-)
ε_f	Flame emissivity (-)
ε_s	Surface emissivity (-)
ρ	Bulk material density (kg/m^3)
σ	Stephan-Boltzmann Constant, $5.67(10)^{-8}$ W/m^2K^4

1. Introduction

Thermal protection from fire in a marine vessel is essential to the safety of crew, passengers and other contents. Even though passive protection can contain the combustion to a small portion of the ship, adjacent corridors and compartments may be affected to the extent that heat or smoke movement can impede egress, rescue efforts, fire fighting, etc. Heat transmission across a fire boundary can be enough to ignite combustibles or create untenable conditions for personnel. Heat transmission from a fire boundary can occur by three modes, conduction through solids, convection by air currents, or thermal radiation from one surface to another. It is this third mode of heat transfer that has been studied during the course of this program.

Radiative heat flux is not currently a criteria for the classification of fire boundaries for commercial vessels. These classifications are defined by Regulation II/2-3 of the International Convention for the Safety of Life at Sea (SOLAS) [1]. The current test method for fire resistance classification is the International Maritime Organization (IMO) Resolution A.517(13) [2], currently under revision. The U.S. Coast Guard has codified its interpretation of the test method in 46 CFR 164.007 and 164.008 [3,4].

Briefly, a class A fire boundary is a bulkhead which is constructed of steel or other equivalent material, is suitably stiffened, and is so constructed as to be capable of preventing the passage of smoke and flame to the end of a one-hour duration of the test method: Recommendation on Fire Test Procedures for A, B, and F Class Divisions (IMO Res. A.517(13)) [2] as it applies to class A bulkheads.

Further refinement of the classification is based on the time period for which the rise of temperature of the unexposed side is limited. In particular, an uninsulated steel bulkhead shall be class A-0, while other classes shall be insulated with a Coast Guard Approved Structural Insulation. The average temperature of the unexposed side will be less than 139°C above the initial temperature without rising, at any one point, including any joint, more than 180°C above the original temperature at the end of 15 minutes for a class A-15; 30 minutes for a class A-30; and 60 minutes for a class A-60 [2-4]. The opposite face of the assembly is exposed to an enclosed furnace which logarithmically rises to 925°C above ambient at the end of the 60-minute test.

The U. S. Coast Guard and other authorities are interested in establishing criteria for thermal radiation from various classifications of insulated and non-insulated bulkhead assemblies. Since glass is also often used for aesthetical purposes to separate areas, such as in vessel corridors, large public spaces, or near life boat embarkation and lowering areas, the concern is that thermal radiation through glass assemblies can block escape routes and ignite combustibles. To provide an equivalent level of safety, the radiation through the assembly should not exceed that of the insulated bulkhead fire boundary. If that means an unnecessarily low level of radiative flux, the criteria may be chosen to provide an adequate level of safety.

This report describes work performed as a foundation study to support an overall program to develop a protocol for measuring the radiant flux through and from glass assemblies. This study was designed to establish a baseline by measuring radiant fluxes from examples of the various classes of fire boundaries. The purpose was to determine the radiative flux from bulkheads which barely meet the temperature limitations of class A bulkheads. An additional aspect to the study was to collect data on the quantity of insulation required to meet fire boundary requirements based on whether the insulation was in or out of the furnace.

The next section of this report presents the approach used in the conduct of the program. Section 3. presents the results for the furnace calibration, bulkhead tests, thermal modeling, and test data comparison and scaling with associated discussion. Conclusions are presented in Section 4. References and Figures are given in Sections 5. and 6. Appendices A through G present detailed test data, transducer calibration information, and thermal modeling input.

2. Approach

This report includes the results of work completed at Southwest Research Institute (SwRI), San Antonio, Texas, under Contract No. F4265087D0026, Delivery Order No. 5162 to the U. S. Coast Guard Research and Development Center, Groton, Connecticut. In short, the work consisted of the construction of a test frame to contain the bulkhead assemblies. Before commencement of evaluation of the bulkheads, the furnace was calibrated to establish radiative and convective fluxes and temperatures during simulated tests. The subsequent tasks included evaluating several of each A-60, A-30, A-15, and A-0 class bulkhead. The evaluations were supplemented with finite element thermal modeling to predict the performance of a particular design and to aid in the selection of insulation

density and thickness to meet the temperature criteria. This was followed by a detailed analysis of the data obtained. The following discussion will present the apparatus and instrumentation used during the furnace calibration and bulkhead tests. Next, the method for each phase of the test work will be presented, including furnace calibration, A-60, A-15, A-30, and A-0 tests, and how the data was to be analyzed.

2.1 Apparatus

2.1.1 Furnace

SwRI's Vertical Furnace is capable of exposing a maximum test specimen of 3.66 m (12.0 ft) high by 3.81 m (12.5 ft) wide. The 0.76-m (30-in.) deep furnace is equipped with nine premixed air/natural gas burners symmetrically placed across the back wall and controlled by a variable air-gas ratio regulator. The flat flame burners have a high swirl and are shaped such that the flame front is widely dispersed over the wall they reside in, and extend over a large area to provide uniform radiant heating within the furnace. Figure 2.1[1] contains a sketch of the furnace. View ports are located on both sides of the furnace to allow observation of the surface exposed to flame.

2.1.2 Test Frame and Bulkhead Construction

The test assemblies were mounted in a frame secured to the front of the furnace. Figure 2.2 shows the design of the frame. The bulkheads were placed in the frame such that it was centered over the nine burners. The specimen bulkheads for all of the tests were mounted in the frame with the stiffeners on the exposed side (i.e., inside the furnace). The frame was designed so that the bulkhead could be easily removed. The tabs which held the bulkhead in place also allowed for its movement due to material expansion during heating.

The bulkheads were constructed in accordance with IMO Res A.517(13) for insulated class A bulkheads. The dimensions of the structural core were 2.44 m high by 1.91 m wide. The core was constructed of hot-rolled mild steel plating with vertical stiffeners spaced at 600 mm. All joints were of continuous welds. The thickness of the steel plating was 4.5 ± 0.5 mm. The vertical stiffeners were 65 ± 5 mm by 65 ± 5 mm with a thickness of 6 ± 1 mm. The steel met the requirements of ASTM

[1]All figures are included in Section 6.0

A131 [5]. This is the ASTM standard for [illegible] steel commonly used in shipbuilding. Refer to Figure 2.3 for a drawing describing the construction of the bulkhead.

Except for class A-0 fire boundaries, the specimen bulkheads were constructed with insulation installed over a structural steel core. The insulation chosen was a mineral wool product by USG Interiors, Inc. Mineral wool was chosen due to its wide usage in the maritime industry. The product designation was "Thermafiber Industrial Felt," USCG Approval No. 164.007/40/0. Their most recent USCG approval (dated 6 February, 1991) indicated that a minimum 64 mm (2.5 in.) thickness with a nominal density of 104 to 112 kg/m^3 (6.5 to 7 lb/ft^3) meets the USCG A-60 requirements (insulation exposed).

It should be noted that the insulation thicknesses listed in Equipment Lists; Items Approved, Certified or Accepted Under Marine Inspection and Navigation Laws [6] was determined assuming the insulation was installed on the exposed side. Insulating the unexposed side, in general, would require a greater thickness of insulation for the same classification, due to the differences in the thermal radiative properties of the steel and the insulation, and the difference in material performance during the test.

The insulation was installed in a manner consistent with its installation when tested for approval per 46 CFR 164.007. Additional guidance on installing insulation, including around the stiffeners, was found in the Guide to Structural Fire Protection Aboard Merchant Vessels, (Navigation and Vessel Inspection Circular No. 6-80) [7].

In general, the insulation was installed with steel pins and clips [7]. The pins were welded to the bulkhead with a capacitor discharge type weld gun and the insulation then impaled on the pins and locked on with washers (also known as speed clips or clinch shields). The typical dimensions for the pins were 3-mm (1/8-in.) diameter pins spaced on 305 mm (12 in) centers with 32-mm (1-1/4-in.) diameter clinch shields. The pins were located approximately 50 mm (2 in) from the edge of the batts, which were supplied in 64 mm by 610 mm by 1220 mm (2.5 in by 2 ft by 4 ft) nominal sizes. Information regarding placement of insulation batts for each test can be found in Appendix A.

2.1.3 Instrumentation and Uncertainty

2.1.3.1 Instrumentation. Data recorded during the furnace calibration and tests included temperatures, furnace pressure and heat flux data. This information was stored electronically using a data acquisition/computer system. The data acquisition system was performed using a Fluke Helios I 2289A computer front end to measure the output of all instruments. Voltages were converted to digital signals with 12 bit accuracy. Signals processed by the Helios were stored by a DEC VAX 11/750 and stored on a hard disk. The data files were subsequently processed and reformatted as needed.

The arrangement of the instrumentation is shown in Figure 2.4. The heat flux transducer placement in the furnace shown was only used during the furnace calibration tests. These circular foil, water-cooled Gardon type, transducers were placed side by side to see the same view. The total heat flux transducers (fluxmeters labeled Rad #1, #2, and #3) had a 180° view. They were located at the upper one-fourth, middle, and lower one-fourth height with respect to the bulkhead and centered horizontally. The radiant heat flux transducers (radiation pyrometers labeled Rad #4, #5, and #6) had a sapphire window with a view angle of 150° (the maximum standard view manufactured). They were placed adjacent to the fluxmeters. The 150° view angle viewed all of the furnace back wall across from the bulkhead. The fluxmeters and pyrometers were both calibrated to indicate incident heat flux and had a range of 0. to 230 kW/m^2 (0. to 20. BTU/ft^2sec). The overrange capability of this transducer is 150%. Further information can be found in Appendix B.

The pyrometers and fluxmeters viewing the unexposed face of the bulkheads were water cooled, Schmidt-Boelter type, with restricted views sized to the degree angle as necessary to view the appropriate area of the test bulkhead. These transducers were obtained from Medtherm Corporation of Huntsville, Alabama. All of the heat flux transducers were of the 64 series.

The test specimen heat flux transducers which viewed the unexposed face of the test assembly during the bulkhead tests were actually total heat flux transducers (fluxmeters of the Schmidt-Boelter thermocouple pile type). The rationale was that these transducers would see a low irradiance compared to the pyrometers in the furnace, since the unexposed surface of the bulkhead would be at a much lower temperature than that of the furnace. Thermal radiation at those lower temperatures occurs at longer wavelengths, which would be absorbed or reflected by a sapphire window at wavelengths greater than 5 μm. It was felt that the fluxmeter under these conditions would primarily indicate

radiant flux, since the transducer was placed a given distance away from the bulkhead and was outside the thermal convective boundary layer of the bulkhead heated surface, thereby minimizing the convective heat fluxes at the face of the transducer. The transducers were water cooled, so that no heat transfer effects should have occurred outside of the sensing area. In addition, a horizontal plate was placed below the transducers to block convective flows near the surface of the transducer (without blocking its view). The specimen fluxmeters were calibrated to indicate incident heat flux and had a range of 0. to 11.4 kW/m^2 (0. to 1.0 BTU/ft^2sec). They were calibrated with and without view restrictors, as discussed in the next paragraph. The overrange capability of this transducer is 500%. In should be noted that these transducers have a "black" surface coating which is calibrated to have a nominal absorptivity of 0.92, over the wavelength range from 0.6 to 15.0 μm. In addition, the method of calibration by the manufacturer can affect the indicated heat flux when used in a configuration different from that of the calibration.

The test specimen fluxmeter placement near the unexposed face was based on view angles of 30° and 60°. Thus, the shape of the area viewed by the specimen fluxmeters was circular. The view of the fluxmeters was only over the bulkhead and did not include the surrounding test frame in its view. The view seen by the five fluxmeters is shown in Figure 2.4. The top, middle, and bottom 30° view fluxmeters were placed so that they extended to one-third of the height of the bulkhead. The 60° view fluxmeter at the center viewed most of the width of the bulkhead. Since it was essential that the view of the fluxmeter not be obstructed by other instrumentation, the 30° center fluxmeter was placed next to the 60° pyrometer, the same distance from the bulkhead surface. In addition to the fluxmeters, one 60° sapphire window-radiant heat flux transducer (pyrometer) was placed adjacent to the 60° view fluxmeter, for comparison purposes. The purpose for this was to clarify any differences between the two types of transducers in this application. The transducers were aligned to view the correct area of the bulkhead with the aid of a laser pointer. All of the furnace and test specimen pyrometers/fluxmeters were furnished with a body thermocouple to monitor the temperature uniformity of the cooling water.

The furnace probes were constructed in accordance with IMO Res A.517(13), as well as the unexposed surface thermocouples with copper disks. All wire was of type K of the appropriate gage. Furnace probe placement is shown in Figure 2.1, while specimen thermocouple placement is shown in Figure 2.3. The specimen thermocouples were attached to the bulkhead using two weld pins and small clips to pinch the thermocouple pad tightly to the steel surface. For the tests where the thermocouple was attached to the insulation, the thermocouple was held in place using a wire mesh

to hold the thermocouple tightly to the surface. The mesh was held in place with the weld pins and clips used to hold the insulation in place. The location of the thermocouple was not varied more than 50 mm from its intended location on the bulkhead. This variation was to prevent the placement of a thermocouple directly over a pin or a joint in the insulation batts, since those features would have represented a very small percentage of the surface area. In addition to these thermocouples, one thermocouple was placed in the furnace building to monitor ambient temperature during the test.

Furnace pressure was monitored with an incline manometer and measured with a Setra Bi-Directional Pressure Transducer Model 264A with a range of ± 250 Pascal (Pa) of water.

2.1.3.2 Instrumentation Calibration. Calibration procedures for all instruments and equipment other than pyrometers and fluxmeters used in this test series are described as part of SwRI's Nuclear Projects Operating Procedure, "Instrumentation Calibration and Repair System," XII-FT-101-2, 1987 [8]. The instruments and equipment are on a routine calibration schedule, and compliance with this schedule was verified before the instrument/equipment was used. All thermocouple wire was purchased with the nuclear critical quality assurance/quality control designation and used for one test only. Before the start of each test, a functional check on all instrumentation was performed.

The pyrometers/fluxmeters which were acquired under this work were calibrated by the manufacturer. The calibration certificates are NIST-traceable and are summarized in Appendix B, Table B.1. The original certificates are on file. As long as the incident heat fluxes seen by these instruments do not exceed their designed capacities, experience has shown that the calibrations are acceptable for a period of approximately one year. Functional calibration checks were performed, and recalibration of the pyrometers/fluxmeters was performed at the completion of the tests to assure that the original calibration was maintained.

2.1.3.3 Instrument Uncertainty. When evaluating the uncertainty in the measurement of a physical quantity, it is necessary to consider each transducer, as well as the system used for recording the output of those instruments.

The thermocouple wire was calibrated by lot from the manufacturer at ±0.4% or ±1.1°C (whichever is greater) and falls within the special limits of accuracy as defined by ANSI MC96.1[9]. The output voltage range expected for furnace temperatures up to 1000°C was 0 to 10 mv.

The accuracy of the heat flux transducers was ±3%, with a maximum non-linearity of ±2% of full range. The output voltage range was 0 to 10 mv. The transducers were re-calibrated as received at the completion of the test series to assure that the calibration of each transducer was maintained.

The furnace pressure transducer accuracy was ± 2.5 Pa with a maximum pressure range of ±250 Pa. The output voltage range was 0 to 5 V.

The electrical signals from the above instruments were converted to digital format as described previously. The internal resolution of the analog to digital conversion was 0.6 μV for DC voltage measurements in the range of ±64 mV. The accuracy stated for the period between calibration was ±0.01% of input ±8.0 μV.

Thus, the overall uncertainty in the instrumentation was not limited by the data acquisition system, but is governed by the individual uncertainties of each transducer. These values do not address additional uncertainties associated with the actual application of use (e.g., the radiative, convective and conductive losses from thermocouples exposed to furnace conditions).

2.2 Furnace Calibration

Furnace calibration was performed to determine the baseline radiative and convective heat fluxes in SwRI's Vertical Furnace for the time-temperature curve of Recommendation on Fire Test Procedures for A, B, and F Class Divisions, IMO Res. A.517(13) [2]. The calibration was determined at three different heights, corresponding to one-fourth, one-half, and three-fourths of the bulkhead height, and over separate test runs. These measurements were completed using three total heat flux meters (fluxmeters) as well as three radiant heat flux meters (pyrometers). Temperature measurements at the calibration locations were also recorded to assure uniformity at the test sample surface.

A total of four calibration tests were performed. The first two were intended to obtain an assurance that the subsequent two full calibration tests on the A-60 bulkheads would be acceptable. The calibration tests were configured the same as an A-60 test, where the mineral wool was exposed to the furnace conditions. The advantage of calibrating the furnace using an actual test bulkhead configuration was that the thermal conditions for the calibration were the same as the thermal

conditions which would exist during the testing of the A-60 and other bulkhead classifications. The calibration bulkhead consisted of assembling an A-60 bulkhead which had three holes to allow for insertion of the pyrometer/fluxmeter probes. The first test (CAL1) followed the standard curve to observe uniformity in the furnace. The second test (CAL2) stepped the furnace temperature and stabilized at several temperature levels, to obtain average readings over a period of time.

The two subsequent calibrations had the full complement of surface temperatures and furnace heat flux transducers. Due to the possible interference, the other five heat flux transducers viewing the sample surface were not installed. Surface and furnace temperatures were recorded. The conduct of these tests was such that the standard temperature curve was followed for the required time period.

2.3 Bulkhead Tests

Several classes of insulated bulkheads were tested. Seven different test configurations were performed. The first configuration was an A-60 bulkhead with the mineral wool insulation exposed to the furnace. The second was also an A-60 configuration, but the insulation was outside of the furnace (the steel was exposed). The third, fourth and fifth configurations consisted of A-30, A-15, and A-0 bulkheads, respectively. The sixth configuration was an A-30 bulkhead comprised of calcium silicate marine board and mineral wool. The third through sixth configuration had the insulation outside the furnace which was the configuration that showed a higher level of radiant heat flux during the A-60 tests. The seventh configuration consisted of an A-15 system with the mineral wool on the exposed face. Three tests of each bulkhead configuration were constructed and tested. Thus, a total of 21 tests were performed.

For each configuration, the specimen bulkheads were constructed to meet the specified class and test configuration. For the classes other than A-0, the construction was such that the temperature rise limit was bracketed (one test exceeded the temperature criteria later in time, the other earlier). This was achieved by varying the thickness and the average density of the insulation to assure that the three tests bracketed the required temperature rise.

Finite-element heat transfer analysis was utilized to aid in the prediction and selection of the material density and thicknesses for the tests. This information, in conjunction with the Guide [7], allowed a determination of the appropriate thickness and density for each of the bulkhead tests to obtain a desired time rating. As indicated in the Guide, if S mm of insulation is required for 60

minutes of thermal protection, 30 minutes of protection can be achieved with 0.75*S mm of insulation, and 15 minutes of insulation can be achieved with 0.5*S mm.

Each test was continued until the average temperature of the surface thermocouples (Ts 1-9, excluding the two on the stiffeners, Ts 10-11) on the unexposed surface rose more than 139°C above the initial temperature. In all cases, the test duration was a minimum of 60 minutes and continued until the temperature requirements were exceeded. This ensured that the main regulatory endpoint of class A was reached.

The data recorded in each test included the radiant heat flux from the unexposed side of the bulkheads, the unexposed surface temperatures, furnace temperatures and pressure, heat flux transducer body temperatures, and ambient temperature.

All steel bulkheads were conditioned prior to test by using a wire brush to clean the surface of dust and light rust. Most of the tests used a new bulkhead, to minimize any problems with changing thermal radiative surface properties due to oxidation. The only specimen bulkheads reused were those A-60 bulkheads which had the insulation exposed, thereby protecting the steel from oxidation. These were reconditioned by wire brush prior to reuse. Each of the test configurations are more clearly outlined below by classification.

2.3.1 A-60 Bulkheads

Two test configurations were used for the Class A-60 fire boundaries. One configuration was with the insulation on the exposed side of the specimen bulkheads. The other was with the insulation on the unexposed side. By varying the density and thickness of the insulation, the required test criteria were met. A total of six tests were performed, three for each configuration.

2.3.2 A-30 Bulkheads

There were two test configurations for the Class A-30 bulkheads. The first configuration, was arrived at by decreasing the insulation thickness from the A-60 bulkhead and placing the insulation on the face which provided the higher level of radiant flux in the Class A-60 tests (i.e., the unexposed side).

The second configuration was designed to accumulate radiant flux data from Class A-30 fire boundaries constructed using calcium silicate marine board. The fire boundary consisted of a structural steel core, mineral wool insulation and calcium silicate marine board to obtain an A-30 classification. The calcium silicate marine board and mineral wool were on the unexposed side (i.e. outside of the furnace). A total of six tests were performed.

2.3.3 A-15 Bulkheads

The two A-15 test configurations were determined by decreasing the thickness of the insulation further and placing the insulation on the exposed face for one configuration and on the unexposed face for the other configuration. A total of six tests were performed.

2.3.4 A-0 Bulkheads

Three tests were performed on bare steel bulkheads. The stiffeners were on the exposed side of the bulkhead (inside the furnace).

2.4 Data Analysis

The analysis included determining the time-radiant flux curve per unit area of radiative surface and the time-cumulative radiant energy curve per unit area of radiative surface. The data from each of the fluxmeters for a given test should be similar, thus the results were averaged to obtain a single time-dependent curve. Since the three tests for each configuration were slightly different, it was necessary to interpolate, to obtain the time-radiant flux and time-cumulative curves for the minimum acceptable required class bulkhead. Dimensional analysis was used to obtain the proper scaling for data comparison.

3. Results and Discussion

The outline for this section of the report will be to present the data separately for each set of tests. First the results of the calibration are presented, followed by the results of the bulkhead tests. For each test run the configuration is noted, along with observations during the tests, and unusual events which need to be described. Due to the volume of data obtained, the following material can

be found in the Appendices: placement of insulation batts (Appendix A), furnace and surface heat fluxes (Appendix C), surface temperatures (Appendix D), furnace temperatures (Appendix E), and heat flux transducer body temperature, ambient temperature and furnace pressure (Appendix F).

It should be noted that, within a given test configuration each test was numbered consecutively, i.e. the first A-60 test was labeled A60-1, while the sixth A-60 test was identified as A60-6. In the data plots the nomenclature adopted was Rad for heat flux transducer, Ts for unexposed surface temperature, Tf for furnace temperature, Tr for heat flux transducer body temperature, Tamb for ambient temperature, and Pf for furnace pressure.

Following the test results presentation, the results of the thermal modeling are presented, even though this was actually intertwined with the tests. The last segment of the results section presents the data comparisons and analyses.

3.1 Furnace Calibration

The first two calibration tests were performed with the furnace heat flux transducers and only four unexposed surface thermocouples. The thermocouples were affixed with different methods to observe the integrity of the bond using ceramic cement, silicone based adhesive, or mechanical fastening using two weld pins and small clips at the perimeter of each pad.

The insulation used for all of the calibration tests was in the density range 108 to 117 kg/m^3 (6.7 to 7.3 lb/ft^3), with a thickness of 64 mm. Further detail regarding the insulation selection can be found in Appendix A. Since the insulation was attached to the face with the stiffeners, an overlap piece was attached to cover the flange (stiffener). For the first two calibration tests, the thickness and width were chosen using the Guide [7]. These dimensions were increased for the third and fourth calibration once it was found that the temperatures at the stiffener were higher than the average temperature.

The heat flux transducers were numbered consecutively from top to bottom. The total heat flux transducers (fluxmeters) were labeled Rad #1, 2, and 3, while the radiant heat flux transducers (pyrometers) were labeled Rad #4, 5, and 6. The total and radiative heat flux within the furnace during the first calibration test (CAL1) can be found in Appendix C. The four surface temperatures recorded are shown in Appendix D. The four thermocouples were arbitrarily placed several

millimeters below the top and middle transducer locations. The two thermocouples labeled Ts2 and Ts4 detached from the bulkhead during the test (at approximately 33 and 27 minutes, respectively); they were fastened with the ceramic cement. A slight bow was observed over the surface of the bulkhead at 34 minutes. The bow was centered at mid-height and at center extended approximately 50 mm into the furnace. The deviation of the actual furnace integrated temperature curve compared to the standard can be found in Appendix A. The data recorded can be found in the appendices as well. Observation showed that the only reliable method for attaching the thermocouples was the mechanical attachment, and this technique was used for all subsequent tests.

The intent of the second calibration run, as mentioned before, was to step and hold the furnace at several temperature levels. Again, the heat flux and surface temperatures recorded can be found in Appendices C and D. Ts2 and 4 from CAL1 were not replaced and did not represent surface temperature. The same bulkhead and insulation from CAL1 was used for this test. Table 3.1 below summarizes the data averaged over the indicated time intervals.

Table 3.1 Averaged Heat Fluxes and Temperatures from Second Calibration Test (CAL2)

HFT No.		Heat Flux (kW/m^2) at Stated Time Interval (minutes)					
		9-17	**21-27**	**30-35**	**40-45**	**49-56**	**62-70**
Total HF	1	38.3	59.6	85.7	128.3	179.6	61.3
	2	38.3	57.0	82.2	117.0	169.8	61.0
	3	40.7	59.1	86.4	124.0	175.6	62.4
	avg	**38.3**	**57.0**	**82.2**	**117.0**	**169.8**	**61.0**
	stdev	1.4	1.3	2.3	5.7	4.9	0.7
Radiant HF	4	19.0	33.1	53.9	83.1	123.5	33.8
	5	18.8	33.1	53.9	83.4	126.6	34.4
	6	18.0	31.9	52.4	81.8	122.7	33.8
	avg	**18.8**	**33.1**	**53.9**	**83.4**	**126.6**	**34.4**
	stdev	0.5	0.7	0.9	0.8	2.1	0.4
Radiant/total (%)		49	58	66	71	75	56
Furnace Temp. (°C)		618	719	817	915	1015	713

Several items are apparent in the data. The first is the remarkable uniformity within the furnace. The standard deviation of the total heat flux from the average was a maximum of 5.7 kW/m^2, while the maximum standard deviation for the radiative flux was 2.1 kW/m^2. Both these values occurred at the higher temperatures in the furnace, an expected result. As shown in the table, the radiative heat fluxes within the furnace varied from 50 to 75% of the total "cold wall" heat flux. This difference will be further discussed in the next section. Again the higher percentage occurred at the higher furnace temperature. Consequently, the convective heat fluxes in the furnace were approximately 50 to 25% of the total "cold wall" heat flux, depending on the furnace temperature. The well-behaved control of the furnace was further demonstrated by comparing the results between the 21-27 and the 62-70 minute intervals where the temperature level was approximately the same. As shown in Table 3.1, the averaged heat fluxes were slightly higher for the latter time period (62-70 minutes) compared to the earlier time (21-27 minutes) although the furnace temperature was approximately the same. This is likely due to the recent adjustment in temperature just before 60 minutes, thus the furnace walls could have been higher in temperature than the furnace gases. The above table is represented graphically in Figure 3.1. Again, it is apparent that the radiative heat fluxes were significantly lower than the black body and total furnace heat fluxes.

For the next two calibration tests, the full instrumentation set was placed, including the furnace heat flux transducers and furnace temperatures, as well as the unexposed surface temperatures. The heat flux transducers viewing the unexposed face were not set up due to the visual interference from the furnace heat flux transducer wiring. The results are found in Appendices C and D. The data between these tests were very similar. This is further illustrated in Table 3.2 where the heat flux data were averaged over a one minute period (30-31 and 60-61 minutes) and compared for tests CAL1, CAL3, and CAL4. As seen, the total and radiative heat flux between tests were very repeatable. An interesting observation is that the middle fluxmeter (Rad #2) was consistently slightly lower than the other two, while the corresponding pyrometer (Rad #5) was consistently slightly higher than the other two pyrometers.

Figure 3.2 shows the average heat fluxes (average of Rad #1, #2, and #3, and the average of #4, #5, and #6) for each of the calibration tests. Figure 3.3 shows the average surface temperatures (average of Ts1-9) for the CAL3 and CAL4 tests. The temperature data for CAL1 and CAL2 are not shown since those tests did not have all nine thermocouples at the proper locations.

Since the furnace temperature curve is a prescribed function of time, it was decided to perform a general curve fit to the data between the first, third and fourth calibration tests. This allows one to characterize the heat fluxes in the furnace as a function of time in equation form, much more useful for numerical modeling. The fit excluded the first three minutes of data and was performed on the averaged indications of the three transducers of the same type. The results and coefficients of the curve fit are shown in Figure 3.4. The only significant deviation in the fit is during the first few minutes, during the start up of the furnace.

Table 3.2 Heat Flux Statistics for Tests CAL1, 3, and 4, Over the Time Periods 30-31 and 60-61 Minutes

HFT No.		Heat Fluxes Averaged from 30-31 Minutes for Test			Heat Fluxes Averaged from 60-61 Minutes for Test		
		CAL1	CAL3	CAL4	CAL1	CAL3	CAL4
Total HF (kW/m^2)	1	92.1	92.4	93.7	134.7	137.8	136.7
	2	91.4	90.7	90.1	129.6	130.5	129.7
	3	94.7	95.6	94.9	139.4	140.1	138.0
	avg	**92.7**	**92.9**	**92.9**	**134.6**	**136.1**	**134.8**
	stdev	1.7	2.5	2.5	4.9	5.0	4.5
Radiant HF (kW/m^2)	4	60.1	59.3	57.1	93.0	93.3	87.3
	5	62.3	64.2	62.6	94.9	99.8	95.9
	6	60.7	62.4	61.3	92.4	97.3	93.9
	avg	**61.0**	**62.0**	**60.3**	**93.4**	**96.8**	**92.4**
	stdev	1.1	2.5	2.9	1.3	3.2	4.5

	Statistics Averaged Over Tests CAL1, CAL3, and CAL4 at 30-31 Minutes for:		Statistics Averaged Over Tests CAL1, CAL3, and CAL4 at 60-61 Minutes for:	
	Total HF (HFT 1-3)	Radiant HF (HFT 4-6)	Total HF (HFT 1-3)	Radiant HF (HFT 4-6)
avg	92.8	61.1	135.2	94.2
stdev	2.0	2.1	4.2	3.5

3.2 Bulkhead Tests

Each of the bulkhead tests were prepared as discussed in Section 2.3. The following discussion will present the summary information gained from all of the tests performed to date, followed by observations and discussion of the results in the subsequent subsections.

Table 3.3 presents a summary of the information obtained from all tests performed. The test I.D. and date of test are shown. The tests are ordered by configuration and decreasing time rating, even though they were not tested chronologically in that order. The test configuration is also shown, consisting of the density and thickness of insulation, and the stiffener overlap dimensions (width x thickness, refer to Figure 2.2). The latter was only applicable for those tests which had the insulation on the exposed face. The initial ambient temperature is shown, as measured by the average of the surface thermocouples (Ts1-9). One of the summary results obtained from the test was a time to exceed the thermal criteria of the test method. This was determined in two ways. Either the average of the surface thermocouples (Ts1-9), excluding the two on the stiffeners, exceeded a 139°C rise in temperature, or the maximum of any surface thermocouple (Ts1-11) exceeded a 180°C rise in temperature from ambient. Both times are shown, and the highlighted number would represent the time used for classifying the bulkhead as per the Standard Fire Test [2]. For conciseness the calibration test data is included here.

Additional test results related to the radiated heat flux are shown in Table 3.4. This includes the peak radiant heat flux (measured from the average of Rad #1, #2, #3, and #5, excluding #4 at any given point in time) and total radiated energy during the one hour exposure.

Other test information such as the insulation batt weights and layout, relative humidity and the percent deviation of the integrated area under the actual furnace temperature curve from the standard can be found in Appendix A, Tables A.1 and A.2. For all of the tests, the greatest furnace deviation was within 1% of the integrated standard temperature curve.

The following subsections present more detailed observations and discussion of the results obtained.

Table 3.3 Bulkhead Test Results Summary for Times to Exceed the Thermal Criteria

Test	Date	Insulation/ Steel Exposed (I/S)	Density (kg/m^3)	Thickness (mm)	Overlap, Width x Depth (mm x mm)	Initial Temp. (Tsavg, °C)	Time to Exceed Average [139 + To] (min)	Time to Exceed Single [180 + To] (min)
CAL1	6-Feb-92	I	111	64	127x32	-[b]	-	-
CAL2	7-Feb-92	I	-[a]	64	127x32	-[b]	-	-
CAL3	10-Feb-92	I	109	64	191x64	20	**54.50**	57.25
CAL4	11-Feb-92	I	111	64	191x64	23	**54.75**	61.75
A60-1	12-Feb-92	I	129	64	254x64	24	**59.75**	68.00
A60-2	14-Feb-92	I	144	64	254x64	22	**68.00**	-[c]
A60-3	18-Feb-92	I	120	64	254x64	27	**55.75**	-[c]
A60-4	25-Feb-92	S	119	127	-	14	60.25	**58.00**
A60-5	12-Mar-92	S	112	127	-	20	52.75	**49.00**
A60-6	12-Mar-92	S	137	127	-	25	65.25	**62.00**
A30-1	26-Mar-92	S	123	95	-	26	43.00	**41.00**
A30-2	1-Apr-92	S	106	95	-	22	35.50	**30.50**
A30-3	6-Apr-92	S	153	64	-	25	**31.75**	**31.75**
A30-4[d]	9-Jun-92	S	134	32	-	24	47.75	**47.00**
A30-5[d]	11-Jun-92	S	NI	-	-	28	**22.00**	24.25
A30-6[d]	15-Jun-92	S	135	19	-	32	**36.67**	37.83
A15-1	20-Apr-92	S	103	32	-	20	14.00	**13.75**
A15-2	21-Apr-92	S	117	32	-	25	14.75	**14.00**
A15-3	15-May-92	S	155	32	-	27	17.25	**14.75**
A15-4	29-Oct-92	I	101	19	127x19	25	**22.50**	25.00
A15-5	30-Oct-92	I	110	13	127x19	30	15.25	**15.00**
A15-6	3-Nov-92	I	139	19	127x19	28	**24.50**	30.25
A0-1	26-Feb-92	S	NI	-	-	27	**4.50**	4.75
A0-2	27-Feb-92	S	NI	-	-	26	**4.00**	4.50
A0-3	28-Feb-92	S	NI	-	-	29	**3.75**	4.25

[a]Test CAL2 used the same insulation and bulkhead from CAL1; the insulation was not replaced, therefore, insulation density was not known.

[b]Surface temperature measurement incomplete, thus it could not be compared to the other tests.

[c]Not exceeded during fire exposure period.

[d]Tests A30-4, -5, and -6 had a 19 mm Marinite panel in addition to the mineral wool insulation shown in the table.

NOTE: *Highlighted text* indicates the time which would be used to classify a bulkhead according to its thermal failure time.

NI - No insulation

Table 3.4 Radiated Heat Fluxes During Bulkhead Tests

Test	Avg HF @ 60 Min (kW/m^2)	Peak HF < = 60 Min (kW/m^2)	Total Radiated Energy @ 60 Min (MJ/m^2)
A60-1	0.77	0.77	0.88
A60-2	0.77	0.77	0.84
A60-3	0.96	0.96	1.23
A60-4	1.46	1.46	0.68
A60-5	1.81	1.81	1.17
A60-6	0.80	0.80	0.46
A30-1	2.00	**2.03**	2.36
A30-2	1.88	**2.03**	3.08
A30-3	2.00	**2.15**	3.77
A30-4	2.25	**2.25**	2.39
A30-5	3.37	**3.75**	7.97
A30-6	3.21	**3.21**	4.44
A15-1	5.27	5.27	10.08
A15-2	5.02	5.02	9.47
A15-3	3.63	3.63	7.18
A15-4	3.92	3.92	6.33
A15-5	5.85	5.85	10.18
A15-6	4.22	4.22	6.72
A0-1	51.15	51.15	104.38
A0-2	51.83	51.83	107.32
A0-3	51.90	51.90	107.49

NOTE: Both peak and average HF columns were extracted from the spatially averaged heat flux data, e.g., the instantaneous average of Rad #1-#3, #5 (see Figures 3.6, 3.8, 3.10, and 3.12) highlighted values indicate that the peak heat flux occurred before the 60-minute period. Note that 60-2 and 60-6 exceeded the criteria after 60 minutes.

3.2.1 A-60 Bulkheads

As seen in Table 3.3, by varying the density of the insulation, it was possible to bracket the temperature criteria for each class of bulkhead. The first A-60 configuration (tests A60-1, 2, and 3) had a single layer of insulation 64 mm (2.5 in.) thick exposed to the furnace, while the second configuration (tests A60-4, 5, and 6) used two layers outside of the furnace. The joints were staggered between layers, and pins were welded accordingly. Photographs of the setup for test A60-1 are shown in Figure 3.5

The heat flux data for the first A-60 test is shown in Appendix C, while the surface temperature information is shown in Appendix D. The furnace temperatures, heat flux transducer body temperatures, and furnace pressure are found in Appendices E and F, respectively. Likewise, the information for the subsequent tests, A60-2 through A60-6, is presented in Appendices C, D, E, and F. This time-history information has been summarized by averaging the appropriate heat flux curves (Rad #1, #2, #3, #5, excluding #4) during the test period, and by averaging the surface temperatures (Ts1-9) during the test. These two plots are shown in Figure 3.6 and 3.7, respectively.

Next, the specific test observations are discussed. The bumps in the heat flux data for test A60-1 at 37 minutes were due to a momentary upset in the flow of cooling water to the transducers.

For test A60-2, the furnace temperature was held constant after 73 minutes until the end of the data. The cooling water to the heat flux transducers was reduced to observe the effect on the indicated heat flux. As expected, the indicated flux decreases a few percent, because the body of the transducer increases, causing more heat to be reradiated away from the transducer which results in a less amount of energy being absorbed by the transducer.

An observation seen for most of the tests where the insulation was exposed was related to the character of the joints between the batts of insulation. Some of the joints appeared to stick together and stay closed, while in other locations the batts appeared to shrink and thus the joint opened appreciably (12 to 25 mm). In general, the insulation appeared grey/black in color and was brittle on the surface. Underneath, the insulation appeared white and was still relatively pliant compared to the original brown pliant texture. The white color probably suggested that the binder was volatilized out of the batt during the exposure. Depending on the length of exposure, the brittle layer varied in thickness from approximately 1/3 to 1/2 the depth.

For the test configuration with the insulation on the unexposed face (tests A60-4, -5, and -6), more of the original brown color remained at the end of the test on the unexposed face. The two layers tended to separate from each other leaving an air gap between them. The first layer which was next to the exposed steel was completely blackened and brittle, while the second layer had approximately 6 mm of which was brittle, with most of the rest being white in color. The exterior retained its original brown color.

Where insulation was located on the unexposed face, sometimes it was necessary to move the location of some of the thermocouples up to 50 mm so that they were not located directly over a joint or pin. This was the case in test A60-4, -5 and -6 where Ts10 and Ts11 were moved up 50 mm from the planned location to miss a pin. For this configuration, the thermocouples were held in place with a wire mesh which was clamped under the round clips holding the insulation in place.

An important feature of the heat flux data observed was the large difference between the total fluxmeters and the radiation pyrometer (Rad #4). This was due to the fact that the pyrometer had a sapphire window which has a low transmittance at wavelengths much greater than 5 μm. This results in a significant amount of the thermal energy which does not reach the transducer surface, since the portion of thermal energy being radiated at longer wavelengths is being absorbed or reflected by the sapphire window. To illustrate the effect, the average surface temperature cannot exceed 159°C (for an assumed ambient of 20°C) at the endpoint criteria for a class A bulkhead. At this temperature the spectral distribution of thermal radiation (assuming a black body distribution) is such that only 10% of the total energy would be incident on the transducer surface.

The A-60 data suggests that the fraction of radiant energy transmitted through the sapphire window and incident on the transducer surface versus the total radiant energy incident on the sapphire window was on the order of 25 to 30% (for the temperatures observed on the unexposed surface). The transducer was calibrated to correct for the reduced transmission through the window (approximately 85%) at wavelengths less than 5 μm, since the transducer was calibrated to indicate incident energy on the transducer surface. This issue is less problematic at higher temperatures since a much higher percentage of the thermal energy is accounted for by the transducer. The same effect was observed for the pyrometers used in the furnace calibration, although the percentage was much higher. The radiant cold wall heat fluxes in a furnace approximately 90-95% of the blackbody heat flux. However, the fluxes in the furnace were approximately 60 to 85% of the theoretical heat flux. It is likely that this effect was due to the transducer, and not due to the actual furnace conditions.

The times for thermal penetration of the bulkhead when the insulation was to the exposed face or to the unexposed face were significantly different. In general, when the steel was exposed, a longer time was required before a significant surface temperature rise was observed. The test configuration was designed to have either configuration meet the same time end point to thermal failure, for comparison purposes. Although the same end point time was achieved (and bracketed, actually), this was not true for the heat flux levels. This was due to the difference in thermal radiative surface properties of the steel and insulation. The heat fluxes at the end of the tests with the insulation outside the furnace were significantly higher, indicating that the remainder of the tests should be performed with the insulation outside of the furnace. This result was based on the fact that for the same surface temperature, less thermal radiation will be emitted from steel compared to the insulation due to the lower surface emissivity of the steel.

Average heat fluxes at the 60-minute mark varied between 0.8 to 1.0 kW/m^2 with the insulation exposed, and were between 0.80 and 1.81 kW/m^2 with the insulation on the unexposed face. Since the heat fluxes were higher when the insulation was on the unexposed face, the subsequent tests were conducted with the insulation on the unexposed face. The heat flux data are shown in Table 3.4 and will be discussed more in a subsequent section.

3.2.2 A-30 Bulkheads

The first two of the A-30 tests (A30-1 and 2) had 1-1/2 layers of insulation (the half layer was placed next to the steel) on the unexposed face, for a total thickness of 96 mm. Both of those tests overshot the desired 30-minute criteria (A30-1 exceeded the criteria at 43 minutes, while A30-2 exceeded the criteria at 35.5 minutes). For this reason, it was decided to use a single layer for the third test. The third A-30 test (A30-3) had a single layer of insulation to try to bracket the 30-minute criteria, but with the higher density material chosen, this test also overshot the desired criteria slightly. Data interpolation/extrapolation issues are further discussed in the data comparison and scaling section. Average heat fluxes at 60 minutes approached 2.0 kW/m^2, while average surface temperatures approached 230°C. Heat flux and surface temperature plots for all six A-30 tests are shown in Figures 3.8 and 3.9, respectively.

The second configuration tested to the A-30 criteria (Tests A30-4, -5, and -6) consisted of a combination of steel, mineral wool insulation, and calcium silicate marine joiner panels. A layer of mineral wool was placed between the steel and the panels; the panels were on the unexposed face of

the assembly. The joiner panels, manufactured by BNZ, were designated as Marinite ML (USCG Approval 164.008/103/0), with dimensions of 1219 by 2438 by 19 mm. The panel had a density of approximately 580 kg/m^3. The panels were assembled with a joint 610 mm from the right edge of the unexposed face of the bulkhead (one full panel and one half- width panel). A metal trim was used at the perimeter of the panels, and along the joint, to simulate conditions similar to that which might be found on a marine vessel. The panel was fastened at the perimeter only to the steel bulkhead, with as small an air gap as possible (the pins prevented a tight contact between the mineral wool and Marinite panel).

For each of the three tests performed, new joiner panels, insulation and steel were used. For A30-4, a thickness of 32 mm of mineral wool was used. During test A30-4, light smoke was observed at 13 minutes emanating from the left and center seam. This had decreased by 26 minutes. The calcium silicate panel began to bow outward, away from the furnace at 54 minutes, while the steel had bowed toward the furnace. At 60 minutes the panel bow was approximately 25 mm outward.

For test A30-5, no mineral wool was used. The joiner panel was placed directly next to the steel bulkhead with an approximate 9-mm air gap. At approximately 20 minutes, light smoke was observed coming from joints in the panel on the unexposed face. At 40 minutes, the joiner panel had discolored slightly, and the vertical joint had warped and opened slightly. The joiner panel had bowed outward approximately 50 mm at the center.

The mineral wool insulation was again used for test A30-6 with the joiner panels, similar to A30-4. However, the insulation thickness was reduced to 19 mm. During test A30-4 one of the furnace thermocouples, Tf5, fell approximately 100 degrees below the rest of the furnace probes over the last 15 minutes of the test. Data for all of the tests was stored every 15 seconds, except for test A30-6, in which data was scanned every 5 seconds.

Heat fluxes at 60 minutes for tests A30-4, -5 and -6 varied from 2.3 to 3.4 kW/m^2, while the surface temperatures were from 220 to 290°C. The surface temperatures during tests A30-4, -5, and -6 all had two places at which the rise in temperature reached a plateau before climbing again. This was indicative of the heat penetration through the two different types of insulation, and subsequent material changes because of decomposition.

One of the heat flux transducers (Rad #5) during tests A30-1, -2, -6, and A60-4 showed a decrease in output slightly before the end of the test. The average heat flux still used these values in the calculation of the average heat flux. This effect could possibly be due to the development of a thermal convective boundary layer on the unexposed face of the assembly or movement of the transducer. The heat flux, surface temperature, and other data for the A-30 tests are shown in the Appendices (C, D, E, and F).

3.2.3 A-15 Bulkheads

The two configurations for the A-15 bulkheads consisted of mineral wool either exposed to the furnace, or unexposed. The first configuration (tests A15-1, -2, and -3) had one layer of 32 mm thick mineral wool on the unexposed face. The density was varied between tests to observe the change in time to thermal failure.

The second configuration (tests A15-4, -5, -6) placed the mineral wool insulation on the exposed face. For tests A15-4 and A15-6 the insulation was 19 mm thick, while test A15-5 used a thickness of 13 mm. The flange overlap was 127 mm wide by 19 mm thick for each of the three tests. Near the end of test A15-4, the bulkhead had bowed approximately 75 mm into the furnace at the center. A similar result was observed in test A15-5, while A15-6 had approximately 50 mm bow at the end of the 60-minute period. These were the last tests to be conducted chronologically. Heat flux and surface temperature plots for all six A-15 tests are shown in Figure 3.10 and 3.11, respectively.

The transient test data can be found in Appendices C, D, E, and F. Average surface temperatures at the end of the tests varied from 290 to 430°C with a corresponding heat flux range of 3.6 to 5.9 kW/m^2 at 60 minutes.

3.2.4 A-0 Bulkheads

The A-0 tests consisted of exposing a bare steel bulkhead to the furnace conditions. The stiffeners faced into the furnace. New bulkheads were constructed for each test. Heat flux and surface temperature plots for all three A-0 tests are shown in Figure 3.12 and 3.13, respectively. Higher surface temperatures were noted, as well as a corresponding increase in heat flux. Average heat fluxes at 60 minutes were 52 kW/m^2, with surface temperatures near 800°C. The data for the A-0 tests are shown in Appendices C, D, E, and F.

During test A0-1, two of the surface thermocouples failed to indicate surface temperature during the test (Ts3 and 10). This was due to shorting and opening of the lead at the plastic connector, which had melted due to the excessive heating.

3.2.5 General Test Comments and Observations

Incident flux received and indicated for bulkhead tests should have been the same as the flux emitted from bulkhead because the gages were calibrated in terms of incident flux. The actual interchange between a bulkhead and an object would be dependent on the radiative properties of both surfaces and the temperature of each. The exception, of course, was Rad #4 which had the sapphire window.

Radiated heat fluxes recorded varied between 40 and 80% of the black body flux that could exist for the surface temperatures recorded. This roughly corresponded to the earlier comment on the difference in radiative properties of the steel and the insulation. The heat flux percentage of black body was lower with the steel on the unexposed face than for the mineral wool. This would be expected to occur, since the mineral wool should have an emissivity around 0.9 to 0.95, while brushed plain carbon steel would be around 0.4. This was not the case for the A-0 tests, where the steel was hot enough to oxidize, thereby increasing the surface emissivity to approximately 0.7. The radiated flux would appear somewhat low for the tests with the insulation on the unexposed face, but it must be realized that the surface temperature measurement in this case probably was slightly high due to the effect of the insulating pad on the temperature reading.

Generally, Rad #1 was the highest of the heat flux transducers viewing the unexposed surface, except for 60-4 and 60-6 near the end of the test. This was probably due to the convective thermal boundary layer developing on the unexposed surface, which was on the order of 0.5 m thick at the top of the bulkhead.

The wide angle Rad #3 was generally lower than that of Rad #2, which had a narrower view. This would be due to the fact that the wider view had a higher percentage of surface area which was over the angle stiffeners, which had additional insulation to compensate for the additional heated surface (for the tests with the insulation to the exposed face). This was especially true where the temperatures recorded at the stiffeners (Ts10 and 11) were lower than the average surface temperature.

Rad #5 was usually, but not consistently, the lower of the heat fluxes recorded. The lower indicating heat fluxes were usually either Rad #3 or #5, not excluding Rad #4 which had the sapphire window.

The heat flux transducers were recalibrated at the completion of testing. They were calibrated as received, without cleaning and refacing with the absorptive coating, so that the change in calibration since manufacture could be determined. The percent change in calibration is shown in Table B.1. All of the re-calibrations were within 3% of the original sensitivities.

For those tests which had steel directly exposed to the furnace, significant oxidation was observed after the test assembly had cooled. Large flakes of oxidized material, varying in thickness up to 0.5 mm, could be removed by brushing the surface. For the most part, the steel retained the majority of its mass, but no determination of load capacity or mass loss was determined.

Fluctuations in the surface temperatures were noted for many of the tests. Even though the furnace temperatures were continually rising with time, the unexposed surface temperature sometimes flattened, or even slightly decreased during several of the tests. There are two factors which could explain this effect. It is possible that convective boundary layer currents were forming, carrying more heat away from the unexposed surface resulting in the same or lower surface temperatures, even though the heat input from the furnace was continually increasing. This effect was noted especially for the mineral wool tests with the insulation on the unexposed surface. It is also true that the thermal characteristics of the mineral wool were changing during the test, probably a greater contributor to the observed phenomena.

3.3 Thermal Modeling

The modeling performed was integrated with the bulkhead tests and used to aid in the prediction of the insulation density and thickness chosen for the next test. The results presented here are intended to be used as a comparison to the actual results obtained. The overall approach to the analysis was to obtain the thermal properties of the insulation and the steel. The properties of steel (density, thermal conductivity and specific heat) were obtained from Reference [10]. The thermal conductivity and specific heat were input as a function of temperature. The insulation properties were provided in the product literature. Since the thermal conductivity as a function of temperature was

non-linear and did not extend to the higher temperatures seen in the furnace, a curve fit/extrapolation was necessary. The equation which best described the temperature dependence was a second degree polynomial fit, where the thermal conductivity increased with temperature. This trend was consistent with data seen for similar types of insulation, such as ceramic fiber blanket.

The next step was to set up the geometry and boundary conditions. The geometry was setup up parametrically to easily vary the thickness and density of insulation. The problem was defined as a one-dimensional model, with the proper thickness of steel and insulation, comprised of 100 nodes to assure convergence. The finite-element heat transfer code allowed for a convective combined with a radiative heat flux boundary conditions. The boundary not exposed to the fire was modeled as an adiabatic surface. Although slightly unrealistic, the results compared very favorably to the test data since the primary mechanism for temperature rise was the transient movement of heat being conducted through the material.

The code used for the modeling effort was FIRES-T3, for Fire Response of Structures-Thermal, Three-dimensional version. This code can evaluate the temperature distribution history of general three-dimensional solids or composite assemblies subjected to fire environments. FIRES-T3 is based on a finite element formulation which considers the temperature dependence of thermal properties and the nonlinearities inherent in modeling fire boundary conditions. The governing equation is a nonlinear, second-order parabolic differential equation referred to as the heat diffusion equation [11]. The data input to the code for each case simulated can be found in Appendix G.

Table 3.5 presents the results of the thermal modeling, including a comparison to the test data where appropriate. Identified are the case number, thermal radiative properties of the exposed surface, which face was exposed, density, thickness, and simulated time to exceed the temperature criteria. The thermal radiative properties (α - absorptivity, ε_f - flame emissivity, ε_s - surface emissivity) were estimated and no attempt was made at performing a rigorous analysis. The objective of the analysis was to judge the density and thickness of material to choose for the subsequent test. The batch of mineral wool insulation obtained had a broad range of densities, though the distribution was weighted toward the density tolerance stated in the literature. The analysis compares well with the actual test results. All other properties remained the same for all runs (i.e., steel plate thickness 4.8 mm, thermal conductivity, specific heat for the steel and insulation and density of the steel). Other radiative and convective properties also remained constant and are shown in Appendix G.

Table 3.5 Thermal Analysis Summary and Comparison to Test Data

Case	α, ε_r, ε_s	Steel/ Ins. exposed	Density (kg/m^3)	Thickness (mm)	Time to exceed 159°C (min)	Test Comparison	
						Time to exceed (avg Ts1-9)	Test ID
1	.6,1.,.88	I	112	64	52.3	53.25 53.25 55.75	CAL3 CAL4 60-3
2	.6,1.,.88	I	144	64	57.2	67.5	60-2
3	.6,1.,.88	S	112	127	64.5	-	-
3a	.9,.7,.7	S	112	127	60.3	-	-
3b	.9,.7,.7	S	120	127	63.5	-	-
3c	.9,.8,.7	S	112	127	58.0	54.00	60-5
4	"	S	120	127	61.2	60.25	60-4
5	"	S	128	127	64.2	-	-
6	"	S	136	127	67.3	65.50	60-6
7	"	S	128	95	42.3	43.00	30-1
7a	"	S	112	95	38.5	35.50	30-2
8	"	S	144	64	26.7	31.75	30-3 (153 kg/m^3)
8a	"	S	112	64	22.7	-	-
8b	"	S	80	64	18.5	-	-
9	"	S	135	51	19.5	-	-
9a	"	S	135	38	14.2	-	-
9b	"	S	135	25	9.5	-	-
10	"	S	136	32	11.8	-	-
10a	"	S	104	32	10.3	14.00	15-1
10b	"	S	144	32	12.2	-	-
10c	"	S	117	32	11.0	14.75	15-2

3.4 Test Data Comparison and Scaling

The main emphasis of this project was to evaluate several classes of bulkheads and determine the levels of radiated heat flux from those boundaries, and the consequences of such temperature-based classifications. Since the method for performing the tests was to bracket the failure time of a particular classification, the data comparison should correlate each configuration to an "ideal" bulkhead which barely met the temperature criteria for that classification. Since all of the tests performed were for class A systems, the comparisons were performed at the 60-minute period, even though the temperature criteria may have been exceeded earlier. The following compares the heat flux and temperature data obtained during this program.

3.4.1 Cumulative and Instantaneous Heat Flux Comparison

The radiated heat flux from the bulkhead during a test can be integrated to obtain a cumulative radiated energy flux curve as a function of time. This is presented in Figures 3.14 to 3.17 for each of the tests performed. For the A-60 tests, the total energy radiated over a 60-minute period varied from 0.5 to 1.2 MJ/m^2 (see Table 3.4). For the A-30 tests, the cumulative radiated energy was less than 5 MJ/m^2, except for A30-5 which rose to about 8 MJ/m^2 at 60 minutes. The A-15 tests had cumulative values of up to 10 MJ/m^2 at 60 minutes, while the A-0 tests had values around 104 to 107 MJ/m^2.

In comparing the heat flux levels observed during the tests, a few points of reference are helpful. The average solar constant has been measured at 1.4 kW/m^2. From published data [12], an irradiance level of 2.75 kW/m^2 would have a tolerable exposure time (time until severe pain occurs) of several hundred seconds. A 7-second exposure would correspond to a tolerable irradiance level of 6.5 kW/m^2, while a 3-second exposure would represent a level of 10 kW/m^2. The auto ignition of wood and paper products generally will occur for incident heat flux levels equal to or greater than 25 kW/m^2.

The thermal radiation recorded from the A-60 tests showed fluxes at approximately 1.5 kW/m^2 at the end of the 60-minute exposure. Although the surface temperatures would cause pain to the touch, the heat flux levels should not present a difficulty for egress or other emergency procedures. However, for materials that are in direct contact with the surface could reach temperatures at which decomposition could occur. This is contrasted with the levels of the A-0 test which approached 52

kW/m^2 at the end of the 60-minute exposure. Peak unexposed surface temperatures were on the order of 800°C.

For the A-30 and A-15 tests the heat fluxes varied between 2 and 5 kW/m^2. This would correspond to a tolerable short duration exposure. The actual tolerance time would depend on the size of the bulkhead being exposed, the view factor to the person or object being exposed, etc.

Figure 3.18 presents the average heat flux at 60 minutes as a function of time to thermal failure for all of the tests performed. The time to thermal failure was based on the average surface temperature (next to last column in Table 3.3), not the single point criteria. This was generated from the data presented in Table 3.3. As expected, the trend is that the heat flux increases with a decrease in the time rating of the bulkhead system. The A-0 data was left off of the plot, since the flux levels were much higher (approximately 52 kW/m^2) and would have reduced the visibility of the data for the insulated tests. This figure would allow one to interpolate between tests to obtain a heat flux for a given class of bulkhead, e.g., the peak HF in a 60 minute period for a typical bulkhead of a given class from A-0 to A60. The curve fit shown includes the A-0 results. One difficulty with this is the obvious difference in heat fluxes of those tests with the insulation to the furnace face as compared to insulation on the unexposed face.

Figure 3.19 shows the total cumulative radiated flux at 60 minutes for each test as a function of time to thermal failure. A similar trend can be observed, where the total radiated energy at 60 minutes increases with a decreasing time to exceed the thermal failure criteria. The A-0 data was left off the plot, since the total radiated energy was significantly higher than for the insulated bulkhead tests (approximately 107 MJ/m^2). Simple interpolation could be performed to obtain the cumulative radiated energy at the 60-minute period for a typical bulkhead of a given class from A-0 to A-60. The next section will discuss a different manner for interpreting this information.

3.4.2 Dimensional Scaling of Temperature and Heat Flux Curves

An alternative approach for evaluating and comparing the test data involved the use of dimensional scaling. The first step in this process was to normalize and use the averaged data to compare the similar tests graphically. The average of Rad #1, 2, 3, and 5 (the total heat flux transducers) was used to produce the heat flux comparison (see, for example, Figure 3.6, for the A-60 tests). The recorded time history temperatures of each bulkhead test were averaged, as measured by

Ts1 through Ts9. Then the initial temperature (To) was subtracted, so that each of the test configuration temperature data could be compared. The comparison temperature plot for the A-60 tests was presented in Figure 3.7. The same comparisons for the A-30, A-15, and A-0 tests were presented in Figures 3.8 through 3.13.

Several observations could be drawn from the above comparisons. First, since the A-0 tests were essentially the same test, and no variation in the setup occurred, the raw data for each test could be averaged together to obtain a single temperature and heat flux profile.

Both the temperature and heat flux data appeared to be amenable to time scaling. The data from the three similar tests could be scaled such that all three temperature and heat flux curves collapse into a single curve representing the result of a classified bulkhead barely meeting the standard thermal requirements. Another way to view this concept is that the data is being interpreted to obtain thermal results of a "perfect" bulkhead classification. Before doing so, it would be prudent to put some science behind the technique.

The method was based on dimensional arguments and heat transfer concepts. Two arguments can be used for the scaling chosen. The first considers the dimensional grouping referred to as the Fourier number, $kt/\rho cL^2$. A dimensionless time, the Fourier number is the ratio of the heat conduction rate to the rate of thermal energy storage in a solid. If the primary mechanisms for energy transfer from one face of the bulkhead to the other was by conduction, taking into account the amount of energy stored in the insulation, then the Fourier number would represent the pertinent phenomena. If each set of three tests were similar thermally (only the density was varied), then an increase in density would correspond to an increase in the time required for the unexposed face to reach the same temperature. This relationship would be linear and allows one to "stretch" or "squeeze" the time scale, making the temperature history curves fall on each other.

The other argument was to observe the one-dimensional, transient heat diffusion equation.

$$\frac{\partial^2 T}{\partial x^2} = \frac{\rho c}{k} \frac{\partial T}{\partial t}$$

As seen, the same physical relationship exists in that an increase in density can be offset by an increase in simulated time to keep the numerical solution of the partial differential equation exactly the same. Thus, the rise in surface temperature during a test is primarily a function of the Fourier number. Also,

it is assumed that the steel has such a high thermal conductivity compared to the insulation, that it can be excluded from the scaling.

The test temperature and heat flux curves were a function of time. The method used to plot the scaled curves was to multiply the actual test time by a scaling factor (which was the classification time rating divided by the actual time to exceed the criteria based on the average of Ts 1-9) and plot the actual temperatures versus the scaled time for each test. The reason for basing the factor on the actual failure time and the rating time (60, 30, or 15 minutes) is that they are the endpoint criteria for interpolating the ideal bulkhead. Table 3.6 presents the scaling factors used for each test curve. Since there was no variation in materials for the A-0 tests, they were not time scaled.

Table 3.6 Table of Time Scale Factors for Bulkhead Tests

Test I.D.	Time Scale Factor
A60-1	60/59.75
A60-2	60/68.00
A60-3	60/55.75
A60-4	60/60.25
A60-5	60/52.75
A60-6	60/65.25
A30-1	30/43.00
A30-2	30/35.50
A30-3	30/31.75
A30-4	30/47.75
A30-5	30/22.00
A30-6	30/36.67
A15-1	15/14.00
A15-2	15/14.75
A15-3	15/17.25
A15-4	15/22.50
A15-5	15/15.25
A15-6	15/24.50

Figure 3.20 shows the collapsed heat flux data for the A-60 tests. The corresponding temperature data is shown in Figure 3.21. Likewise, the scaled data for the A-30 and A-15 tests are shown in Figures 3.22 through 3.25. As observed, the three scaled tests collapse very well into one curve. These collapsed curves can now be averaged and a single equation could be generated to describe the surface temperature or heat flux as a function of time for each classification rating. The curves of the cumulative heat flux were not scaled, but could also be scaled with similar comparative results expected.

With the heat flux curves now scaled, it is possible to identify the heat flux and cumulative heat flux at the 60 minute scaled time. This is shown in Table 3.7 for the A-60 tests. The heat flux can be seen by following the vertical line at 60 minutes in Figure 3.20 up to the heat flux curves for each test and reading the indicated flux, which is shown in Table 3.7. As discussed previously, the heat flux is greater when the insulation was on the unexposed face, however, the cumulative heat flux was lower for the A-60 tests. This relationship is the same for the A-15 tests at 15 minute scaled time. It may not be the same for the A-30 and A-15 tests at 60 minutes.

Table 3.7 Heat Flux and Cumulative Heat Flux at 60 Minutes (Scaled Time) for the A-60 and A-0 Tests

Test	Actual test time	Heat Flux(kW/m^2)	Cumulative Heat Flux (MJ/m^2)
A60-1	59.75	0.77	0.87
A60-2	68.00	0.92	1.25
A60-3	55.75	0.86	1.00
Average		**0.85**	**1.04**
A60-4	60.25	1.48	0.70
A60-5	52.75	1.13	0.49
A60-6	65.25	1.51	0.82
Average		**1.37**	**0.67**
A0-1	60.00	51.15	104.38
A0-2	60.00	51.83	107.32
A0-3	60.00	51.90	107.49
Average		**51.6**	**106.40**

Thus, the averaged heat flux and cumulative data shown in Table 3.7 represents the results which would be obtained from a Class A-60 and A-0 bulkhead barely meeting the requirements of the classification. The summary average from the scaled data for the A-30 and A-15 tests could not be included in Table 3.7, since in scaled time most of the tests did not reach 60 minutes (see Figures 3.22 and 3.24).

Another way to view the comparative results from the tests is to compare the Fourier number for each test as a function of the time to thermal failure. Since the previous discussion showed that for a given temperature rise (in this case the temperature rise to thermal failure), a linear relationship should exist between the time for that to occur and the density times the thickness squared (ρL^2). This assumes that the specific heat and thermal conductivity are the same in the comparison. Thus, for those tests which utilized mineral wool insulation only, the comparison can be shown. Table 3.8 presents this information, which is shown graphically in Figure 3.26. As seen in the figure, indeed a linear relationship is shown for those tests with the mineral wool exposed to the furnace. A separate linear relationship is also observed for those tests which exposed the steel (insulation on the cold face). This result highlights the fact that in spite a number of possible nonlinearities in material behavior, heat transfer, and geometry, that the fundamental principles of heat transfer dominate the process.

An additional point which can be drawn from Figure 3.26 is related to the ratio of the slopes between the two curve fits. Previously, it was mentioned that approximately twice the thickness of insulation was required to meet the same temperature requirements when the insulation was placed on the unexposed face. Assuming the density is approximately the same, the ratio of the two slopes (83.12/23.579) should correspond to the ratio of the square of the thicknesses required for insulation on the cold face compared to the hot face. The square root of this ratio is 1.9, a number very close to 2, thereby confirming the previous statement.

It should be noted that a rigorous dimensional analysis has not been performed. Additional non-dimensional parameters (or pi terms) can be identified which would increase the success of the characterization of the thermal system. Parameters involving thermal radiation and convection would be required, as well as separate terms to describe the thermal properties of each material present. A simplified scaling approach has been presented, which helps to substantiate the physical relationships which exist in this thermal system. It would be ill-advised to extrapolate this information to thermal protection systems composed of different materials or of combinations which would attempt to extrapolate this relationship beyond the scope of the present data. Notwithstanding the inherent

cautions, this information can be of great use to the modeling community for the prediction and enhancement of fire safety systems aboard ships and other structures. One issue not addressed with this type of fundamental analysis is the possible problems associated with the durability of the material, or its unusual behavior during a fire exposure, such as cracks, spalling etc.

Table 3.8 Density Times Thickness Squared for Bulkhead Tests

Test ID	Density (kg/m^3)	Mineral Wool Thickness (mm)	ρL^2	Time to Exceed Average (min)
CAL3	109.50	63.50	0.442	54.50
CAL4	110.78	63.50	0.447	54.75
A60-1	128.55	63.50	0.518	59.75
A60-2	143.91	63.50	0.580	68.00
A60-3	119.90	63.50	0.483	55.75
A60-4	119.44	127.00	1.927	60.25
A60-5	111.97	127.00	1.806	52.75
A60-6	136.80	127.00	2.206	65.25
A30-1	122.94	95.25	1.115	43.00
A30-2	106.13	95.25	0.963	35.50
A30-3	153.36	63.50	0.618	31.75
A15-1	102.93	31.75	0.104	14.00
A15-2	117.18	31.75	0.118	14.75
A15-3	154.96	31.75	0.156	17.25
A15-4	101.17	19.05	0.037	22.50
A15-5	110.46	12.70	0.018	15.25
A15-6	139.27	19.05	0.051	24.50

4. Conclusions

The baseline data obtained from this research program has reached several objectives. The data presented included unexposed surface temperatures and heat fluxes from a variety of Class A bulkheads. This is summarized below.

The furnace calibration work performed has shown that the furnace heat fluxes were reasonably uniform over the surface where the bulkheads were located. The portion of "cold wall" convective heat flux measured showed that radiative heat transfer accounts for 50 to 75% of the total heat transfer within the furnace. It is likely that this percentage is higher due to the nature of the sapphire window as discussed previously.

The most significant results obtained from this test series has been in the development of a database of unexposed surface temperatures and heat fluxes for Class A-60, A-30, A-15, and A-0 bulkheads. The data, presented in the results, contains information very useful for fully characterizing the behavior of insulated and uninsulated bulkhead systems. This information can be used to predict the actual expected levels of radiation in the event of fire, and also to determine regulatory guidelines for the use of these materials and alternative materials, such as glass. As seen in the literature, the thermal radiation measured brackets the range of acceptable exposure levels, depending on the class and configuration of bulkhead tested.

For the class A-60 tests, heat fluxes at the end of the 60 minute exposure ranged from 0.8 to 1.8 kW/m^2, with cumulative radiated energy between 0.5 to 1.2 MJ/m^2. For the A-30 tests, heat fluxes at the end of the 60 minute exposure ranged from 1.9 to 3.8 kW/m^2, with cumulative radiated energy between 2.4 to 9 MJ/m^2. For the A-15 tests, heat fluxes at the end of the 60 minute exposure ranged from 3.6 to 5.9 kW/m^2, with cumulative radiated energy between 6.3 to 10.2 MJ/m^2. For the A-0 tests, heat fluxes at the end of the 60 minute exposure were approximately 52 kW/m^2, with cumulative radiated energy near 106 MJ/m^2.

The data obtained has been subjected to dimensional analysis, with a high degree of correlation. This will be very useful for the prediction and modeling of fires in marine vessel construction. The analysis has shown that the primary factors affecting the thermal protection offered by mineral wool are the density and thickness of material used. This excludes any effects of material degradation due to method of attachment, bulkhead movement during an actual fire, etc. In no case should the analysis be extrapolated to other materials or different configurations without validation, since the behavior and thermal properties may be different than those analyzed here.

The thermal modeling performed has been very useful in selecting the density and thickness of insulation to meet the requirements of the project to bracket the thermal failure of each bulkhead for each classification. In addition, the comparison to the test data has shown that the analysis in

general were within 15% of the test results. This provides a basis for validation of the finite element method, as applied to the thermal analysis of an insulated marine boundary subjected to fire conditions. Also, the capability of the finite-element method would allow for the modeling of more complex configurations, i.e. to include the 2-dimensional effects of the stiffeners, 3-dimensional effects of the pins, and to broaden the scope to other materials and geometries, for which sufficient input data is available.

Based on experimental results, it has been shown that approximately twice the thickness of insulation was required to meet the same thermal criteria when the insulation was placed on the unexposed face as compared to placing it on the exposed face of the steel bulkhead. Although both configurations were investigated during this program, it should be remembered that the Standard Test Method only requires the insulation to be tested on the exposed face. Thus several of the tests conducted were not necessarily representative of what may occur in a qualification test for an insulation product. It was the purpose of conducting those tests to achieve a worst case where the heat fluxes would be higher.

5. References

1. Regulation II/2-3 of the International Convention for the Safety of Life at Sea (SOLAS), International Maritime Organization, London 1986.
2. Recommendation on Fire Test Procedures for "A," "B," and "F" Class Divisions, IMO Res. A.517(13), in Fire Test Procedures, International Maritime Organization, London 1984.
3. 46 CFR 164.007, Structural Insulation, United States Coast Guard, Department of Transportation, 1989.
4. 46 CFR 164.008, Bulkhead Panels, United States Coast Guard, Department of Transportation, 1989.
5. Standard Specification for Structural Steel For Ships, ASTM A 131, American Society of Testing and Materials, Philadelphia, PA.
6. Equipment Lists; Items Approved, Certified or Accepted Under Marine Inspection and Navigation Laws, U.S. Coast Guard, COMDTINST M16714.3C.
7. Guide to Structural Fire Protection Aboard Merchant Vessels, U.S. Coast Guard, Navigation and Vessel Inspection Circular No. 6-80, 2 April 1980.
8. Nuclear Projects Operating Procedure, "Instrumentation Calibration and Repair System," XII-FT-101-2, Southwest Research Institute, 1987.
9. American National Standards Institute, MC96.1.
10. The SFPE Handbook of Fire Protection Engineering, NFPA and SFPE, Mass, 1990.
11. R.H. Iding, Z. Nizamuddin, and B. Bresler. FIRES-T3 A Computer Program for the Fire Response of Structures - Thermal Three-Dimensional Version. UCB FRB 77-15, University of California, Berkeley, 1977.
12. Bioastronautics Databook, NASA-SP-3006.

6. Figures

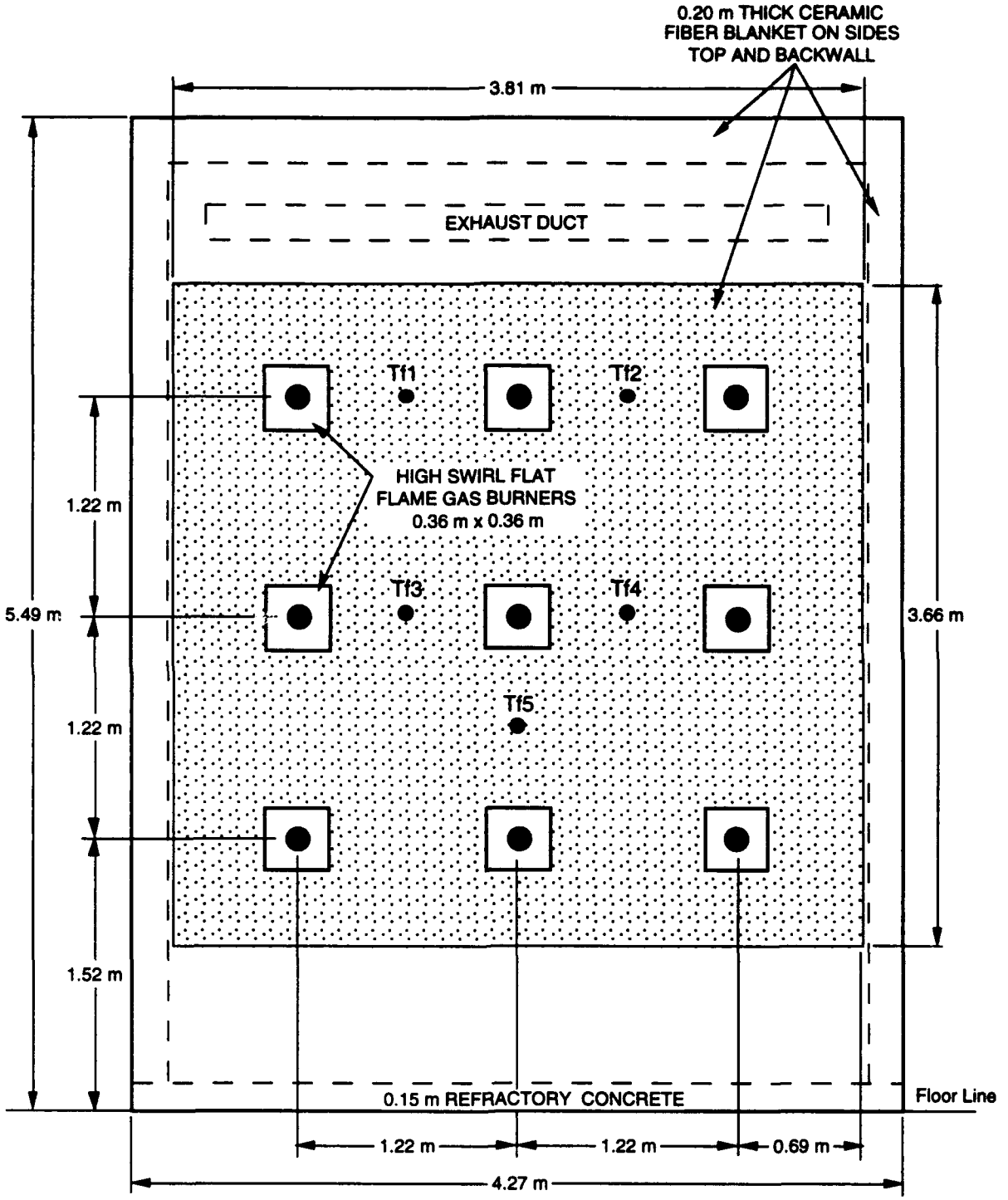

Figure 2.1 Furnace description, showing furnace probe locations (Tf1-5)

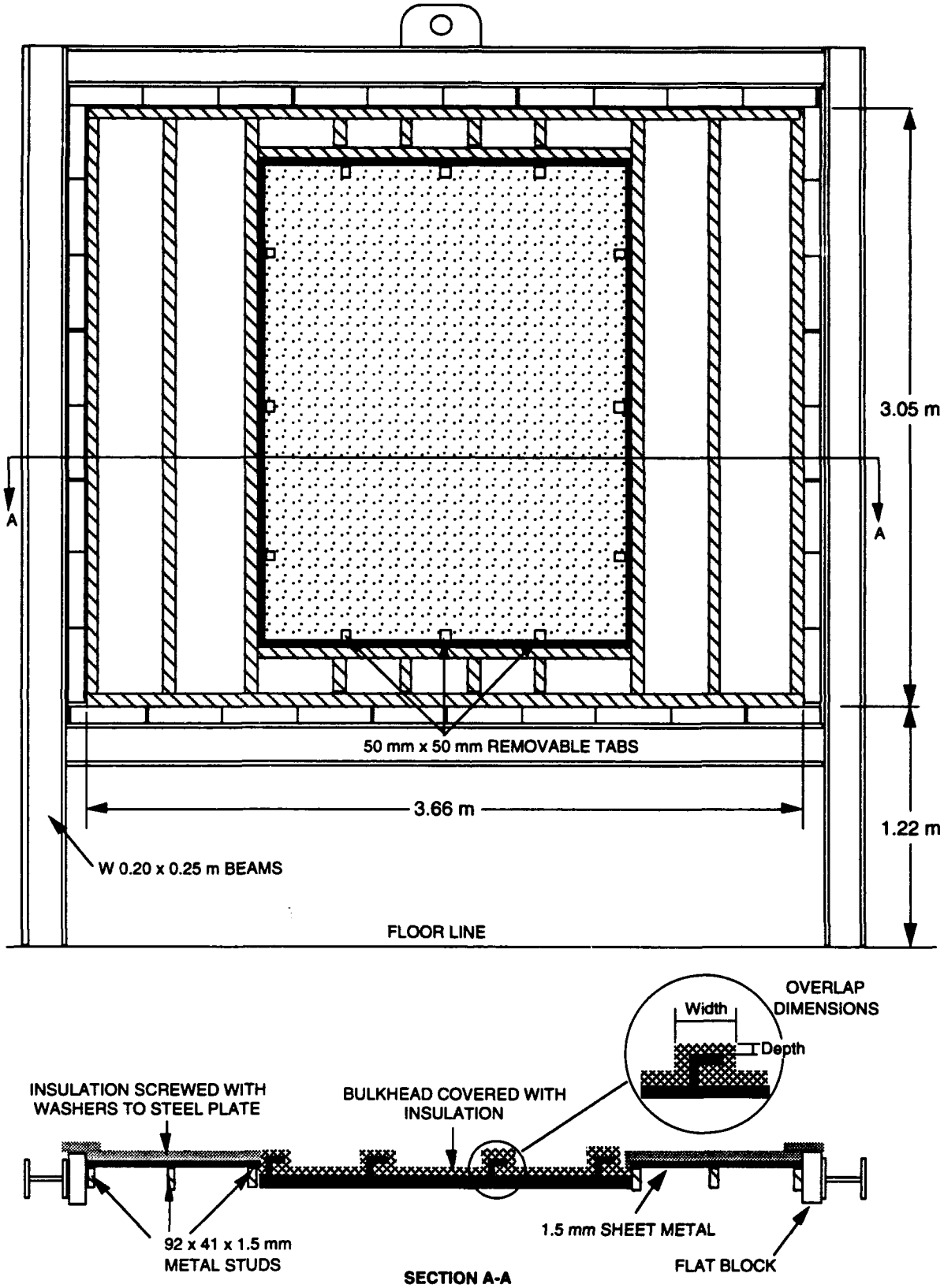

Figure 2.2 Test frame design showing bulkhead location

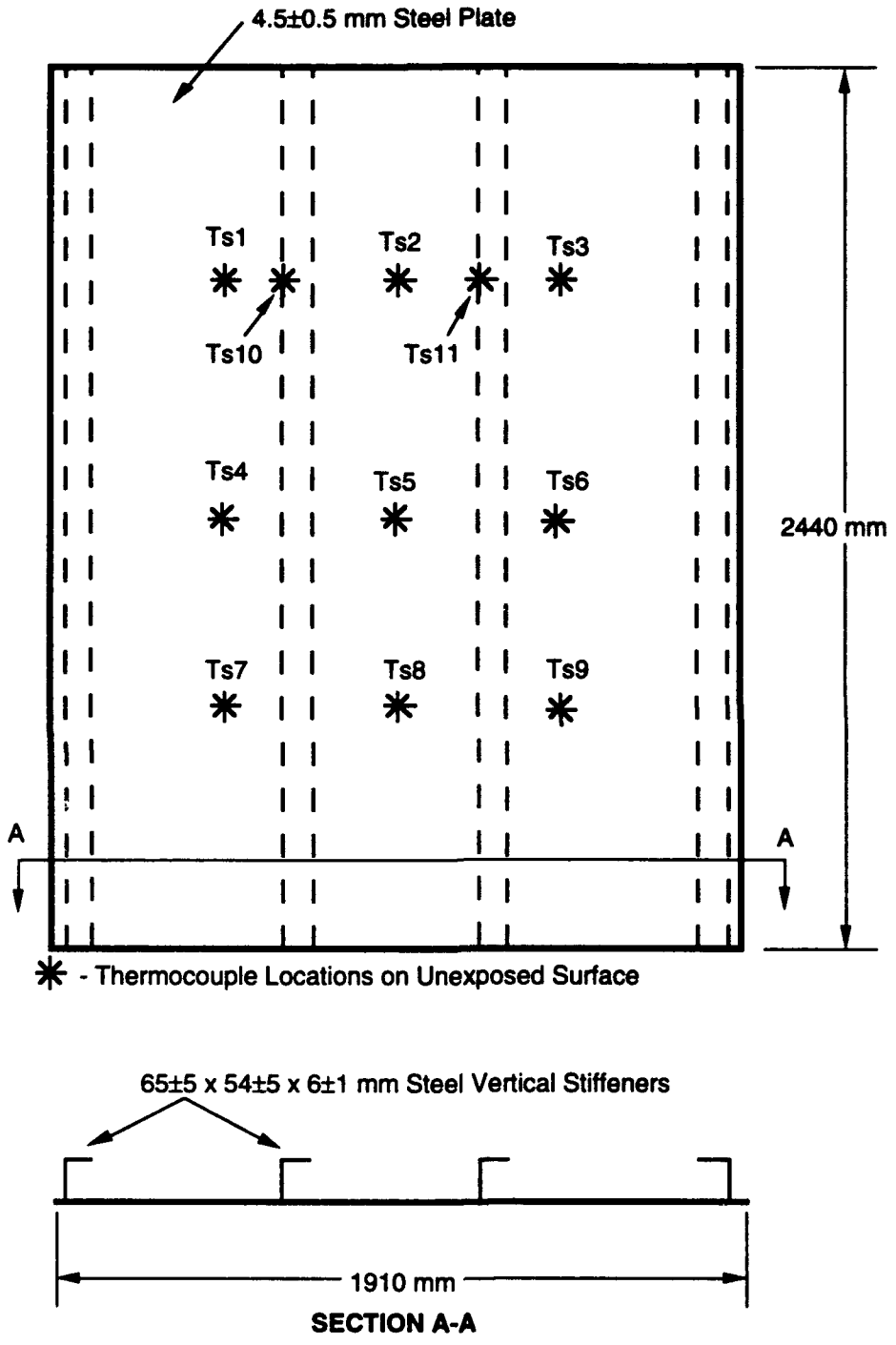

Figure 2.3 Construction of bulkhead, showing thermocouple locations (Ts1 - 11)

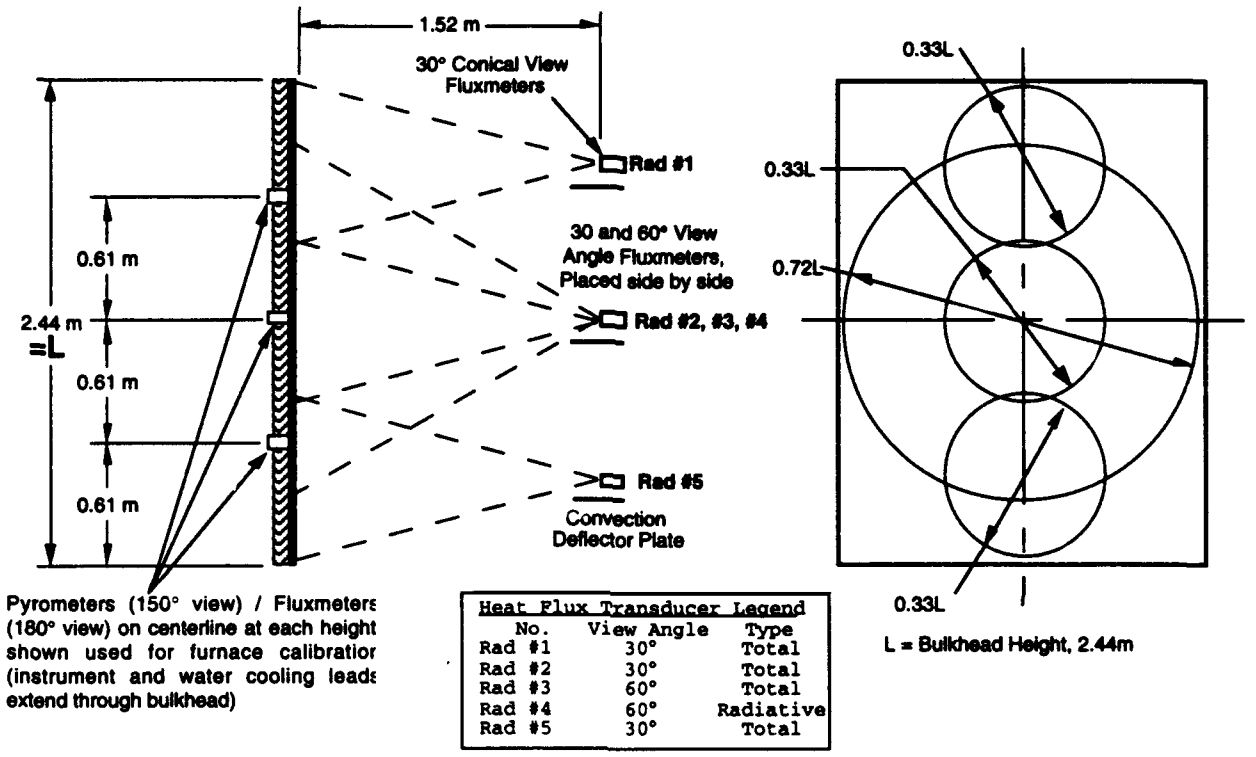

Figure 2.4 Heat flux transducer locations with respect to bulkhead

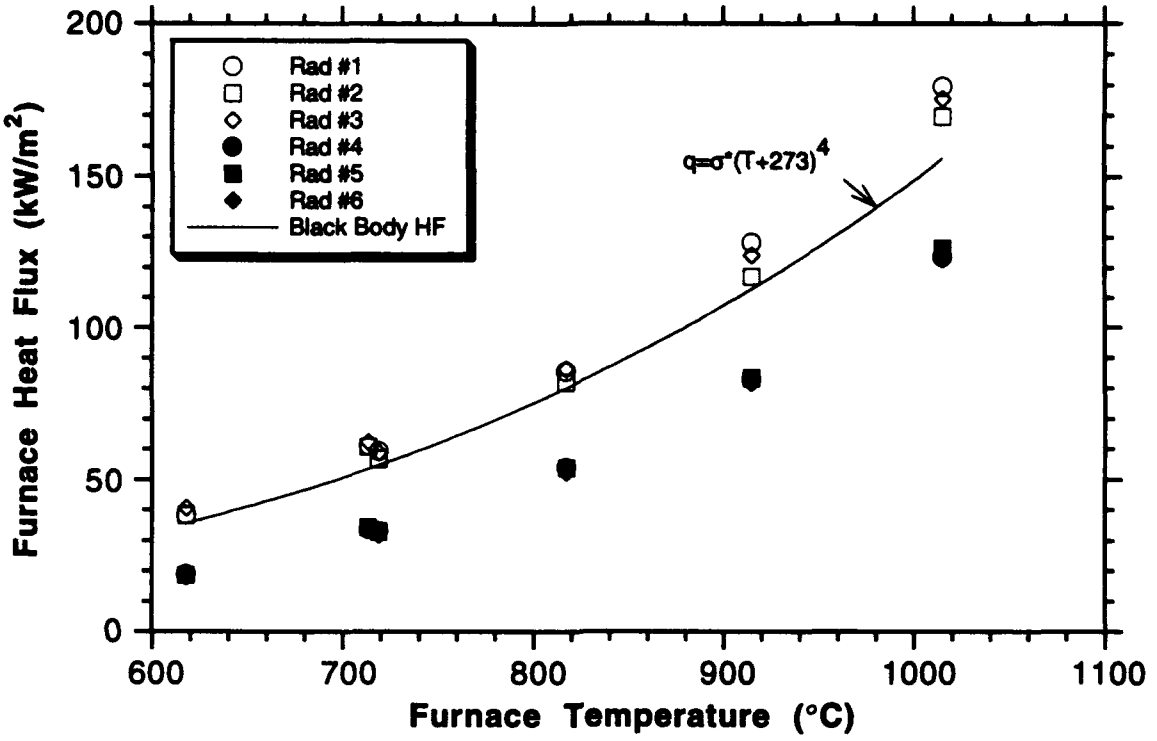

Figure 3.1 Time averaged heat flux and furnace temperature from test CAL2 (data from Table 3.1)

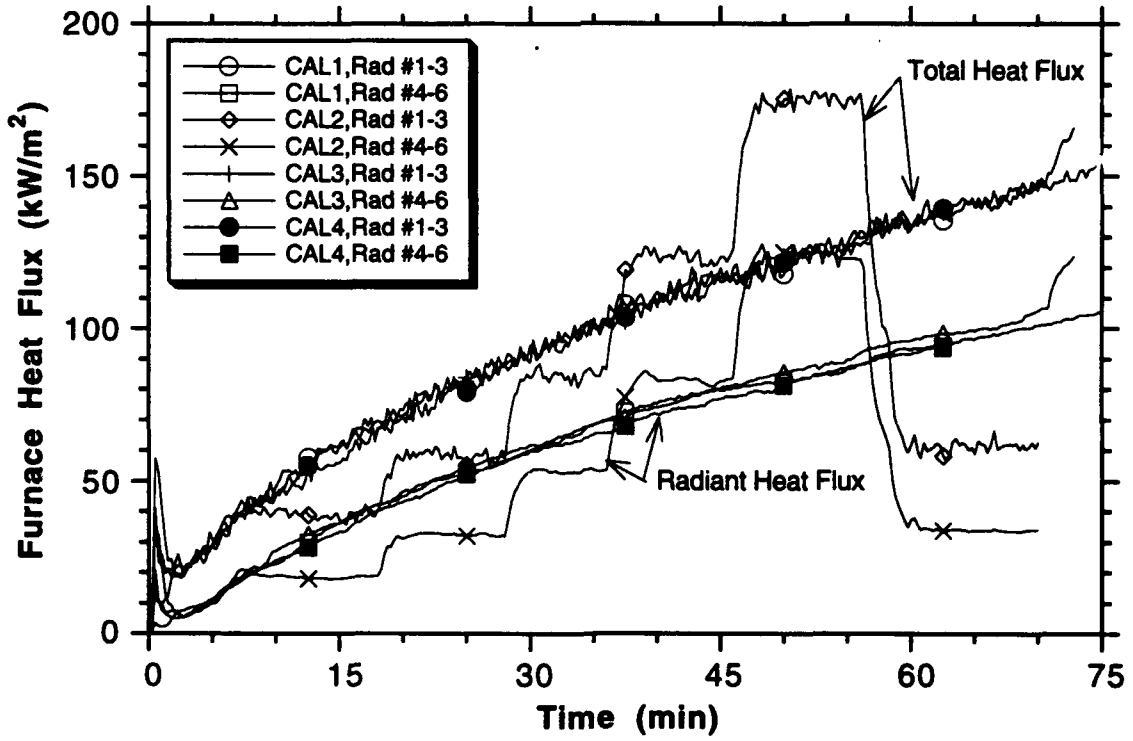

Figure 3.2 Average heat fluxes for CAL1, CAL2, CAL3, and CAL4 tests

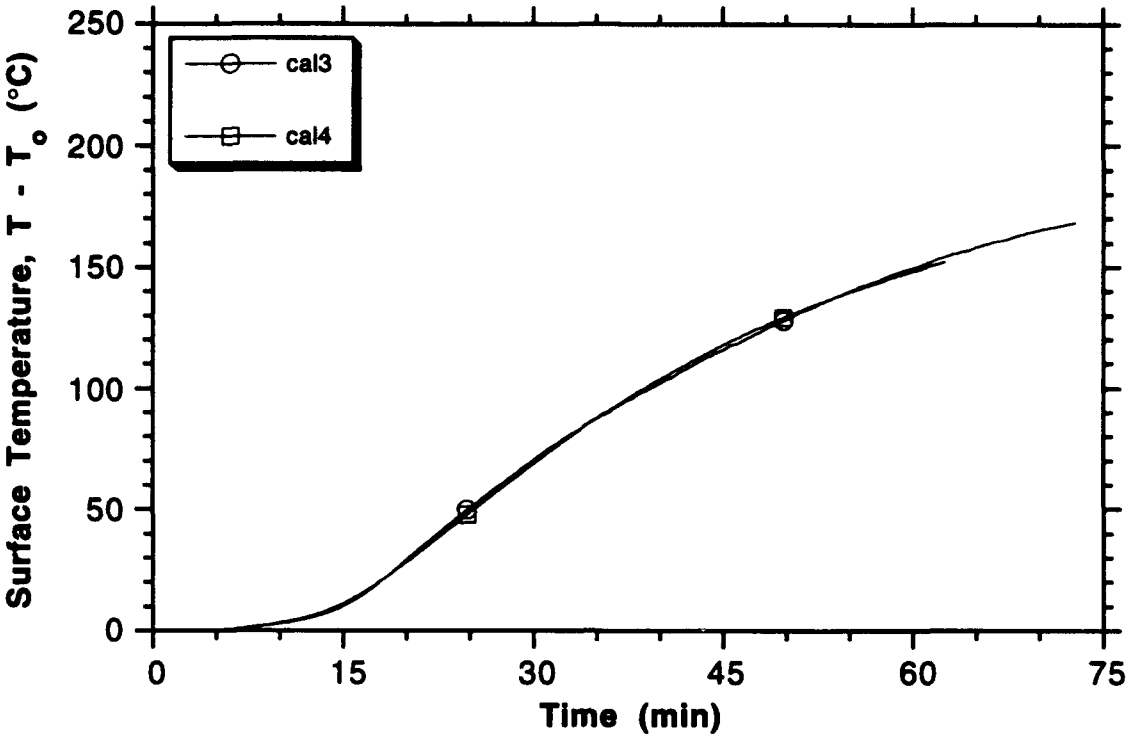

Figure 3.3 Average Surface Temperatures for CAL3 and CAL4 tests; average of Ts1-9 above initial ambient temperature

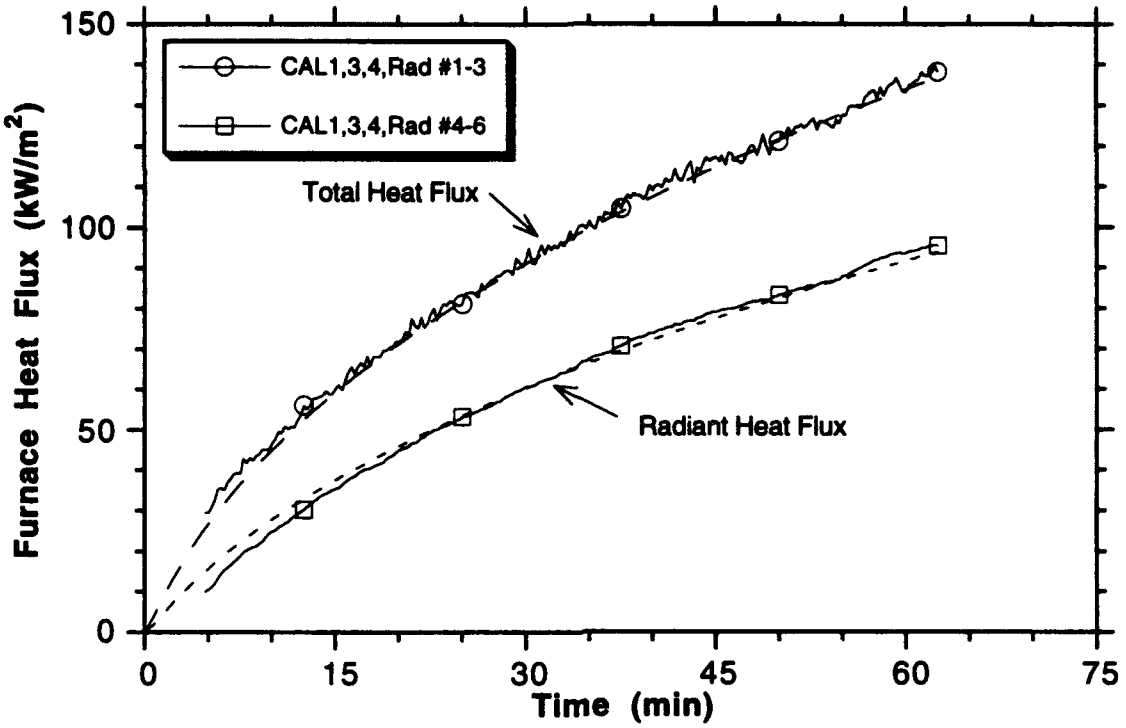

Total Heat Flux Curve Fit

HF=m1*5.67e-11*(345*ln(8*x+1)+293)^m2		
	Value	Error
m1	0.58788242458	0.0894897
m2	3.7241548355	0.0195464
R	0.99791470098	NA

Radiative Heat Flux Curve Fit

HF=m1*5.67e-11*(345*ln(8*x+1)+293)^m2		
	Value	Error
m1	0.0264628476	0.00582864
m2	4.0736034233	0.028252
R	0.9970335932	NA

Figure 3.4 Time averaged heat fluxes from tests CAL1, 3, and 4; two curves from each test are shown, the first for the average of total fluxmeters (Rad #1-3), the second for the average of the radiation pyrometers (Rad #4-6); the corresponding curve fits are shown (the fit excludes the data for the first 5 minutes)

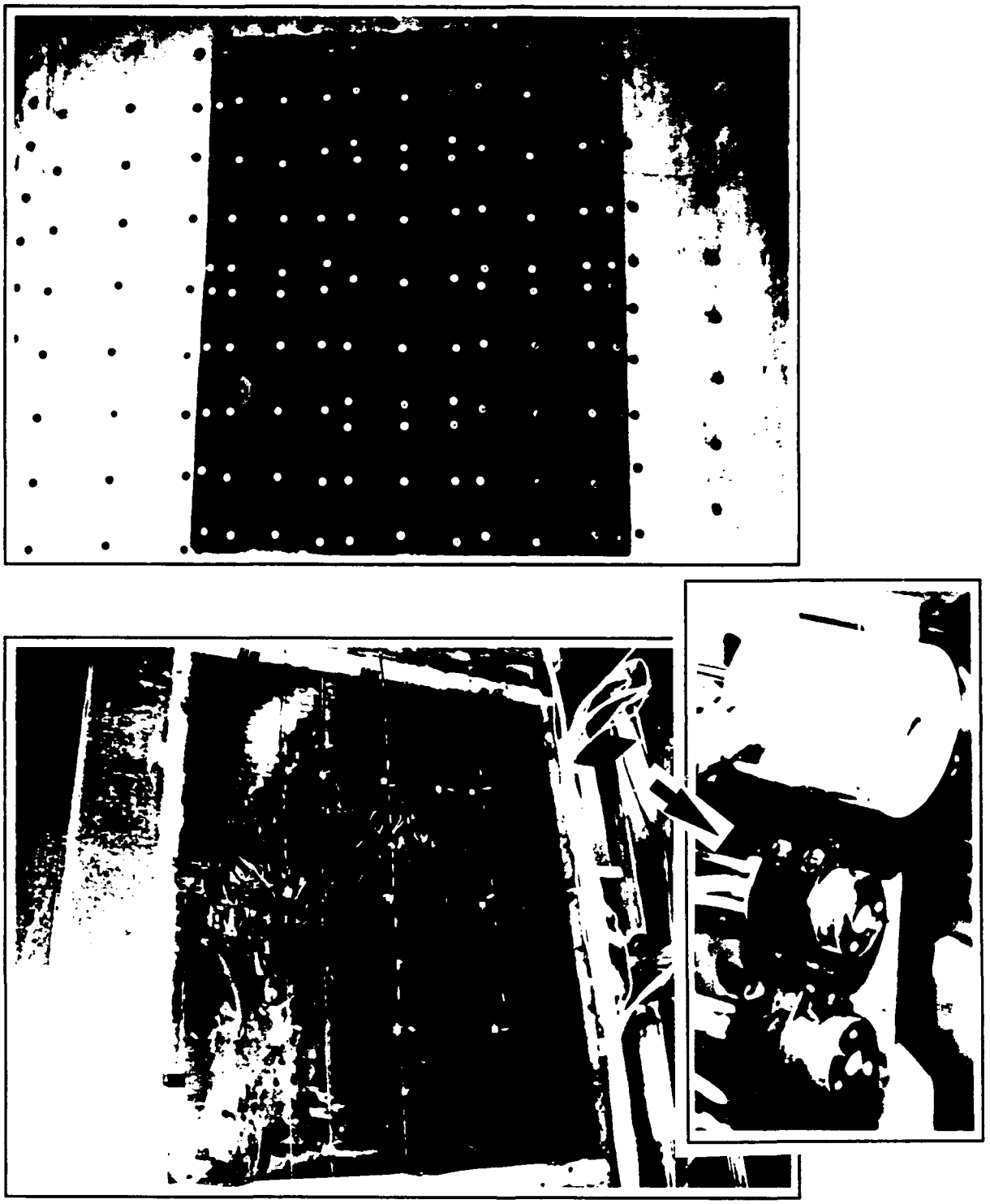

Figure 3.5 Photographs of setup for test A60-1; the top panel shows the exposed insulated face before placement on furnace; the lower panel shows the unexposed steel face with instrumentation; the inset is a closeup of the 30° and 60° HF transducers viewing the middle of the bulkhead

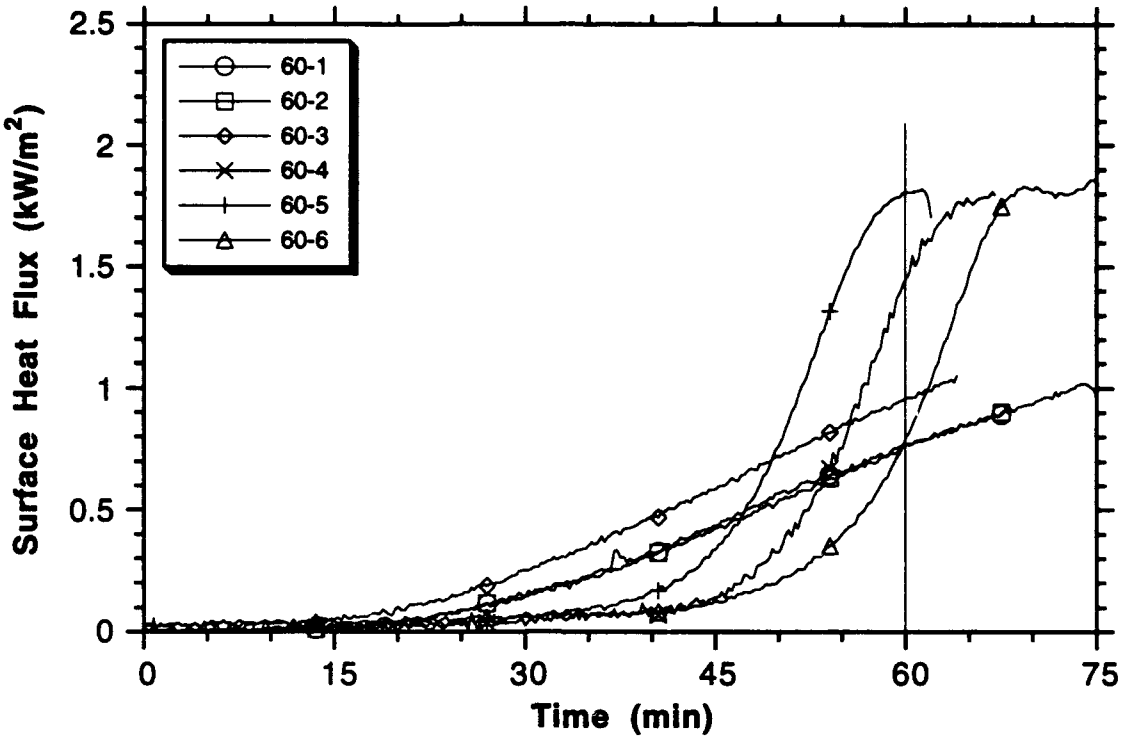

Figure 3.6 Averaged heat flux comparison for A-60 tests

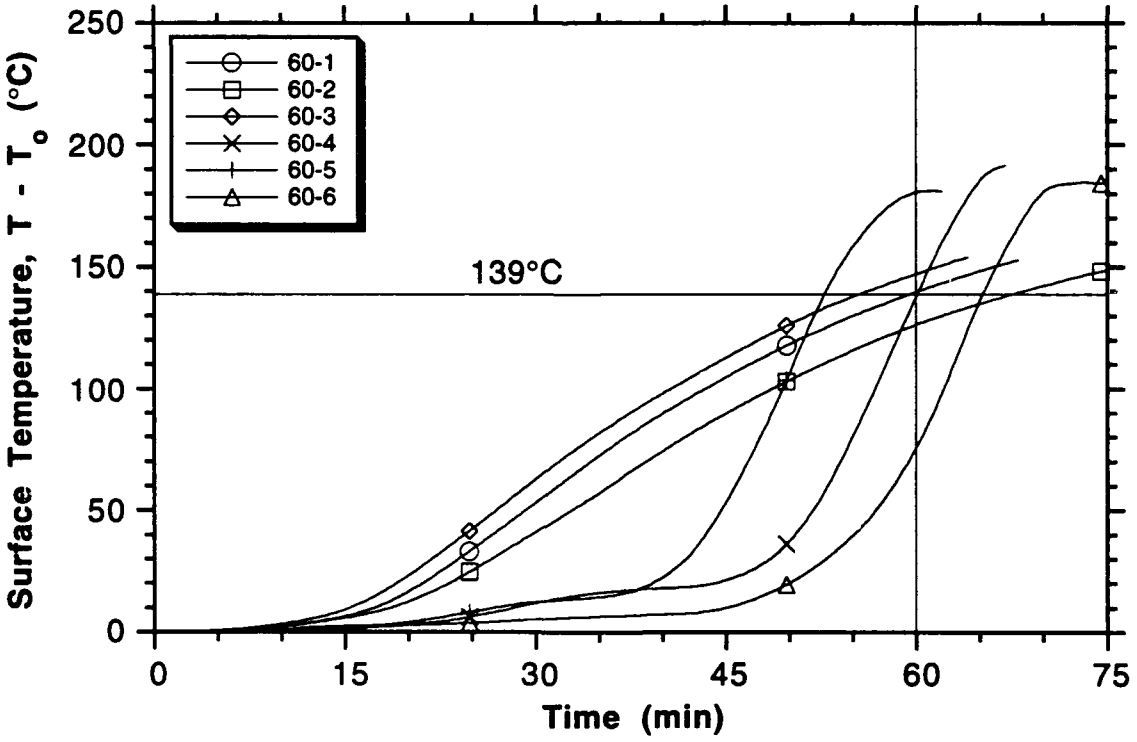

Figure 3.7 Averaged temperature comparison for A-60 tests

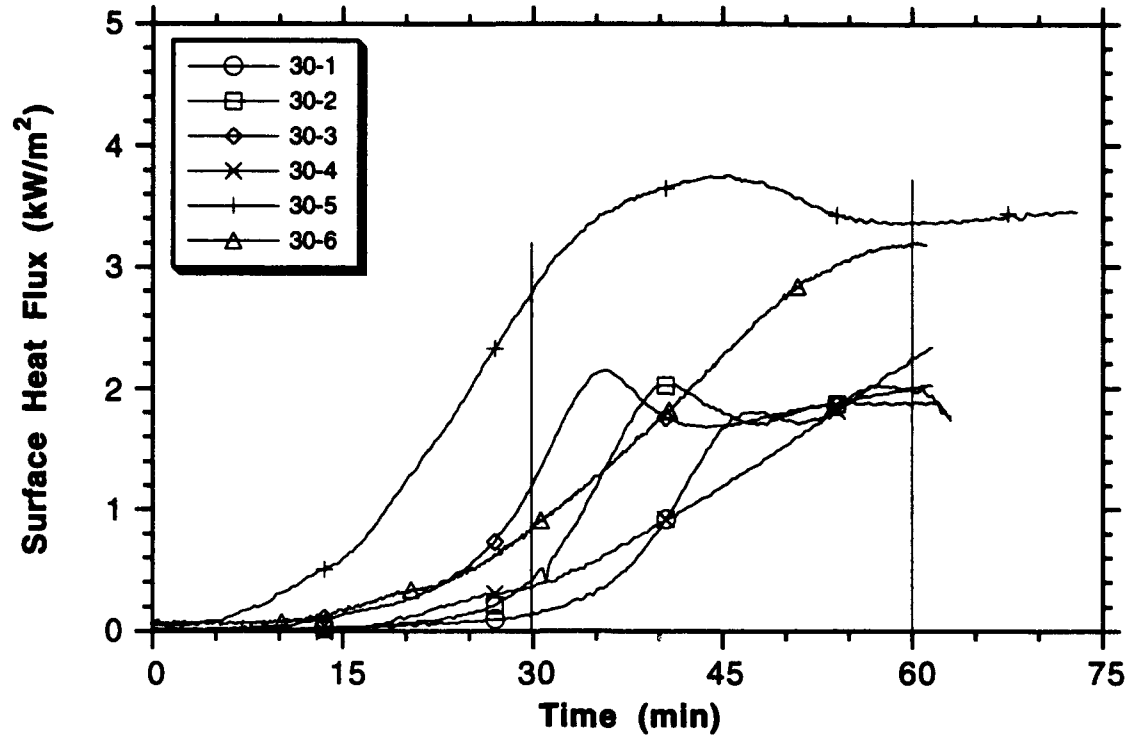

Figure 3.8 Averaged heat flux comparison for A-30 tests

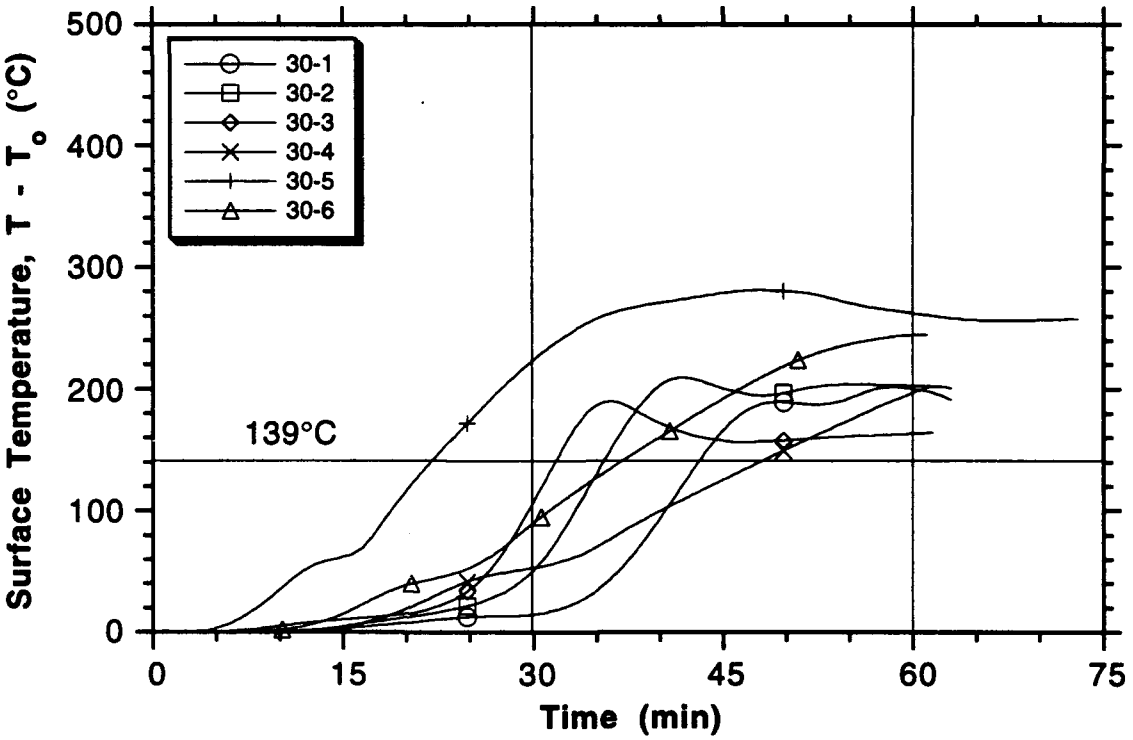

Figure 3.9 Averaged temperature comparison for A-30 tests

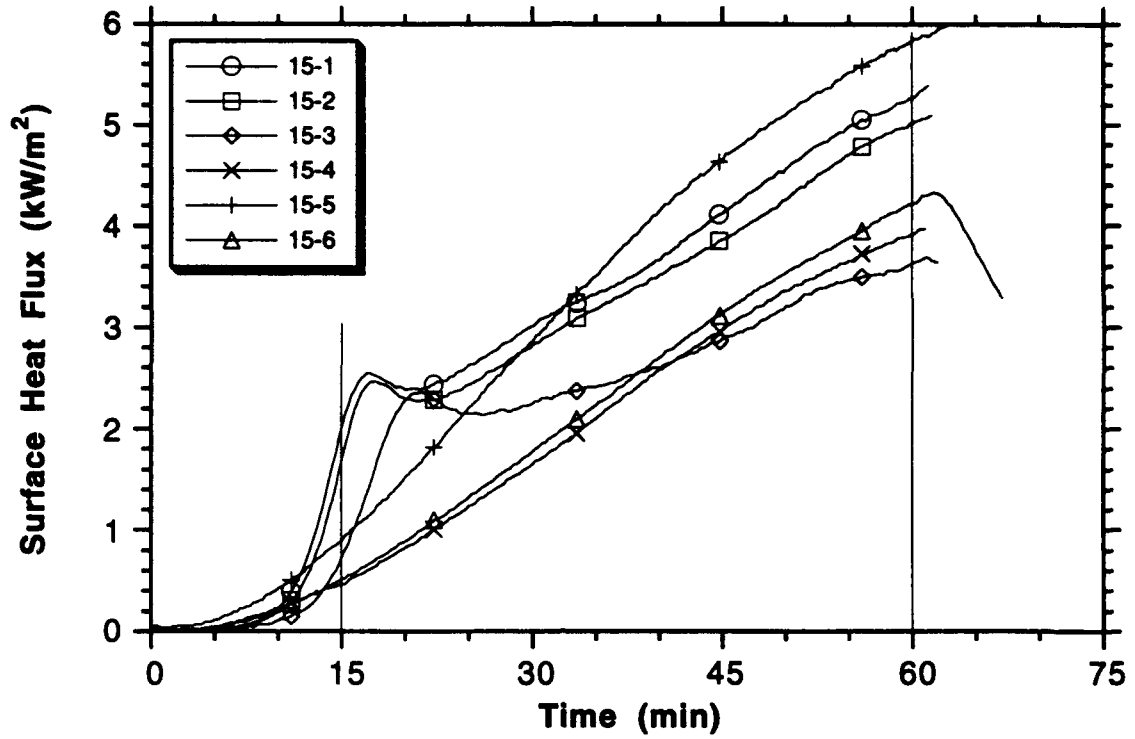

Figure 3.10 Averaged heat flux comparison for A-15 tests

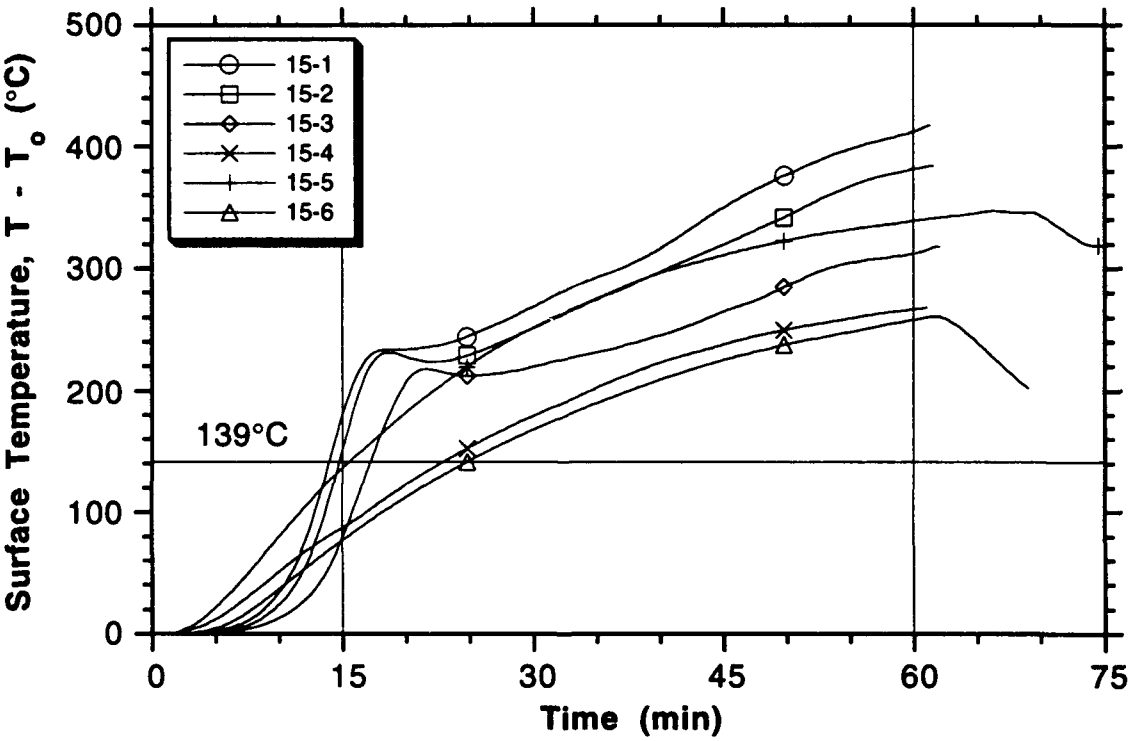

Figure 3.11 Averaged temperature comparison for A-15 tests

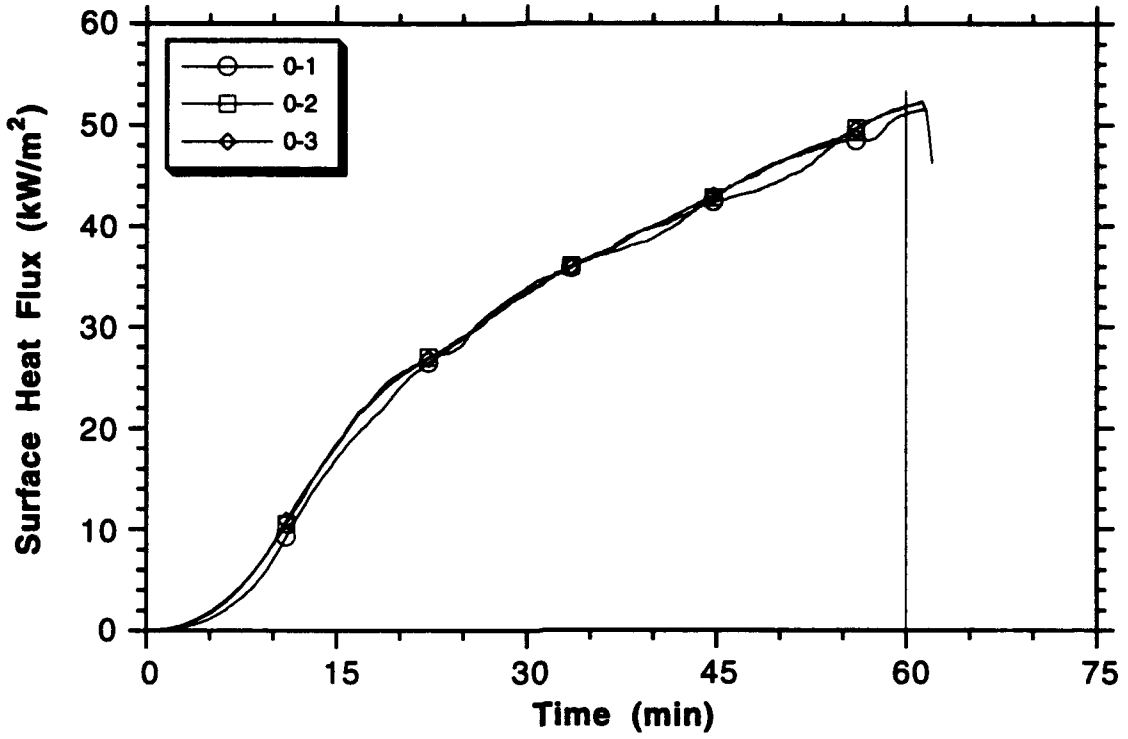

Figure 3.12 Averaged heat flux comparison for A-0 tests

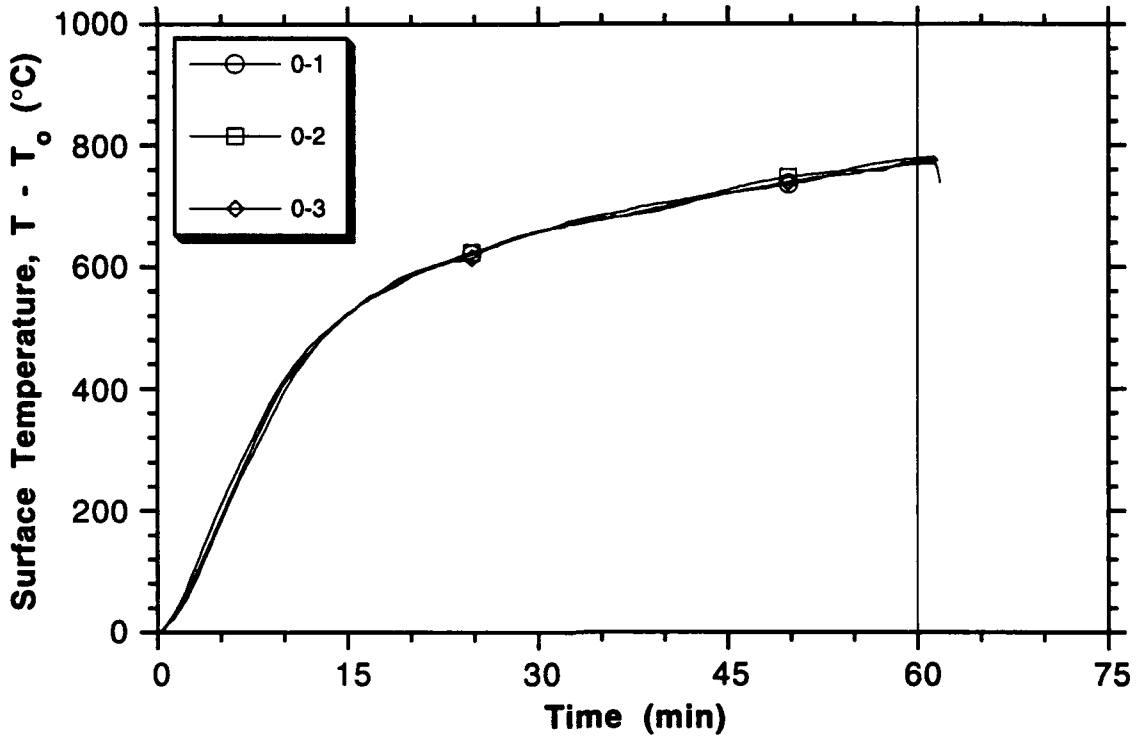

Figure 3.13 Averaged temperature comparison for A-0 tests

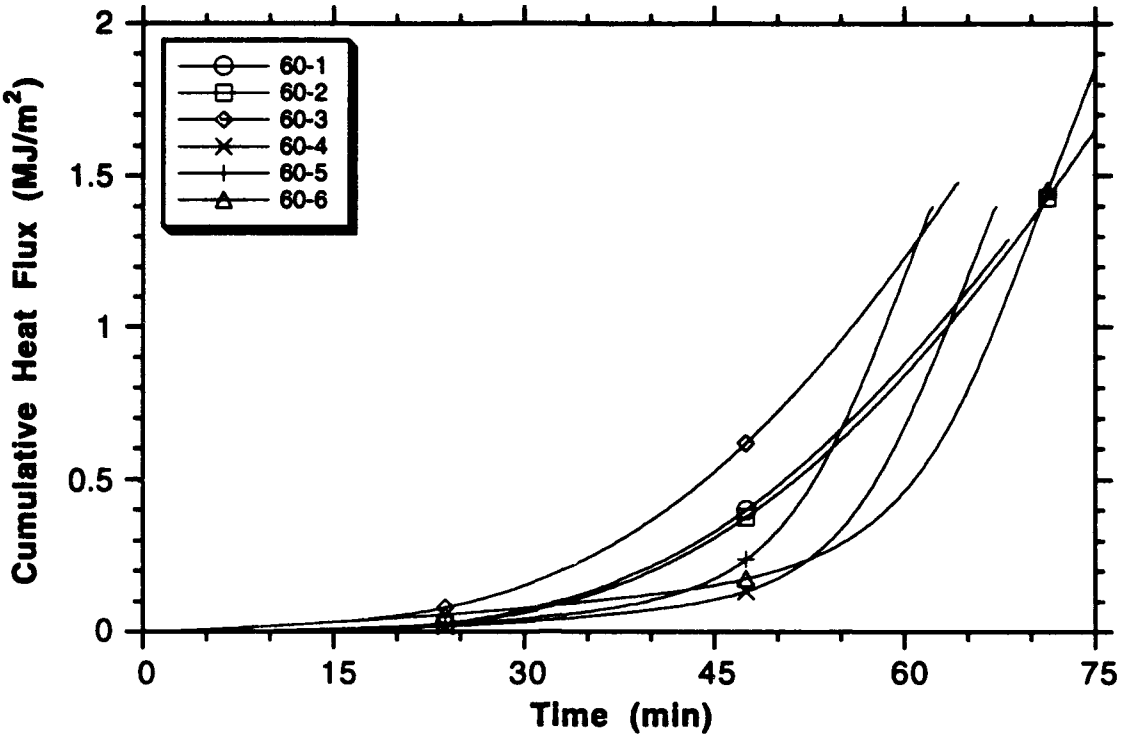

Figure 3.14 Cumulative heat flux comparison for A-60 tests

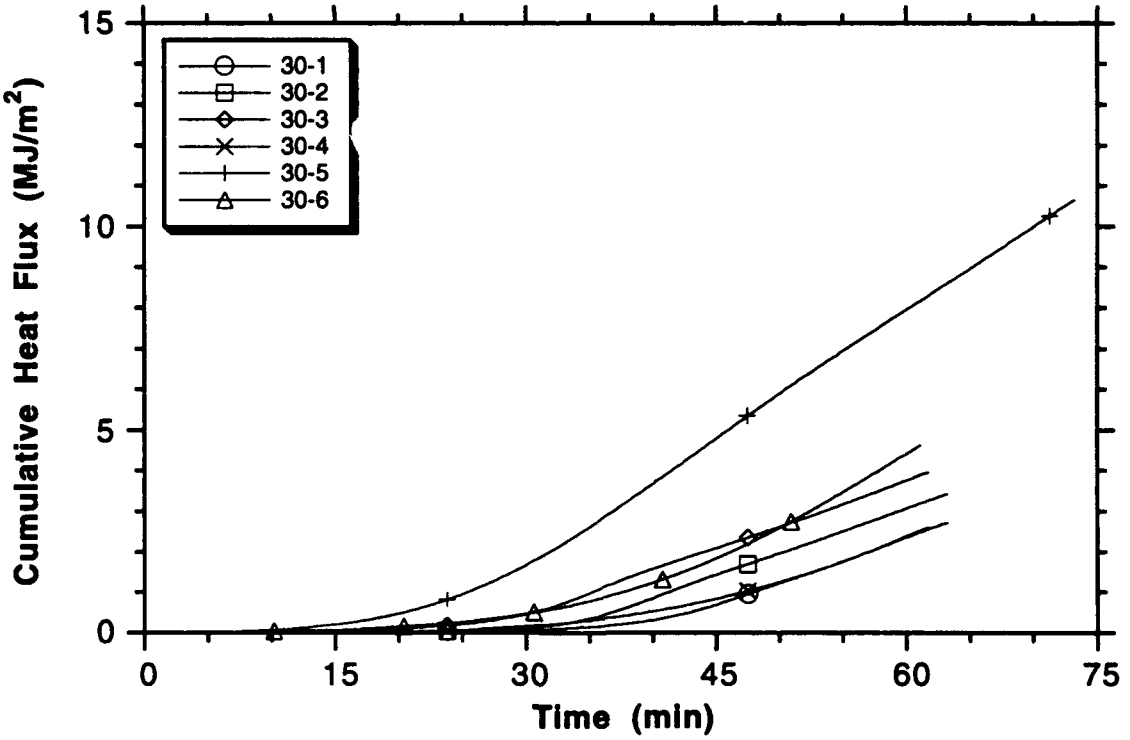

Figure 3.15 Cumulative heat flux comparison for A-30 tests

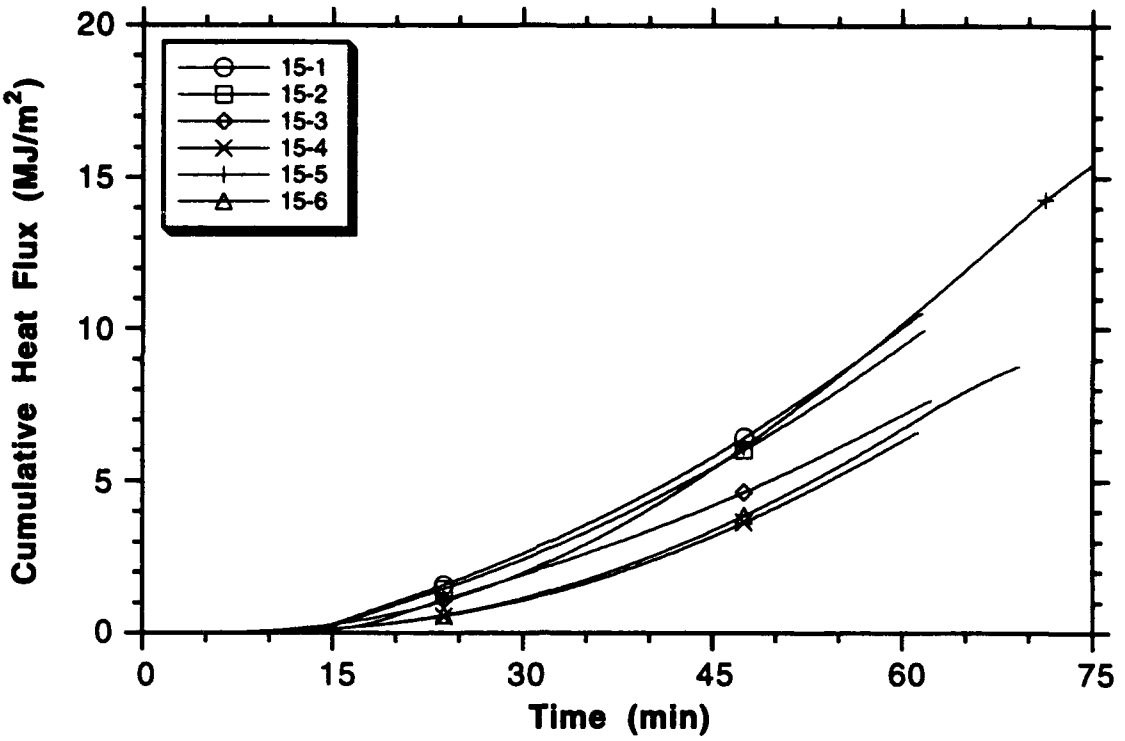

Figure 3.16 Cumulative heat flux comparison for A-15 tests

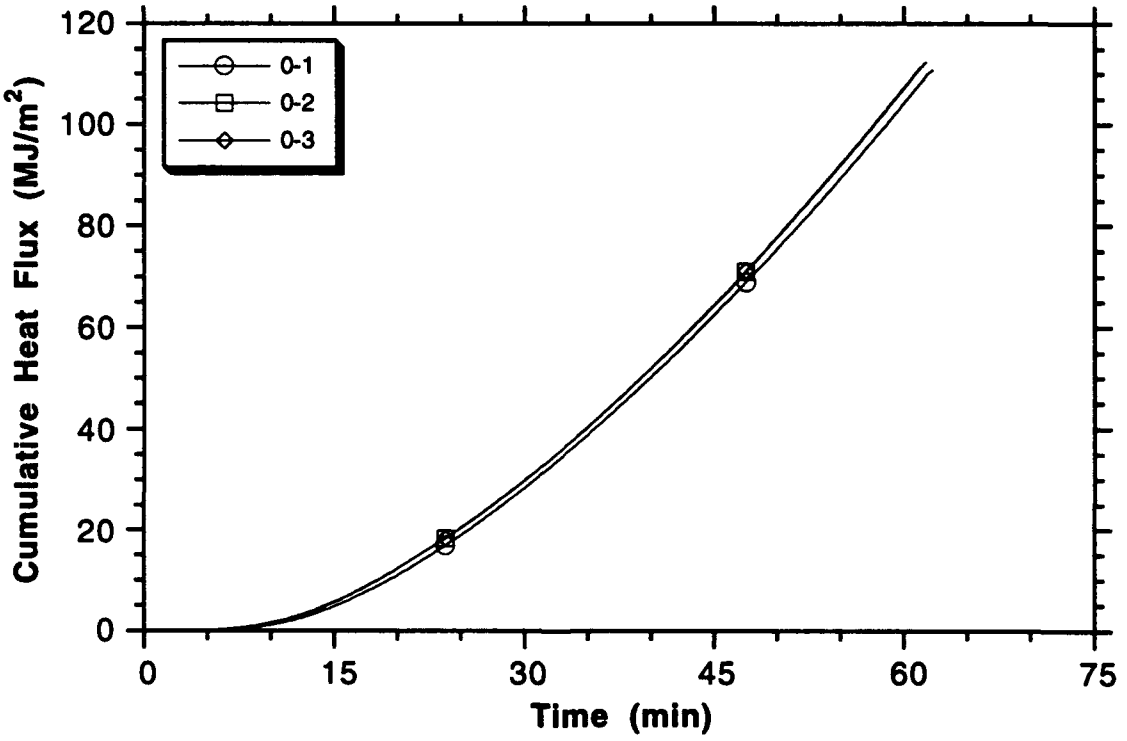

Figure 3.17 Cumulative heat flux comparison for A-0 tests

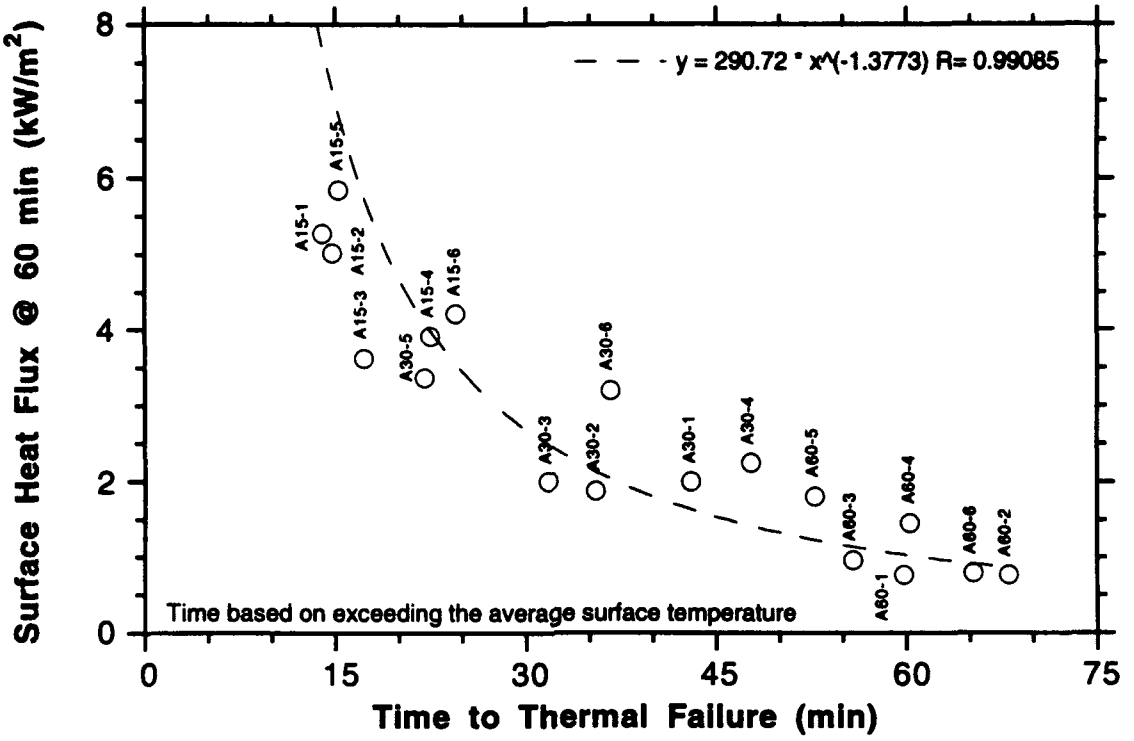

Figure 3.18 Radiated Heat Flux at 60 minutes as a function of time to thermal failure

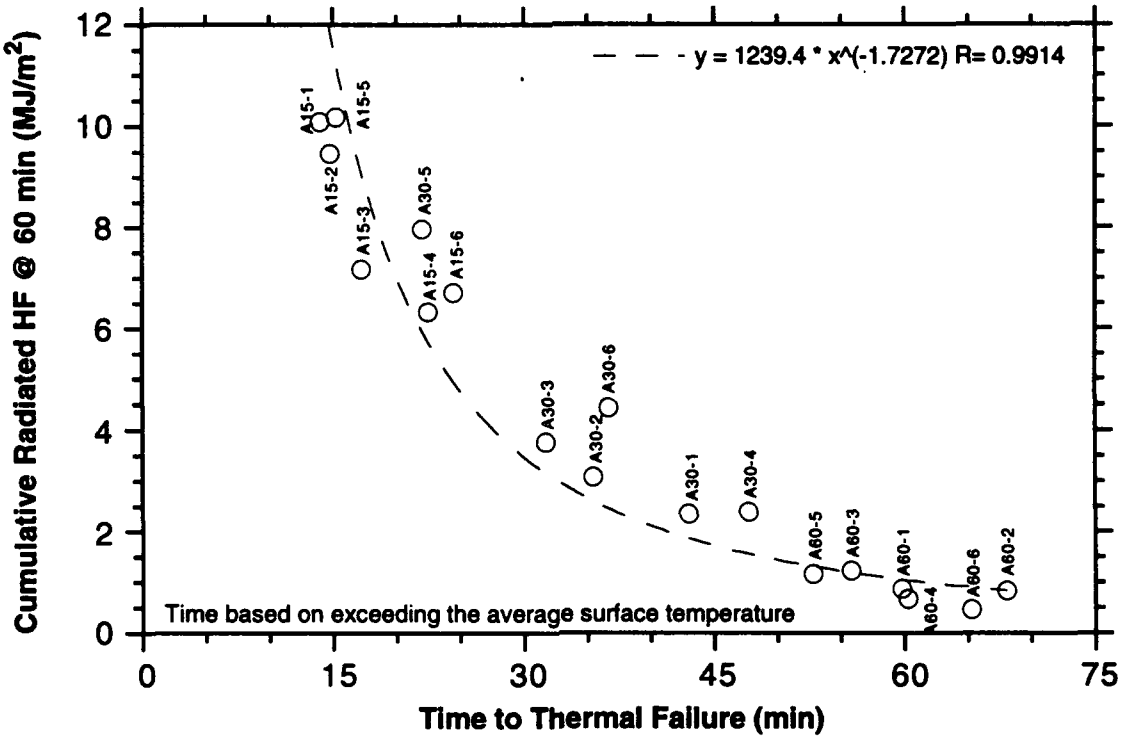

Figure 3.19 Cumulative Radiated Heat Flux at 60 minutes as a function of time to thermal failure

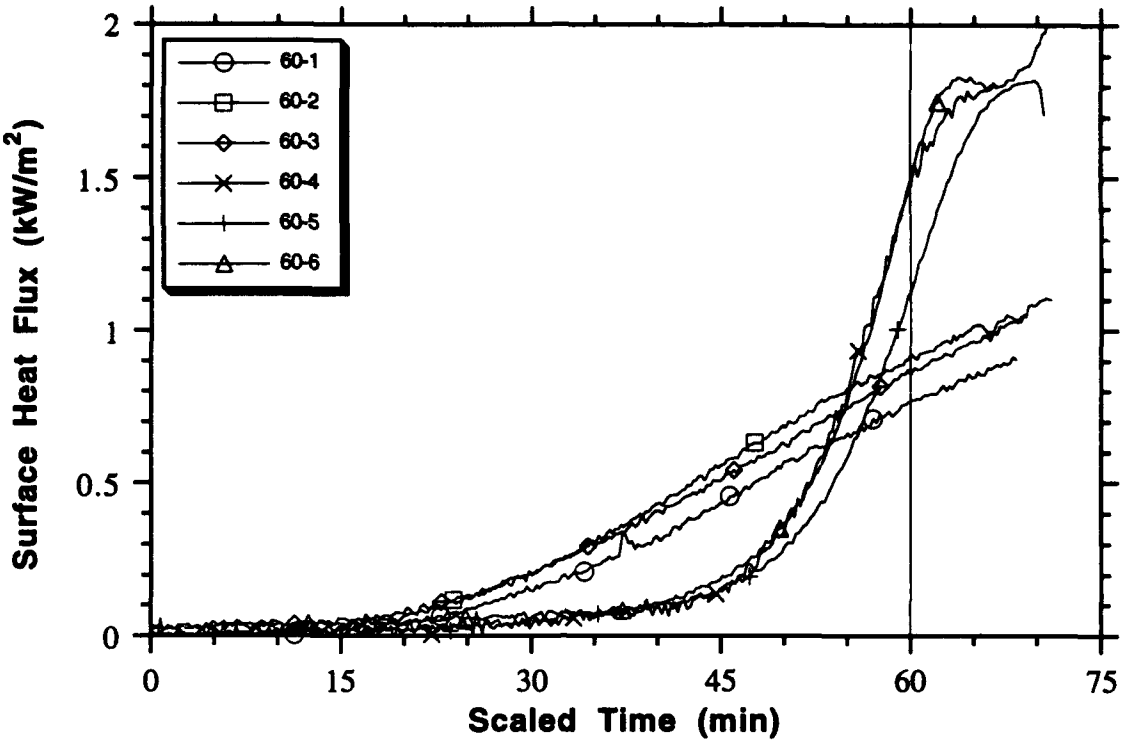

Figure 3.20 Time scaled heat flux data for A-60 tests

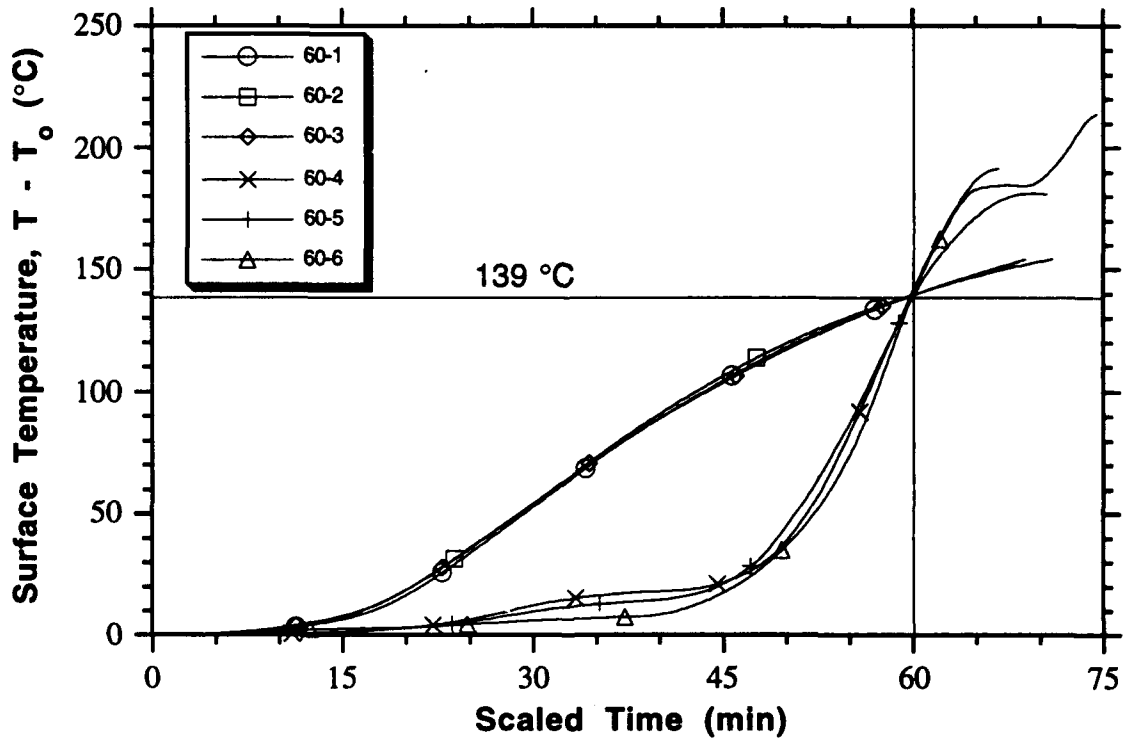

Figure 3.21 Time scaled temperature data for A-60 tests

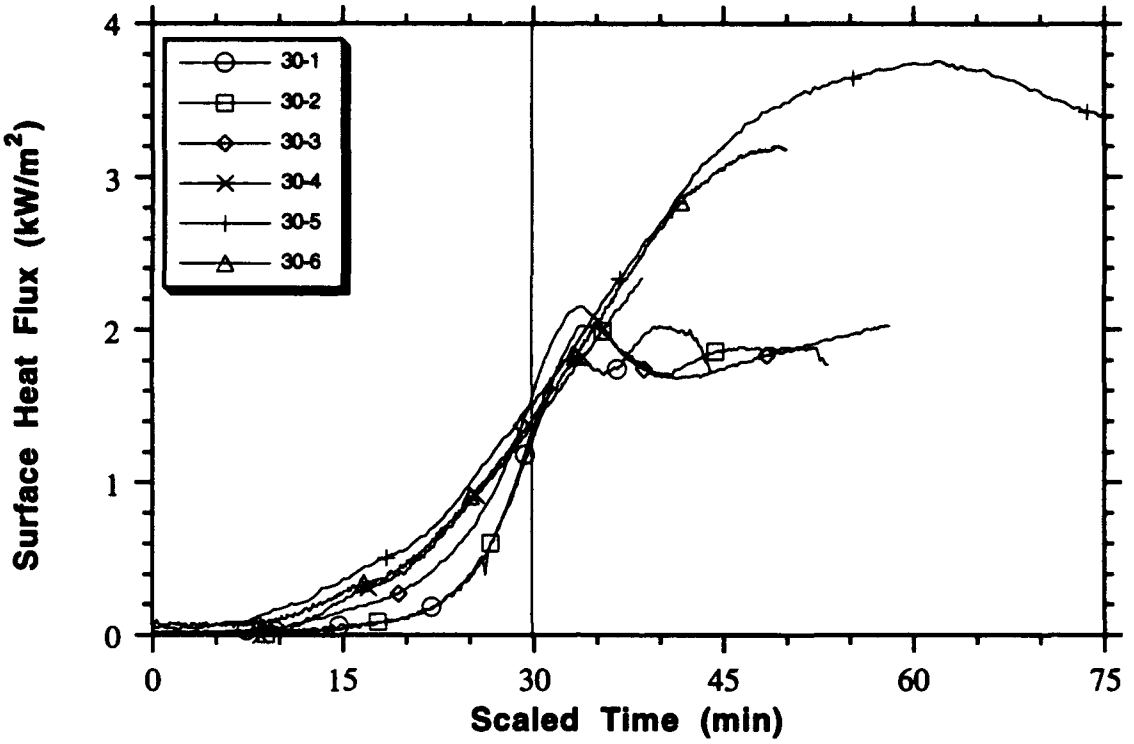

Figure 3.22 Time scaled heat flux data for A-30 tests

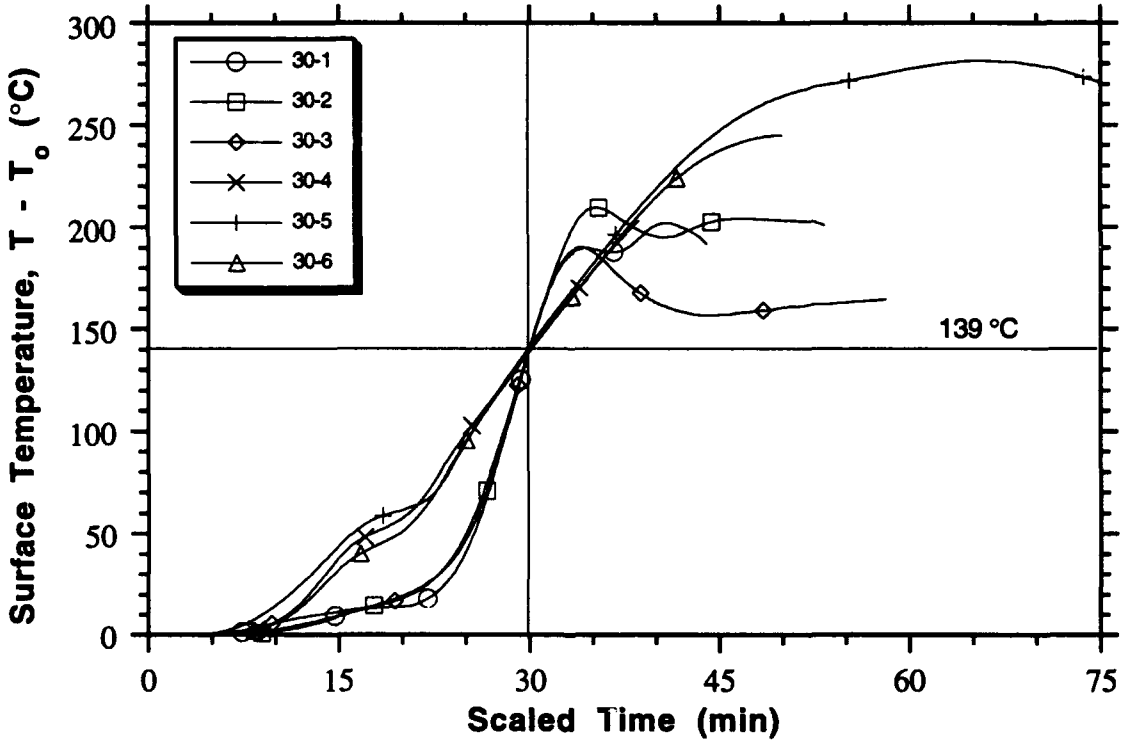

Figure 3.23 Time scaled temperature data for A-30 tests

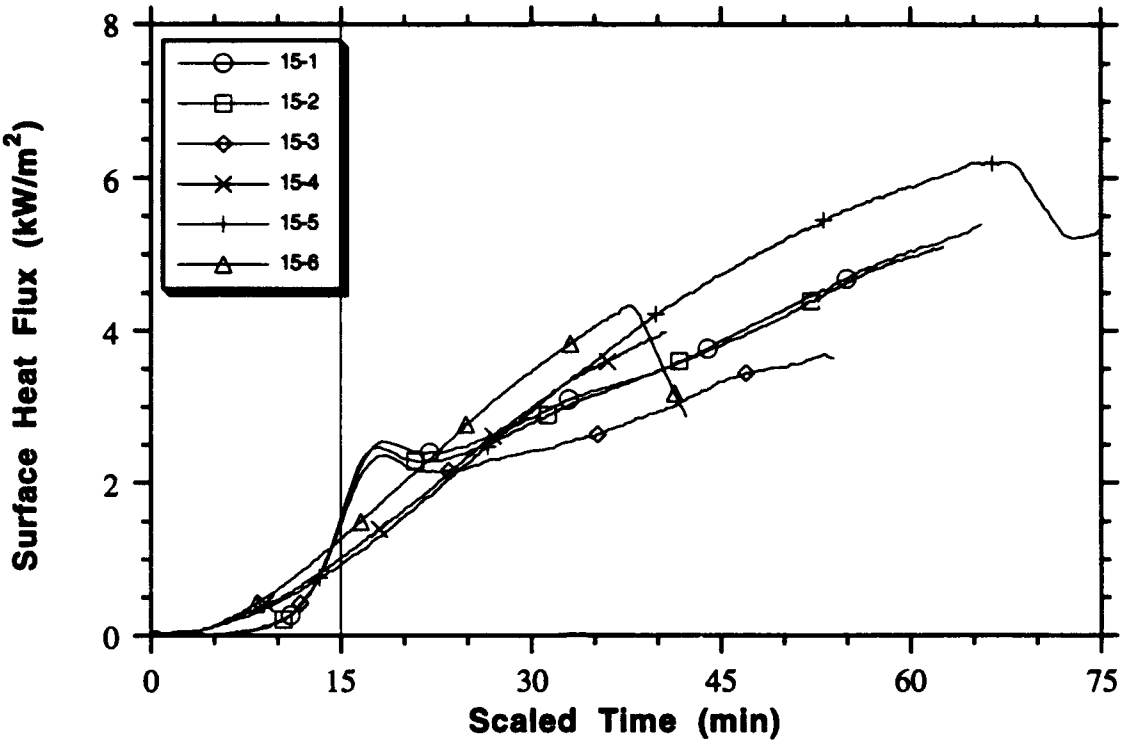

Figure 3.24 Time scaled heat flux data for A-15 tests

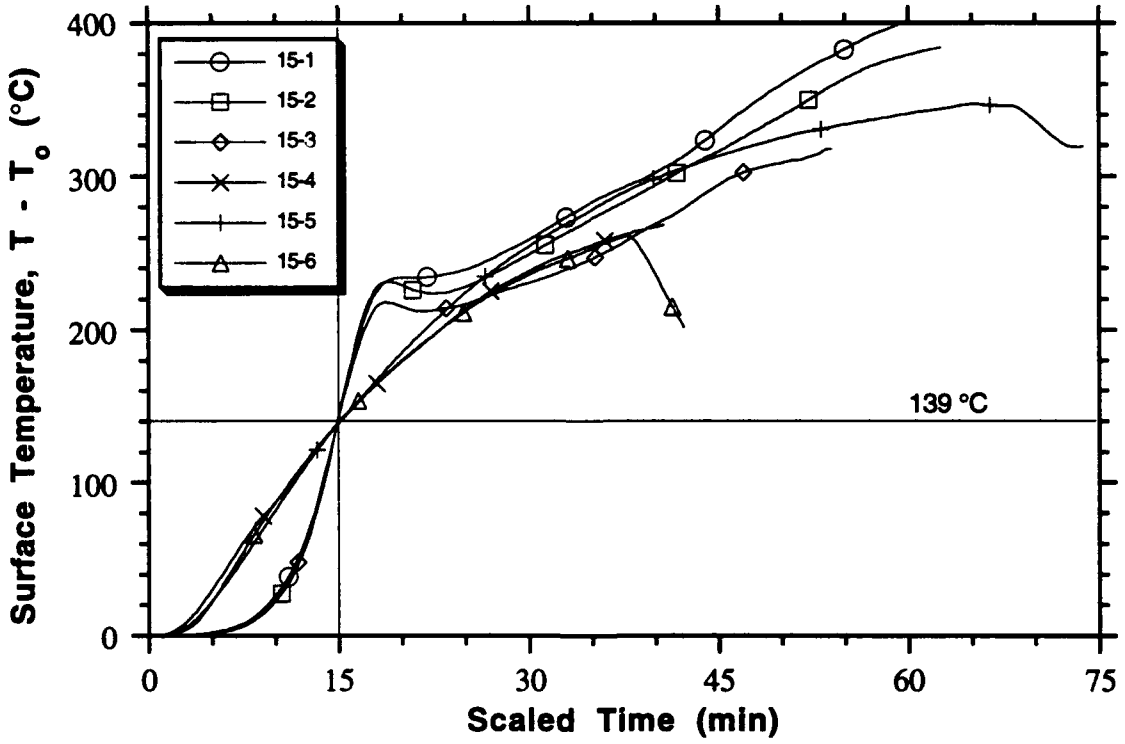

Figure 3.25 Time scaled temperature data for A-15 tests

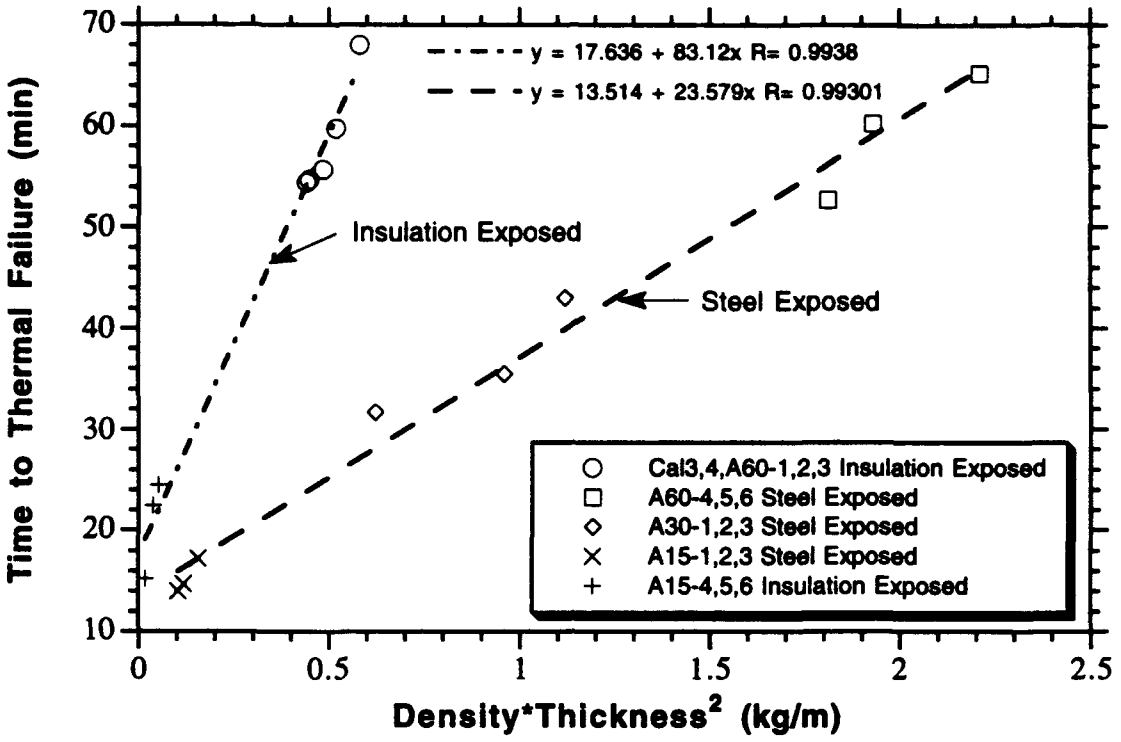

Figure 3.26 Time to thermal failure as a function of density times thickness squared (ρL^2)

Appendix A

Placement of Insulation Batts/Additional Test Information

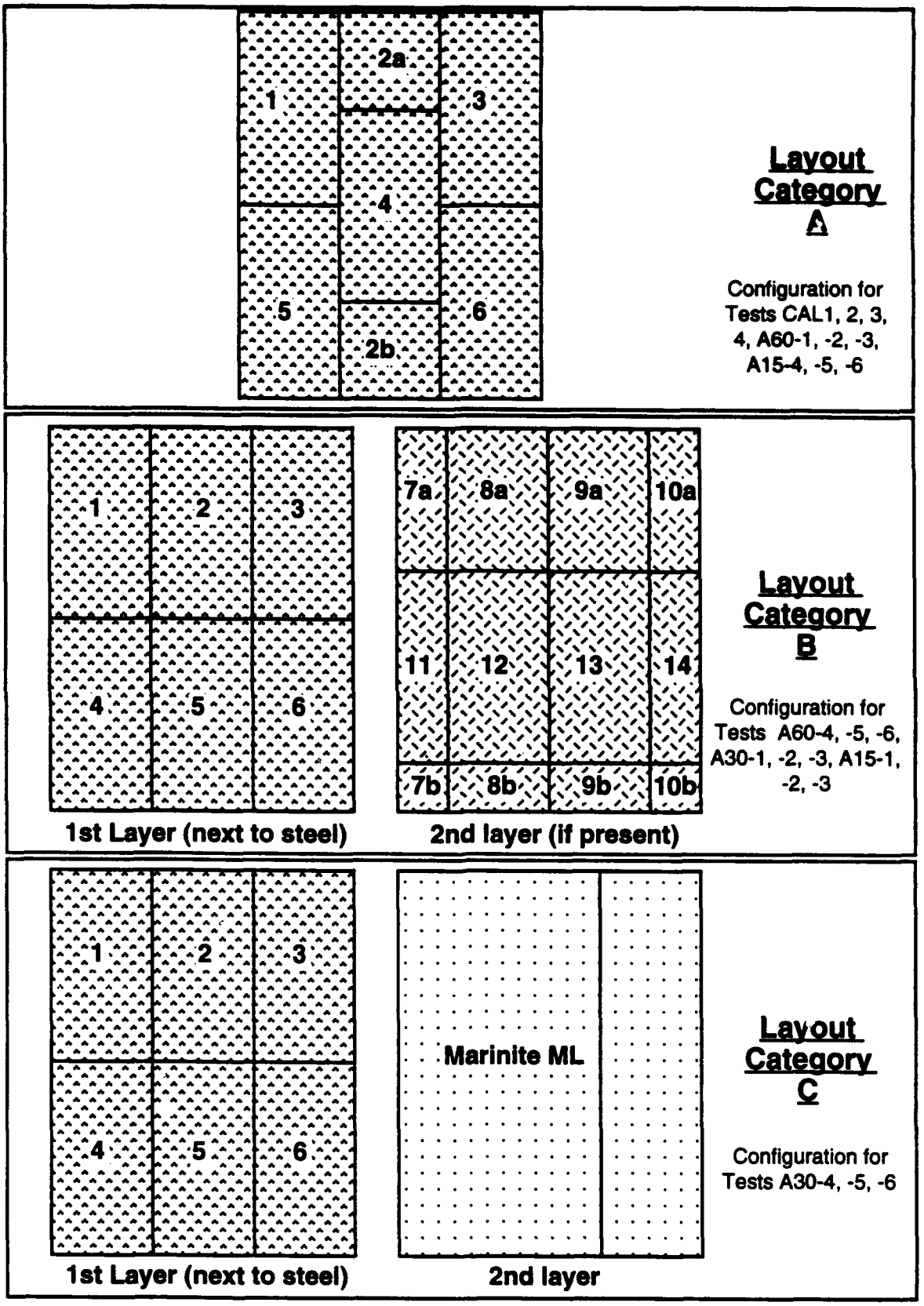

Figure A.1 Insulation layout for bulkhead tests

Table A.1 Test Mineral Wool Insulation Batt Layout (refer to Figure A.1); Weight of Each Batt Shown, in Kilograms, Before Cutting, Nominal Batt Size 610 mm by 1220 mm by 64 mm

Test	Layout Category (cf Fig. A.1)	Layer Thickness (mineral wool, unless otherwise specified)	Insulation or Steel Exposed	1	2	3	4	5	6	7	8	9	10	11	12	13	14	Flange Overlap (left, right)		Average Weight (kg)	Average Density (kg/m^3)
CAL1	A	1 layer, 64 mm	I	5.2	5.1	5.2	5.1	5.3	5.5	-	-	-	-	-	-	-	-	5.1	5.5	5.2	111
CAL2	A	1 layer, 64 mm	I	Same insulation as above						-	-	-	-	-	-	-	-	-	-	-	-
CAL3	A	1 layer, 64 mm	I	5.1	5.1	5.1	5.1	5.1	5.5	-	-	-	-	-	-	-	-	5.1	5.5	5.2	109
CAL4	A	1 layer, 64 mm	I	5.2	5.1	5.2	5.1	5.3	5.5	-	-	-	-	-	-	-	-	5.2	5.2	5.2	111
A60-1	A	1 layer, 64 mm	I	6.1	6.1	6.1	6.0	6.0	6.0	-	-	-	-	-	-	-	-	5.9	6.2	6.1	129
A60-2	A	1 layer, 64 mm	I	6.8	6.8	6.8	6.8	6.8	6.8	-	-	-	-	-	-	-	-	6.7	6.8	6.8	144
A60-3	A	1 layer, 64 mm	I	5.7	5.7	5.6	5.7	5.7	5.6	-	-	-	-	-	-	-	-	5.6	5.7	5.7	120
A60-4	B	1st layer 64 mm, 2nd layer 64 mm	S	5.7	5.7	5.7	5.7	5.7	5.7	5.6	5.6	5.6	5.6	5.6	5.6	5.6	5.6	-	-	5.6	119
A60-5	B	1st layer 64 mm, 2nd layer 64 mm	S	5.4	5.4	5.4	5.4	5.4	5.4	5.2	5.3	5.3	5.2	5.2	5.2	5.2	5.2	-	-	5.3	112
A60-6	B	1st layer 64 mm, 2nd layer 64 mm	S	6.5	6.5	6.5	6.5	6.5	6.5	6.4	6.4	6.4	6.4	6.4	6.4	6.4	6.4	-	-	6.5	137
A30-1	B	1st layer 32 mm, 2nd layer 64 mm	S	5.9	5.9	5.9	5.9	5.9	5.9	5.8	5.8	5.8	5.8	5.8	5.8	5.8	5.8	-	-	5.8	123
A30-2	B	1st layer 32 mm, 2nd layer 64 mm	S	5.0	5.0	5.0	5.0	5.0	5.0	4.9	5.0	5.1	5.1	4.9	5.0	5.0	5.1	-	-	5.0	106
A30-3	B	1 layer 64 mm	S	7.3	7.2	7.2	7.3	7.3	7.3	-	-	-	-	-	-	-	-	-	-	7.2	153
A30-4	C	1st layer 32 mm, 2nd layer 19 mm Marinite ML	S	6.4	6.4	6.4	6.4	6.4	6.4	-	-	-	-	-	-	-	-	-	-	6.4	134
A30-5	C	1 layer 19 mm Marinite ML	S	-	-	-	-	-	-	-	-	-	-	-	-	-	-	-	-	-	-
A30-6	C	1st layer 19 mm, 2nd layer 19 mm Marinite ML	S	6.4	6.4	6.4	6.4	6.4	6.4	-	-	-	-	-	-	-	-	-	-	6.4	135
A15-1	B	1 layer, 32 mm	S	4.9	4.9	4.9	4.9	4.9	4.9	-	-	-	-	-	-	-	-	-	-	4.9	103
A15-2	B	1 layer, 32 mm	S	5.5	5.5	5.5	5.5	5.5	5.5	-	-	-	-	-	-	-	-	-	-	5.5	117
A15-3	A	1 layer 32 mm	S	7.3	7.3	7.3	7.3	7.3	7.3	-	-	-	-	-	-	-	-	-	-	7.3	155
A15-4	A	1 layer 19 mm	I	4.8	4.8	4.8	4.8	4.8	4.8	-	-	-	-	-	-	-	-	4.8	4.8	4.8	101
A15-5	A	1 layer 13 mm	I	5.2	5.2	5.2	5.2	5.2	5.2	-	-	-	-	-	-	-	-	5.2	5.2	5.2	110
A15-6	A	1 layer 19 mm	I	6.6	6.6	6.6	6.6	6.6	6.6	-	-	-	-	-	-	-	-	6.6	6.6	6.6	139

Average weight calculated excluding the overlap pieces

Table A.2 Additional Bulkhead Test Information

Test	Initial Relative Humidity (%)	Average HF at Failure Time (based on Tsavg1-9) (kW/m^2)	Integrated Furnace Temperature at 60 Min., (∫[Tf-To] dt) (°C*min)	Furnace Integrated Temperature Deviation from Standard (%)
CAL1	39	-	-	-
CAL2	NA	-	-	-
CAL3	76	-	46583	-0.13%
CAL4	76	-	46428	-0.47%
A60-1	64	0.77	46542	-0.22%
A60-2	89	0.92	46331	-0.68%
A60-3	21	0.86	46543	-0.22%
A60-4	64	1.48	46553	-0.20%
A60-5	36	1.13	46488	-0.34%
A60-6	36	1.51	46584	-0.13%
A0-1	46	0.91	46325	-0.69%
A0-2	35	1.05	46565	-0.17%
A0-3	36	1.04	46514	-0.28%
A30-1	61	1.37	46219	-0.92%
A30-2	50	1.31	46583	-0.14%
A30-3	70	1.61	46448	-0.43%
A15-1	52	1.52	46394	-0.54%
A15-2	56	1.58	46377	-0.58%
A15-3	66	1.47	46344	-0.65%
A30-4	81	1.38	46579	-0.14%
A30-5	82	1.52	46683	0.08%
A30-6	NA	1.42	46239	-0.87%
A15-4	66	1.03	46416	-0.49%
A15-5	58	0.95	46273	-0.80%
A15-6	44	1.28	46185	-0.99%

NOTE: Furnace Deviation Calculated based on temperature rise from ambient; the IMO Standard integrated furnace curve, $\int 345\ln(8t+1)dt$, is 46646 °C*min at 60 minutes. Integrated area calculated by trapezoidal rule integration from average furnace temperature rise from ambient.

Appendix B

Heat Flux Transducer Calibration Information

Table B.1 Heat Flux Transducer Calibration Summary

	Number	Heat Flux Transducer Type	Model No.	Serial No.	Location During Use	Pre-Test Calibrated Sensitivity			Post-Test as Received Calibration Sensitivity			Percent Change in Calibration (%)
						mV	at W/cm²	(mV/[W/cm²])	mV	at W/cm²	(mV/[W/cm²])	
Calibration Tests	1	180° THF	64-20-18K	74041	top of furnace	9.34	20	0.0467	9.20	20	0.0460	-1.50
	2	180° THF	64-20-18K	74041	middle of furnace	8.75	20	0.0438	8.58	20	0.0429	-1.94
	3	180° THF	64-20-18K	74043	bottom of furnace	9.32	20	0.0466	9.18	20	0.0459	-1.50
	4	150° RHF	64-20-18K/SW-1C-150	74044	top of furnace	7.23	20	0.0362	7.11	20	0.0356	-1.66
	5	150° RHF	64-20-18K/SW-1C-150	74045	middle of furnace	7.09	20	0.0355	7.09	20	0.0355	0.00
	6	150° RHF	64-20-18K/SW-1C-150	74046	bottom of furnace	7.07	20	0.0354	6.99	20	0.0350	-1.13
Bulkhead Tests	1	30° THF	64-1-18K/VRW-30C	74047	top of bulkhead	0.556	1	0.0556	9.61	17	0.0565	1.67
	2	30° THF	64-1-18K/VRW-30C	74048	middle of bulkhead	0.570	1	0.0570	9.71	17	0.0571	0.21
	3	60° THF	64-1-18K/NW-1C-60C	740410	middle of bulkhead	2.54	1	0.2540	14.15	5.5	0.2573	1.29
	4	60° RHF	64-1-18K/SW-1C-60C	740411	middle of bulkhead	2.33	1	0.2330	12.46	5.5	0.2265	-2.77
	5	30° THF	64-1-18K/VRW-30C	74049	bottom of bulkhead	0.506	1	0.0506	8.45	17	0.0497	-1.77

THF - Total Heat Flux Transducer, or Fluxmeter
RHF - Radiative Heat Flux Transducer, or Pyrometer, using a sapphire window
Post-Test as received Calibration refers to the re-calibration of the transducers at the conclusion of testing without refurbishing the face of the transducer.

Appendix C

Furnace and Surface Heat Fluxes

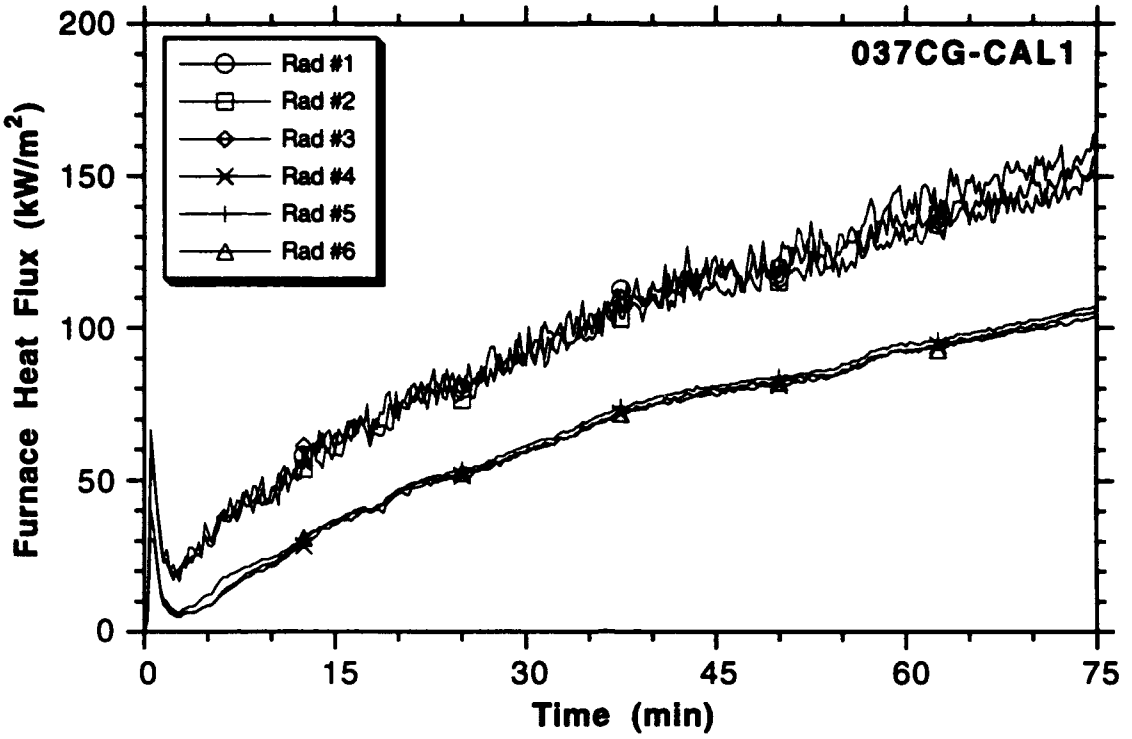
037CG-CAL1
Rad #1
Rad #2
Rad #3
Rad #4
Rad #5
Rad #6
Furnace Heat Flux (kW/m^2)
Time (min)
0
50
100
150
200
0
15
30
45
60
75

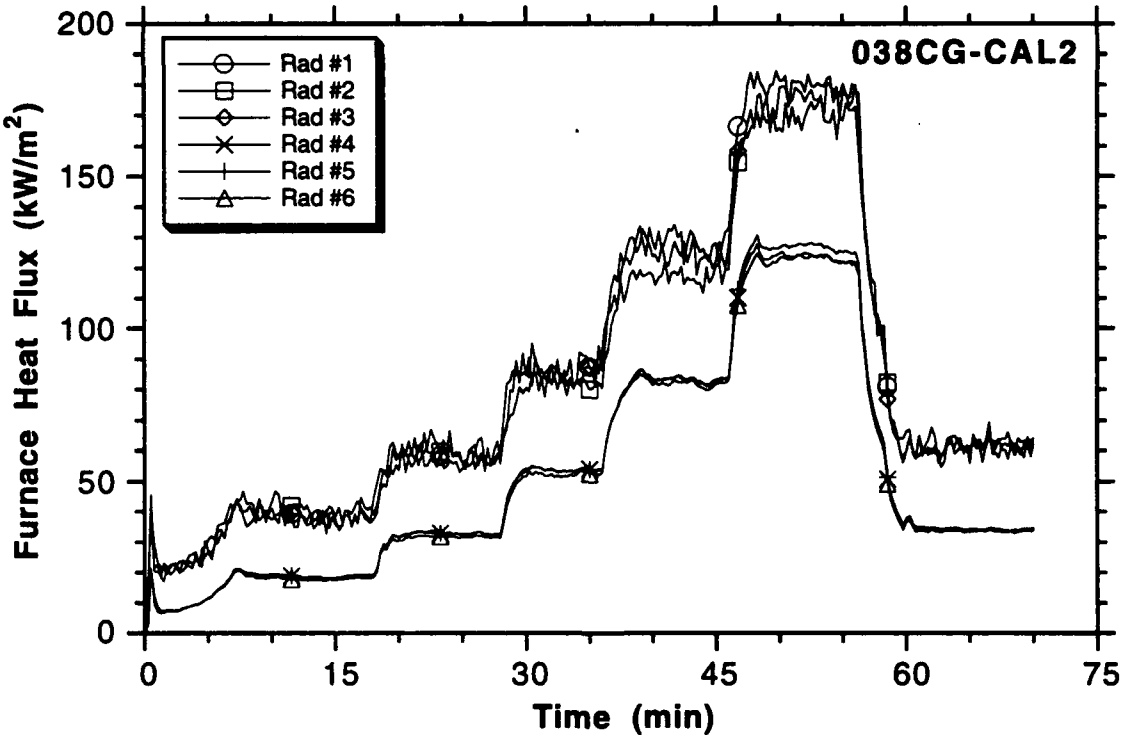
038CG-CAL2
Rad #1
Rad #2
Rad #3
Rad #4
Rad #5
Rad #6
Furnace Heat Flux (kW/m^2)
Time (min)
0
50
100
150
200
0
15
30
45
60
75

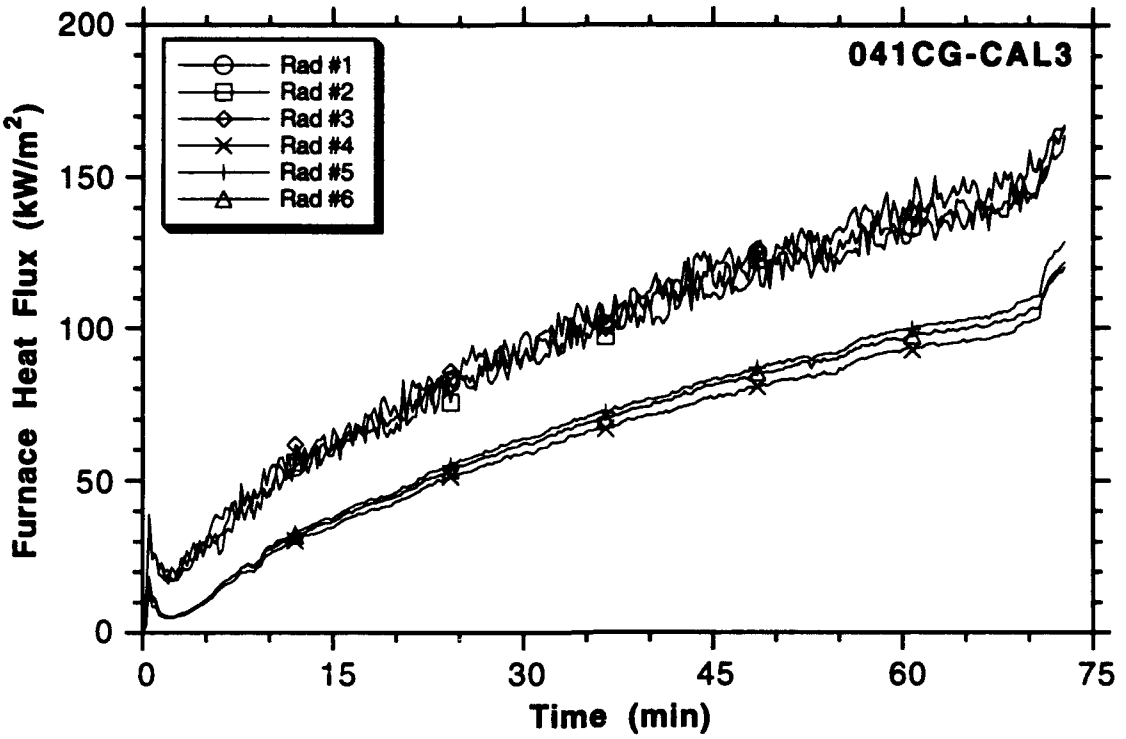
041CG-CAL3
Rad #1
Rad #2
Rad #3
Rad #4
Rad #5
Rad #6
Furnace Heat Flux (kW/m^2)
Time (min)
0
50
100
150
200
0
15
30
45
60
75

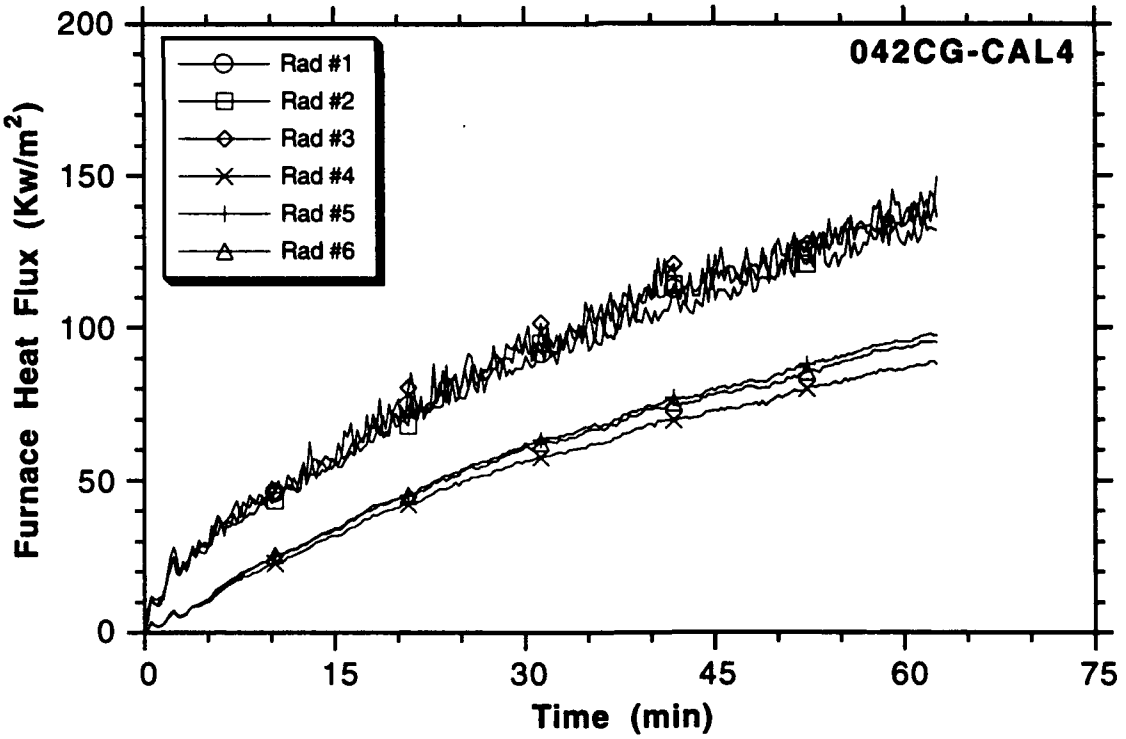
042CG-CAL4
Rad #1
Rad #2
Rad #3
Rad #4
Rad #5
Rad #6
Furnace Heat Flux (Kw/m^2)
Time (min)
0
50
100
150
200
0
15
30
45
60
75

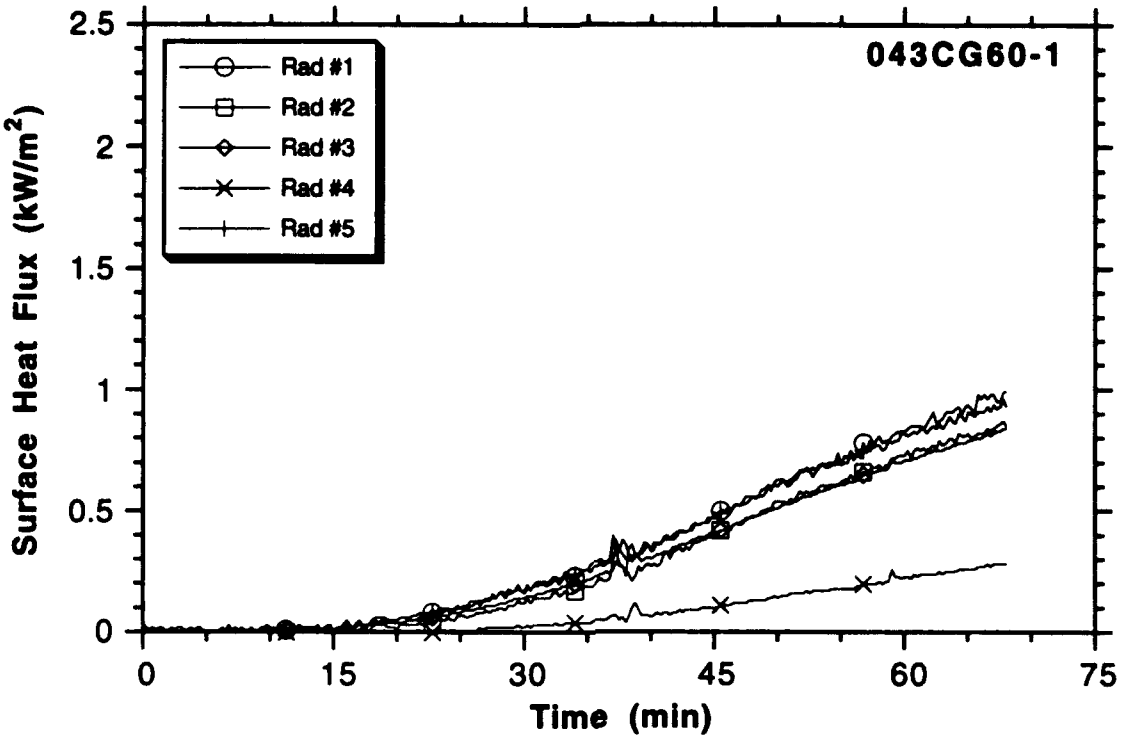
043CG60-1
Rad #1
Rad #2
Rad #3
Rad #4
Rad #5
Surface Heat Flux (kW/m^2)
Time (min)
0
0.5
1
1.5
2
2.5
0
15
30
45
60
75

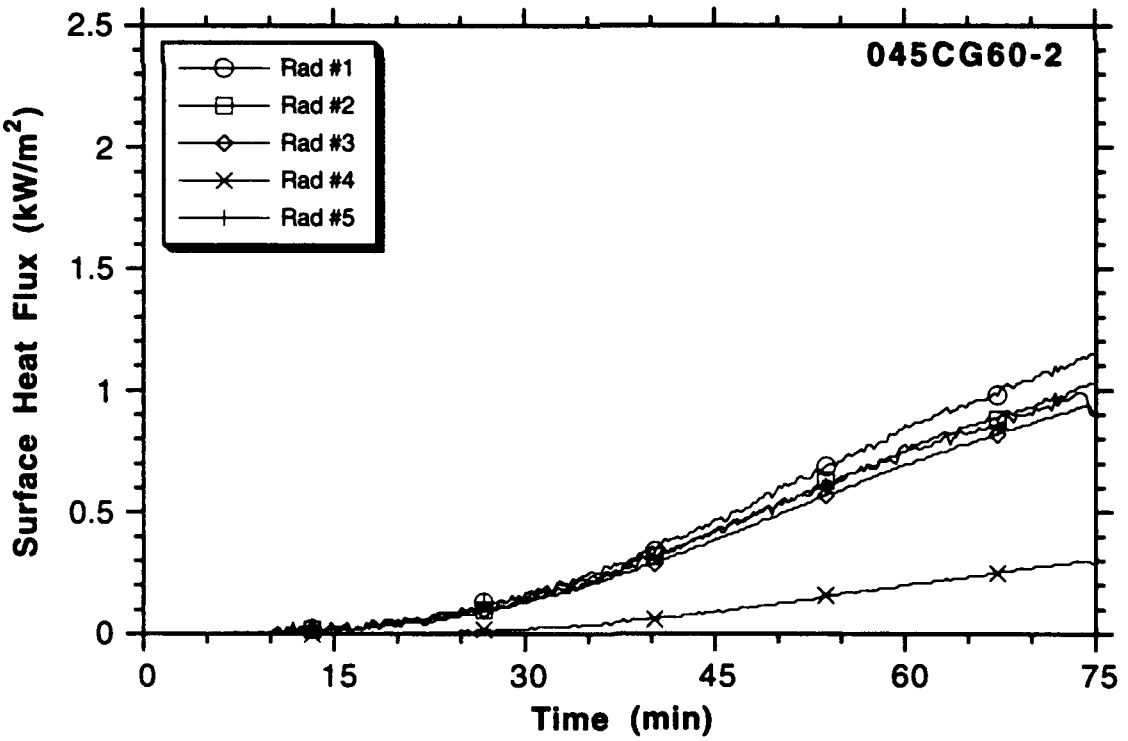
045CG60-2
Rad #1
Rad #2
Rad #3
Rad #4
Rad #5
Surface Heat Flux (kW/m^2)
Time (min)
0
0.5
1
1.5
2
2.5
0
15
30
45
60
75

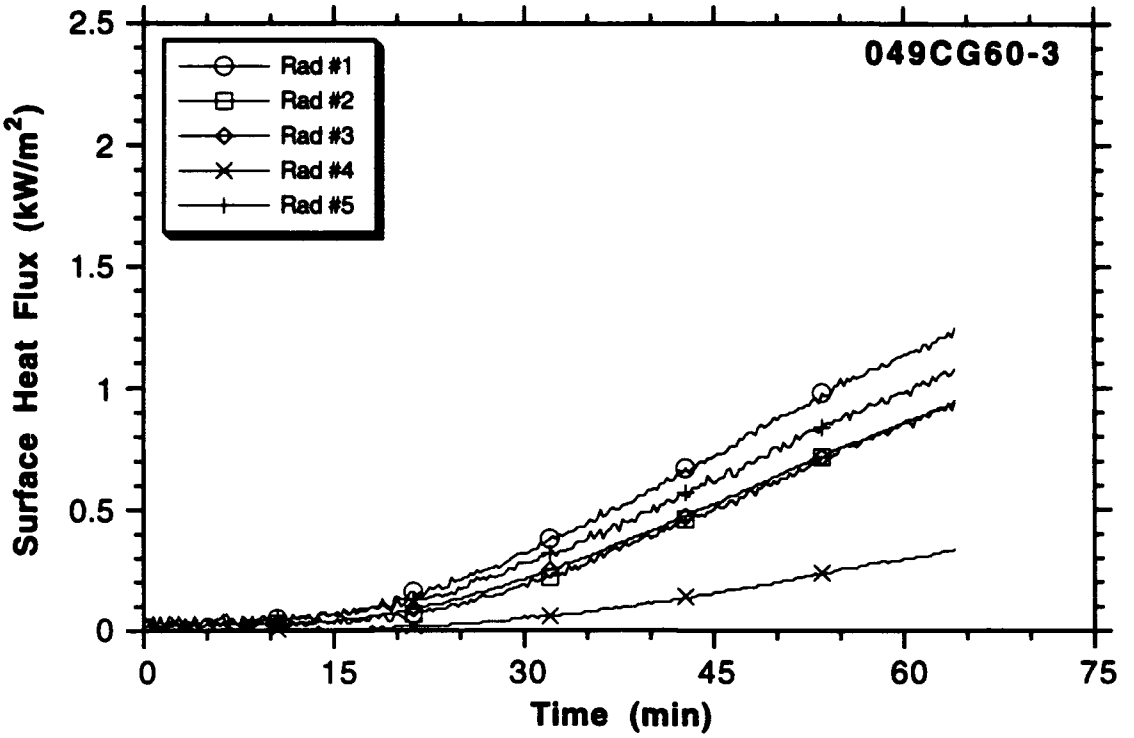
049CG60-3
Rad #1
Rad #2
Rad #3
Rad #4
Rad #5
Surface Heat Flux (kW/m^2)
Time (min)
0
0.5
1
1.5
2
2.5
0
15
30
45
60
75

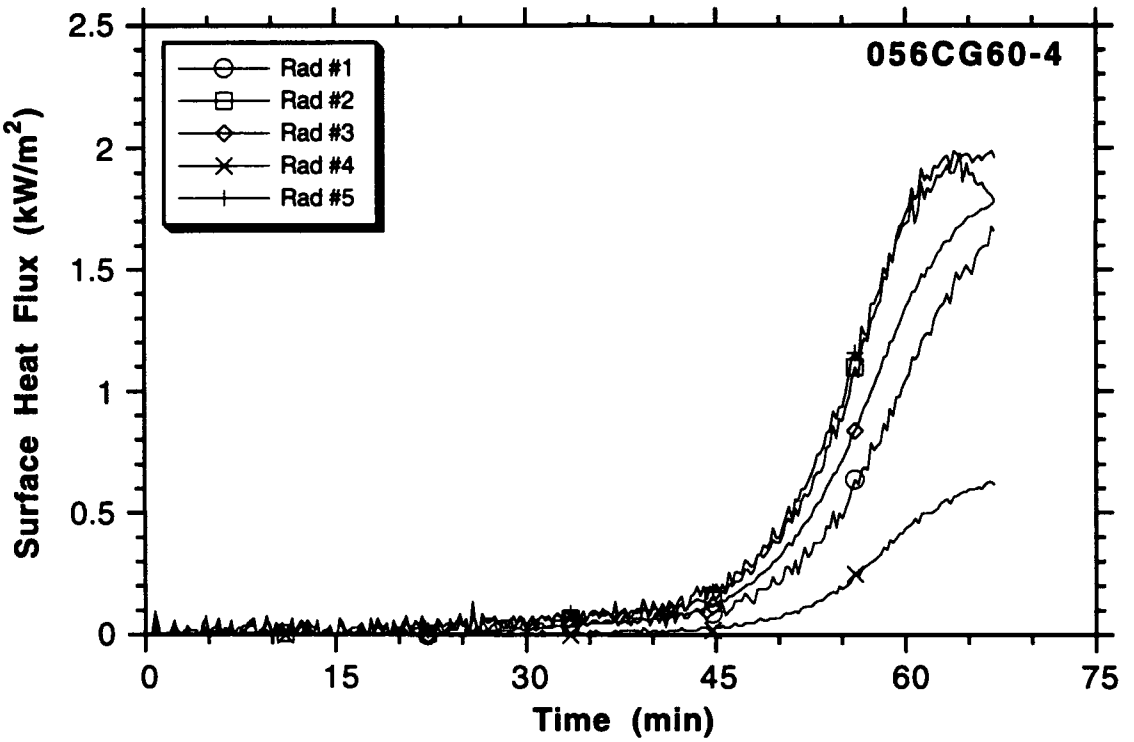
056CG60-4
Rad #1
Rad #2
Rad #3
Rad #4
Rad #5
Surface Heat Flux (kW/m^2)
Time (min)
0
0.5
1
1.5
2
2.5
0
15
30
45
60
75

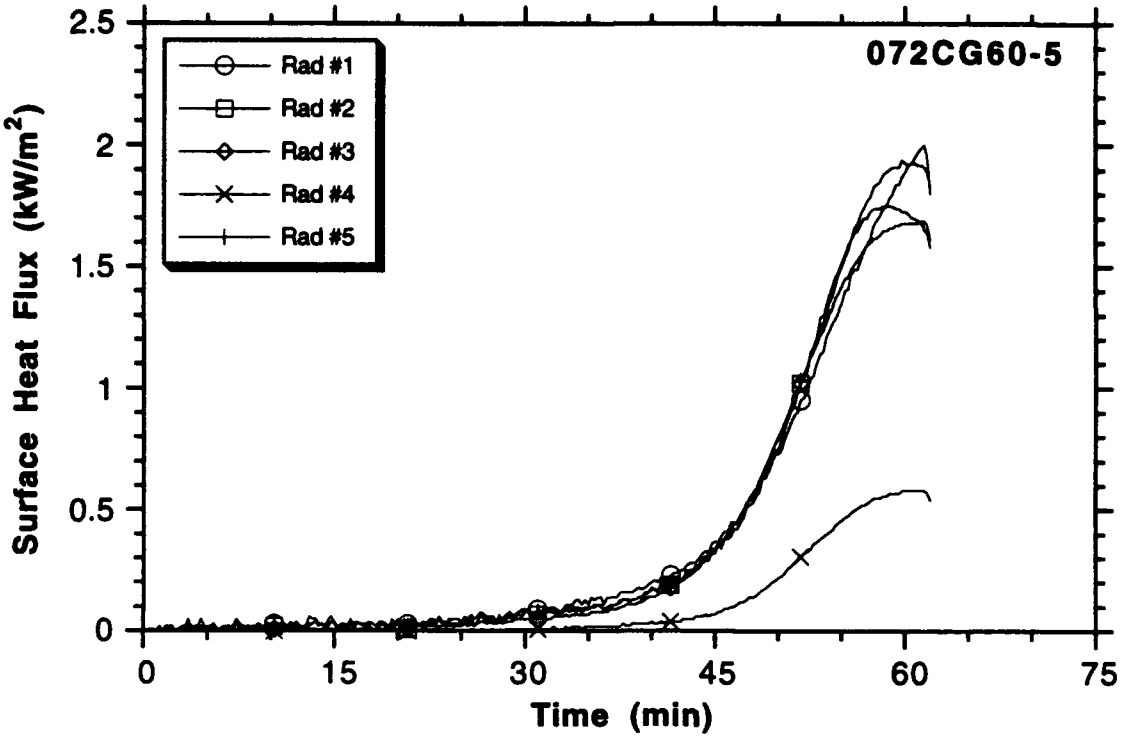
072CG60-5
Rad #1
Rad #2
Rad #3
Rad #4
Rad #5
Surface Heat Flux (kW/m^2)
Time (min)
0
0.5
1
1.5
2
2.5
0
15
30
45
60
75

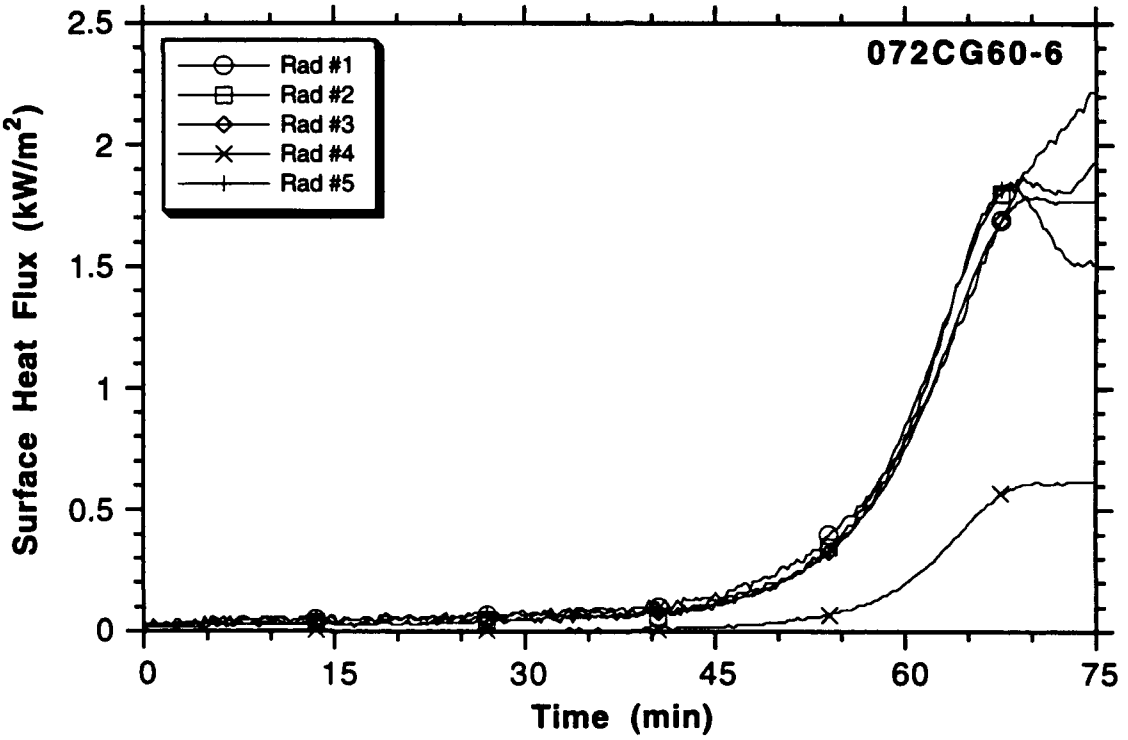
072CG60-6
Rad #1
Rad #2
Rad #3
Rad #4
Rad #5
Surface Heat Flux (kW/m^2)
Time (min)
0
0.5
1
1.5
2
2.5
0
15
30
45
60
75

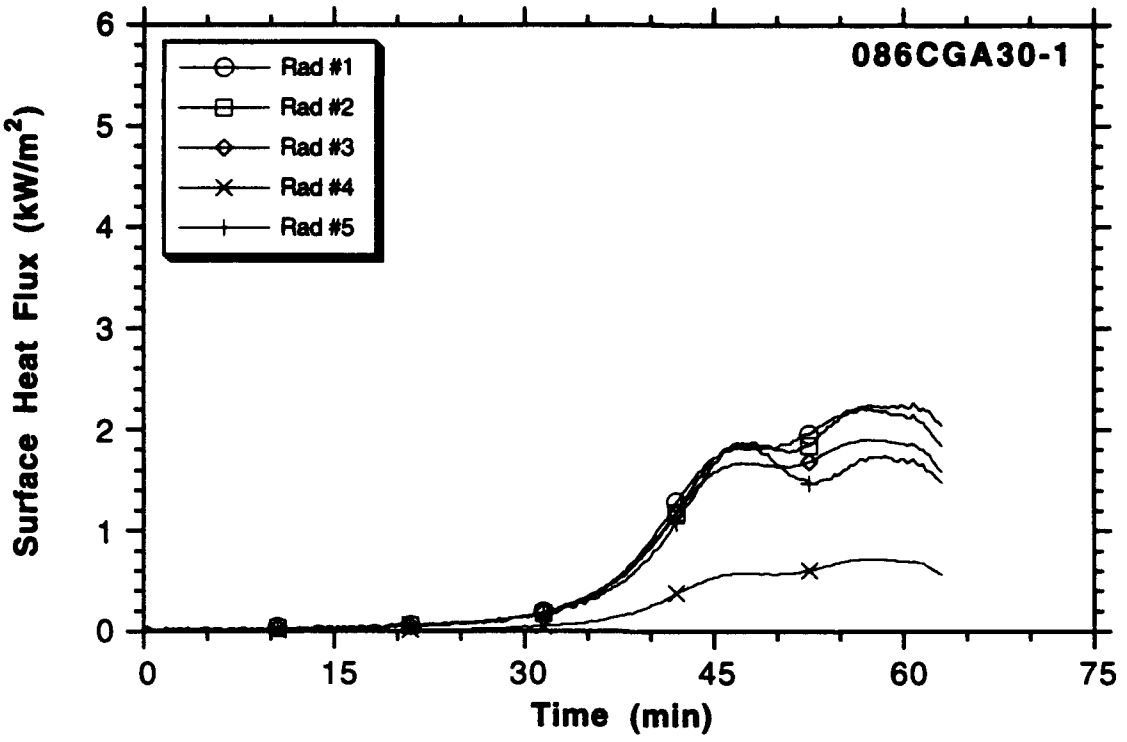
086CGA30-1
Rad #1
Rad #2
Rad #3
Rad #4
Rad #5
Surface Heat Flux (kW/m²)
Time (min)
0
15
30
45
60
75
1
2
3
4
5
6

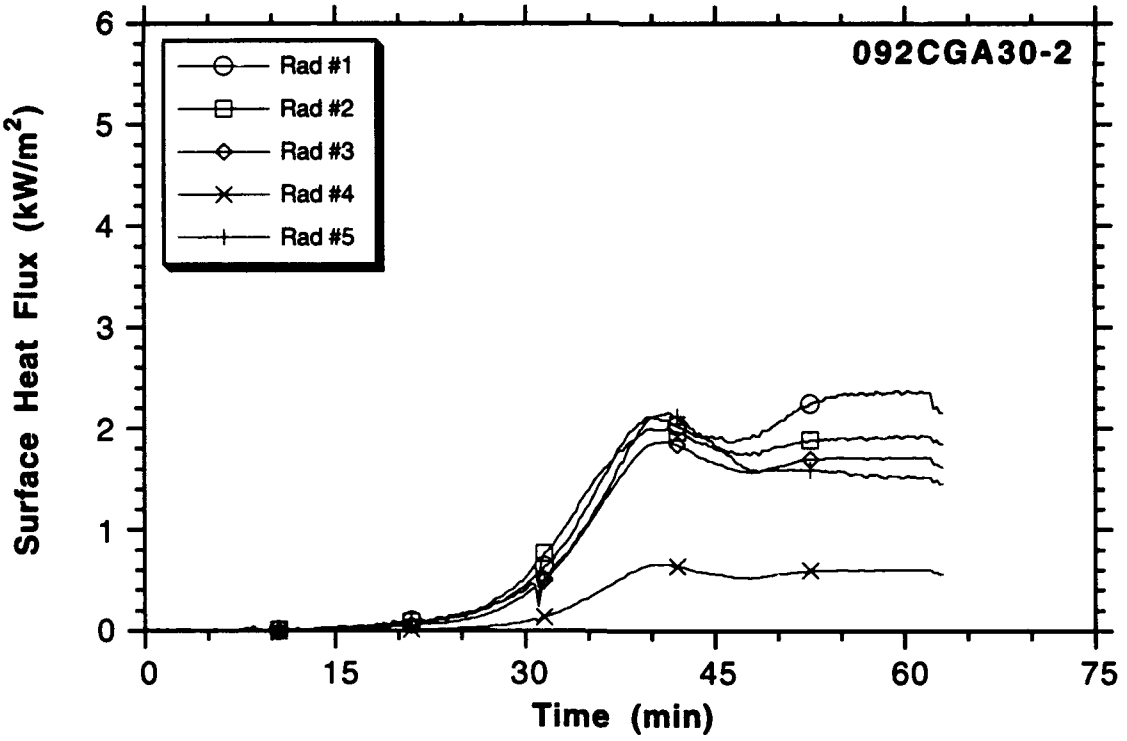
092CGA30-2
Rad #1
Rad #2
Rad #3
Rad #4
Rad #5
Surface Heat Flux (kW/m²)
Time (min)
0
15
30
45
60
75
1
2
3
4
5
6

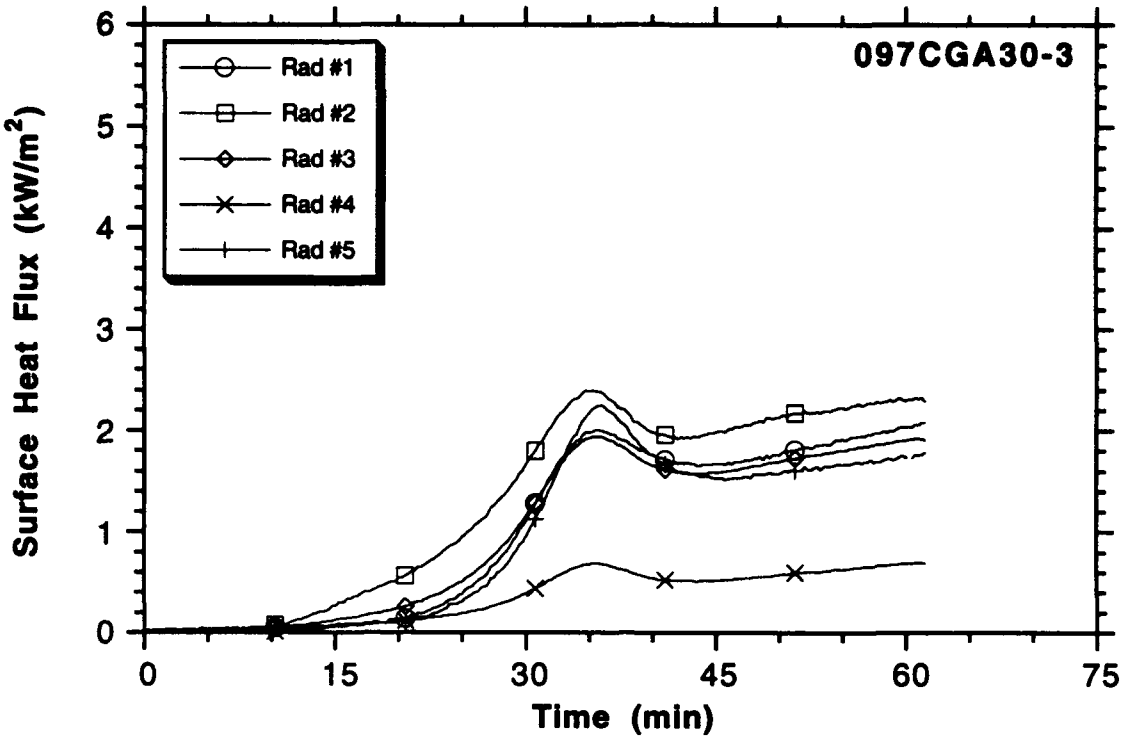
097CGA30-3
Rad #1
Rad #2
Rad #3
Rad #4
Rad #5
Surface Heat Flux (kW/m²)
Time (min)
0
1
2
3
4
5
6
0
15
30
45
60
75

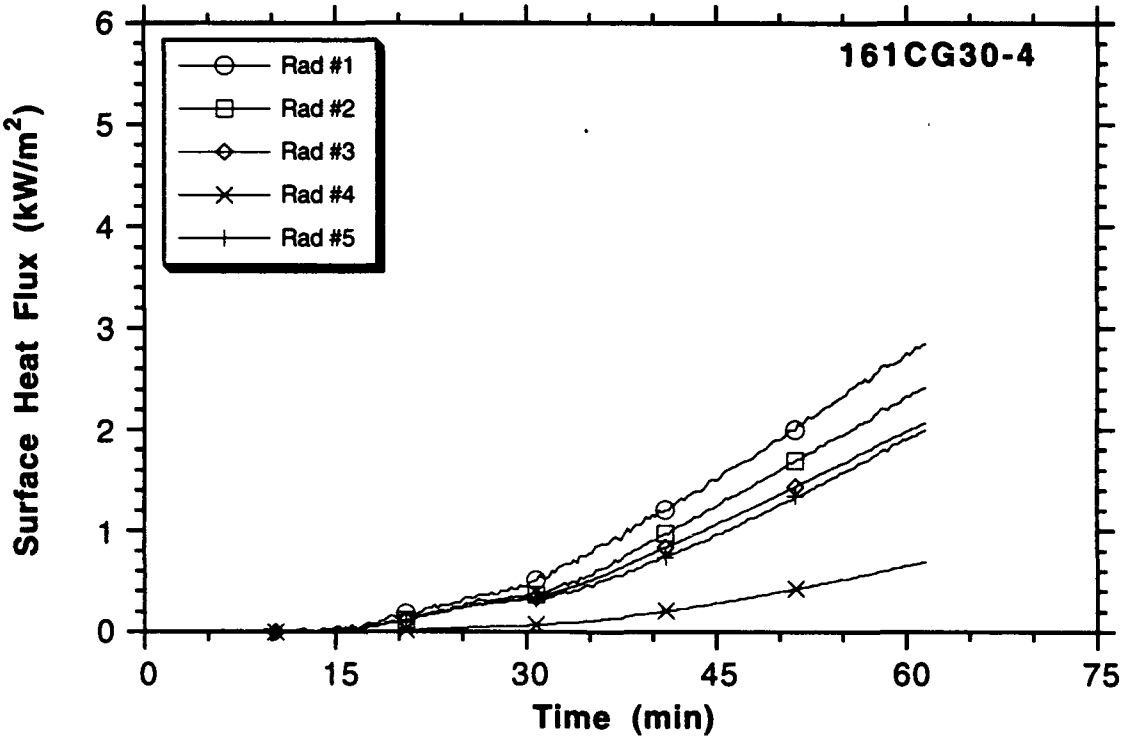
161CG30-4
Rad #1
Rad #2
Rad #3
Rad #4
Rad #5
Surface Heat Flux (kW/m²)
Time (min)
0
1
2
3
4
5
6
0
15
30
45
60
75

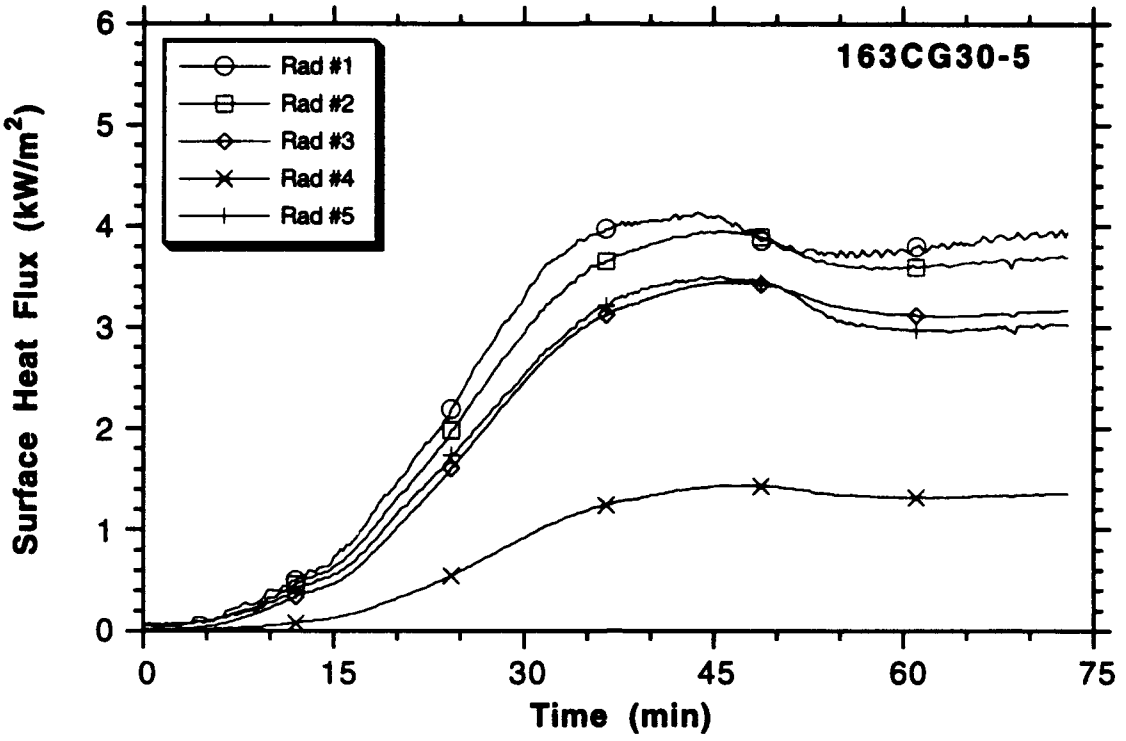
163CG30-5
Rad #1
Rad #2
Rad #3
Rad #4
Rad #5
Surface Heat Flux (kW/m^2)
Time (min)
0
1
2
3
4
5
6
0
15
30
45
60
75

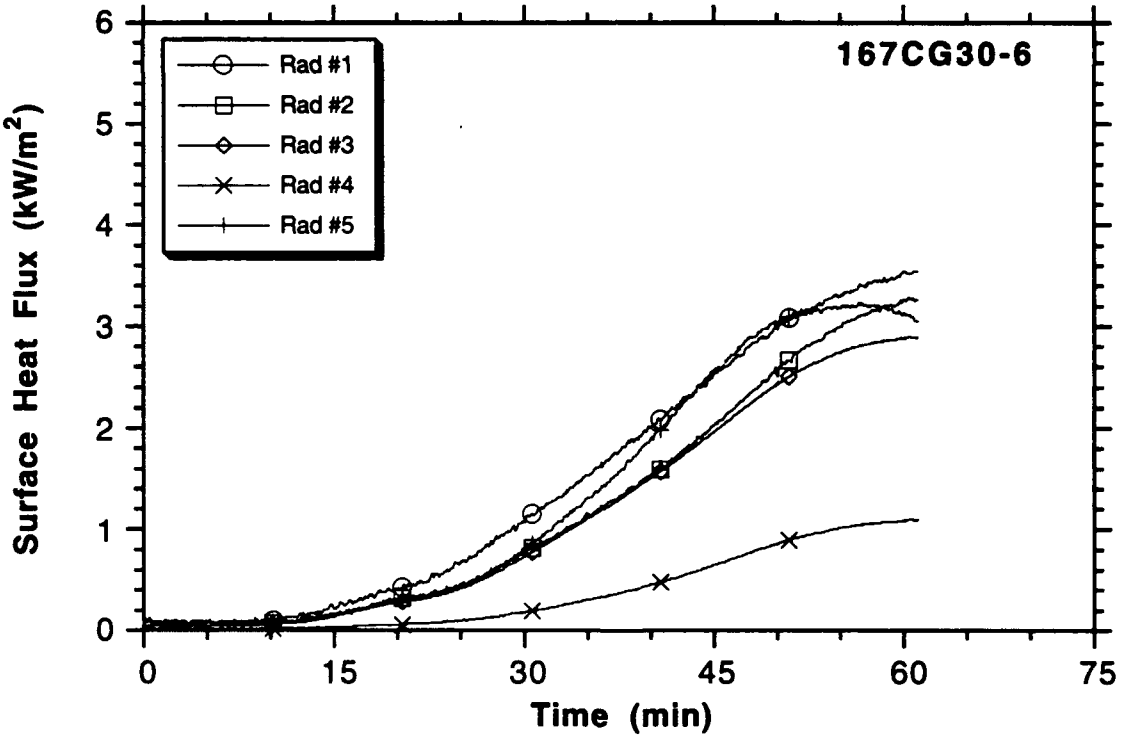
167CG30-6
Rad #1
Rad #2
Rad #3
Rad #4
Rad #5
Surface Heat Flux (kW/m^2)
Time (min)
0
1
2
3
4
5
6
0
15
30
45
60
75

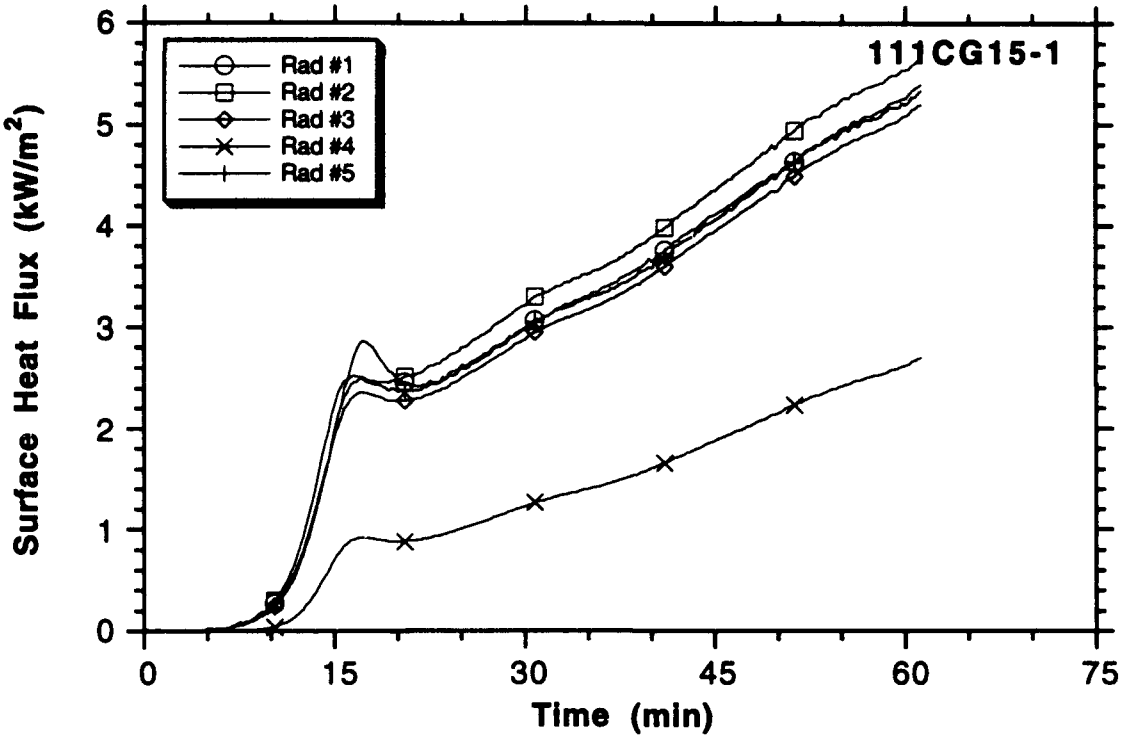
111CG15-1
Rad #1
Rad #2
Rad #3
Rad #4
Rad #5
Surface Heat Flux (kW/m²)
Time (min)
0
1
2
3
4
5
6
0
15
30
45
60
75

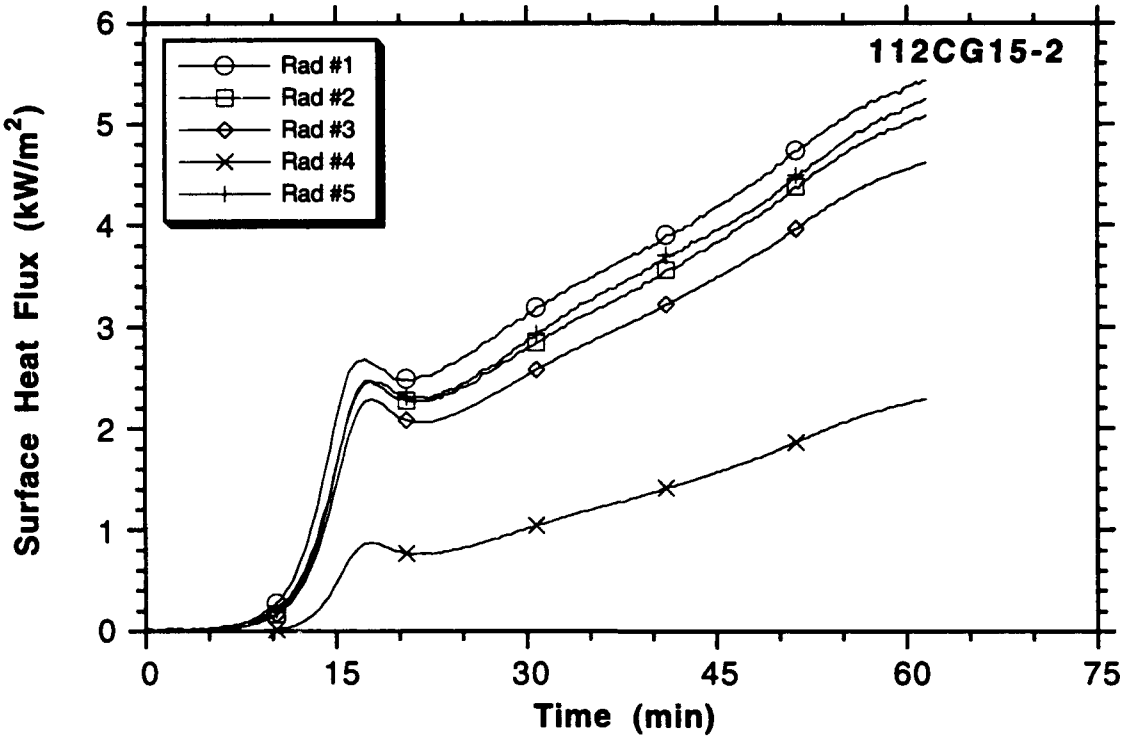
112CG15-2
Rad #1
Rad #2
Rad #3
Rad #4
Rad #5
Surface Heat Flux (kW/m²)
Time (min)
0
1
2
3
4
5
6
0
15
30
45
60
75

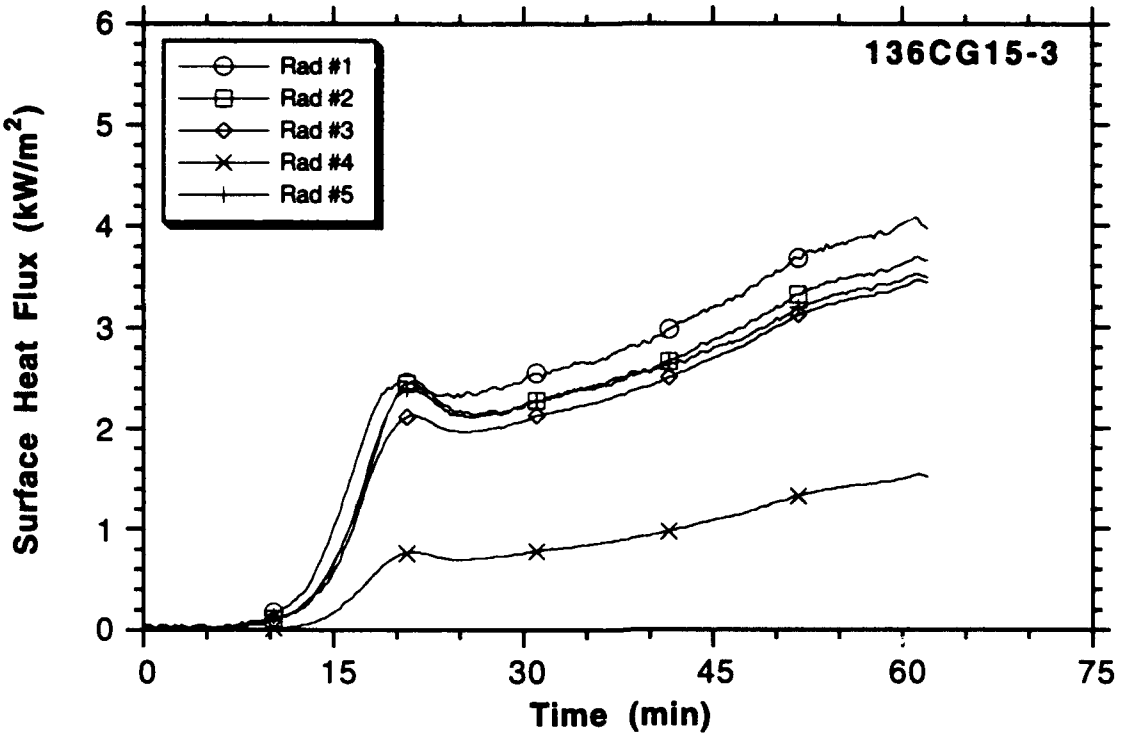
136CG15-3
Rad #1
Rad #2
Rad #3
Rad #4
Rad #5
Surface Heat Flux (kW/m²)
Time (min)
0
1
2
3
4
5
6
0
15
30
45
60
75

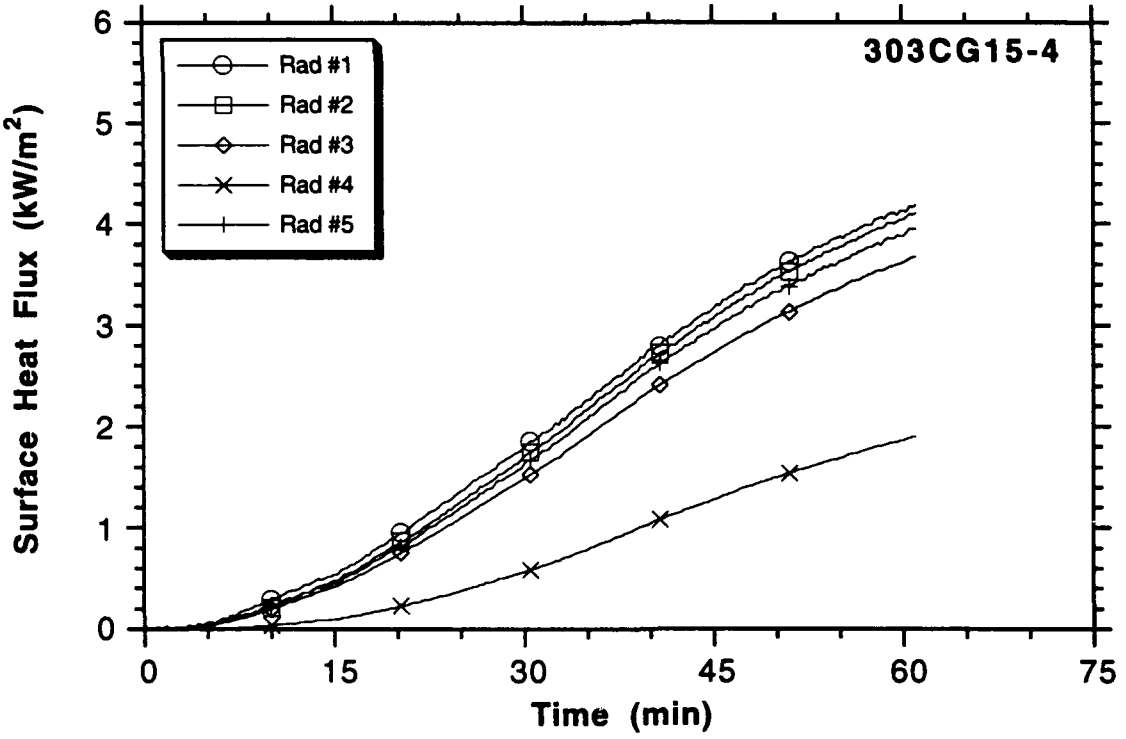
303CG15-4
Rad #1
Rad #2
Rad #3
Rad #4
Rad #5
Surface Heat Flux (kW/m²)
Time (min)
0
1
2
3
4
5
6
0
15
30
45
60
75

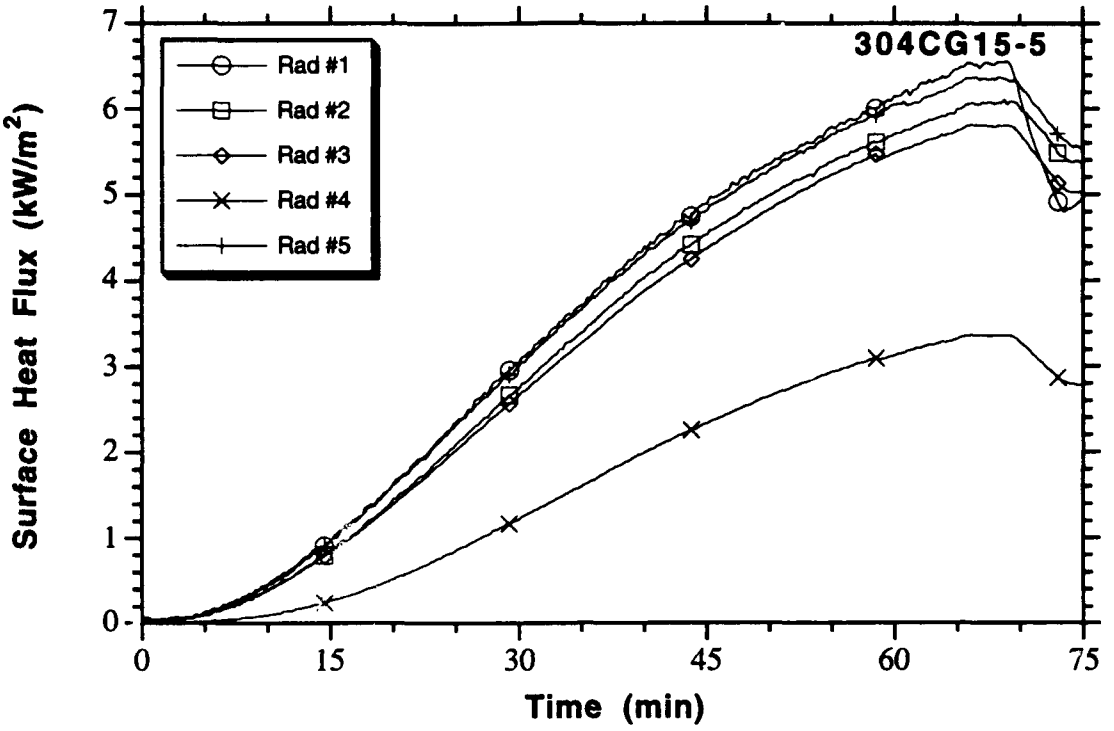
304CG15-5
Rad #1
Rad #2
Rad #3
Rad #4
Rad #5
Surface Heat Flux (kW/m²)
Time (min)
0
1
2
3
4
5
6
7
0
15
30
45
60
75

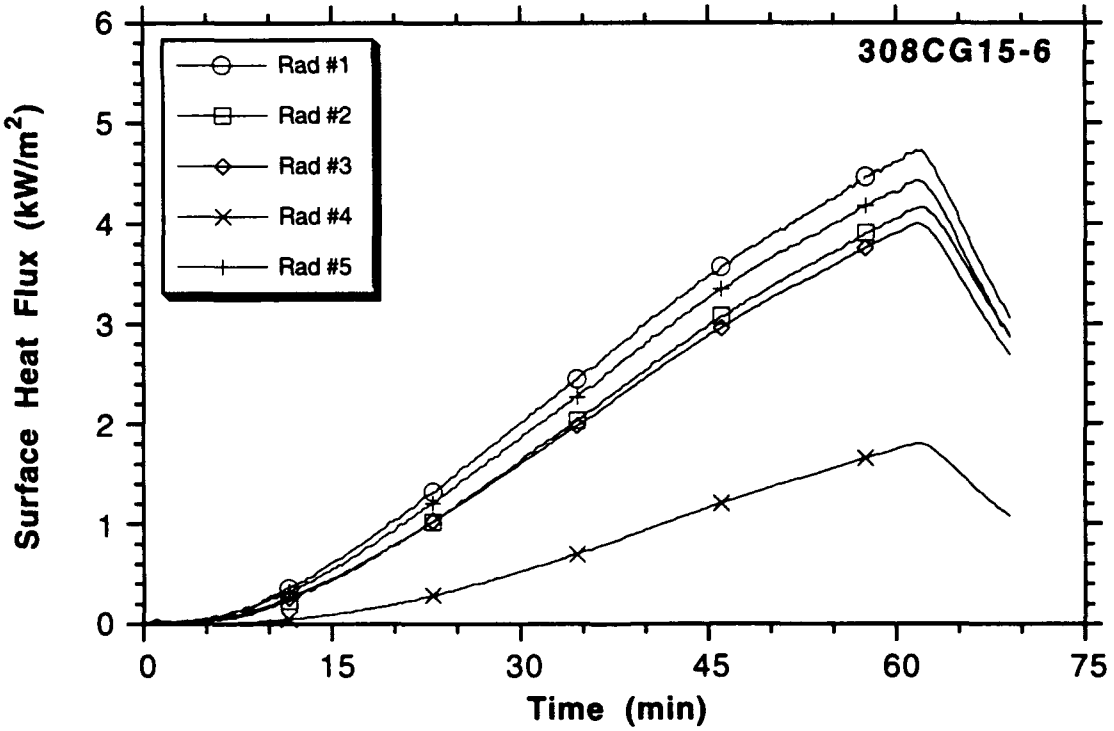
308CG15-6
Rad #1
Rad #2
Rad #3
Rad #4
Rad #5
Surface Heat Flux (kW/m²)
Time (min)
0
1
2
3
4
5
6
0
15
30
45
60
75

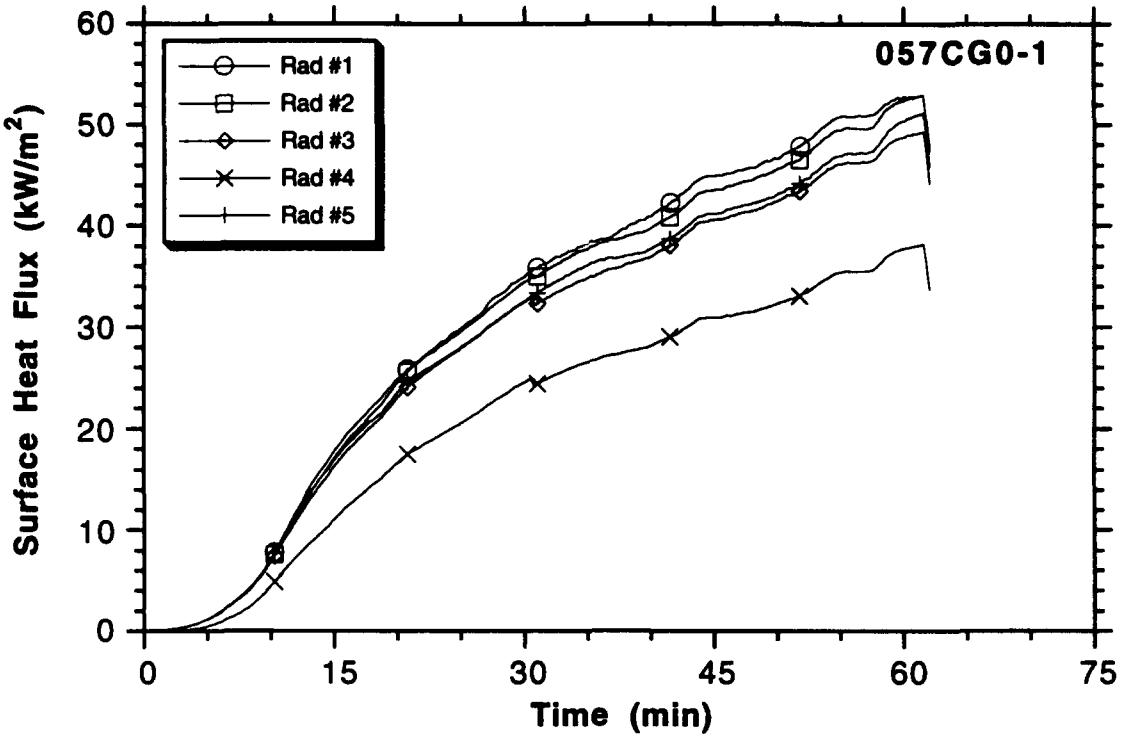
057CG0-1
Rad #1
Rad #2
Rad #3
Rad #4
Rad #5
Surface Heat Flux (kW/m²)
Time (min)
0
10
20
30
40
50
60
0
15
30
45
60
75

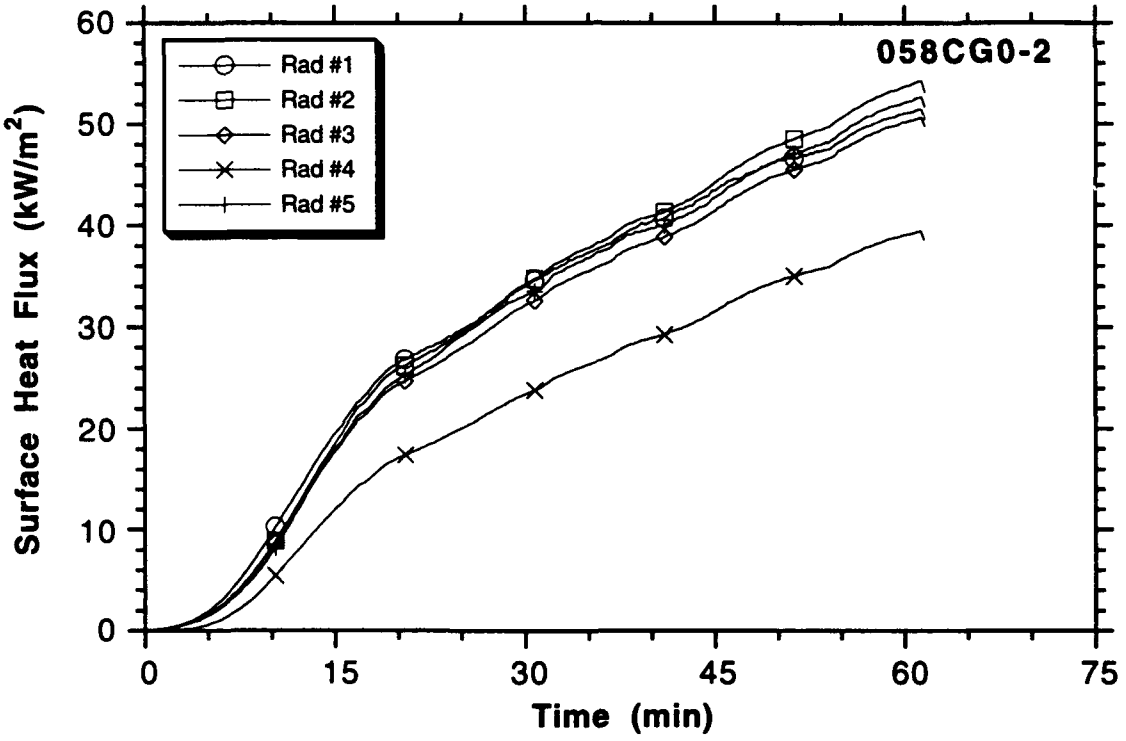
058CG0-2
Rad #1
Rad #2
Rad #3
Rad #4
Rad #5
Surface Heat Flux (kW/m²)
Time (min)
0
10
20
30
40
50
60
0
15
30
45
60
75

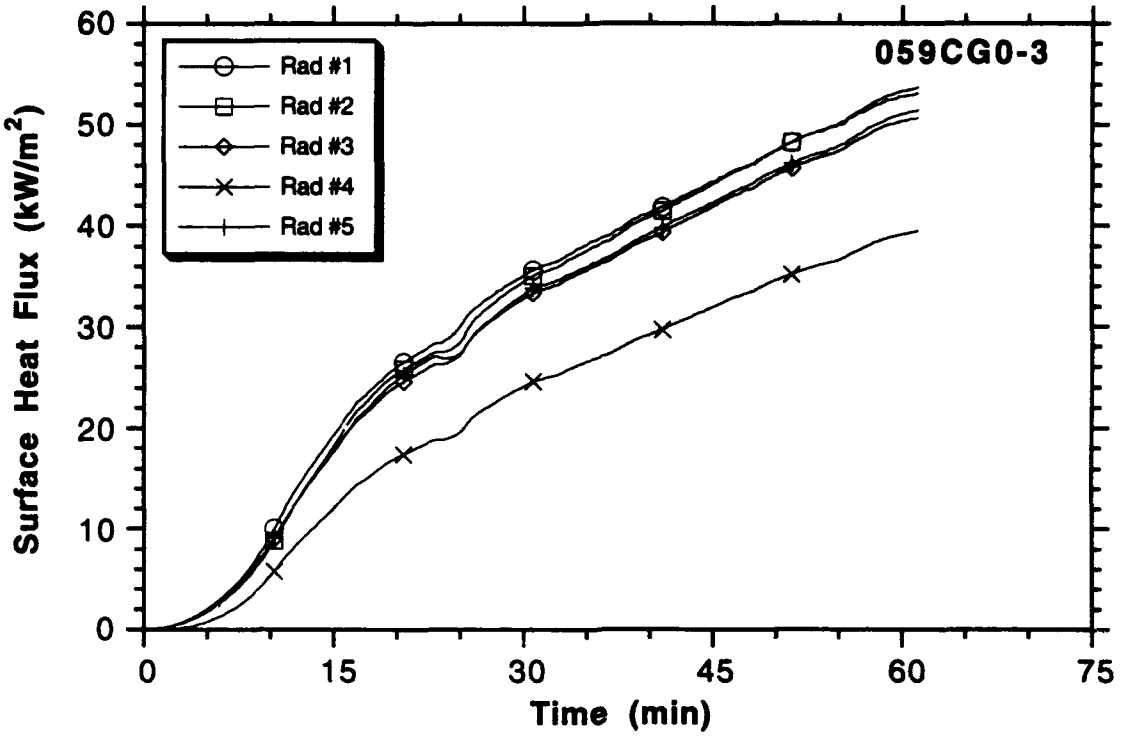
059CG0-3
Rad #1
Rad #2
Rad #3
Rad #4
Rad #5
Surface Heat Flux (kW/m^2)
Time (min)
0
10
20
30
40
50
60
0
15
30
45
60
75

Appendix D

Surface Temperatures During Bulkhead Tests

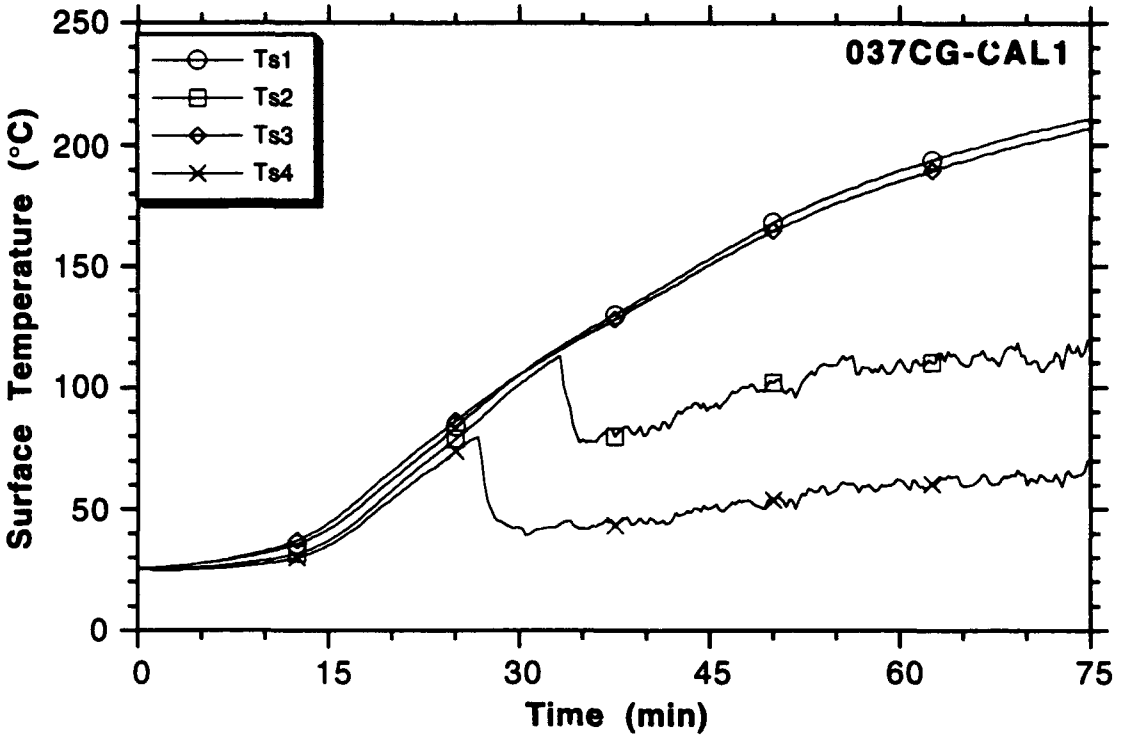
037CG-CAL1
Ts1
Ts2
Ts3
Ts4
Surface Temperature (°C)
Time (min)
0
50
100
150
200
250
0
15
30
45
60
75

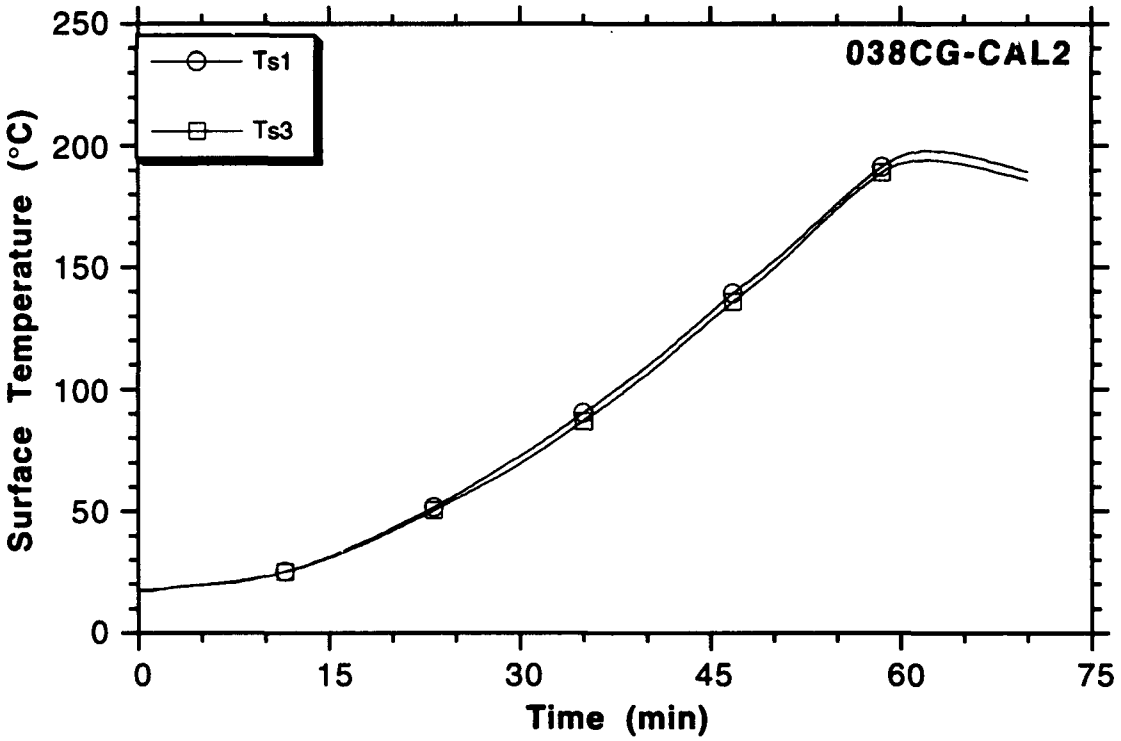
038CG-CAL2
Ts1
Ts3
Surface Temperature (°C)
Time (min)
0
50
100
150
200
250
0
15
30
45
60
75

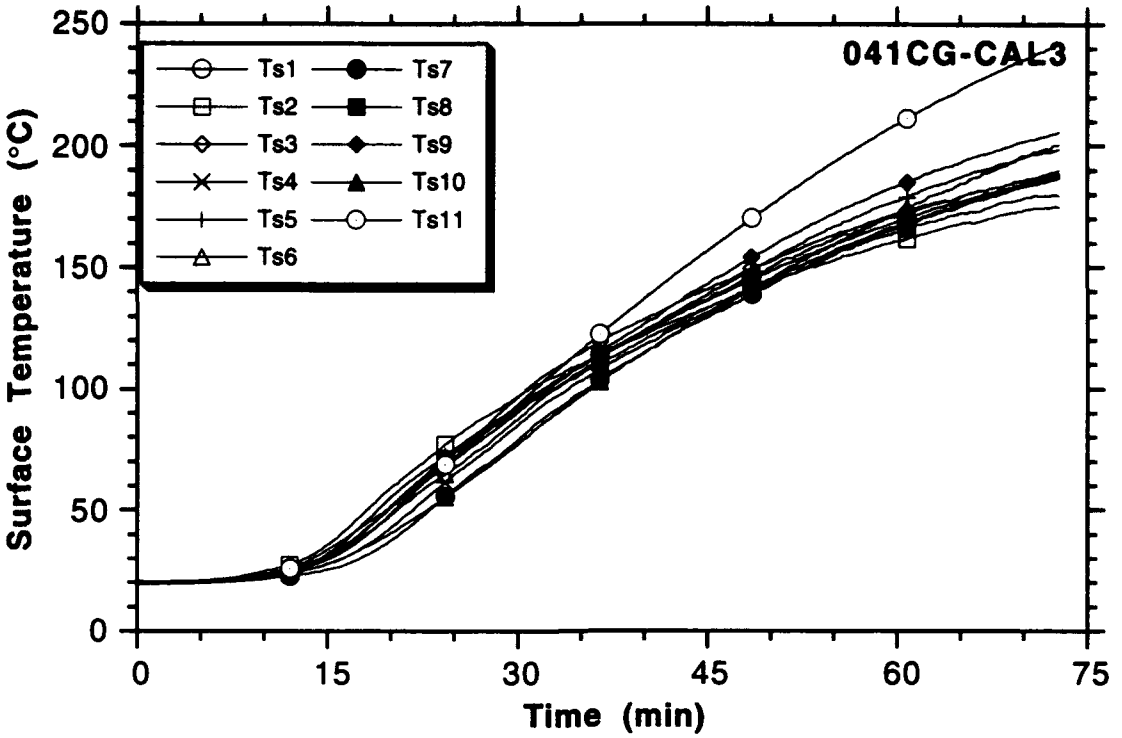
041CG-CAL3
Ts1
Ts2
Ts3
Ts4
Ts5
Ts6
Ts7
Ts8
Ts9
Ts10
Ts11
Surface Temperature (°C)
Time (min)
0
50
100
150
200
250
0
15
30
45
60
75

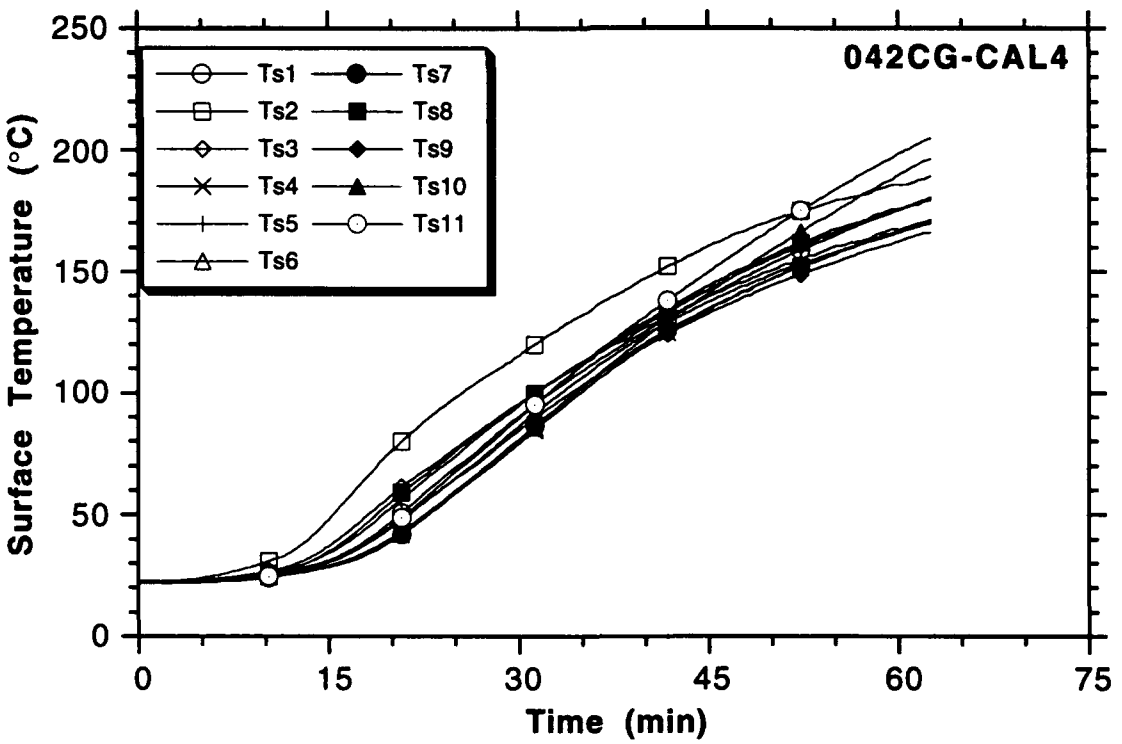
042CG-CAL4
Ts1
Ts2
Ts3
Ts4
Ts5
Ts6
Ts7
Ts8
Ts9
Ts10
Ts11
Surface Temperature (°C)
Time (min)
0
50
100
150
200
250
0
15
30
45
60
75

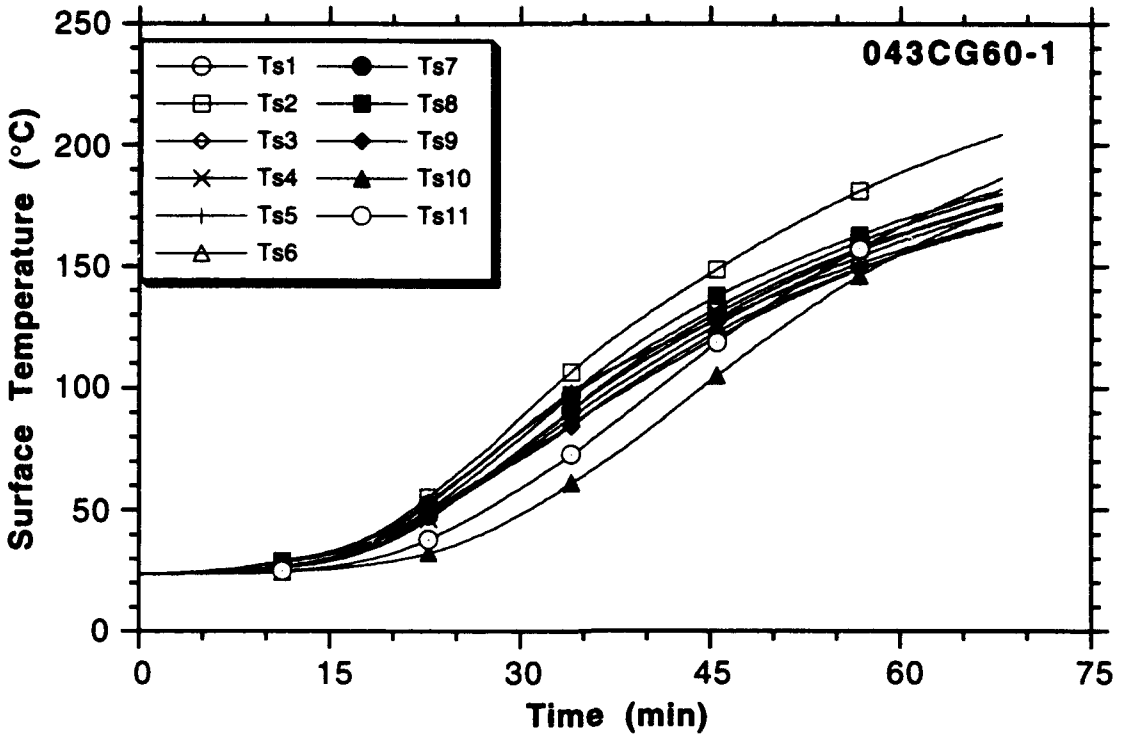
043CG60-1
Ts1
Ts2
Ts3
Ts4
Ts5
Ts6
Ts7
Ts8
Ts9
Ts10
Ts11
Surface Temperature (°C)
Time (min)
0
50
100
150
200
250
0
15
30
45
60
75

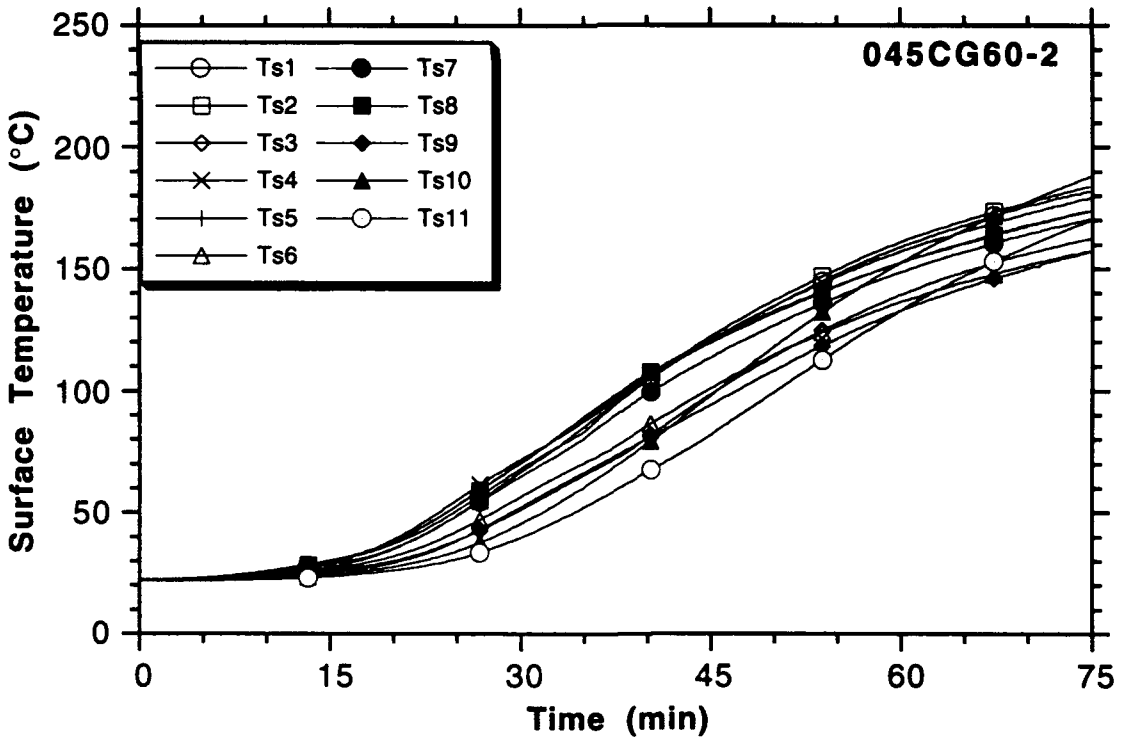
045CG60-2
Ts1
Ts2
Ts3
Ts4
Ts5
Ts6
Ts7
Ts8
Ts9
Ts10
Ts11
Surface Temperature (°C)
Time (min)
0
50
100
150
200
250
0
15
30
45
60
75

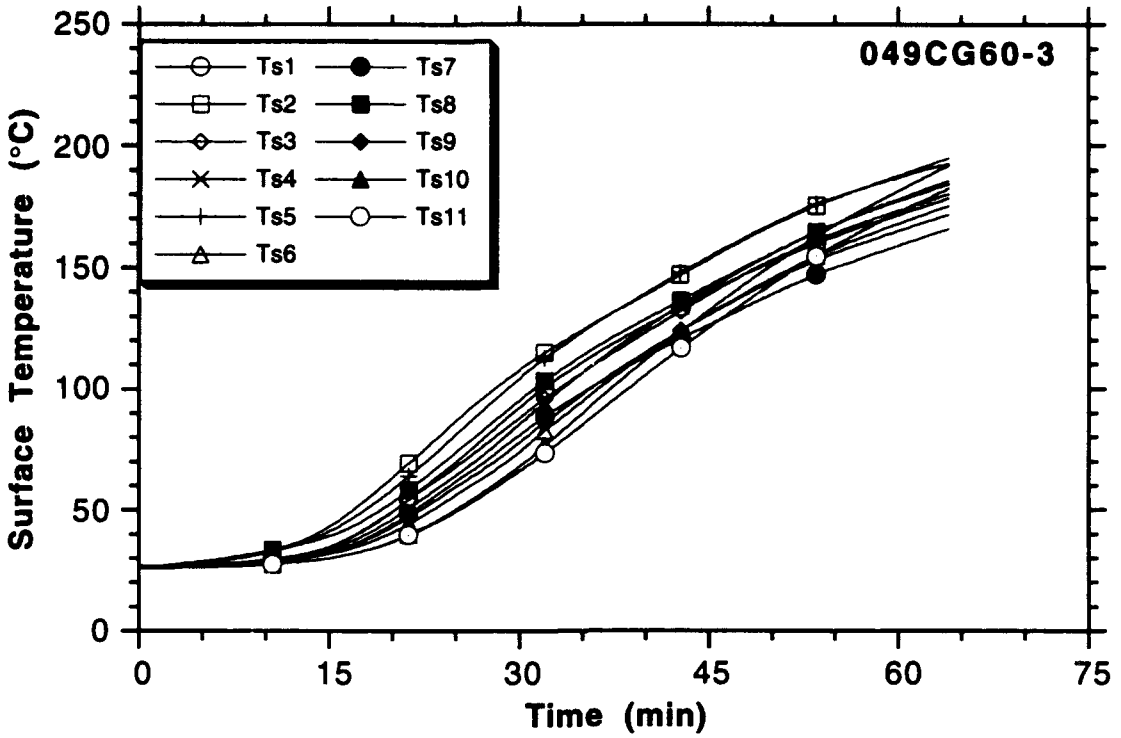
049CG60-3
Ts1
Ts2
Ts3
Ts4
Ts5
Ts6
Ts7
Ts8
Ts9
Ts10
Ts11
Surface Temperature (°C)
Time (min)
0
50
100
150
200
250
0
15
30
45
60
75

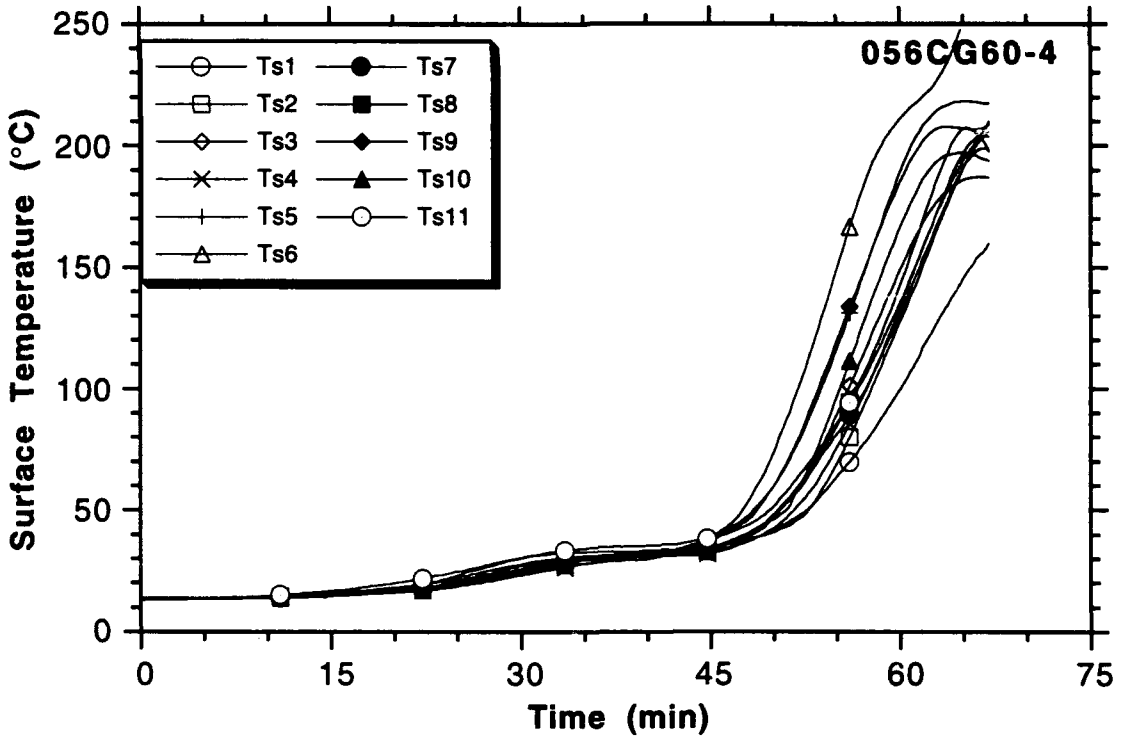
056CG60-4
Ts1
Ts2
Ts3
Ts4
Ts5
Ts6
Ts7
Ts8
Ts9
Ts10
Ts11
Surface Temperature (°C)
Time (min)
0
50
100
150
200
250
0
15
30
45
60
75

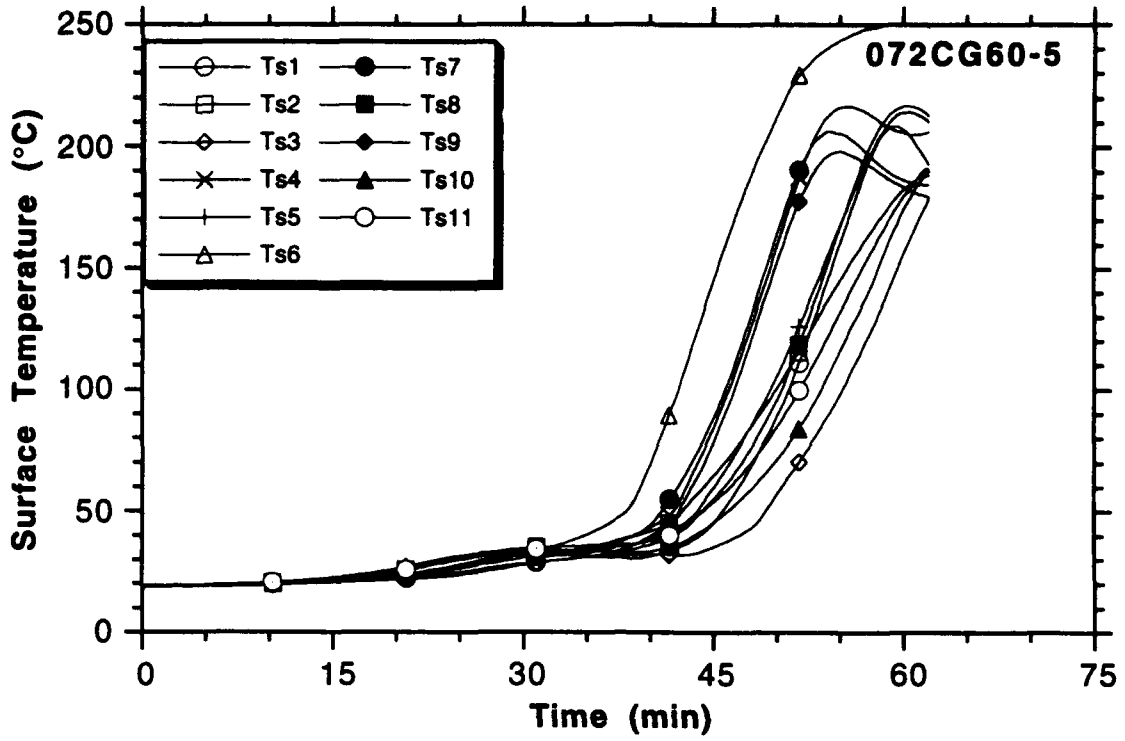
072CG60-5
Ts1
Ts2
Ts3
Ts4
Ts5
Ts6
Ts7
Ts8
Ts9
Ts10
Ts11
Surface Temperature (°C)
Time (min)
0
50
100
150
200
250
0
15
30
45
60
75

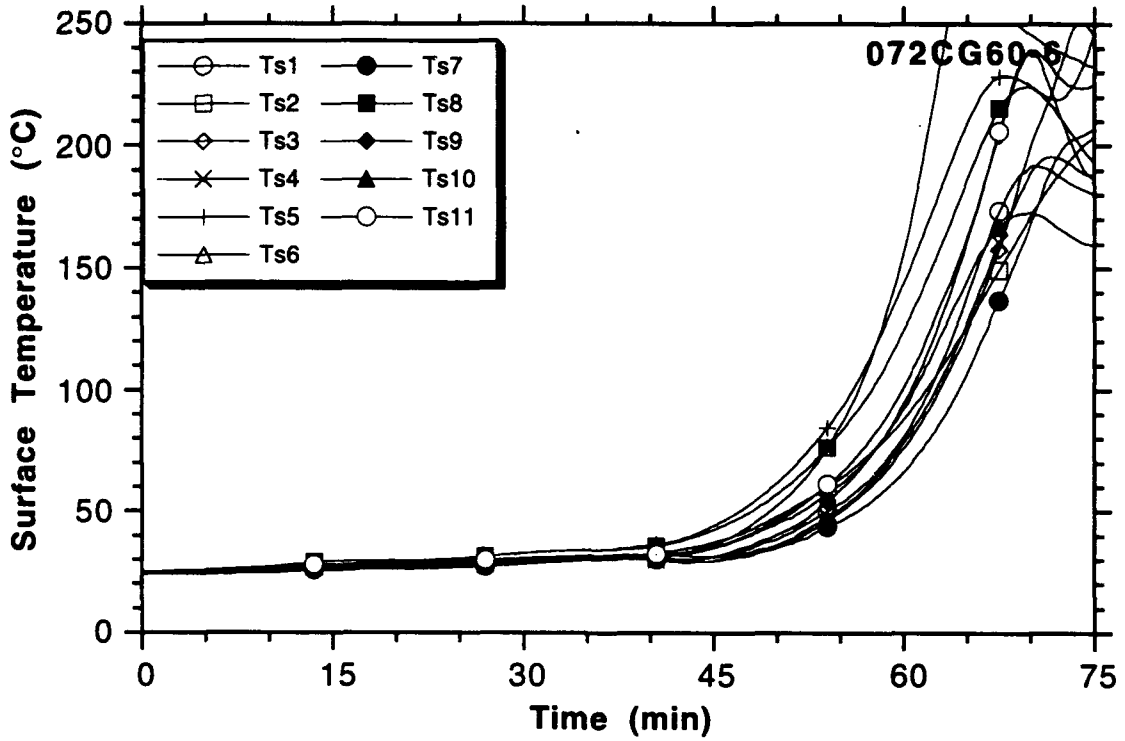
072CG60-6
Ts1
Ts2
Ts3
Ts4
Ts5
Ts6
Ts7
Ts8
Ts9
Ts10
Ts11
Surface Temperature (°C)
Time (min)
0
50
100
150
200
250
0
15
30
45
60
75

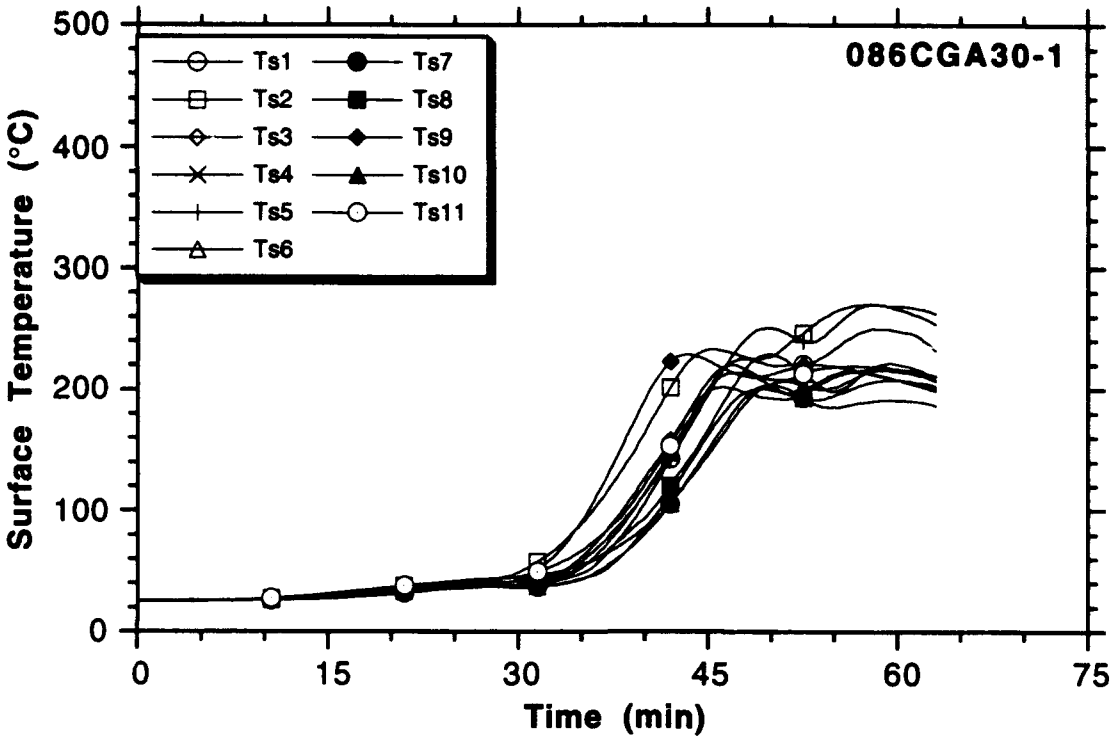
086CGA30-1
Ts1
Ts2
Ts3
Ts4
Ts5
Ts6
Ts7
Ts8
Ts9
Ts10
Ts11
Surface Temperature (°C)
Time (min)
0
100
200
300
400
500
0
15
30
45
60
75

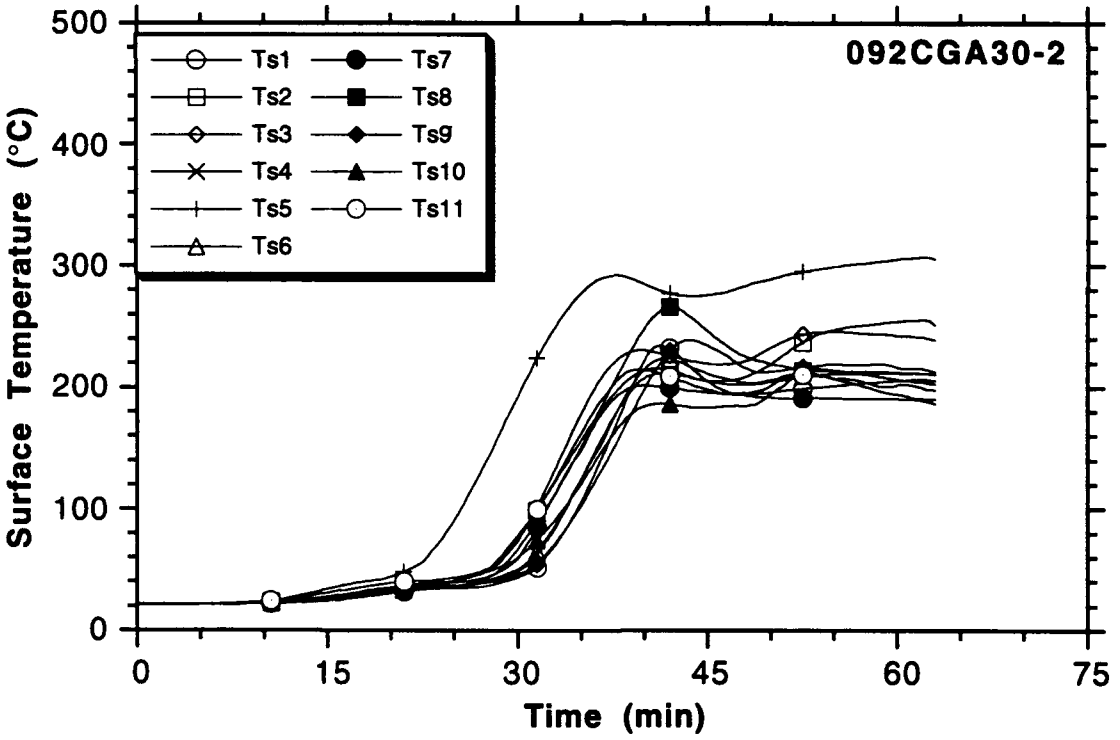
092CGA30-2
Ts1
Ts2
Ts3
Ts4
Ts5
Ts6
Ts7
Ts8
Ts9
Ts10
Ts11
Surface Temperature (°C)
Time (min)
0
100
200
300
400
500
0
15
30
45
60
75

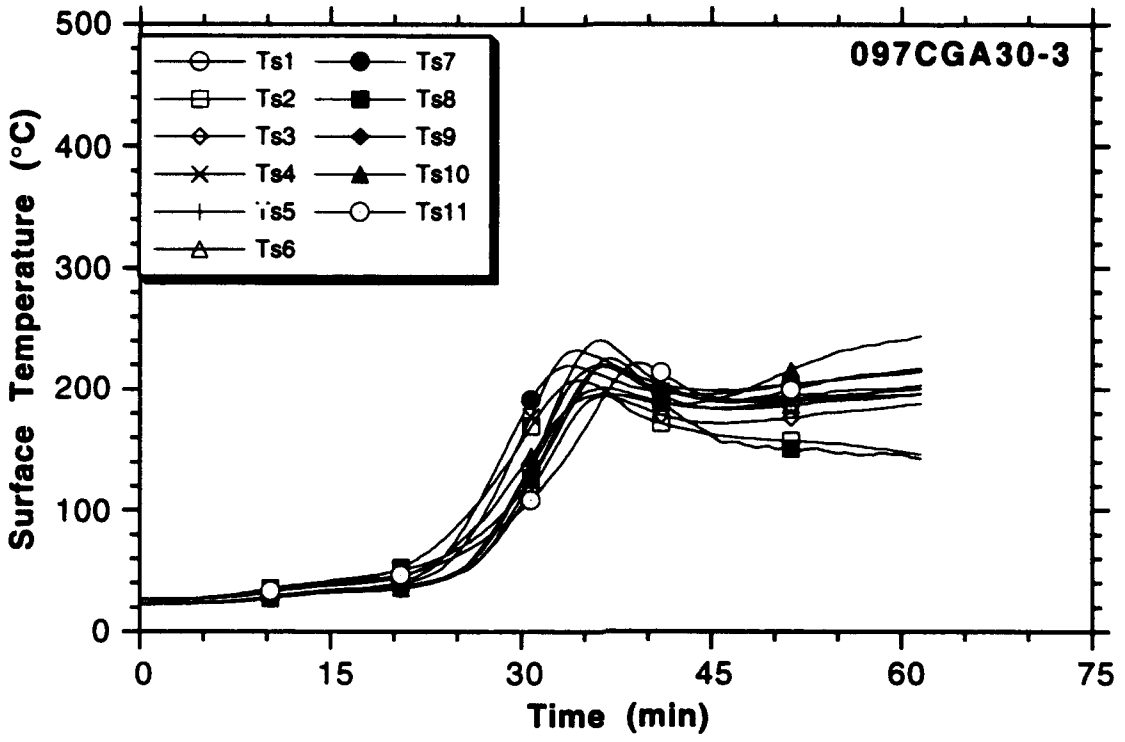
097CGA30-3
Ts1
Ts2
Ts3
Ts4
Ts5
Ts6
Ts7
Ts8
Ts9
Ts10
Ts11
Surface Temperature (°C)
Time (min)
0
100
200
300
400
500
0
15
30
45
60
75

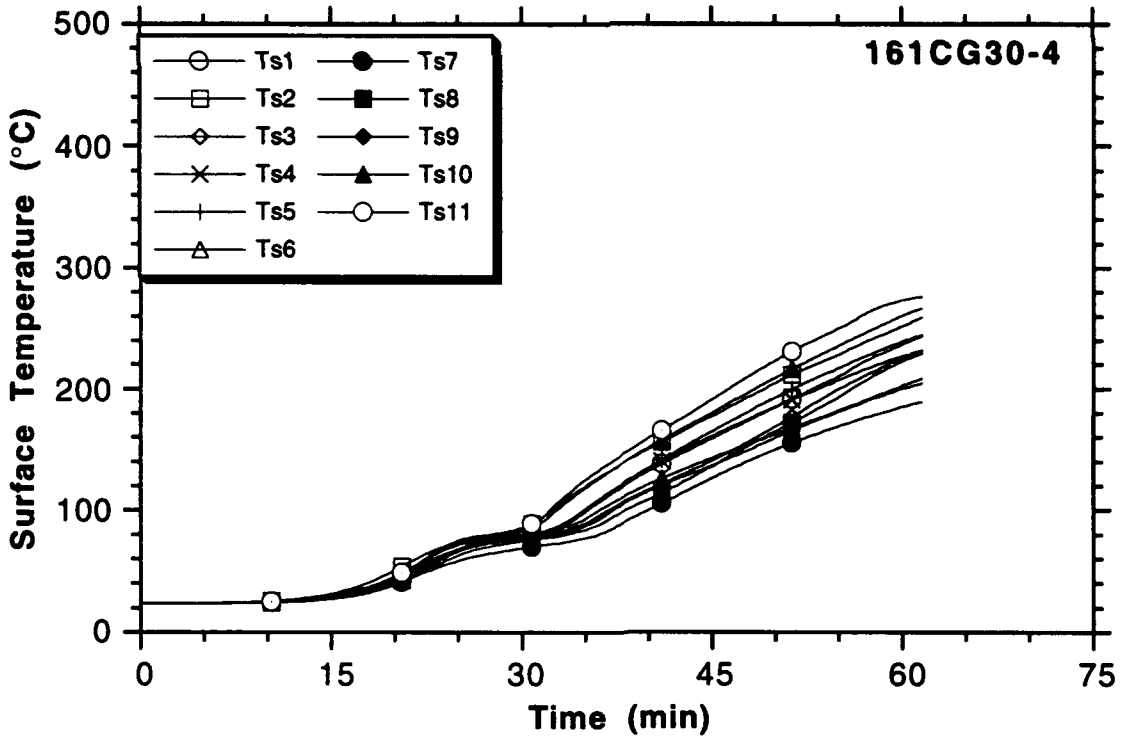
161CG30-4
Ts1
Ts2
Ts3
Ts4
Ts5
Ts6
Ts7
Ts8
Ts9
Ts10
Ts11
Surface Temperature (°C)
Time (min)
0
100
200
300
400
500
0
15
30
45
60
75

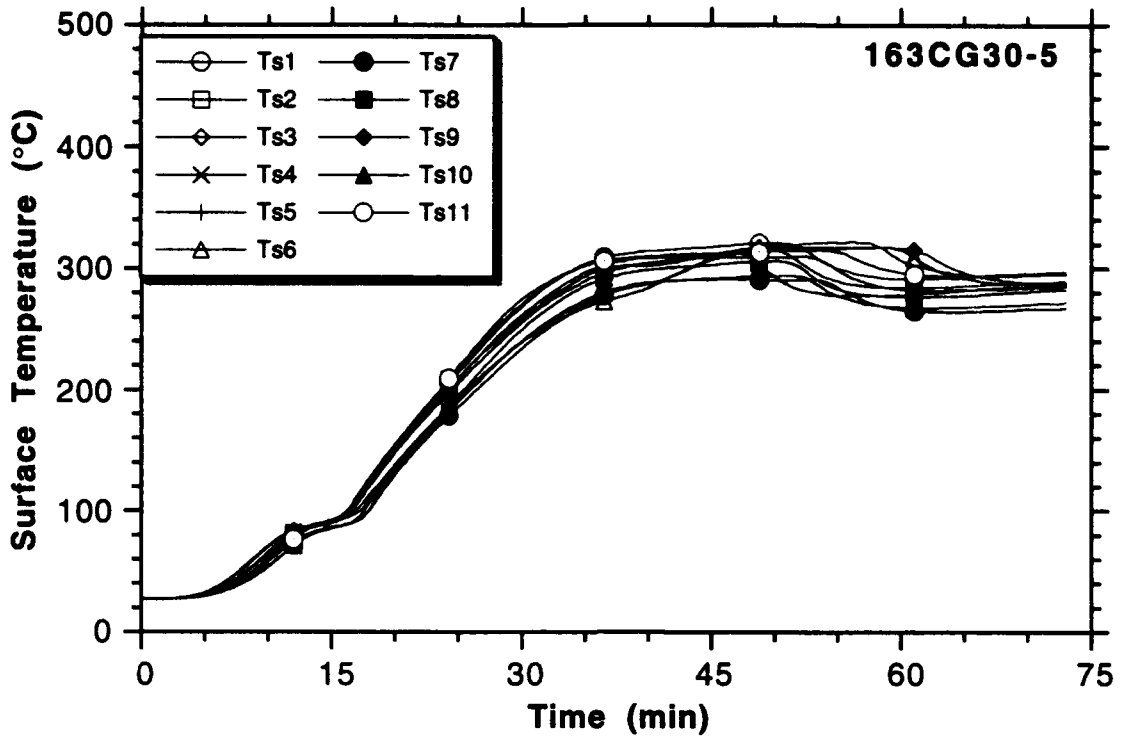
163CG30-5
Ts1
Ts2
Ts3
Ts4
Ts5
Ts6
Ts7
Ts8
Ts9
Ts10
Ts11
Surface Temperature (°C)
Time (min)
0
100
200
300
400
500
0
15
30
45
60
75

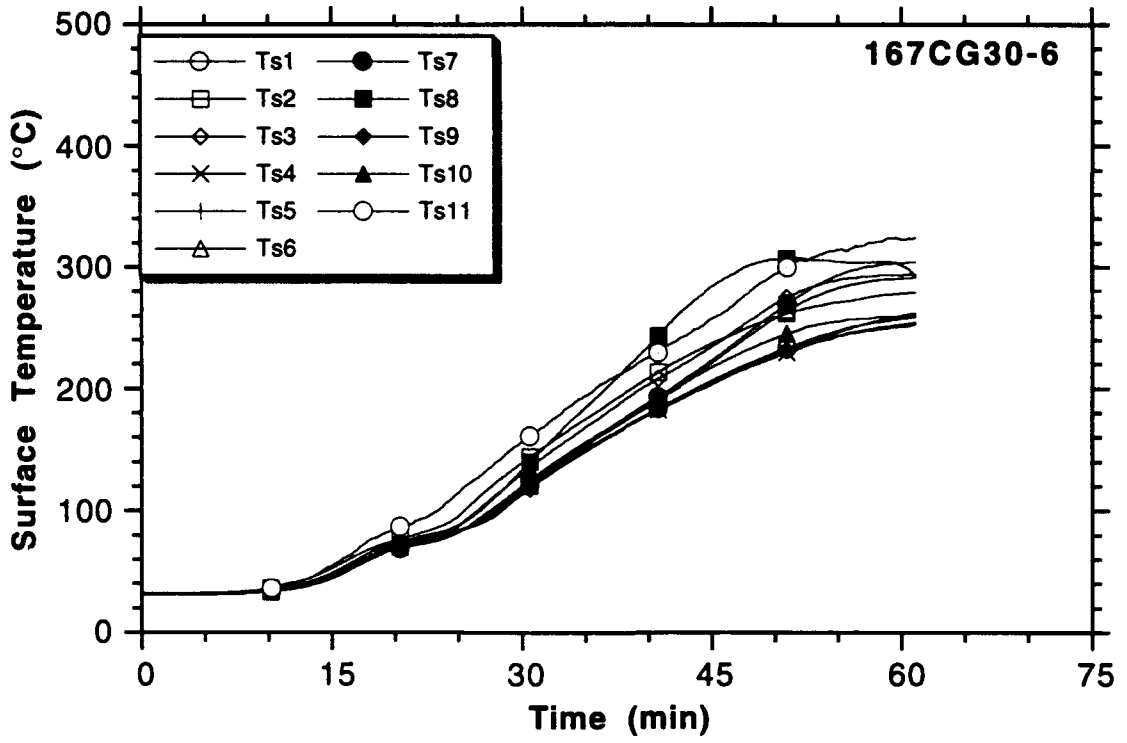
167CG30-6
Ts1
Ts2
Ts3
Ts4
Ts5
Ts6
Ts7
Ts8
Ts9
Ts10
Ts11
Surface Temperature (°C)
Time (min)
0
100
200
300
400
500
0
15
30
45
60
75

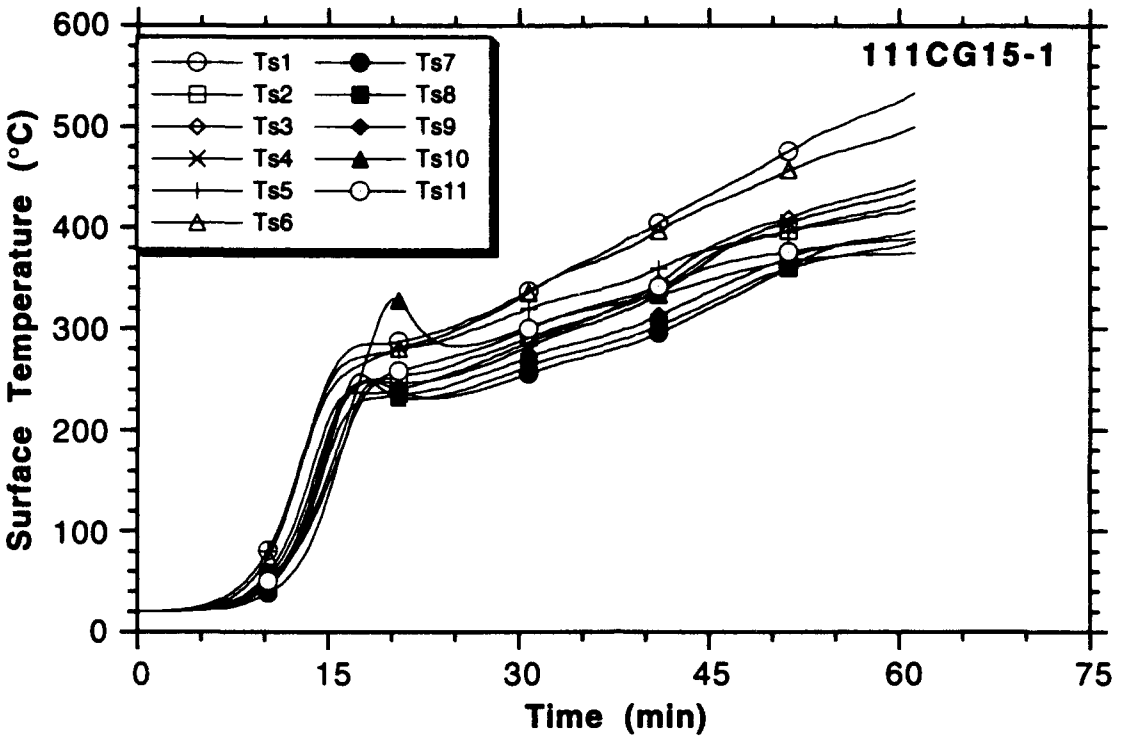
111CG15-1
Ts1
Ts2
Ts3
Ts4
Ts5
Ts6
Ts7
Ts8
Ts9
Ts10
Ts11
Surface Temperature (°C)
Time (min)
0
100
200
300
400
500
600
0
15
30
45
60
75

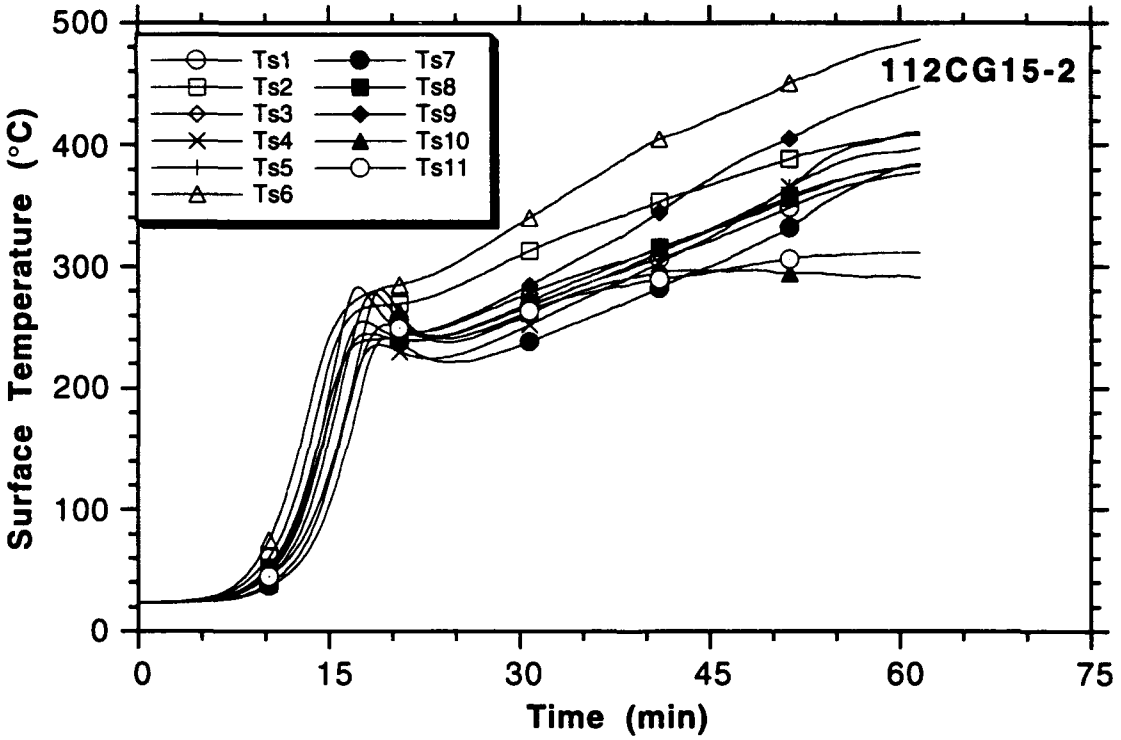
112CG15-2
Ts1
Ts2
Ts3
Ts4
Ts5
Ts6
Ts7
Ts8
Ts9
Ts10
Ts11
Surface Temperature (°C)
Time (min)
0
100
200
300
400
500
0
15
30
45
60
75

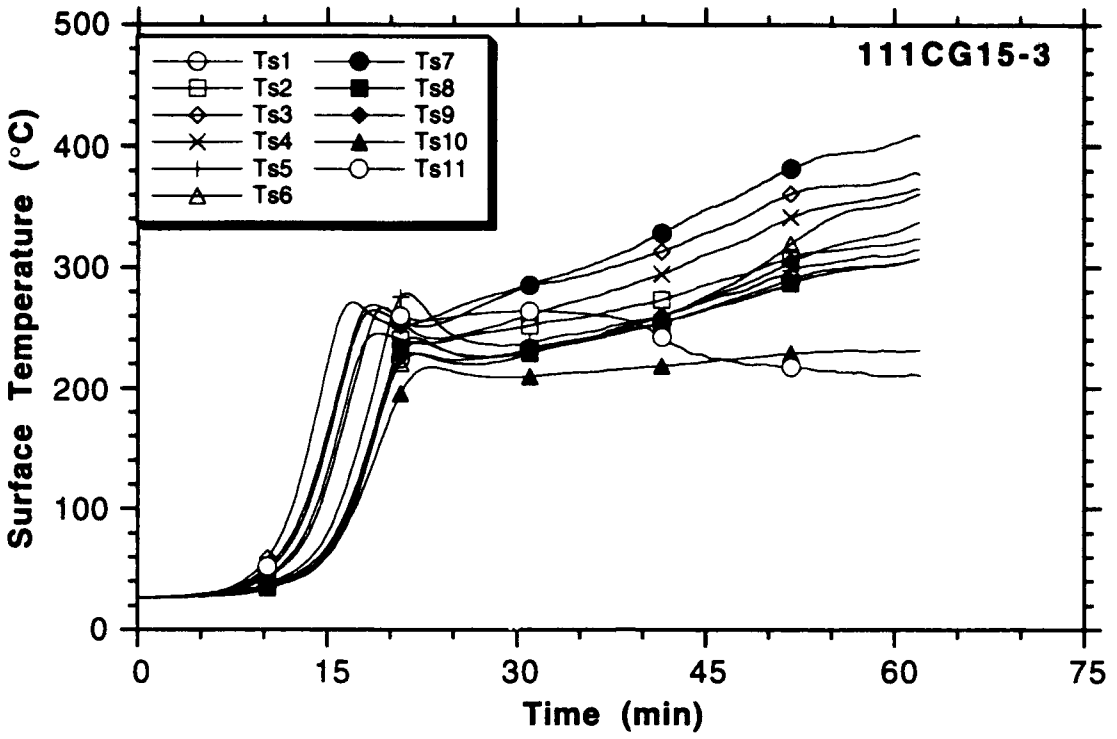
111CG15-3
Ts1
Ts2
Ts3
Ts4
Ts5
Ts6
Ts7
Ts8
Ts9
Ts10
Ts11
Surface Temperature (°C)
Time (min)
0
100
200
300
400
500
0
15
30
45
60
75

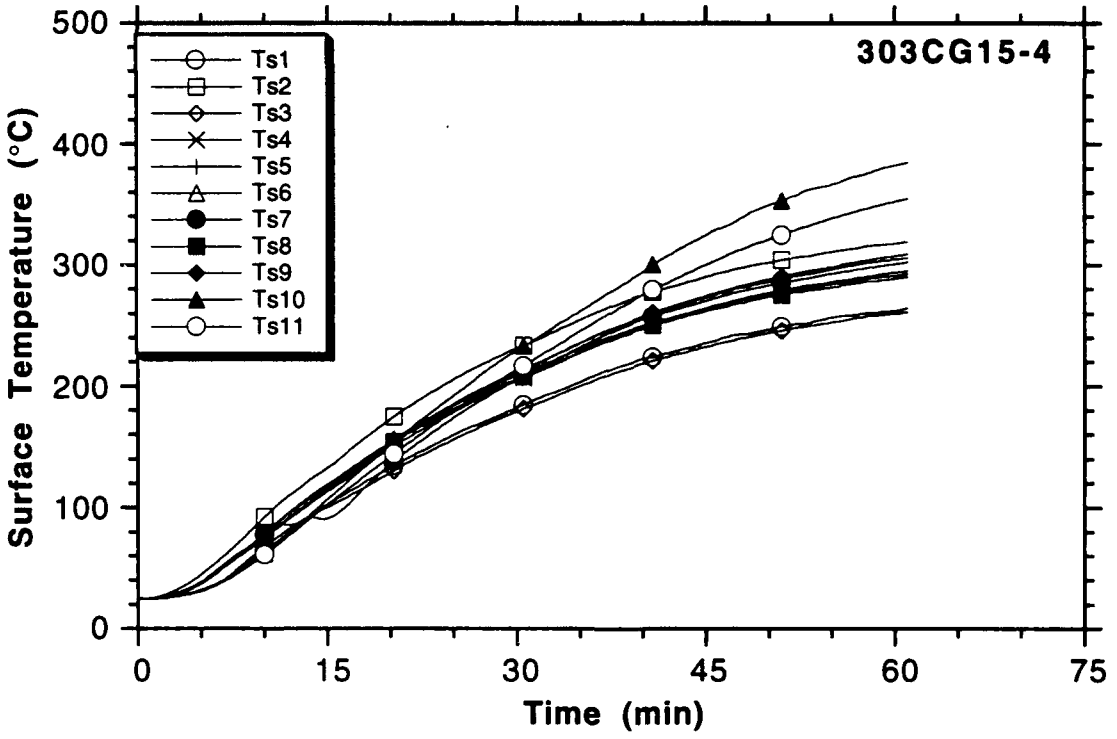
303CG15-4
Ts1
Ts2
Ts3
Ts4
Ts5
Ts6
Ts7
Ts8
Ts9
Ts10
Ts11
Surface Temperature (°C)
Time (min)
0
100
200
300
400
500
0
15
30
45
60
75

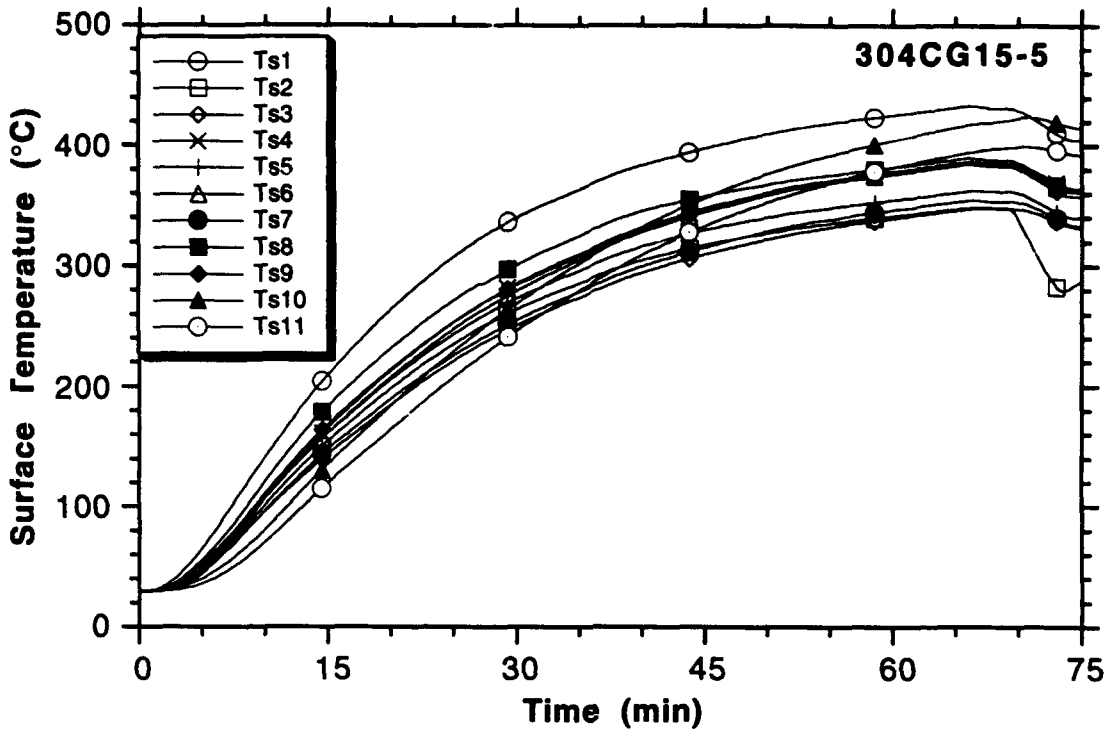
304CG15-5
Ts1
Ts2
Ts3
Ts4
Ts5
Ts6
Ts7
Ts8
Ts9
Ts10
Ts11
Surface Temperature (°C)
Time (min)
0
100
200
300
400
500
0
15
30
45
60
75

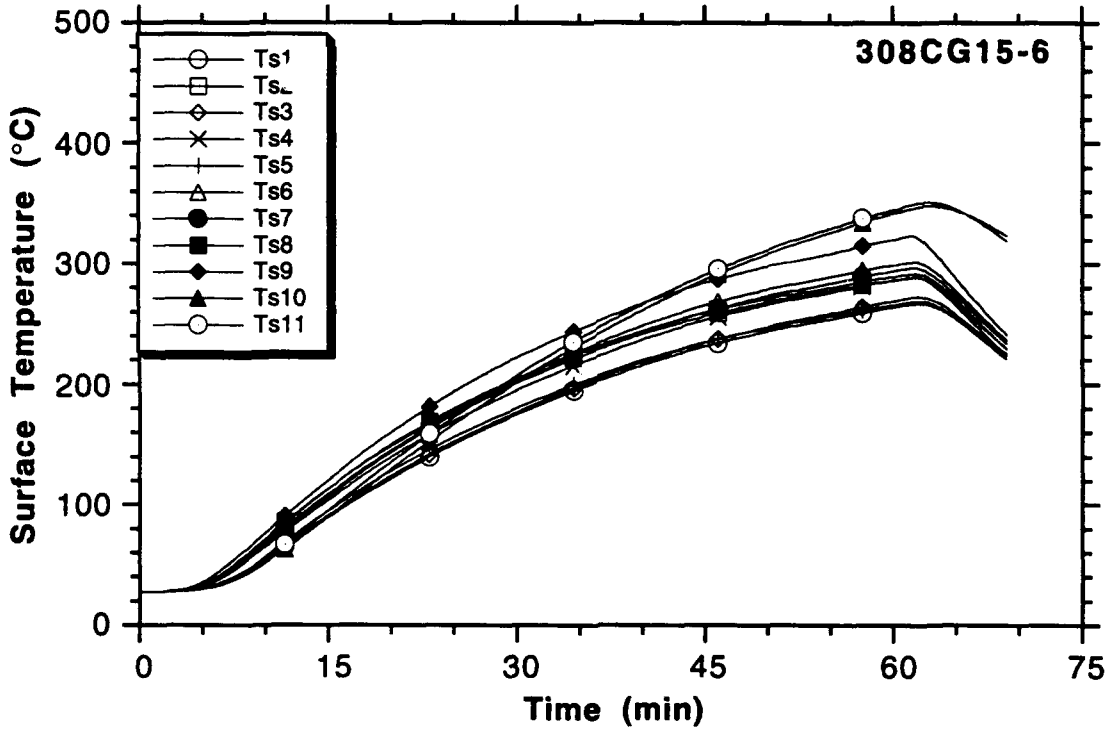
308CG15-6
Ts1
Ts2
Ts3
Ts4
Ts5
Ts6
Ts7
Ts8
Ts9
Ts10
Ts11
Surface Temperature (°C)
Time (min)
0
100
200
300
400
500
0
15
30
45
60
75

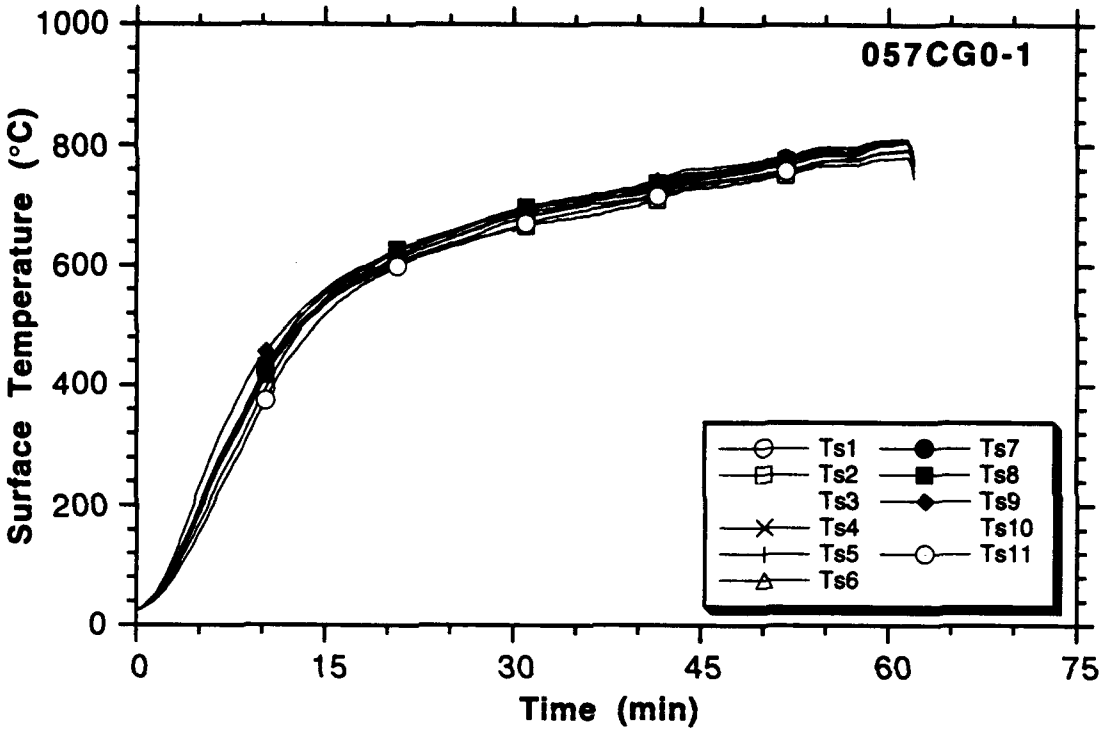
057CG0-1
Surface Temperature (°C)
Time (min)
Ts1
Ts2
Ts3
Ts4
Ts5
Ts6
Ts7
Ts8
Ts9
Ts10
Ts11

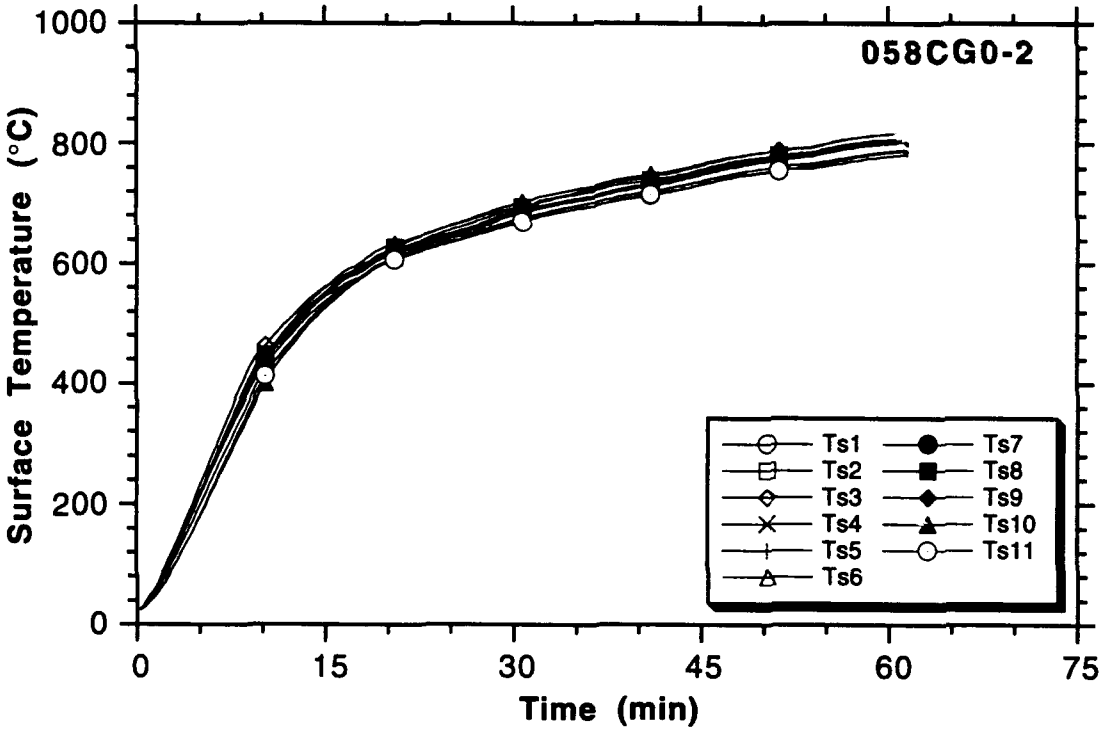
058CG0-2
Surface Temperature (°C)
Time (min)
Ts1
Ts2
Ts3
Ts4
Ts5
Ts6
Ts7
Ts8
Ts9
Ts10
Ts11

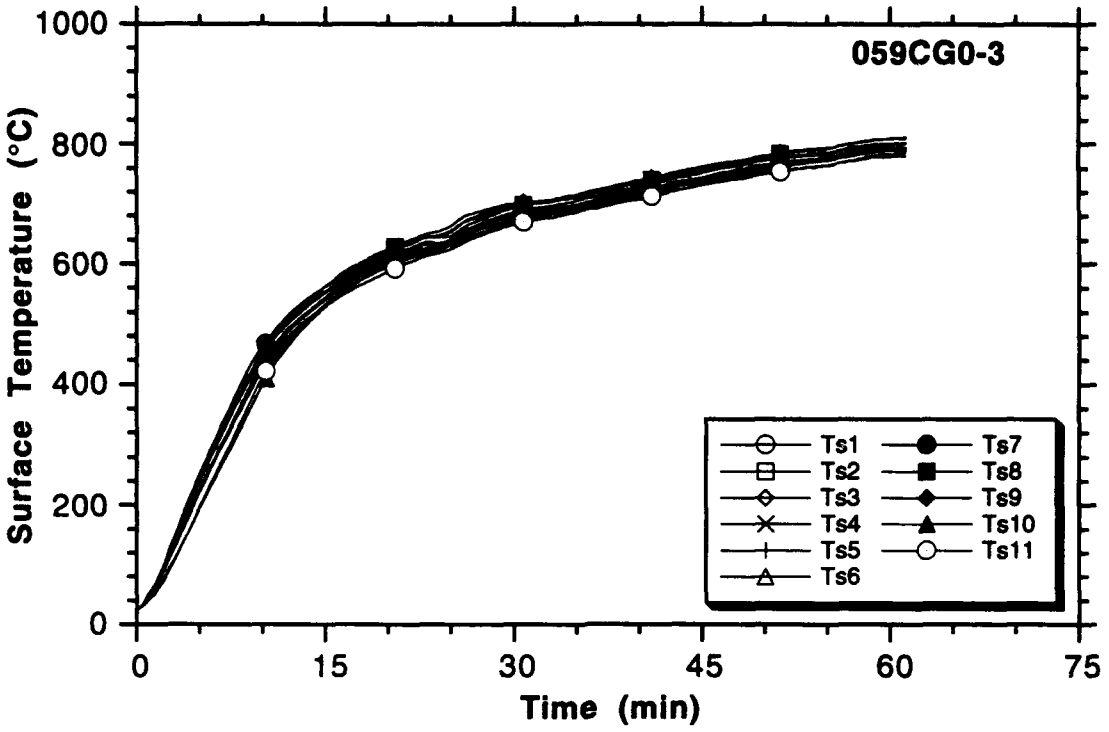
059CG0-3
Surface Temperature (°C)
1000
800
600
400
200
0
0
15
30
45
60
75
Time (min)
Ts1
Ts2
Ts3
Ts4
Ts5
Ts6
Ts7
Ts8
Ts9
Ts10
Ts11

Appendix E

Furnace Temperatures During Bulkhead Tests

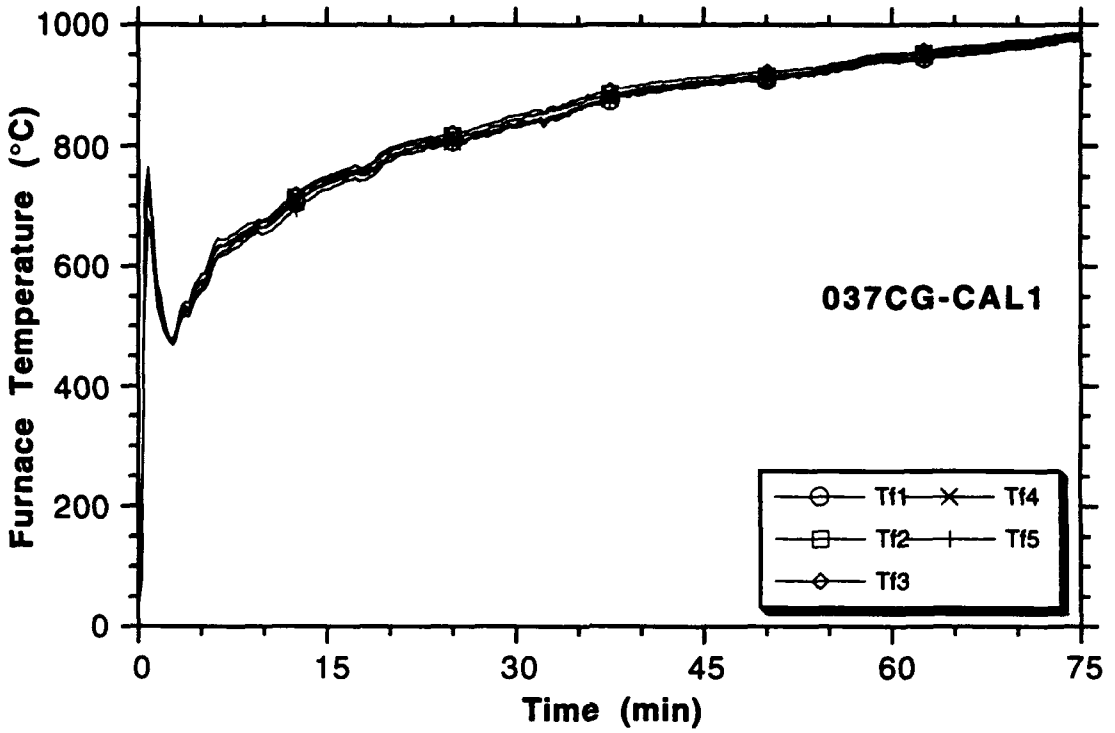
Furnace Temperature (°C)
1000
800
600
400
200
0
0
15
30
45
60
75
Time (min)
037CG-CAL1
Tf1
Tf2
Tf3
Tf4
Tf5

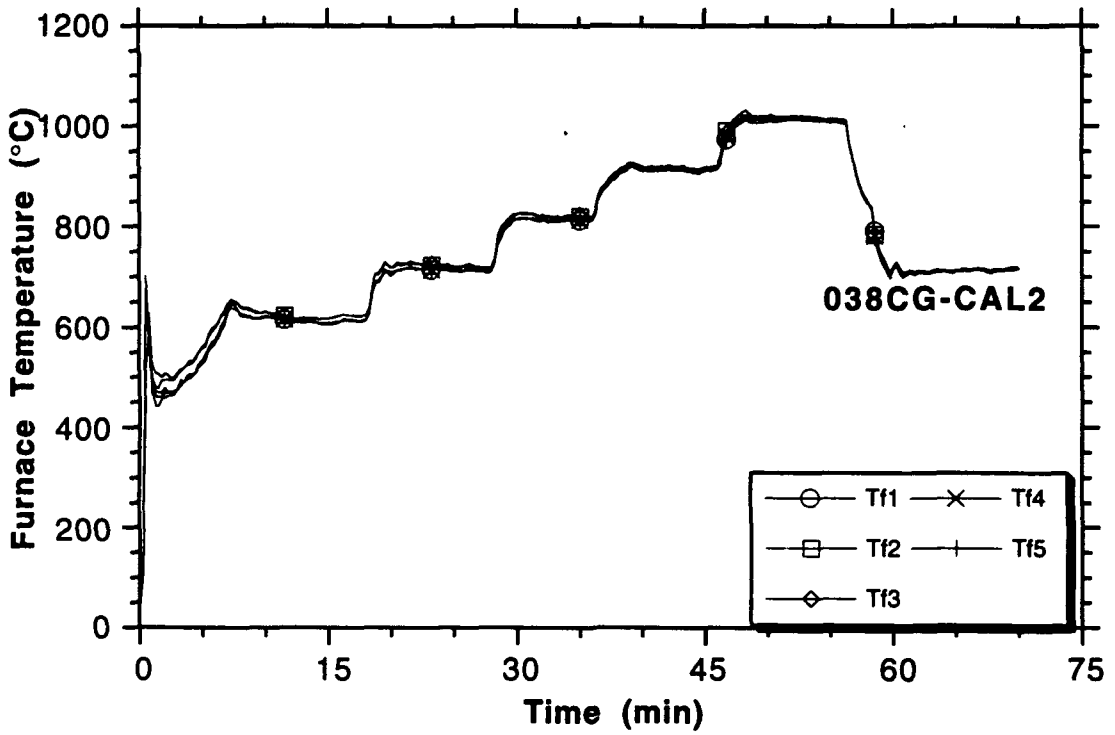
Furnace Temperature (°C)
1200
1000
800
600
400
200
0
0
15
30
45
60
75
Time (min)
038CG-CAL2
Tf1
Tf2
Tf3
Tf4
Tf5

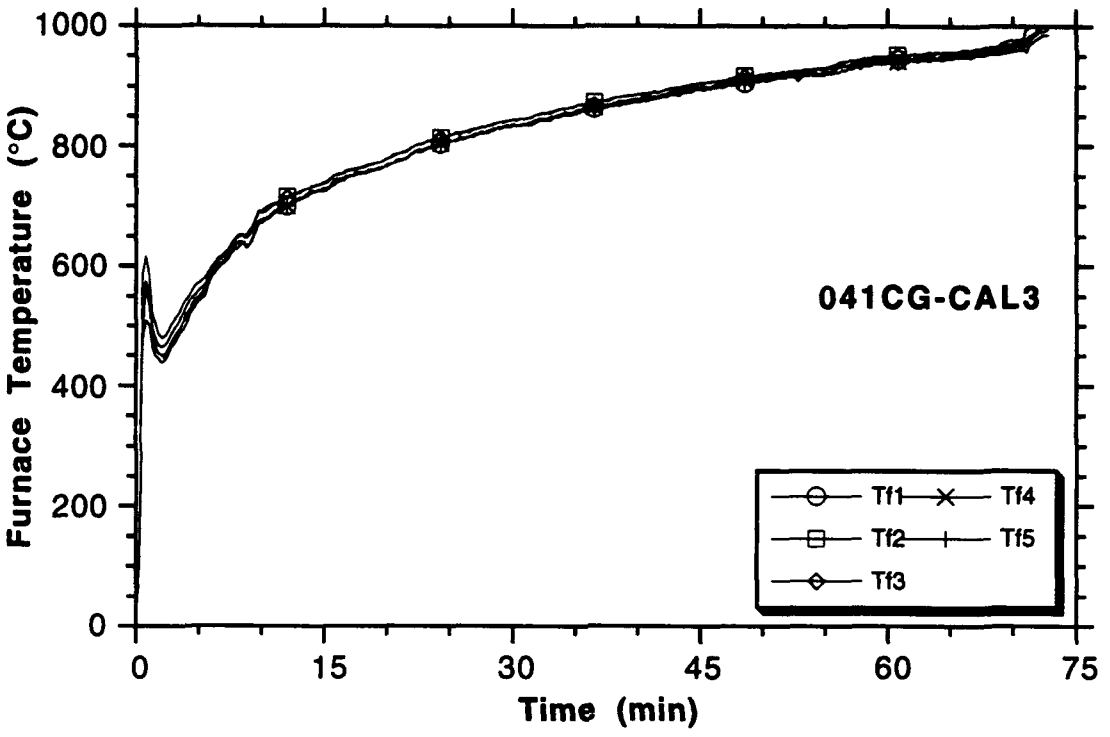
1000
800
600
400
200
0
Furnace Temperature (°C)
041CG-CAL3
Tf1
Tf4
Tf2
Tf5
Tf3
0
15
30
45
60
75
Time (min)

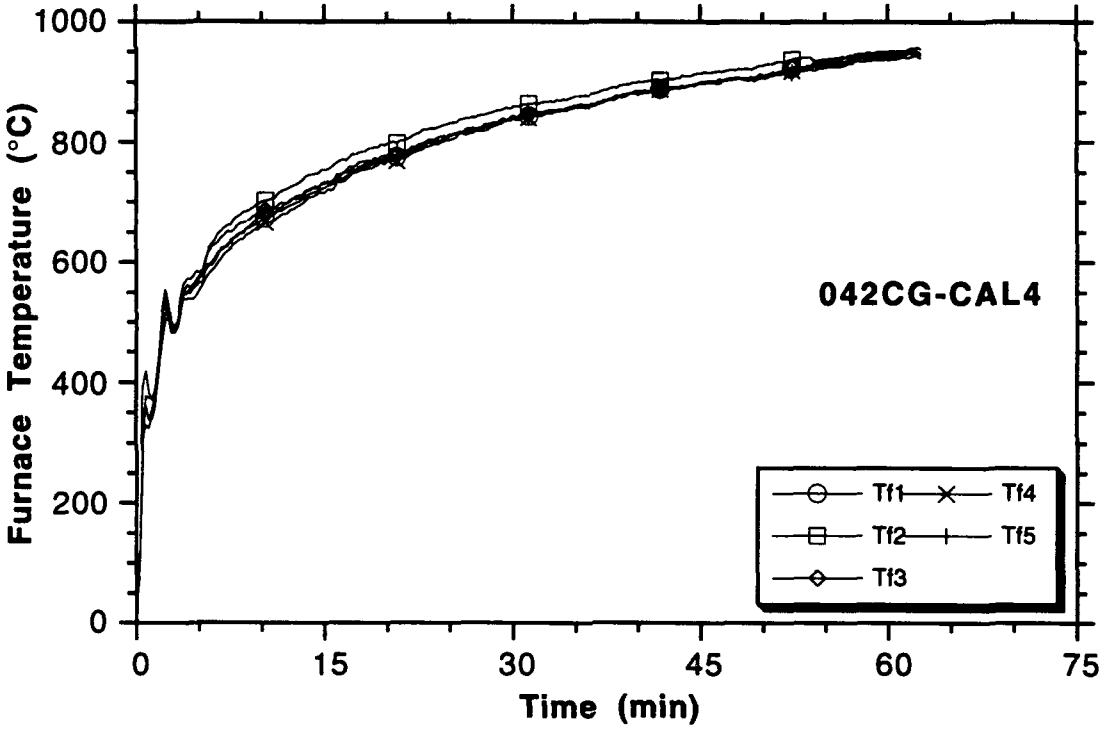
1000
800
600
400
200
0
Furnace Temperature (°C)
042CG-CAL4
Tf1
Tf4
Tf2
Tf5
Tf3
0
15
30
45
60
75
Time (min)

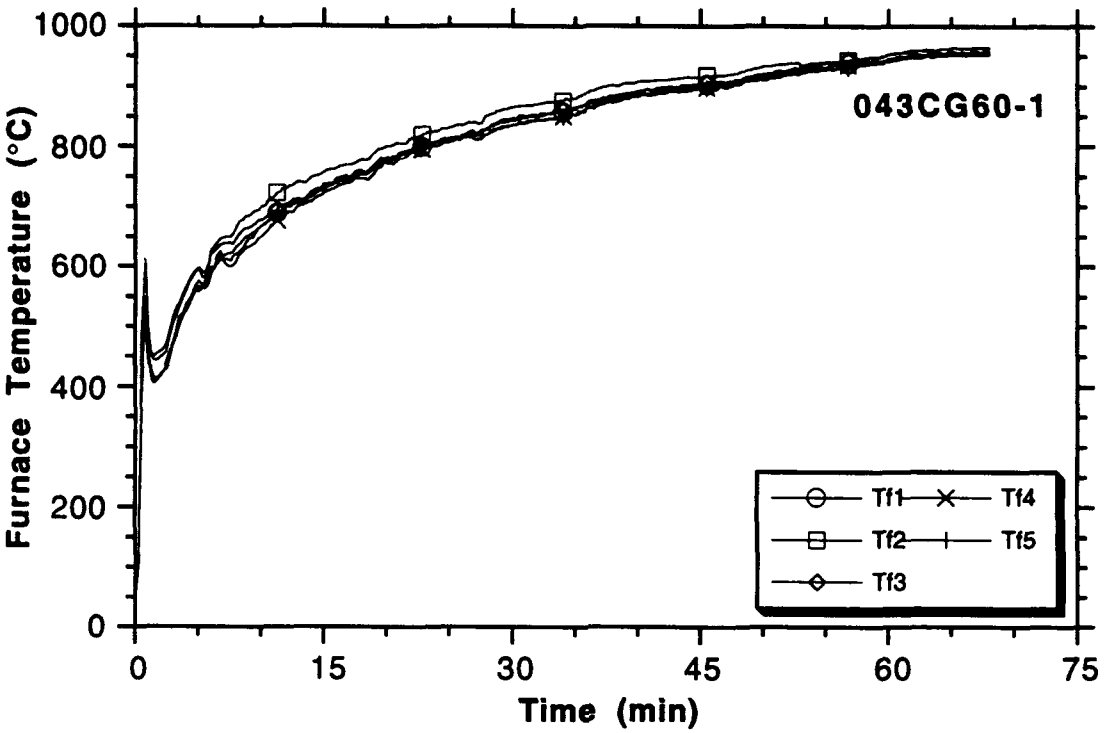
1000
800
600
400
200
0
Furnace Temperature (°C)
043CG60-1
Tf1
Tf4
Tf2
Tf5
Tf3
0
15
30
45
60
75
Time (min)

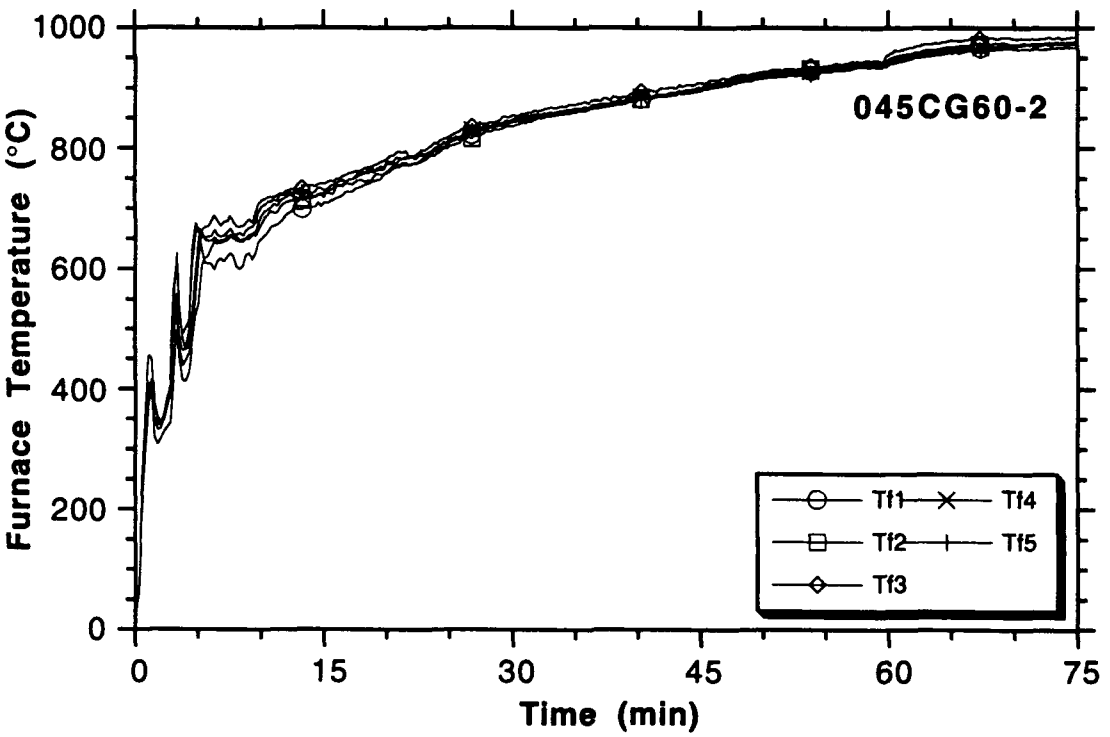
1000
800
600
400
200
0
Furnace Temperature (°C)
045CG60-2
Tf1
Tf4
Tf2
Tf5
Tf3
0
15
30
45
60
75
Time (min)

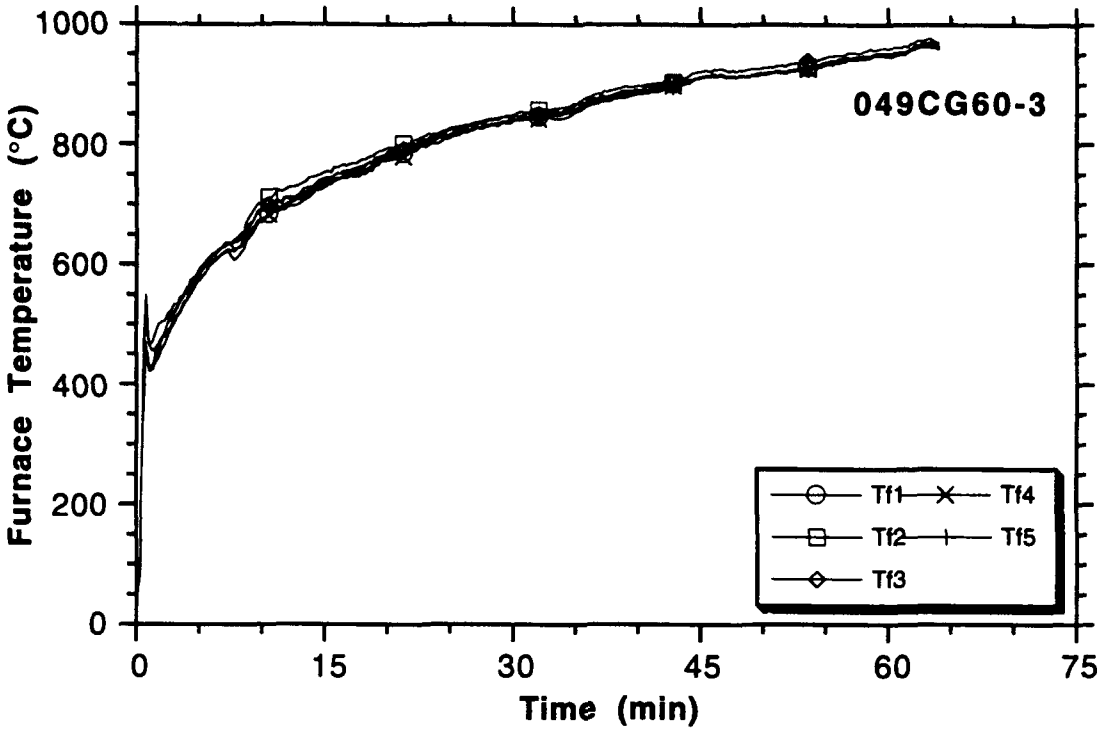
049CG60-3
Furnace Temperature (°C)
Time (min)
Tf1
Tf2
Tf3
Tf4
Tf5
0
200
400
600
800
1000
0
15
30
45
60
75

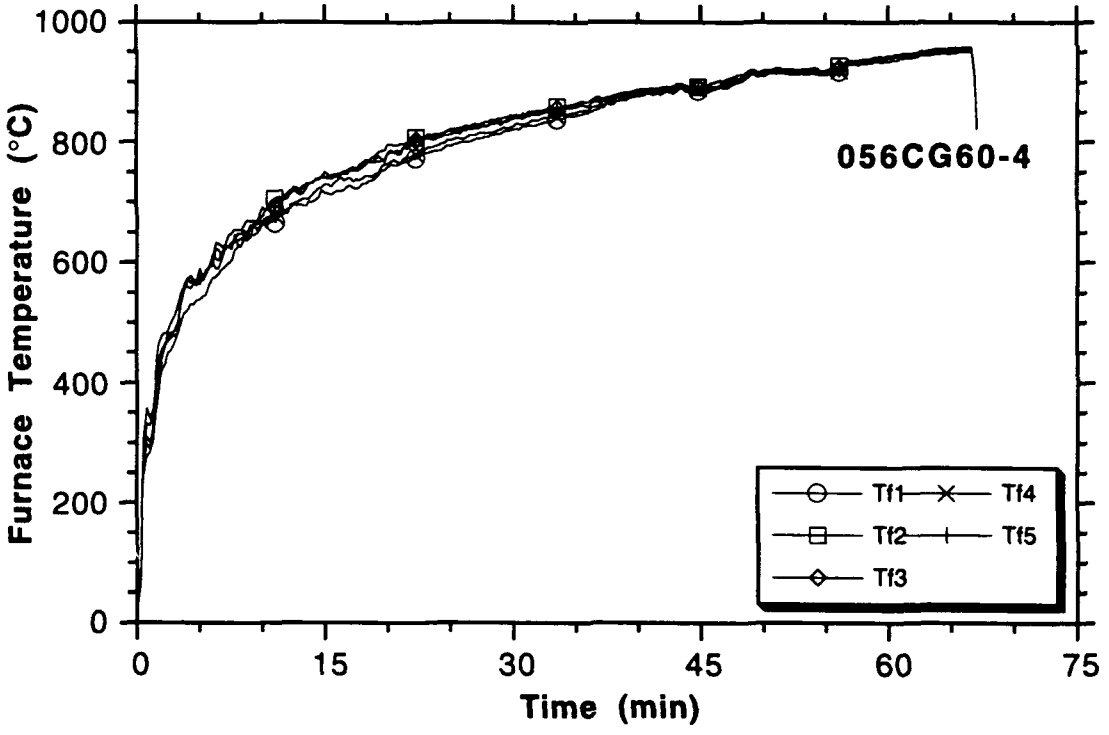
056CG60-4
Furnace Temperature (°C)
Time (min)
Tf1
Tf2
Tf3
Tf4
Tf5
0
200
400
600
800
1000
0
15
30
45
60
75

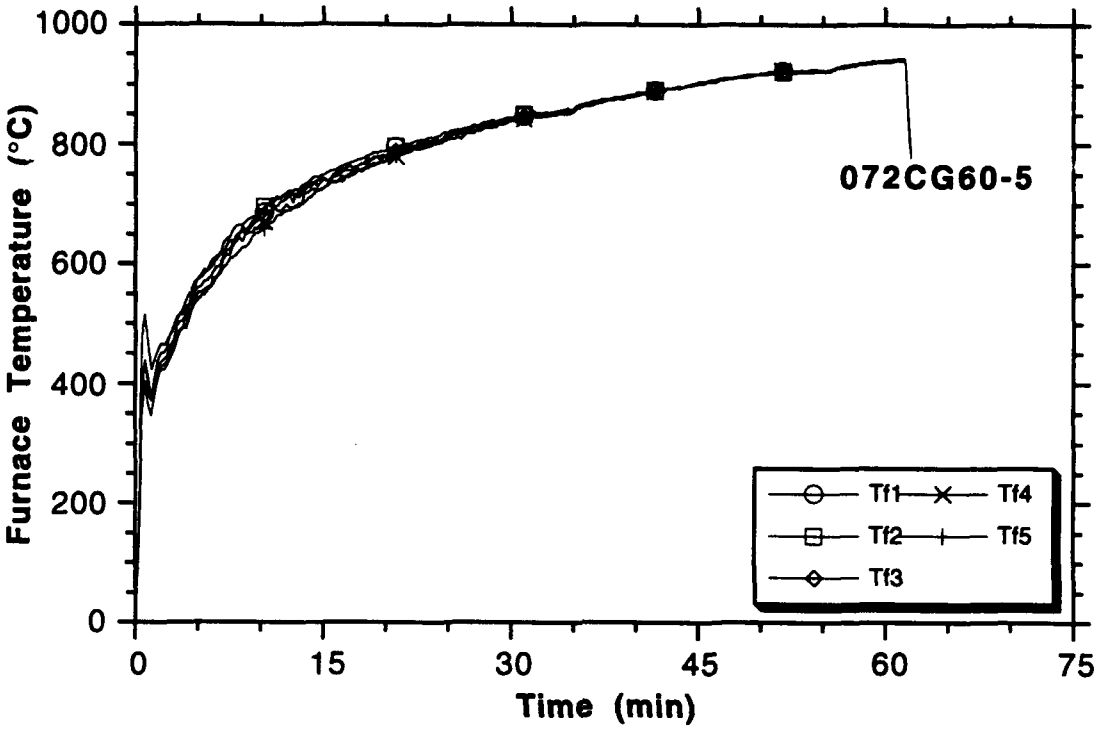
1000
800
600
400
200
0
Furnace Temperature (°C)
0
15
30
45
60
75
Time (min)
072CG60-5
Tf1
Tf4
Tf2
Tf5
Tf3

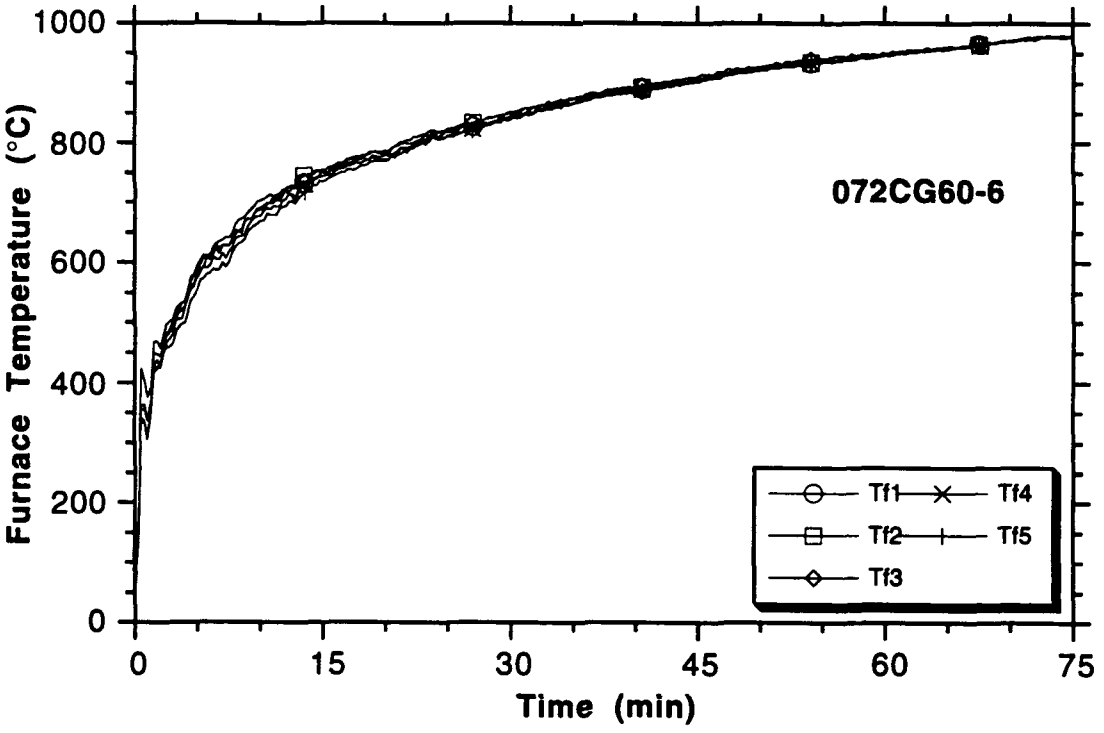
1000
800
600
400
200
0
Furnace Temperature (°C)
0
15
30
45
60
75
Time (min)
072CG60-6
Tf1
Tf4
Tf2
Tf5
Tf3

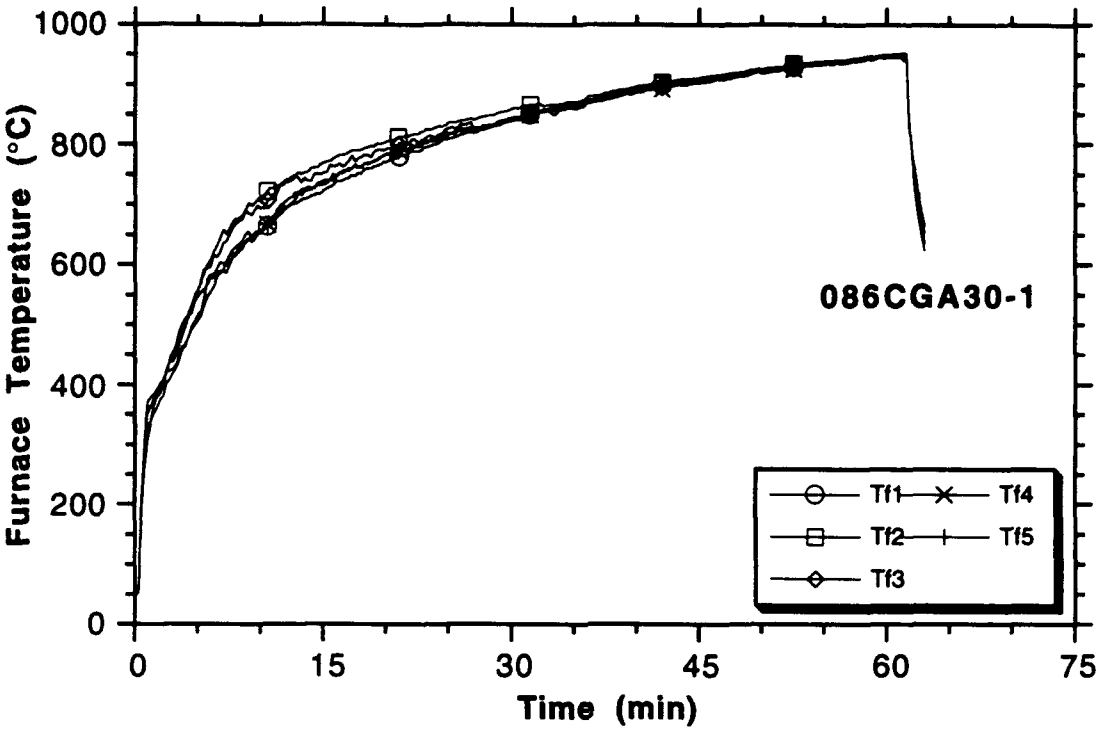
1000
800
600
400
200
0
Furnace Temperature (°C)
0
15
30
45
60
75
Time (min)
086CGA30-1
Tf1
Tf2
Tf3
Tf4
Tf5

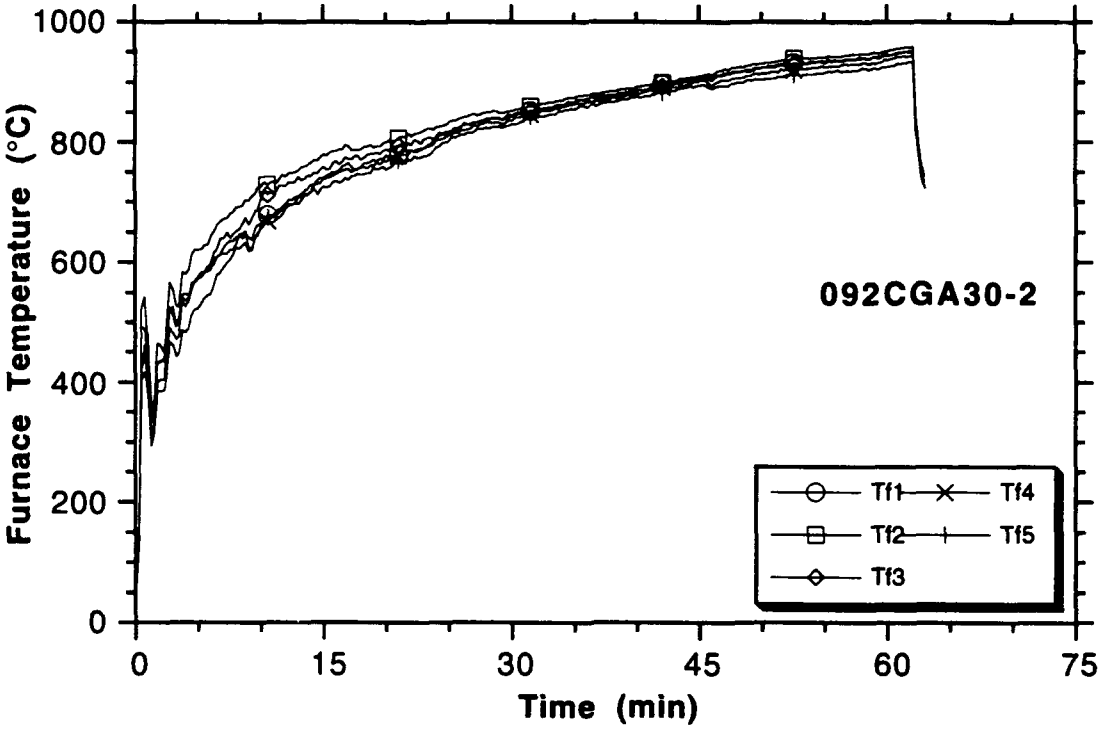
1000
800
600
400
200
0
Furnace Temperature (°C)
0
15
30
45
60
75
Time (min)
092CGA30-2
Tf1
Tf2
Tf3
Tf4
Tf5

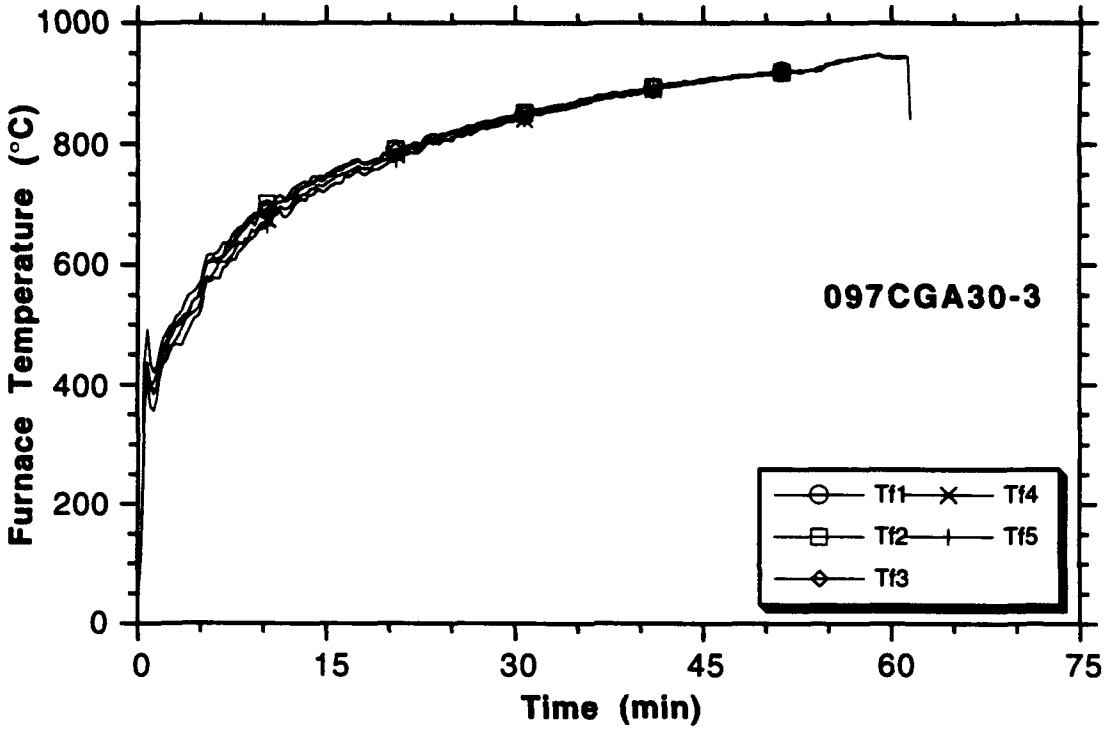
1000
800
600
400
200
0
Furnace Temperature (°C)
0
15
30
45
60
75
Time (min)
097CGA30-3
Tf1
Tf4
Tf2
Tf5
Tf3

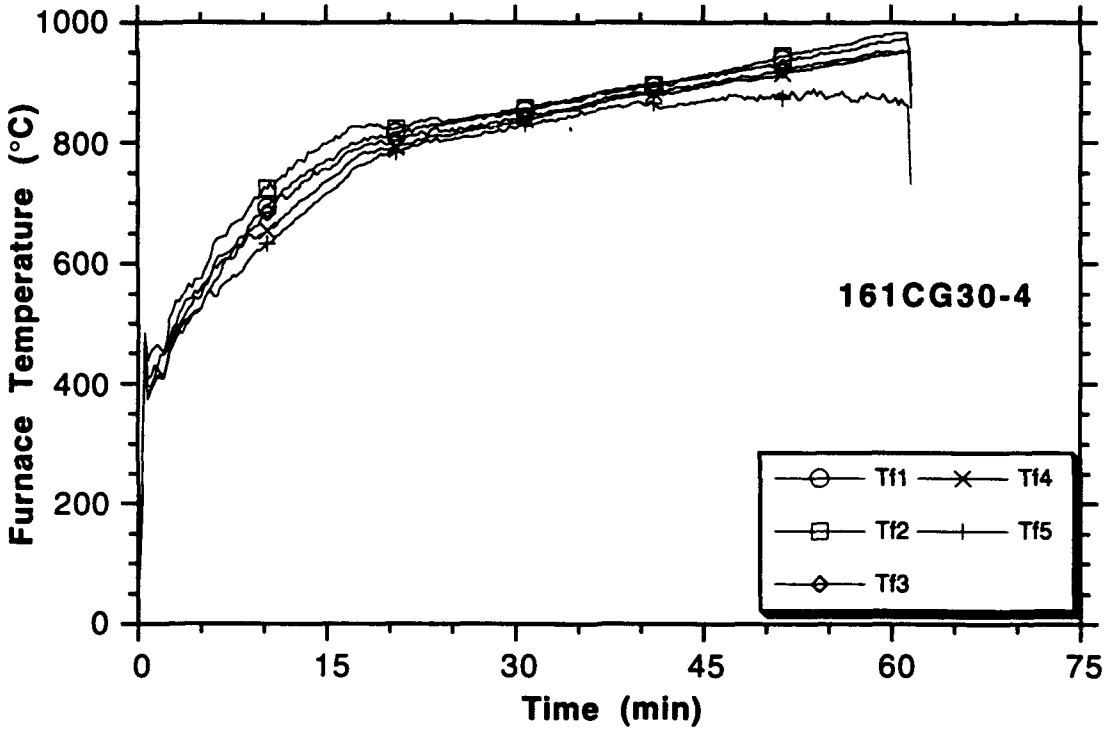
1000
800
600
400
200
0
Furnace Temperature (°C)
0
15
30
45
60
75
Time (min)
161CG30-4
Tf1
Tf4
Tf2
Tf5
Tf3

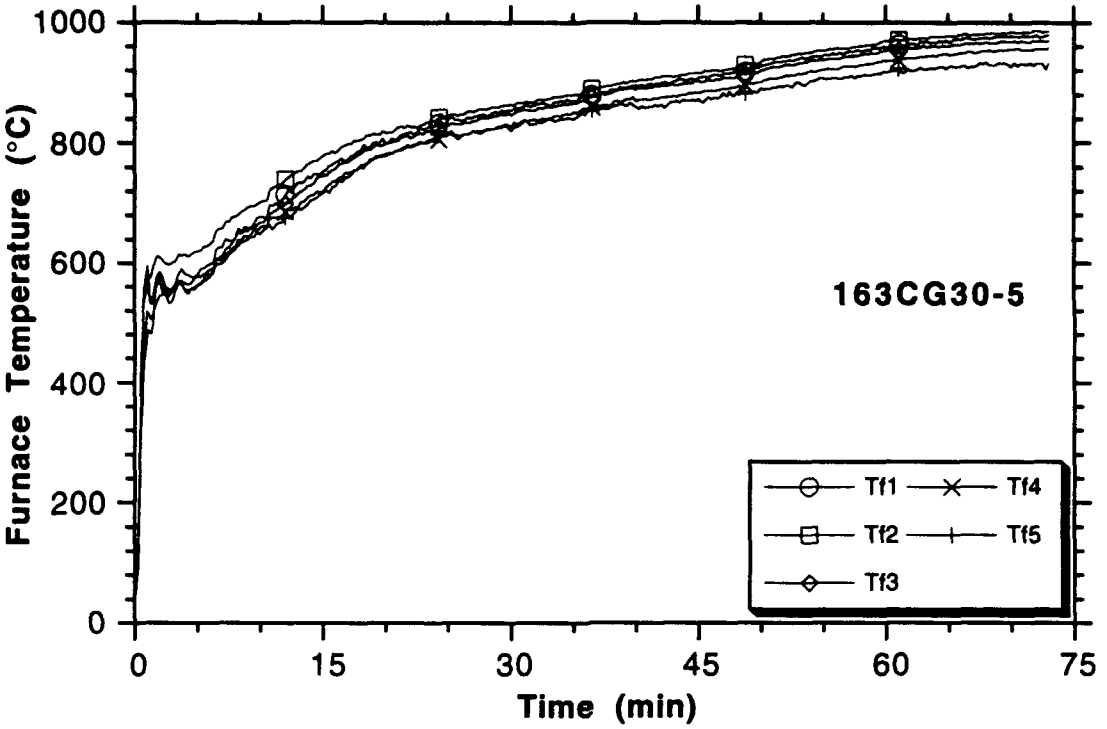
1000
800
600
400
200
0
Furnace Temperature (°C)
0
15
30
45
60
75
Time (min)
163CG30-5
Tf1
Tf4
Tf2
Tf5
Tf3

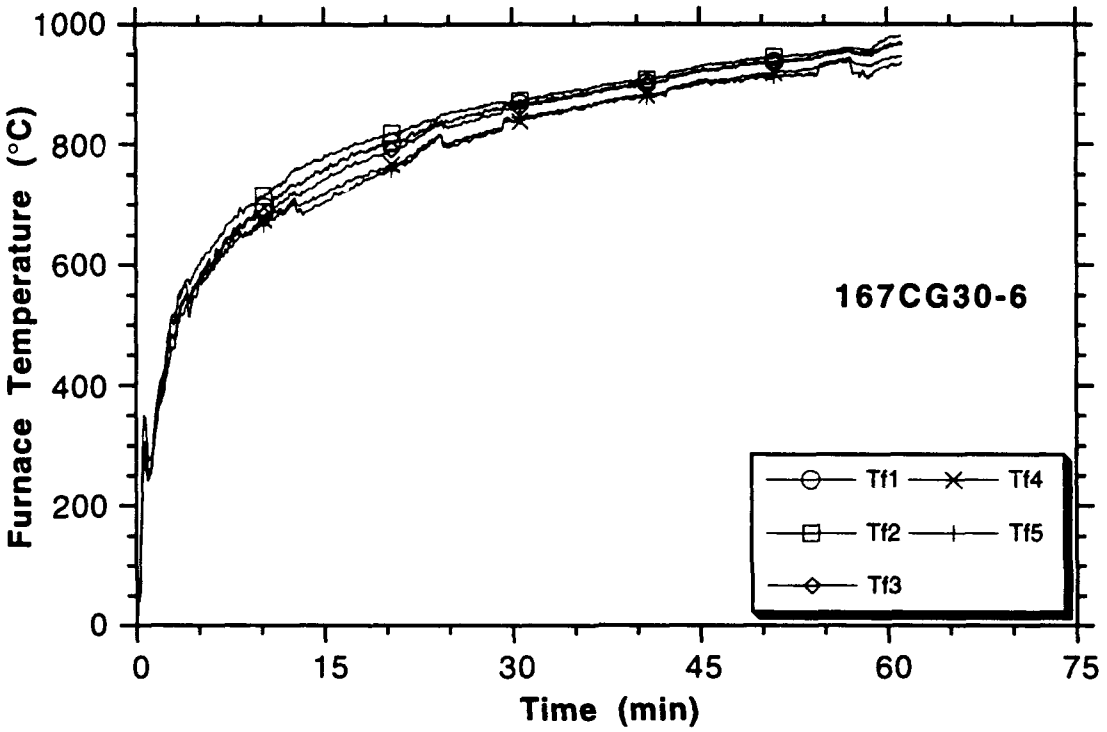
1000
800
600
400
200
0
Furnace Temperature (°C)
0
15
30
45
60
75
Time (min)
167CG30-6
Tf1
Tf4
Tf2
Tf5
Tf3

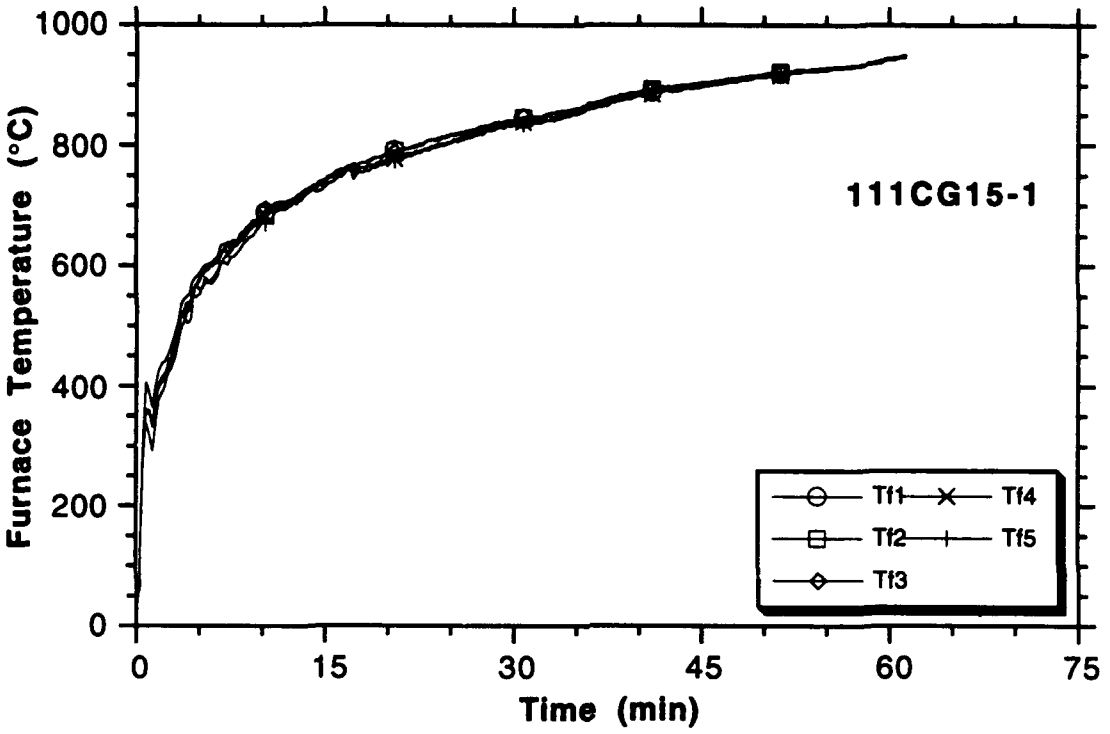
1000
800
600
400
200
0
Furnace Temperature (°C)
0
15
30
45
60
75
Time (min)
111CG15-1
Tf1
Tf4
Tf2
Tf5
Tf3

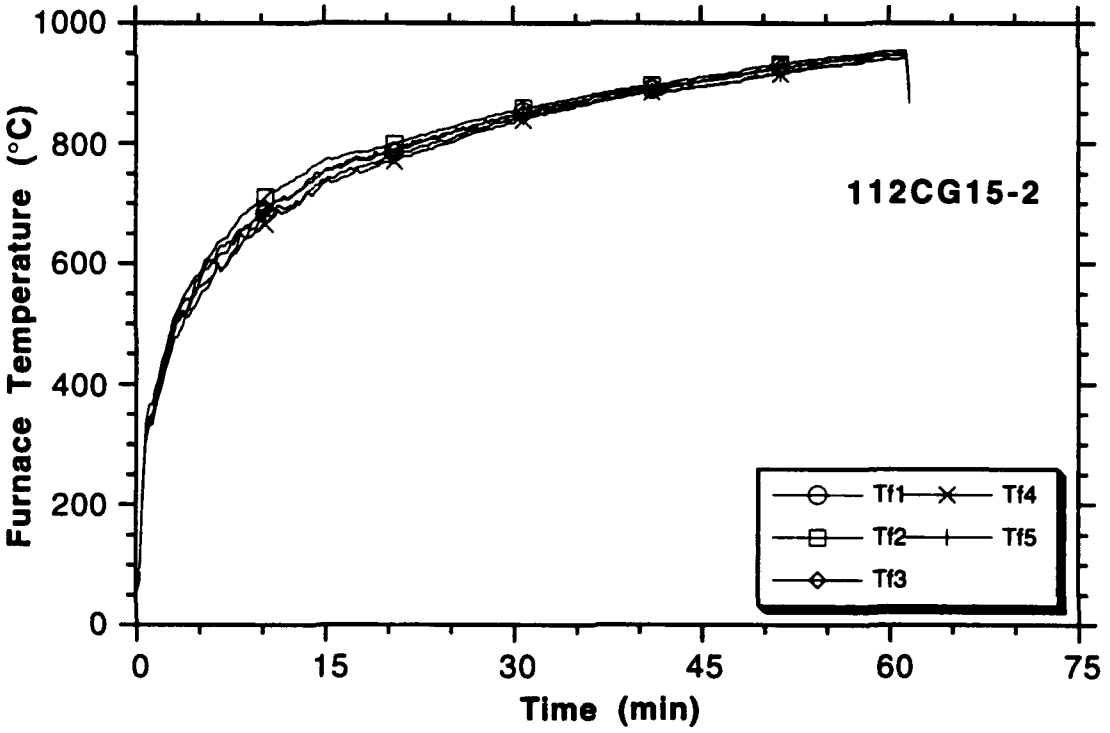
1000
800
600
400
200
0
Furnace Temperature (°C)
0
15
30
45
60
75
Time (min)
112CG15-2
Tf1
Tf4
Tf2
Tf5
Tf3

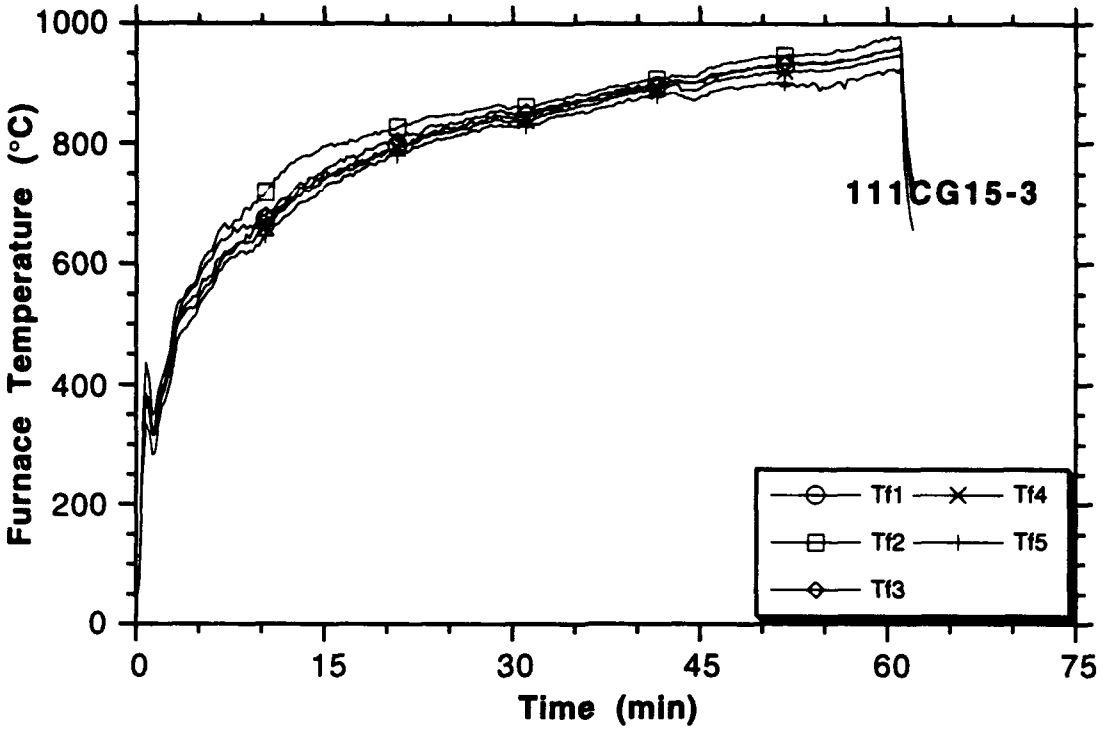
111CG15-3
Furnace Temperature (°C)
Time (min)
Tf1
Tf2
Tf3
Tf4
Tf5
0
200
400
600
800
1000
0
15
30
45
60
75

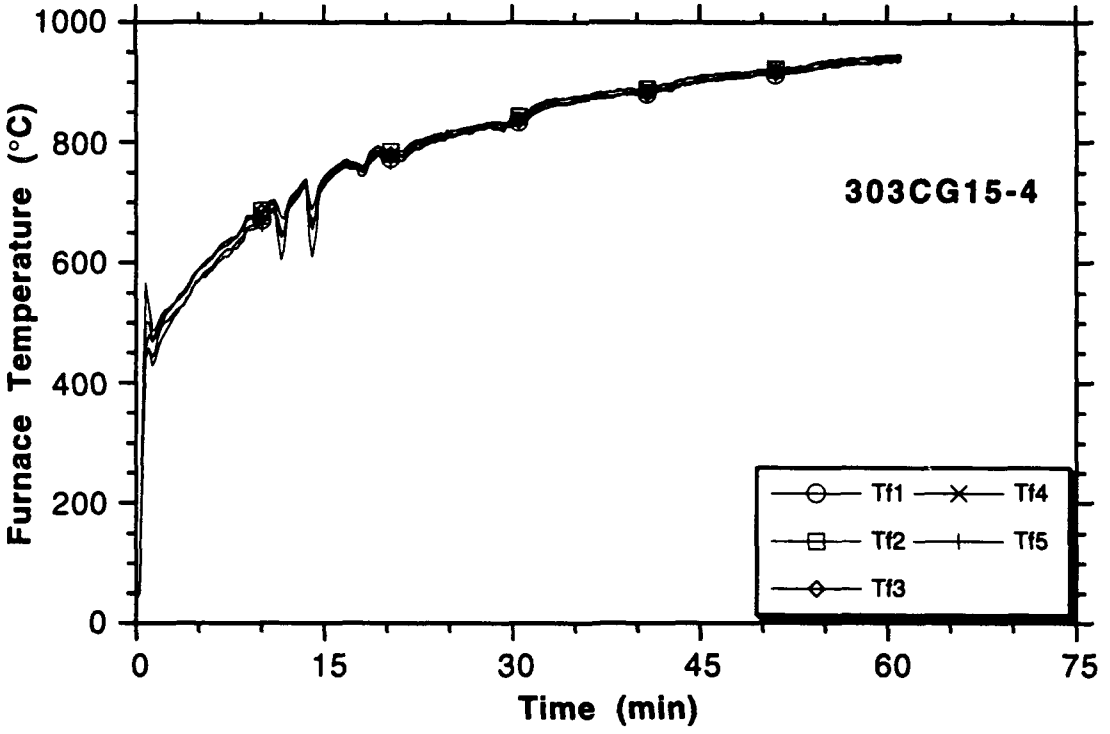
303CG15-4
Furnace Temperature (°C)
Time (min)
Tf1
Tf2
Tf3
Tf4
Tf5
0
200
400
600
800
1000
0
15
30
45
60
75

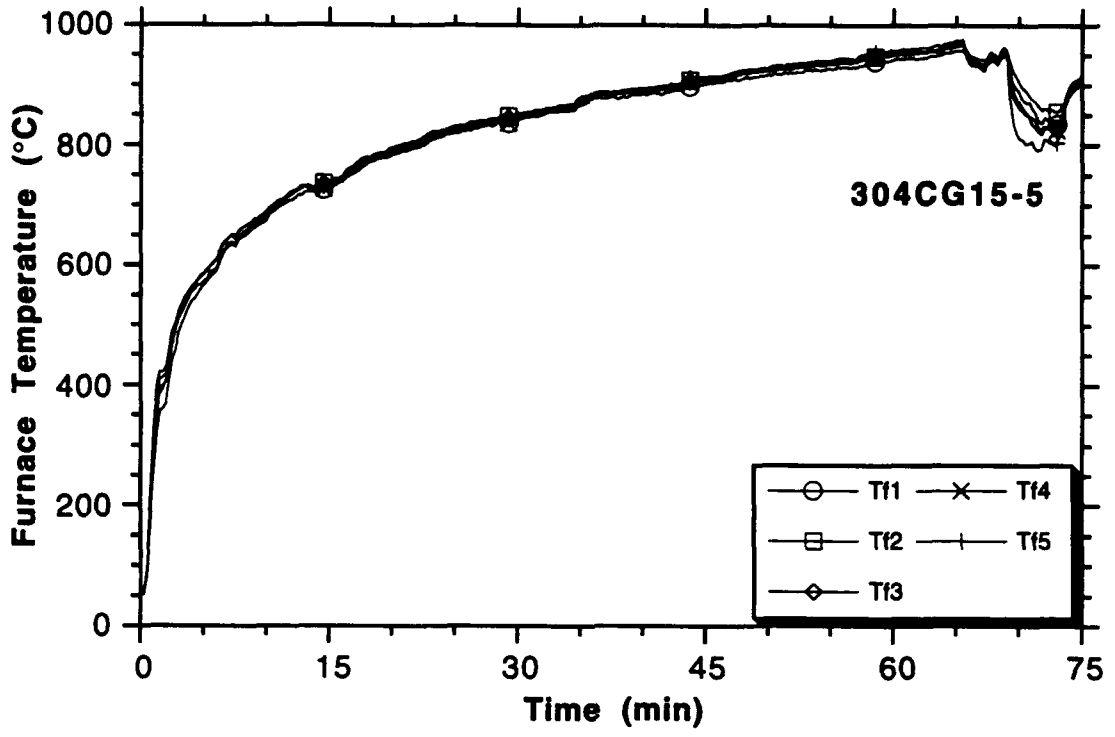
1000
800
600
400
200
0
Furnace Temperature (°C)
0
15
30
45
60
75
Time (min)
304CG15-5
Tf1
Tf4
Tf2
Tf5
Tf3

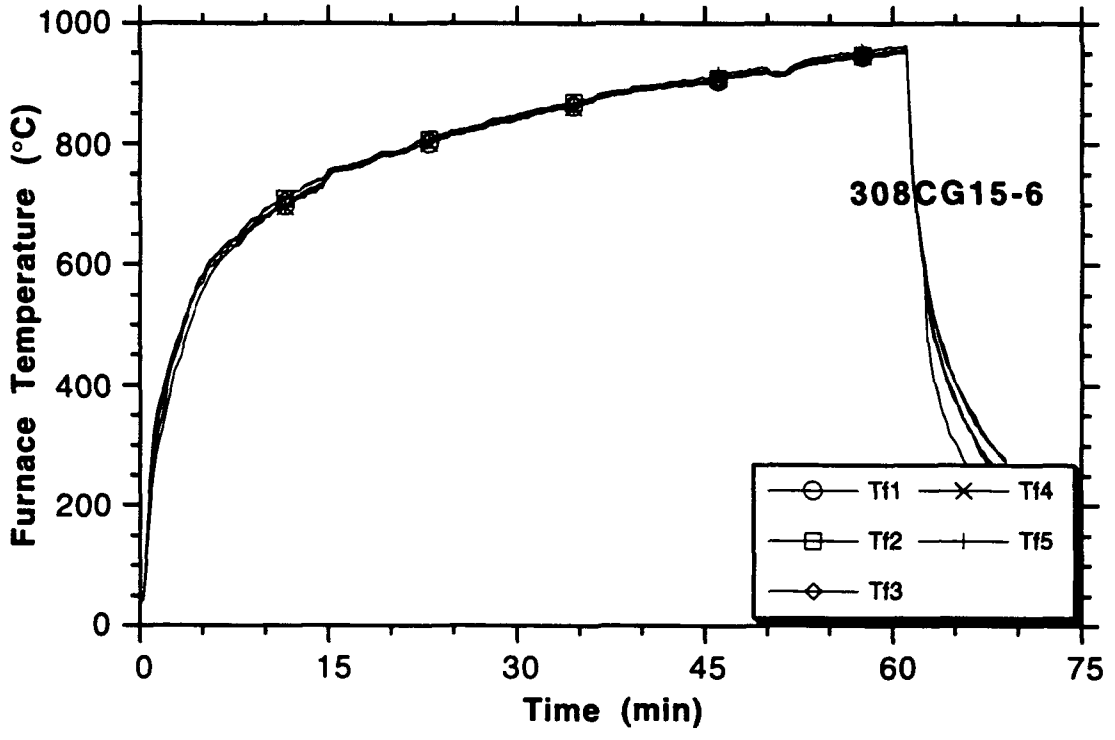
1000
800
600
400
200
0
Furnace Temperature (°C)
0
15
30
45
60
75
Time (min)
308CG15-6
Tf1
Tf4
Tf2
Tf5
Tf3

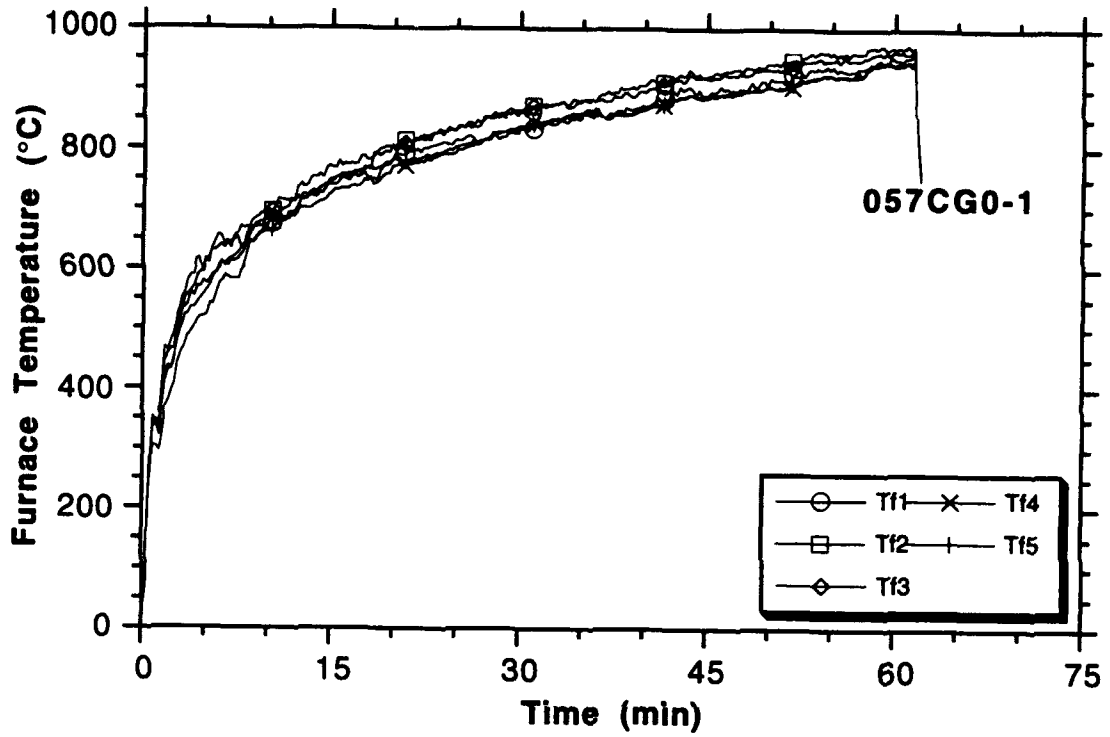
Furnace Temperature (°C)
1000
800
600
400
200
0
0
15
30
45
60
75
Time (min)
057CG0-1
Tf1
Tf4
Tf2
Tf5
Tf3

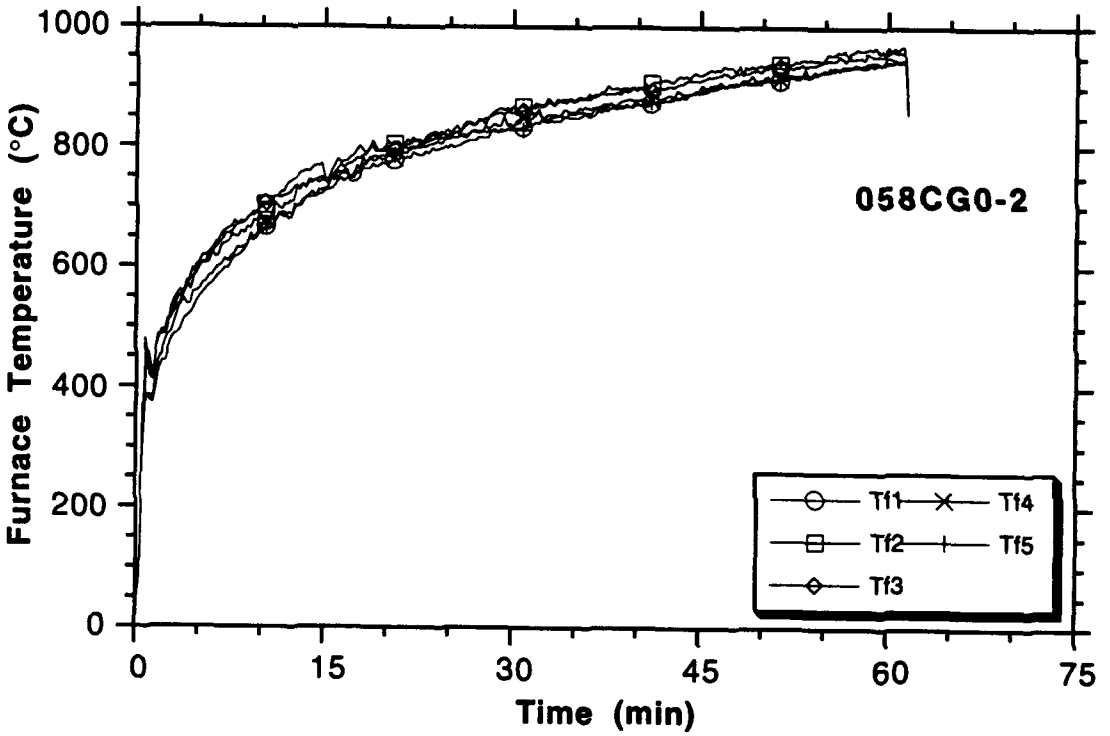
Furnace Temperature (°C)
1000
800
600
400
200
0
0
15
30
45
60
75
Time (min)
058CG0-2
Tf1
Tf4
Tf2
Tf5
Tf3

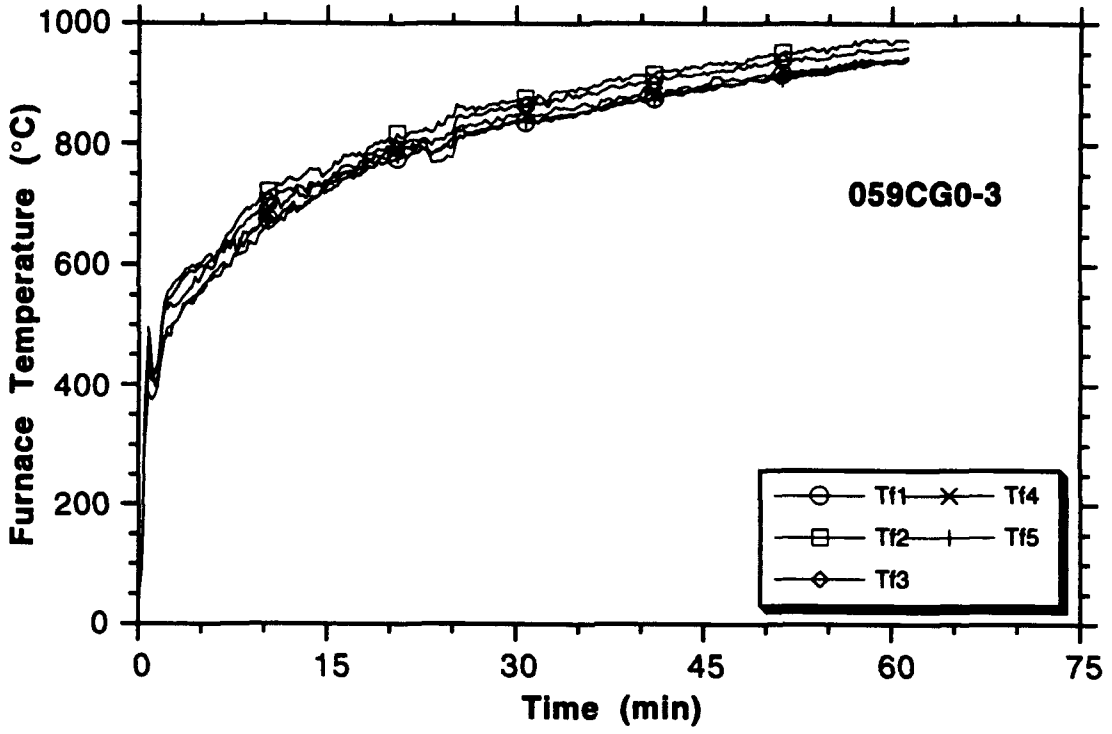
1000
800
600
400
200
0
Furnace Temperature (°C)
0
15
30
45
60
75
Time (min)
059CG0-3
Tf1
Tf2
Tf3
Tf4
Tf5

Appendix F

Heat Flux Transducer Body Temperature, Ambient Temperature and Furnace Pressure During Bulkhead Tests

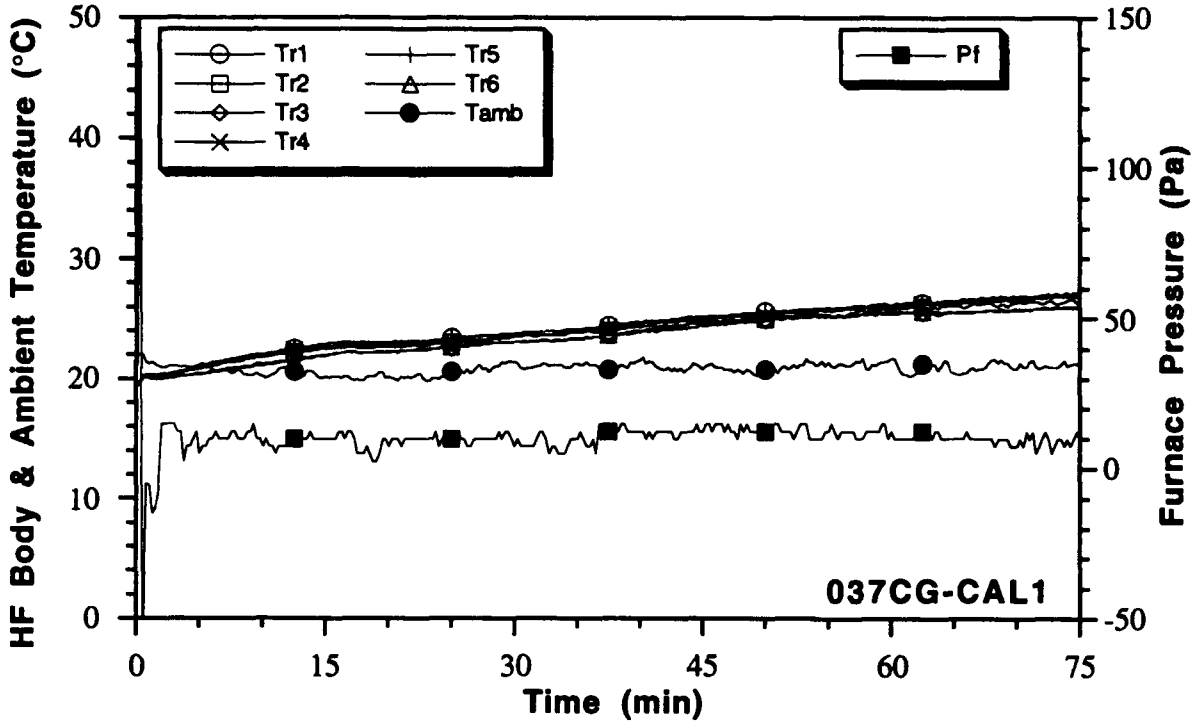
Tr1
Tr2
Tr3
Tr4
Tr5
Tr6
Tamb
Pf
HF Body & Ambient Temperature (°C)
Furnace Pressure (Pa)
Time (min)
037CG-CAL1
0
10
20
30
40
50
-50
0
50
100
150
0
15
30
45
60
75

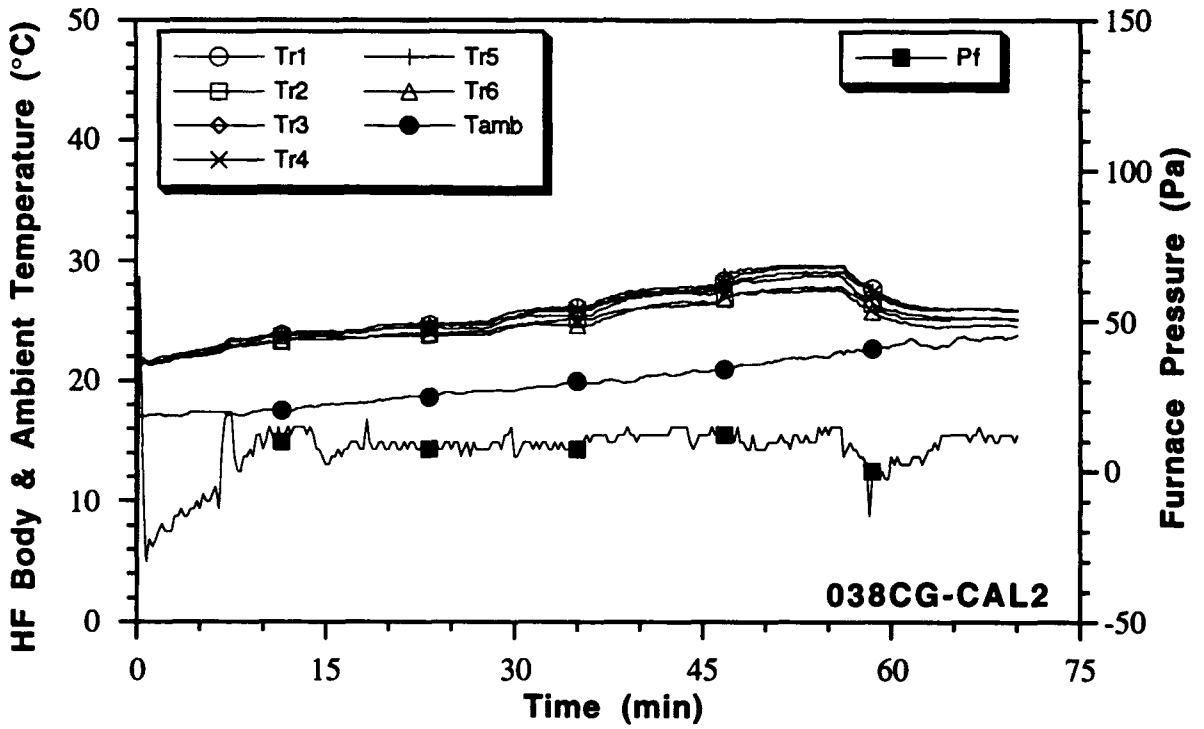
Tr1
Tr2
Tr3
Tr4
Tr5
Tr6
Tamb
Pf
HF Body & Ambient Temperature (°C)
Furnace Pressure (Pa)
Time (min)
038CG-CAL2
0
10
20
30
40
50
-50
0
50
100
150
0
15
30
45
60
75

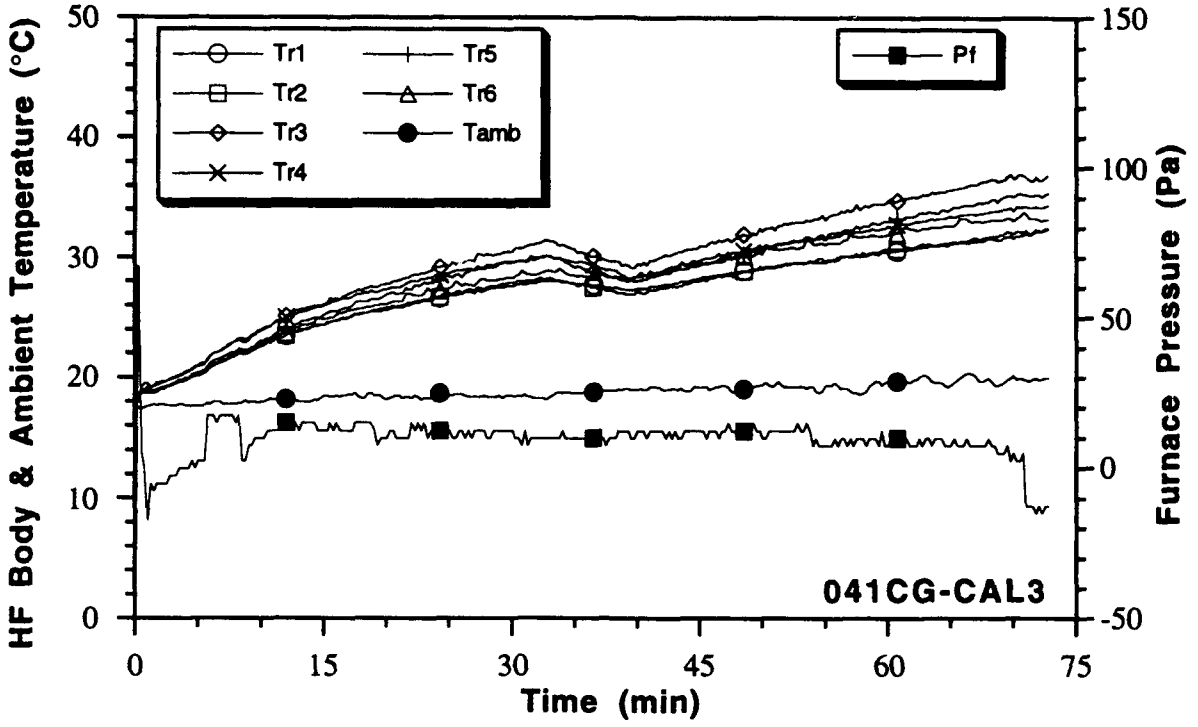
Tr1
Tr2
Tr3
Tr4
Tr5
Tr6
Tamb
Pf
041CG-CAL3
HF Body & Ambient Temperature (°C)
Furnace Pressure (Pa)
Time (min)
0
10
20
30
40
50
-50
0
50
100
150
0
15
30
45
60
75

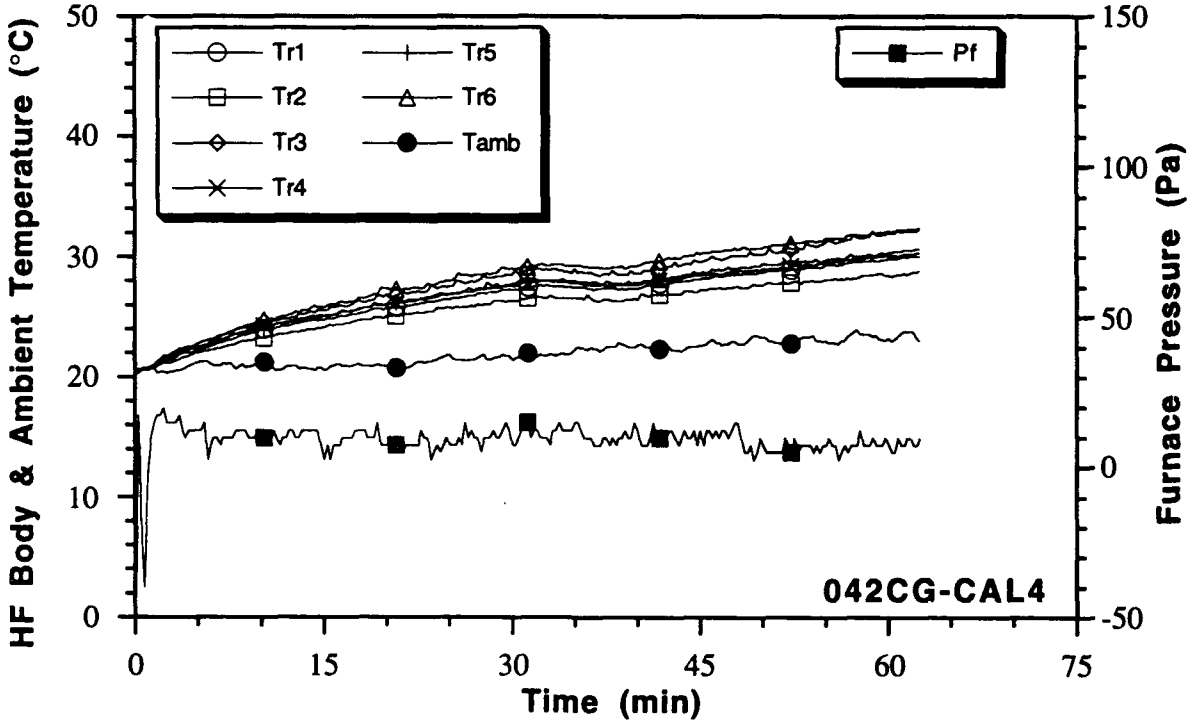
Tr1
Tr2
Tr3
Tr4
Tr5
Tr6
Tamb
Pf
042CG-CAL4
HF Body & Ambient Temperature (°C)
Furnace Pressure (Pa)
Time (min)
0
10
20
30
40
50
-50
0
50
100
150
0
15
30
45
60
75

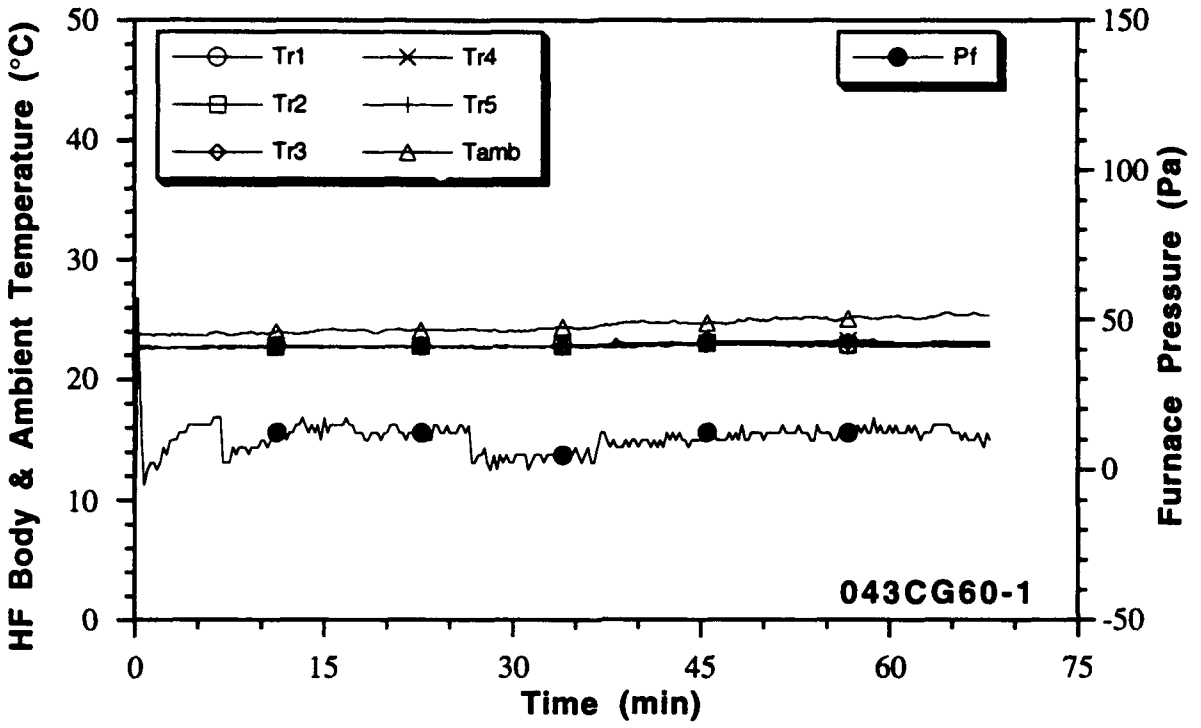
Tr1
Tr2
Tr3
Tr4
Tr5
Tamb
Pf
HF Body & Ambient Temperature (°C)
Furnace Pressure (Pa)
Time (min)
043CG60-1
0
10
20
30
40
50
-50
0
50
100
150
0
15
30
45
60
75

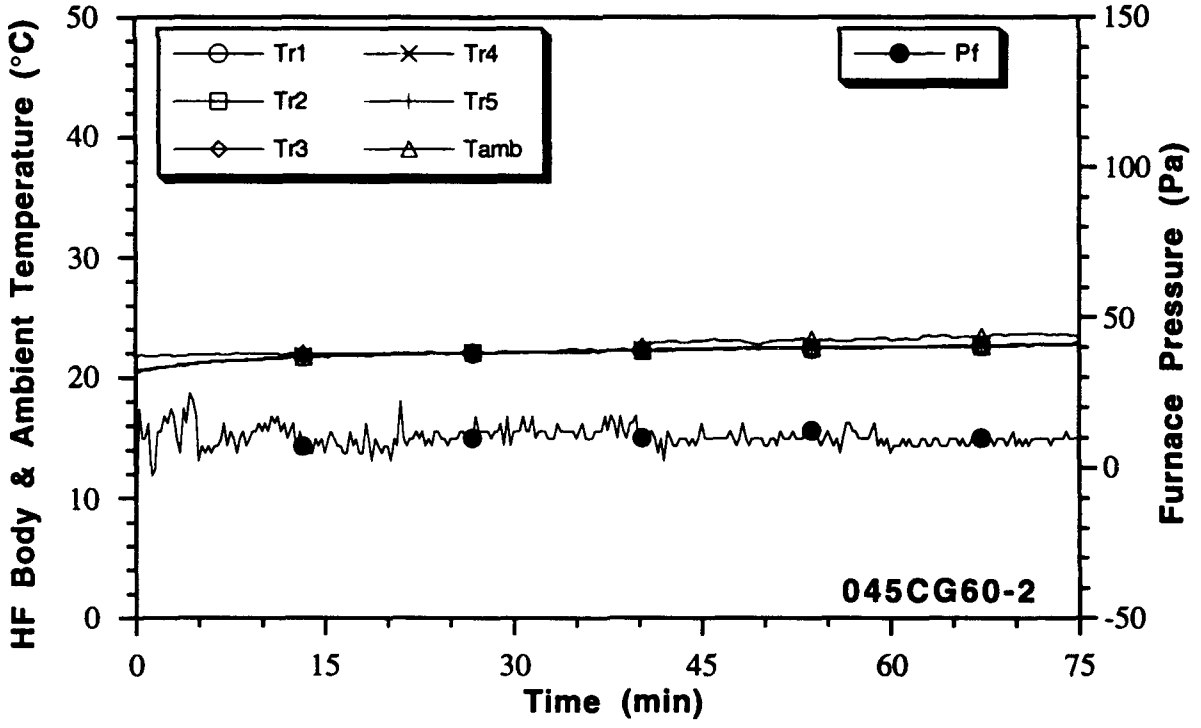
Tr1
Tr2
Tr3
Tr4
Tr5
Tamb
Pf
HF Body & Ambient Temperature (°C)
Furnace Pressure (Pa)
Time (min)
045CG60-2
0
10
20
30
40
50
-50
0
50
100
150
0
15
30
45
60
75

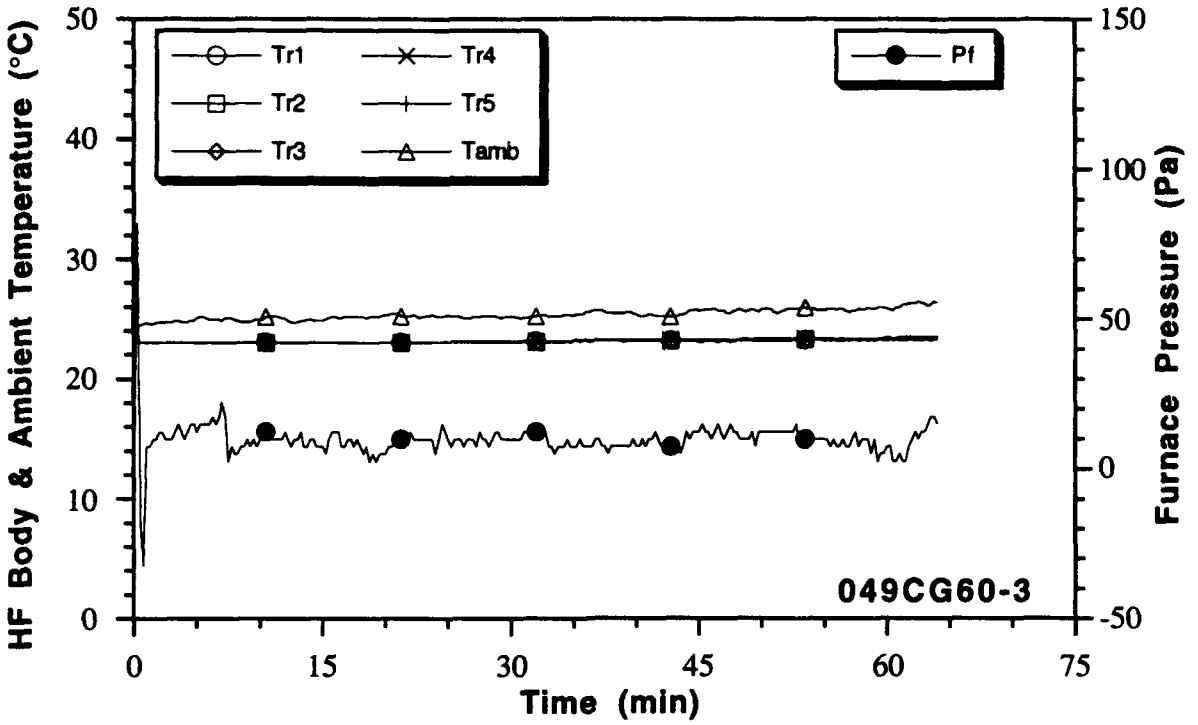
HF Body & Ambient Temperature (°C)
Furnace Pressure (Pa)
Time (min)
Tr1
Tr2
Tr3
Tr4
Tr5
Tamb
Pf
049CG60-3
0
10
20
30
40
50
-50
0
50
100
150
0
15
30
45
60
75

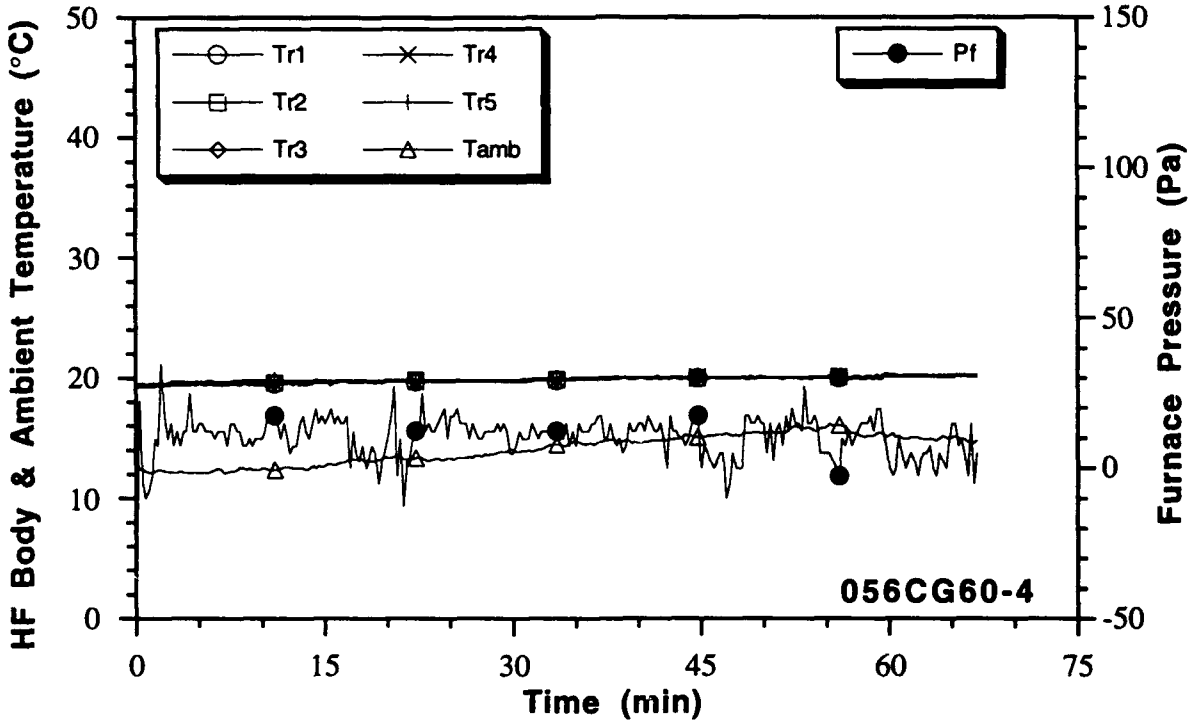
HF Body & Ambient Temperature (°C)
Furnace Pressure (Pa)
Time (min)
Tr1
Tr2
Tr3
Tr4
Tr5
Tamb
Pf
056CG60-4
0
10
20
30
40
50
-50
0
50
100
150
0
15
30
45
60
75

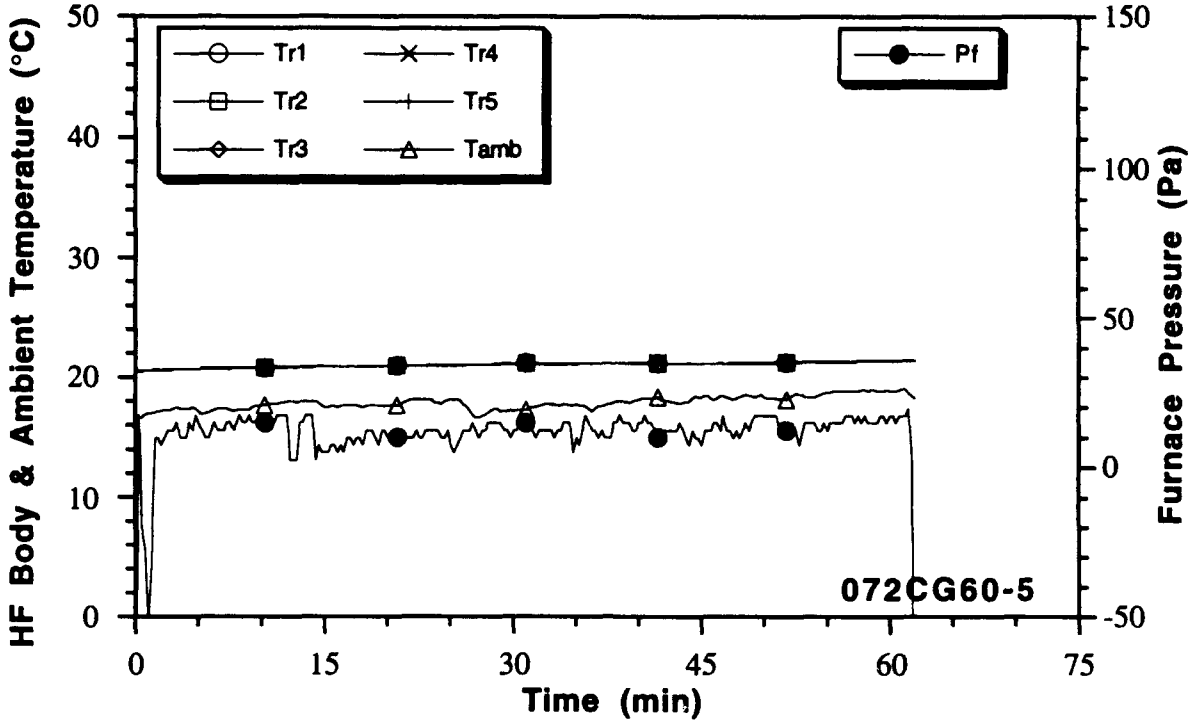
HF Body & Ambient Temperature (°C)
Furnace Pressure (Pa)
Time (min)
Tr1
Tr2
Tr3
Tr4
Tr5
Tamb
Pf
072CG60-5
0
10
20
30
40
50
-50
0
50
100
150
0
15
30
45
60
75

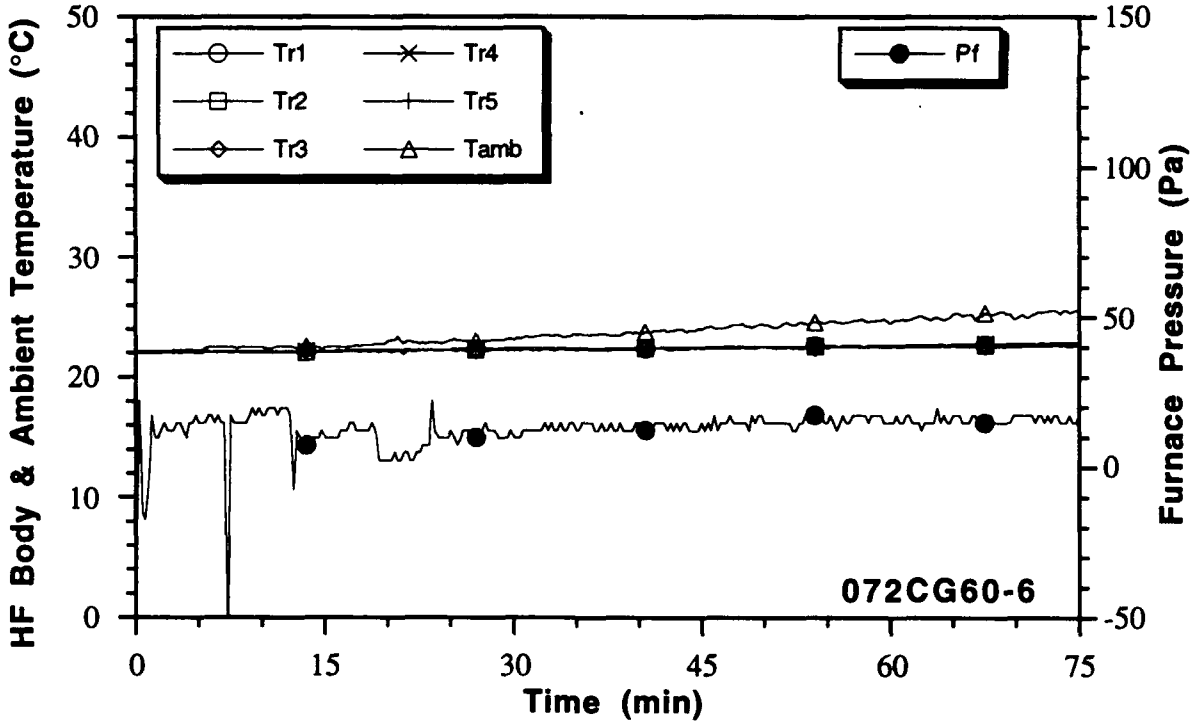
HF Body & Ambient Temperature (°C)
Furnace Pressure (Pa)
Time (min)
Tr1
Tr2
Tr3
Tr4
Tr5
Tamb
Pf
072CG60-6
0
10
20
30
40
50
-50
0
50
100
150
0
15
30
45
60
75

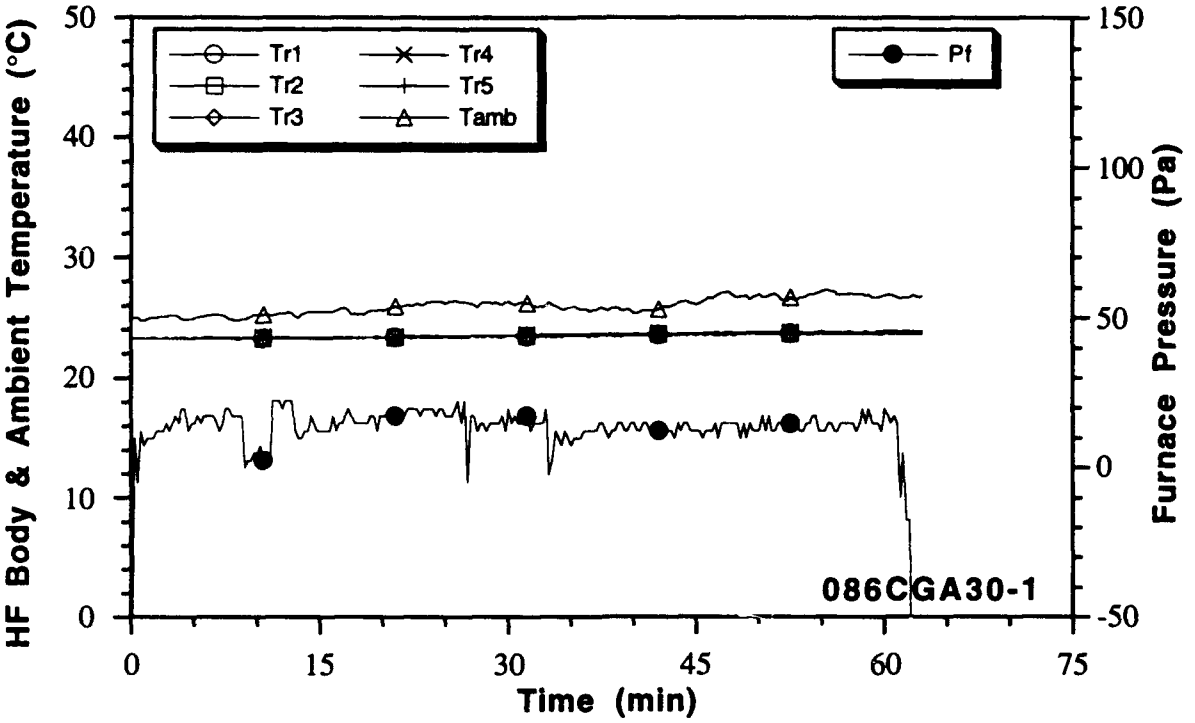
Tr1
Tr2
Tr3
Tr4
Tr5
Tamb
Pf
HF Body & Ambient Temperature (°C)
Furnace Pressure (Pa)
Time (min)
086CGA30-1
0
10
20
30
40
50
-50
0
50
100
150
0
15
30
45
60
75

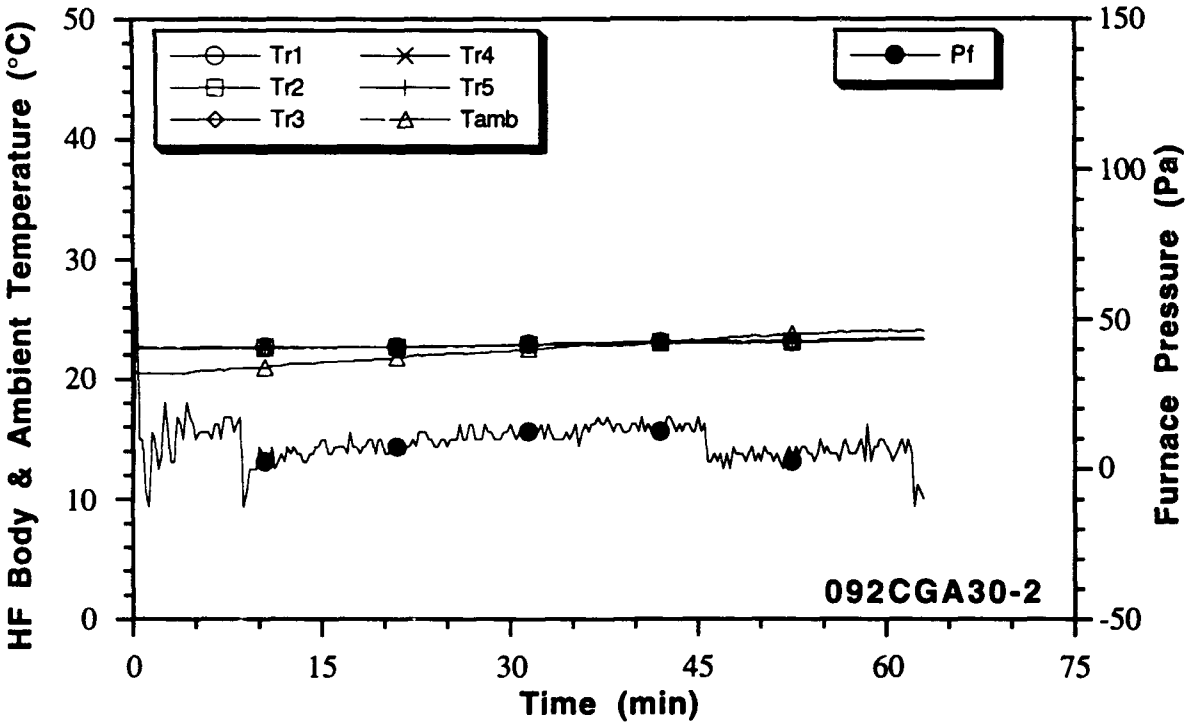
Tr1
Tr2
Tr3
Tr4
Tr5
Tamb
Pf
HF Body & Ambient Temperature (°C)
Furnace Pressure (Pa)
Time (min)
092CGA30-2
0
10
20
30
40
50
-50
0
50
100
150
0
15
30
45
60
75

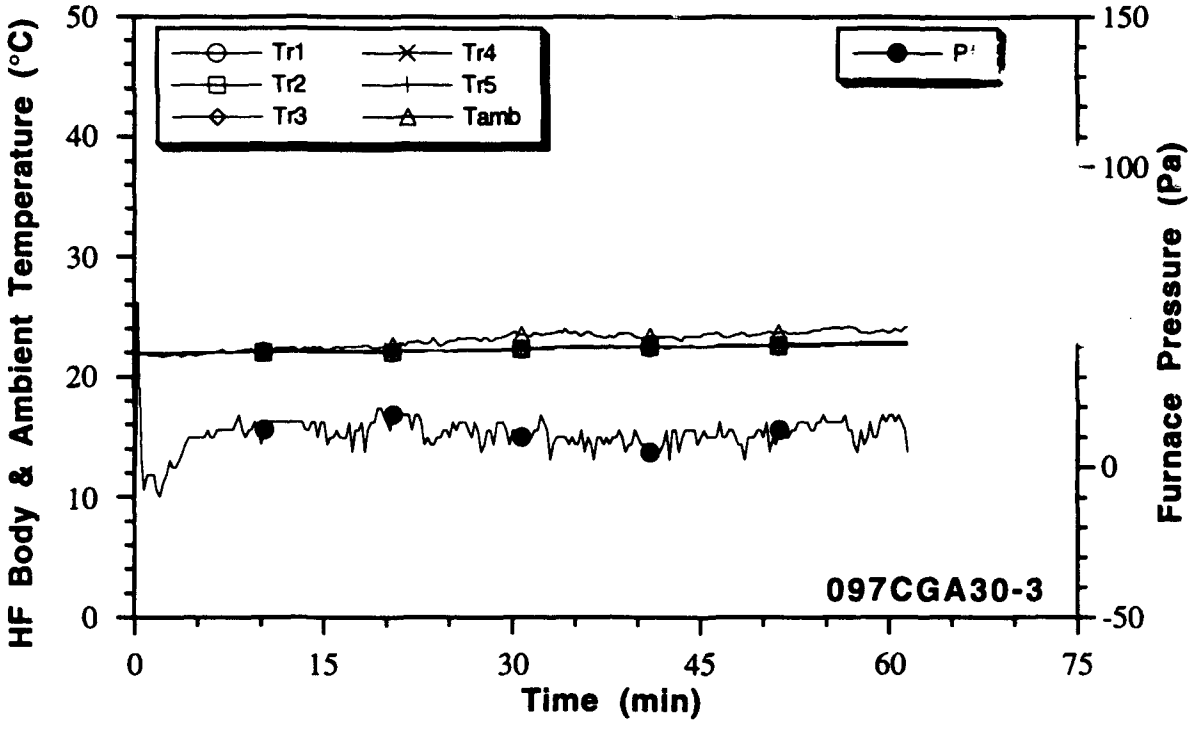
HF Body & Ambient Temperature (°C)
Furnace Pressure (Pa)
Time (min)
Tr1
Tr2
Tr3
Tr4
Tr5
Tamb
Pf
097CGA30-3
0
10
20
30
40
50
150
100
0
-50
0
15
30
45
60
75

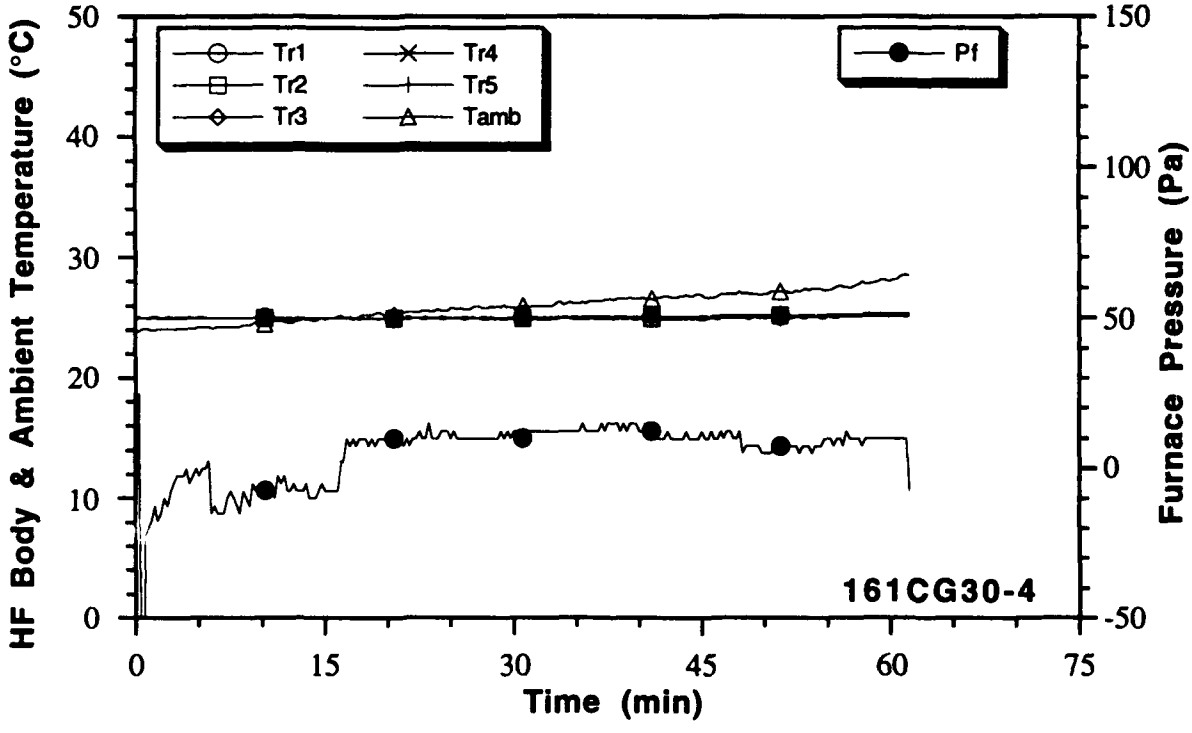
HF Body & Ambient Temperature (°C)
Furnace Pressure (Pa)
Time (min)
Tr1
Tr2
Tr3
Tr4
Tr5
Tamb
Pf
161CG30-4
0
10
20
30
40
50
150
100
50
0
-50
0
15
30
45
60
75

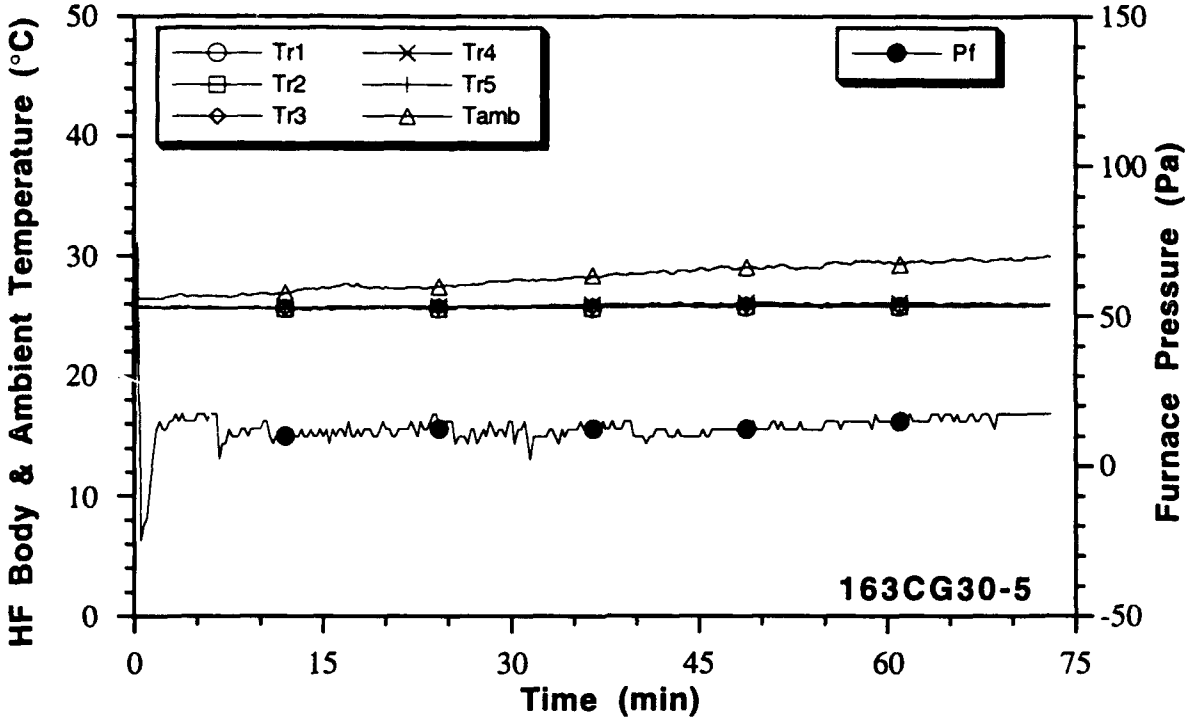
Tr1
Tr2
Tr3
Tr4
Tr5
Tamb
Pf
HF Body & Ambient Temperature (°C)
Furnace Pressure (Pa)
Time (min)
163CG30-5
0
10
20
30
40
50
-50
0
50
100
150
0
15
30
45
60
75

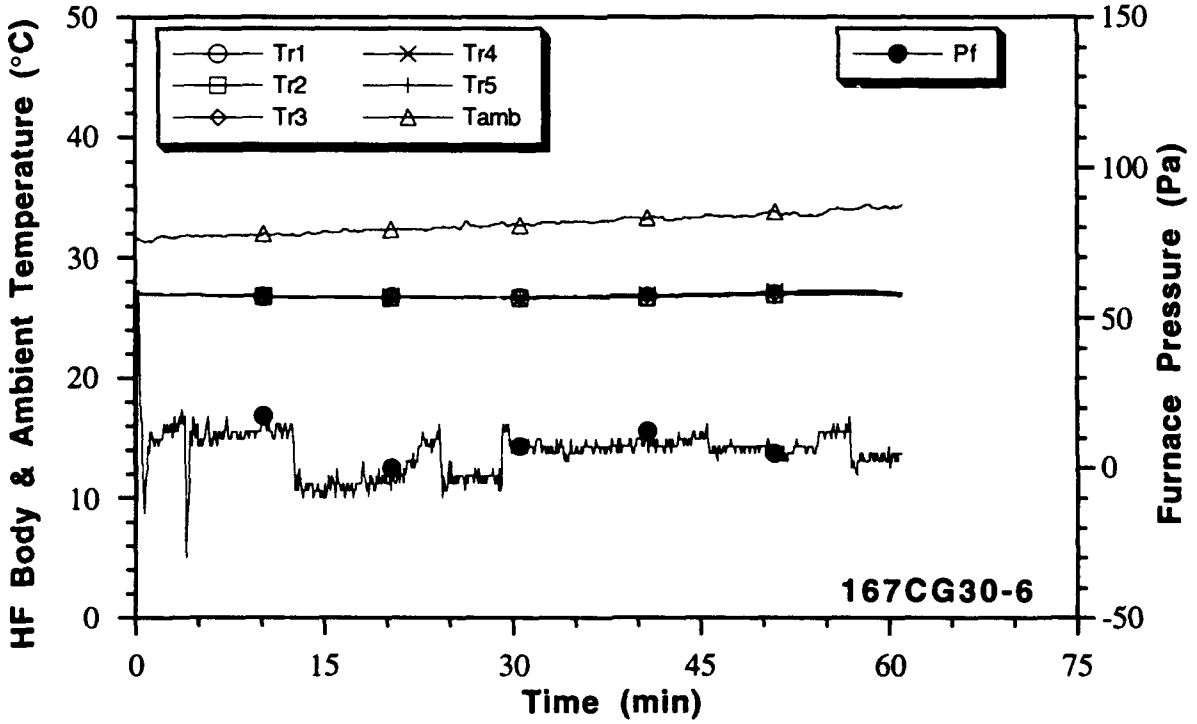
Tr1
Tr2
Tr3
Tr4
Tr5
Tamb
Pf
HF Body & Ambient Temperature (°C)
Furnace Pressure (Pa)
Time (min)
167CG30-6
0
10
20
30
40
50
-50
0
50
100
150
0
15
30
45
60
75

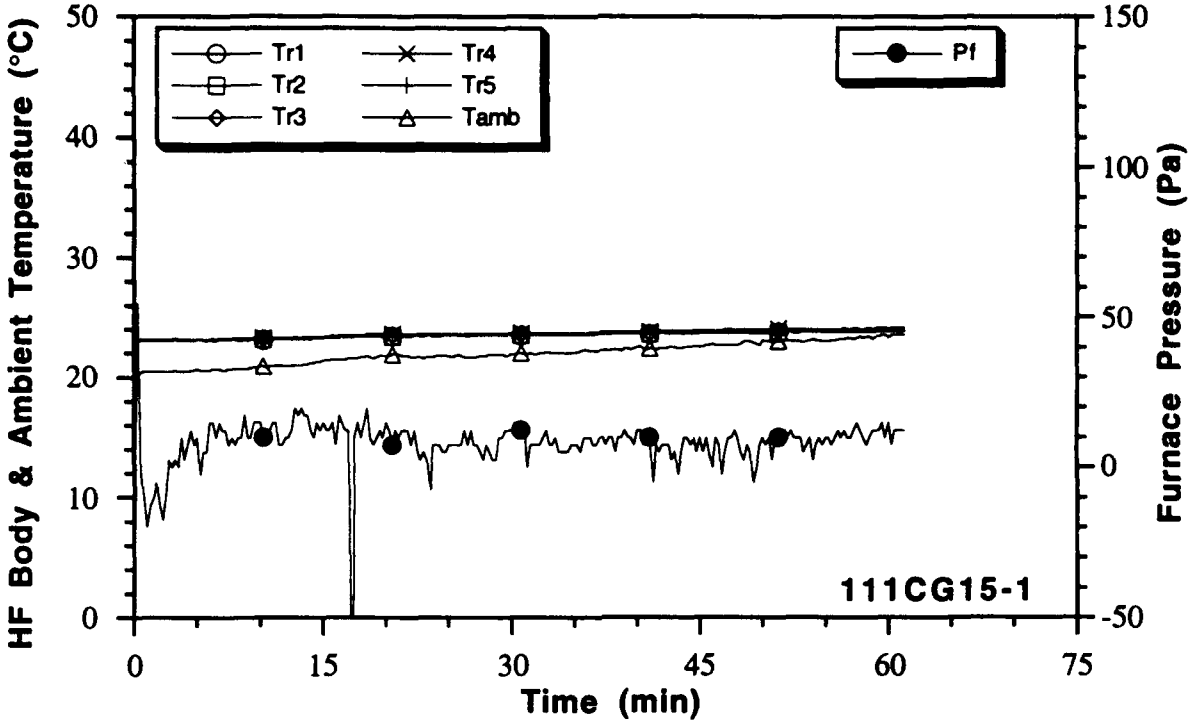
Tr1
Tr2
Tr3
Tr4
Tr5
Tamb
Pf
HF Body & Ambient Temperature (°C)
Furnace Pressure (Pa)
Time (min)
111CG15-1
0
10
20
30
40
50
-50
0
50
100
150
0
15
30
45
60
75

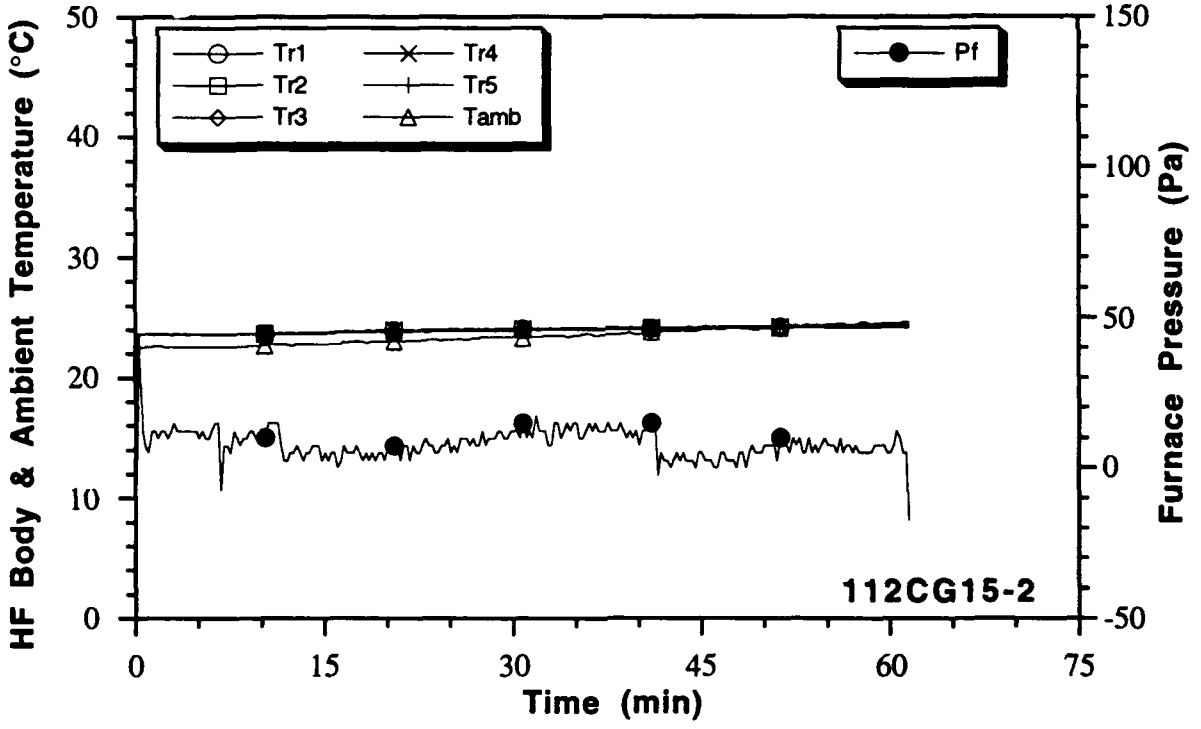
Tr1
Tr2
Tr3
Tr4
Tr5
Tamb
Pf
HF Body & Ambient Temperature (°C)
Furnace Pressure (Pa)
Time (min)
112CG15-2
0
10
20
30
40
50
-50
0
50
100
150
0
15
30
45
60
75

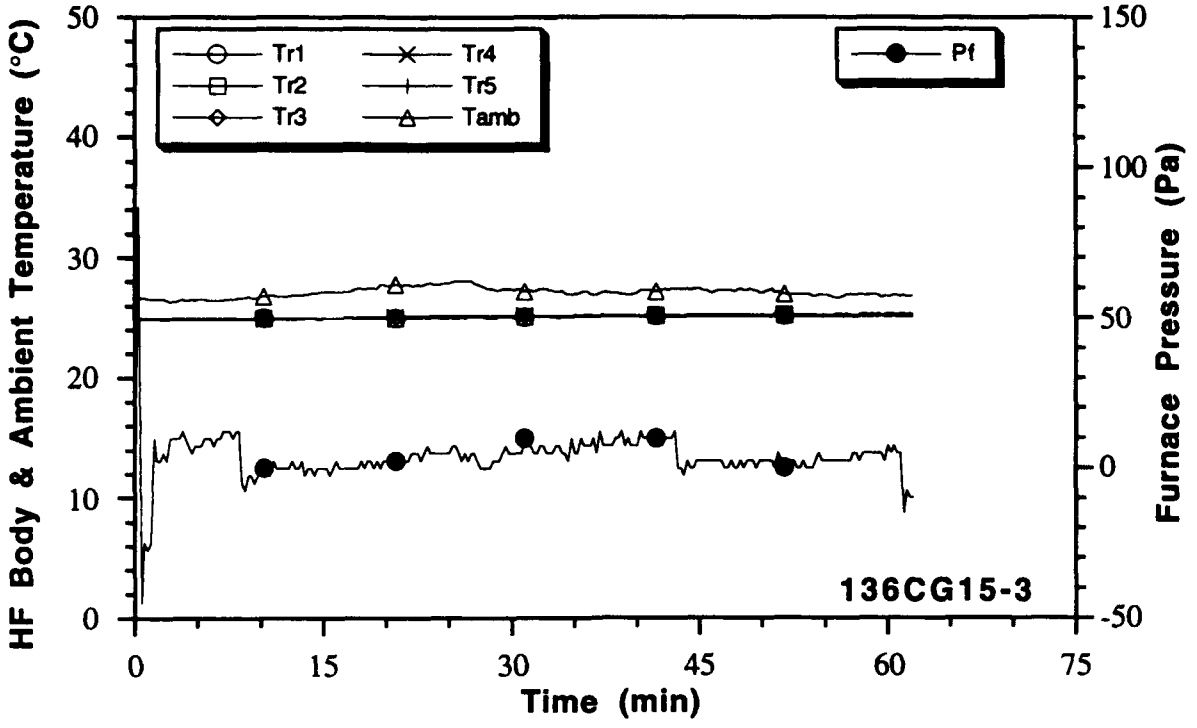
Tr1
Tr2
Tr3
Tr4
Tr5
Tamb
Pf
HF Body & Ambient Temperature (°C)
Furnace Pressure (Pa)
Time (min)
136CG15-3
0
10
20
30
40
50
-50
0
50
100
150
0
15
30
45
60
75

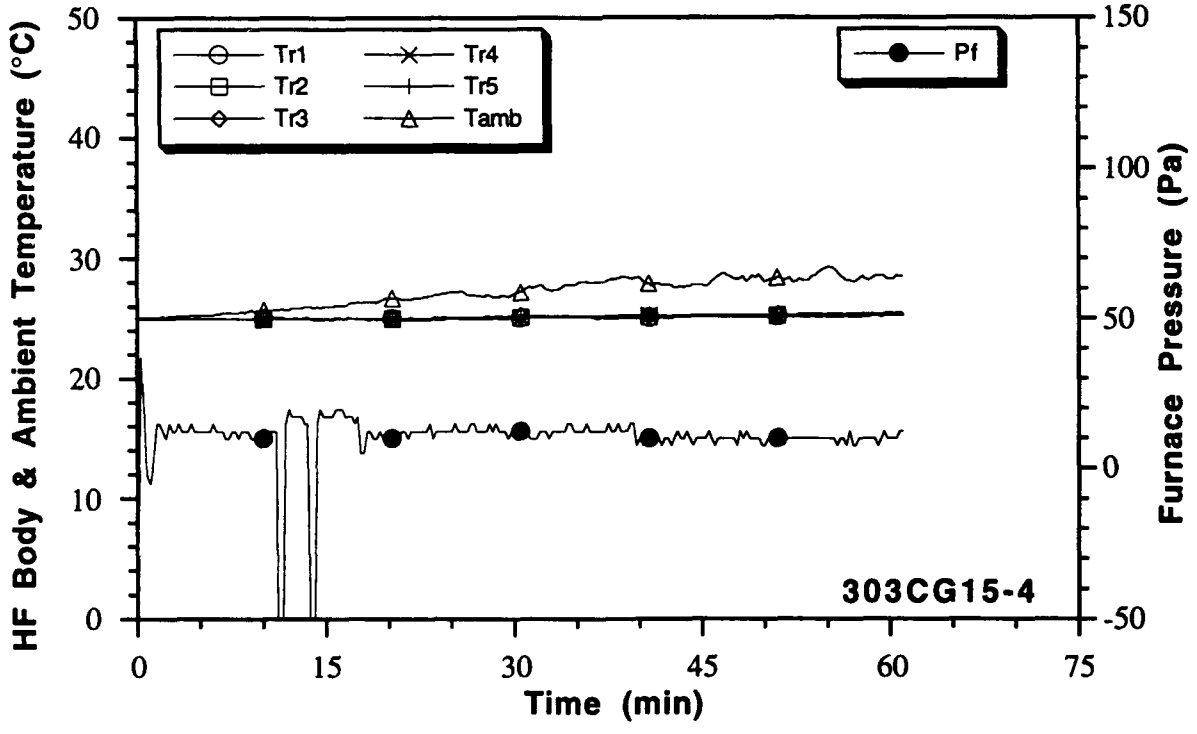
Tr1
Tr2
Tr3
Tr4
Tr5
Tamb
Pf
HF Body & Ambient Temperature (°C)
Furnace Pressure (Pa)
Time (min)
303CG15-4
0
10
20
30
40
50
-50
0
50
100
150
0
15
30
45
60
75

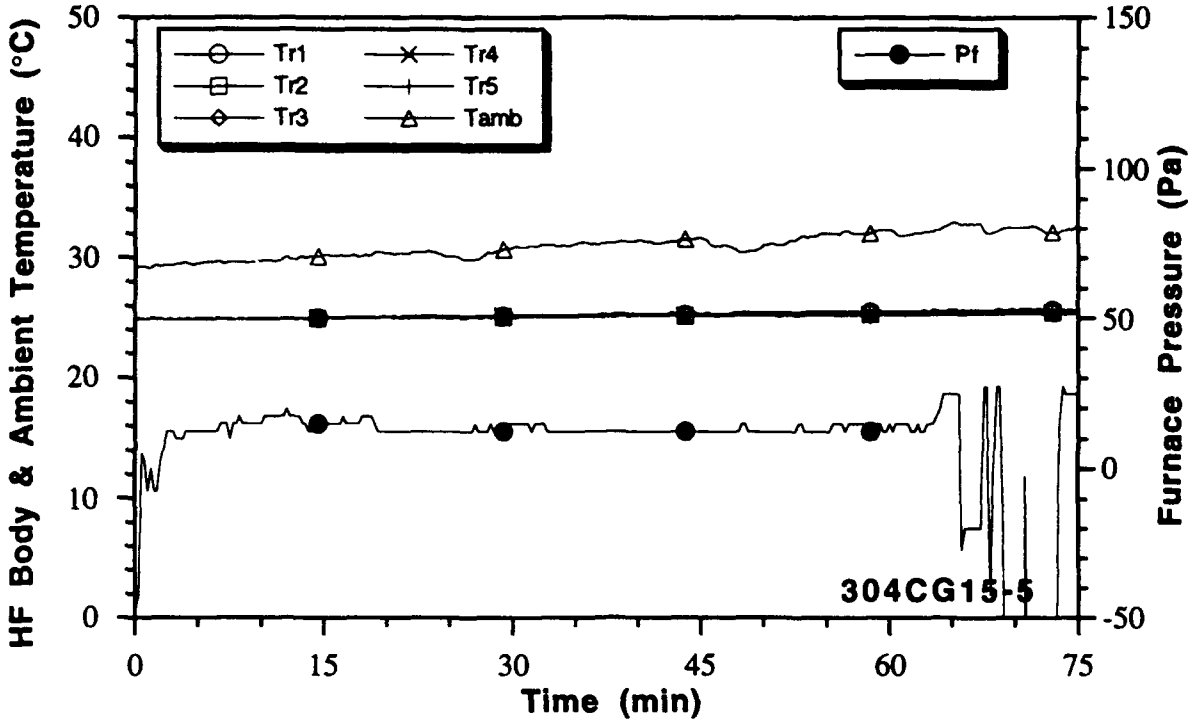
Tr1
Tr2
Tr3
Tr4
Tr5
Tamb
Pf
HF Body & Ambient Temperature (°C)
Furnace Pressure (Pa)
Time (min)
304CG15-5
0
10
20
30
40
50
-50
0
50
100
150
0
15
30
45
60
75

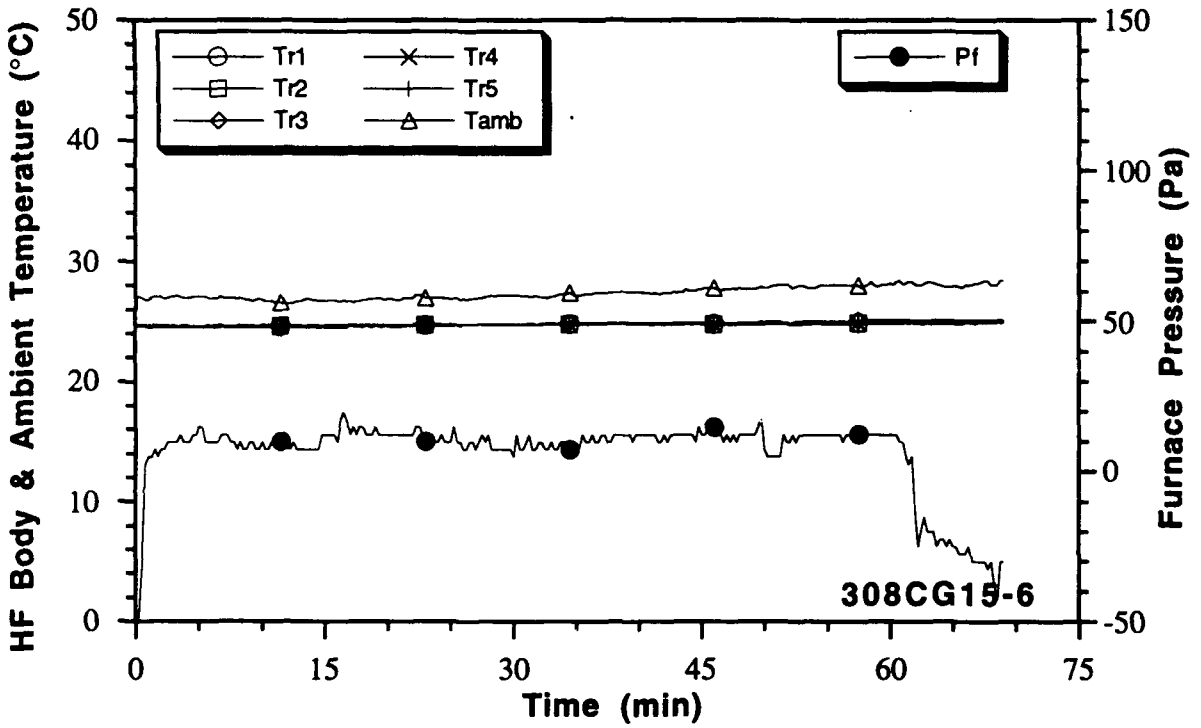
Tr1
Tr2
Tr3
Tr4
Tr5
Tamb
Pf
HF Body & Ambient Temperature (°C)
Furnace Pressure (Pa)
Time (min)
308CG15-6
0
10
20
30
40
50
-50
0
50
100
150
0
15
30
45
60
75

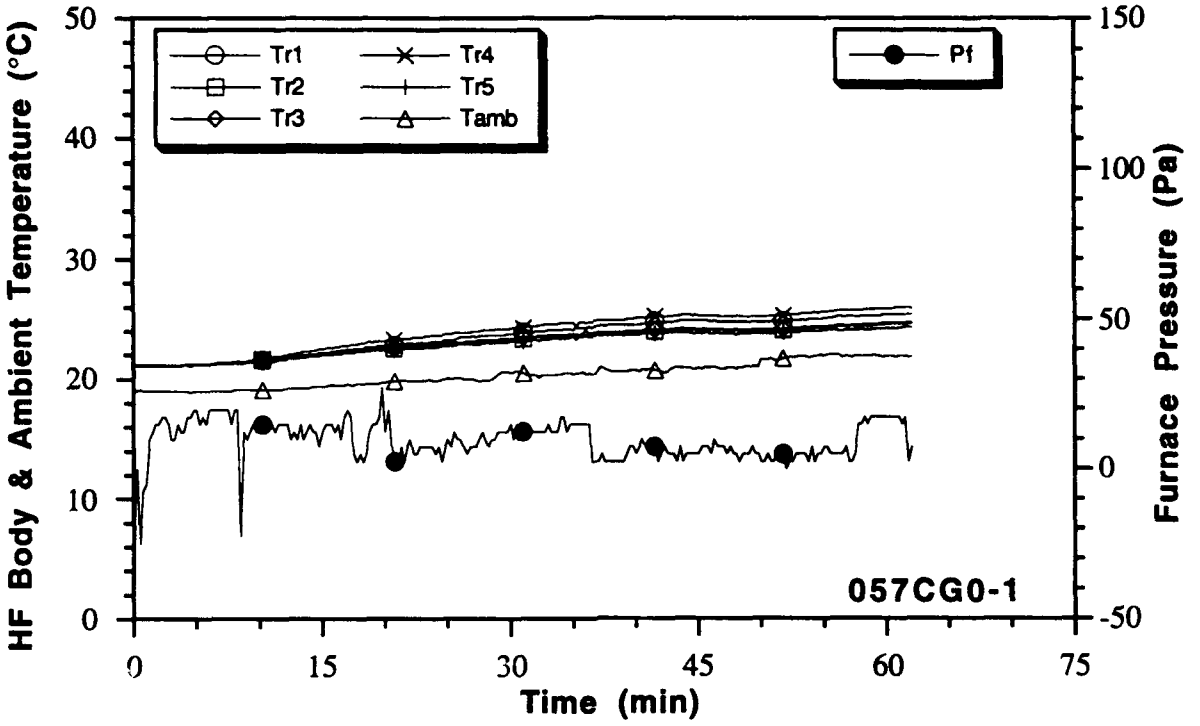
Tr1
Tr2
Tr3
Tr4
Tr5
Tamb
Pf
HF Body & Ambient Temperature (°C)
Furnace Pressure (Pa)
Time (min)
057CG0-1
0
10
20
30
40
50
-50
0
50
100
150
0
15
30
45
60
75

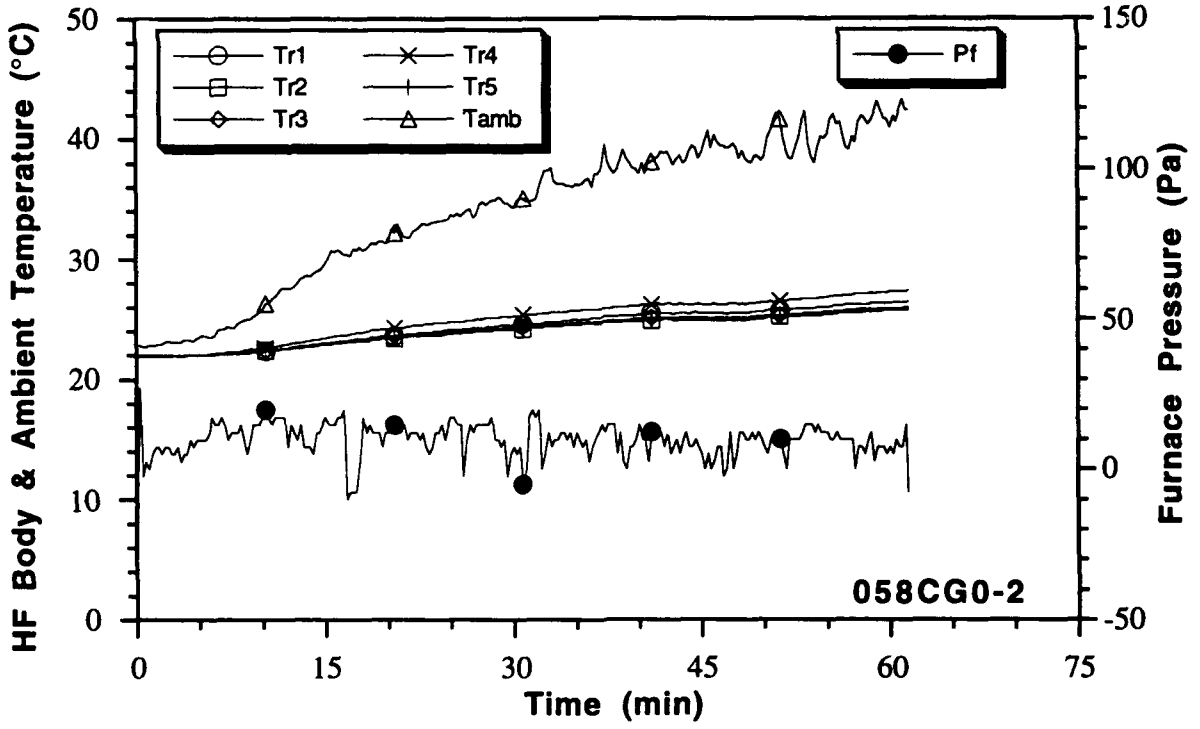
Tr1
Tr2
Tr3
Tr4
Tr5
Tamb
Pf
HF Body & Ambient Temperature (°C)
Furnace Pressure (Pa)
Time (min)
058CG0-2
0
10
20
30
40
50
-50
0
50
100
150
0
15
30
45
60
75

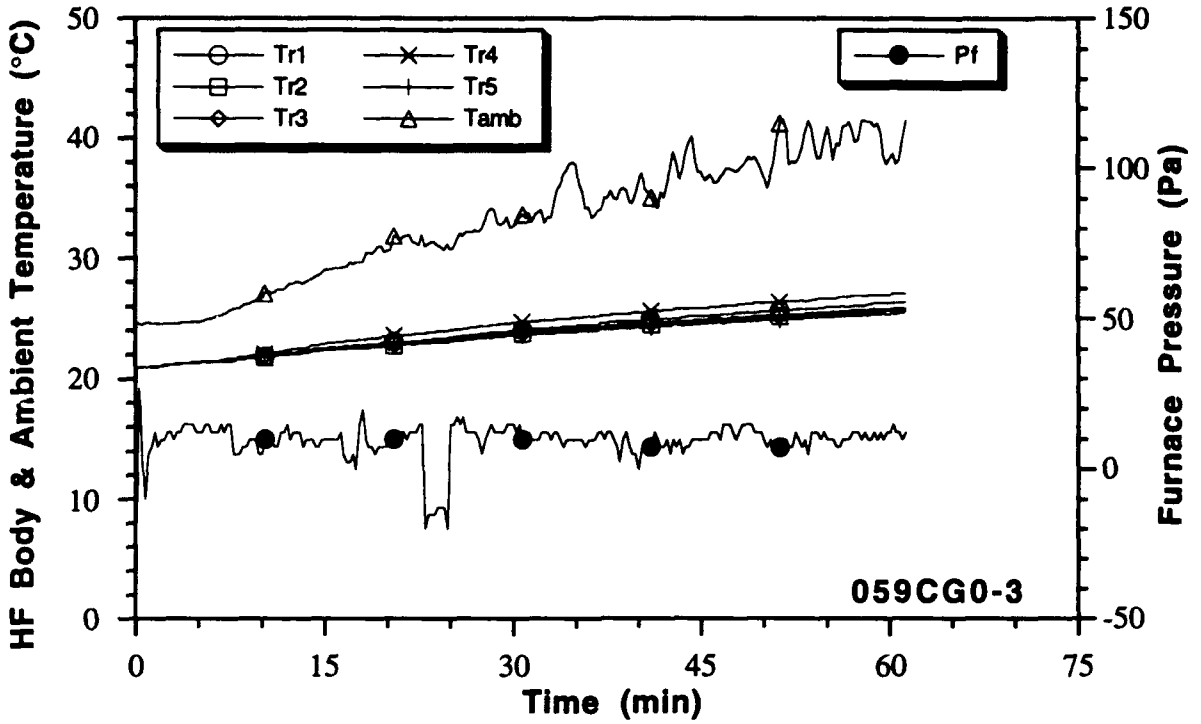
Tr1
Tr2
Tr3
Tr4
Tr5
Tamb
Pf
059CG0-3
HF Body & Ambient Temperature (°C)
Furnace Pressure (Pa)
Time (min)
0
10
20
30
40
50
-50
0
50
100
150
0
15
30
45
60
75

Appendix G
Thermal Modeling Input

MATERIAL PROPERTIES

Steel:

Thickness	4.76 mm	(3/16 in.)
Density	7690 kg/m^3	(480 lb/ft^3)

Thermal Conductivity

T(°C)	K (W/mK)	T (°F)	K (BTU/hrftF)
-17.8	51.9	0	30
315.6	42.7	600	24.7
593.3	34.8	1100	20.1
1093.3	25.9	2000	15
1371.1	25.9	2500	15

Specific Heat

T (°C)	C (J/kgK)	T (°F)	C (BTU/lbF)
-17.8	448	0	0.107
398.9	602	750	0.144
593.3	720	1100	0.172
1371.1	720	2500	0.172

Mineral Wool:

Thickness	25 to 127 mm
Density	80 to 144 kg/m^3

Thermal Conductivity

T(°C)	K (W/mK)	T (°F)	K (BTU/hrftF)
20.0	0.035	68	0.020
100.0	0.045	212	0.026
200.0	0.064	392	0.037
500.0	0.168	932	0.097
800.0	0.342	1472	0.198
926.7	0.436	1700	0.252
1093.3	0.579	2000	0.335

Specific Heat

T (°C)	C (J/kgK)	T (°F)	C (BTU/lbF)
20.0	879	68	0.21
100.0	879	212	0.21
200.0	1213	392	0.29
800.0	2008	1472	0.48
1093.3	2008	2000	0.48

BOUNDARY CONDITIONS AND MODELING DETAILS

1-d
100 nodes, 99 elements
elements 1-6 steel, the rest were insulation
10 second time steps
nonlinear boundary conditions, allowing convection and radiation at exposed face
- convection factor 25 W/m^{2}K (4.4. BTU/hrft^{2}F), with power of 1
- surface absorptivity, 0.6 to 0.9
- flame emissivity, 1. to 0.7
- surface emissivity, 0.88 to .7 (refer to table 3.5)

non-exposed face insulated
initial temperature of 20 °C (68 °F)
0.005 permissible relative error for fire boundary condition iteration
-.8 overconvergence factor for fire boundary condition iteration